Synthesis of Novel Dihydropentalenes, Pentalenides and Hydropentalenides

Boyt, Stuart

Award date:
2019

Awarding institution:
University of Bath

Synthesis of Novel Dihydropentalenes, Pentalenides and Hydropentalenides

Stuart Matthew Boyt

A thesis submitted for the degree of Doctor of Philosophy

University of Bath

Department of Chemistry

September 2019

Acknowledgements

I would like to thank:

Dr. Ulrich Hintermair for pitching this intriguing project and giving me the guidance I needed to explore it. And also for putting up with my tendency to get distracted by side-projects!

Dr. Gabriele Kociok-Kohn for assistance with XRD, especially running measurements on our air sensitive samples, and Dr. Tim Woodman for advice regarding NMR and for help with running a variety of NMR experiments

Professor Geoff Cloke and Dr. Alexander Kilpatrick for their advice about pentalenide chemistry, and for providing the sample of dilithium pentalenide that started this project off

Professor David Procter for his suggestions about samarium chemistry which enabled the problems of pinacol coupling to be overcome

Stefanie Federle for her care and patience, and for keeping me smiling even in the midst of thesis writing

Maya Singer Hobbs for being my constant companion in the lab, and for reading through my thesis in its roughest state

Kasia Maltby for being a great office mate, and for all the times spent at her place drinking too much vodka

Matt O'Neill, Matt Surman, Dan Berry and David Williamson for all the times playing board games together, and for all the inane chat that provided a needed distraction from all the chemistry talk

All the Hinterbears past and present for creating a pleasant work environment these past four years

My parents, Graham and Amelia, and my brothers, Jamie and Alex, for all their support through my years of study

Abstract

Pentalenides are dianionic ligands that can be thought of as two fused cyclopentadienides. They have drawn attention due to the interesting structural and electronic properties of pentalenide complexes of s, p, d and f block elements. However, exploration of the organometallic chemistry of these ligands has been limited by the difficulties associated with synthesising the precursors for these species. In **Chapter 1** the current literature regarding pentalenide synthesis is reviewed. Pyrolytic and solution phase routes to the ligand precursors, typically dihydropentalenes, are discussed, as well as their conversion into mono- and dianionic derivatives. Select examples of synthesising organometallic pentalenide compounds from these precursors are also discussed.

In **Chapter 2** the synthesis of phenyl-substituted dihydropentalenes is described. Attempts to synthesise di-, tri-, penta- and hexa-phenyl dihydropentalenes are detailed, and a straightforward, high-yielding synthesis of 1,3,4,6-tetraphenyldihydropentalene is reported, with a variety of reagents being shown to facilitate its formation. **Chapter 3** details the conversion of 1,3,4,6-tetraphenyldihydropentalene into its mono- and dianionic derivatives, and the characterisation of these anions by NMR and XRD. This chapter includes the first pentalenide to be characterised with different alkali metals. Solubility issues with the dilithium, disodium and dipotassium salts of tetraphenyldihydropentalenide were overcome by synthesising hetero-bimetallic alkali metal salts, the first such pentalenide species to be described.

In **Chapter 4** the synthesis of dihydropentalenes bearing both methyl and phenyl substituents is documented. The deprotonation of these dihydropentalenes, which leads to formation of the first vinyl-dihydropentalenide anions, is also described.

Table of contents

Abbreviations

Å	Angstrom
Ar	Aryl
Bn	Benzo
Bu	Butyl
C	Celsius
COD	Cyclooctadiene
COT	Cyclooctatetraene
Cp^-	Cyclopentadienide
CpH	Cyclopentadiene
$(CpH)_2$	Dicyclopentadiene
Cp*H	1,2,3,4,5-pentamethylcyclopentadiene
Ct	Centroid
DFT	Density functional theory
DME	Dimethoxyethane
d	Doublet
ε	Molar extinction coefficient
Et	Ethyl
Fv	Fulvene
η	Hapticity
HMBC	Heteronuclear multiple bond correlation
HMDS	Hexamethyldisilazide
HSQC	Heteronuclear single quantum coherence
K_a	Acid dissociation constant
L	Ligand

LVT	Low-valent titanium
m	Meta
m	Multiplet
M	Metal
Me	Methyl
NBS	N-bromosuccinimide
NMR	Nuclear magnetic resonance
o	Ortho
OR	Alkoxide
p	Para
Ph	Phenyl
PhMe	Toluene
Pn^{2-}	Pentalenide
Pn*	1,3,4,5,6-pentamethyl-2-methylene-1,2-dihydropentalene
Pn^{*2-}	1,2,3,4,5,6-hexamethylpentalenide
PnH^{-}	Hydropentalenide
$Pn^{*}H^{-}$	1,2,3,4,5,6-hexamethylhydropentalenide
PnH_2	Dihydropentalene
Pr	Propyl
Pyr	Pyridine
q	Quartet
QSAR	Quantitative structure-activity relationship
r.t	Room temperature
s	Singlet
t	Tert

t	Triplet
THF	Tetrahydrofuran
TIPS	Tri(isopropyl)silyl
TLC	Thin-layer chromatography
TMEDA	Tetramethylethylenediamine
TMS	Trimethylsilyl
UV/Vis	Ultraviolet-Visible
XRD	X-ray diffraction

Chapter 1: Introduction

Statement of authorship

This declaration concerns the article entitled:			
Chapter 1: Introduction Pg. 11-53 of this thesis			
Publication status (tick one) **Draft manuscript** ☐ **Submitted** ☐ **In review** ☐ **Accepted** ☐ **Published** X			
Publication details (reference)	Boyt, S.M.; Jenek, N.A.; Hintermair, U.; Synthesis of organometallic pentalenide complexes. *Dalton Trans.*, **2019**, *48*, 5107-5124		
Candidate's contribution to the paper (provide details, and also indicate as a percentage)	**Formulation of ideas:** Contributed to the devising of the article and outlining the focuses. Compiled the relevant literature to be reviewed **(60%)** **Design of methodology:** N/A **Experimental work:** N/A **Presentation of data in journal format:** Wrote the bulk of text in the article, as well as made the majority of the diagrams. Inserted most of the references **(60%)**		
Statement from Candidate	This paper reports on original research I conducted during the period of my Higher Degree by Research candidature.		
Signed		**Date**	20/09/2019

1.1 Pentalene and pentalenides

Pentalene (**Pn**, C_8H_6) has long fascinated theoretical and synthetic organic chemists for its anti-aromatic 8π system.[1] Unlike the flexible 8π cyclooctatetraene (**COT**, C_8H_8) **Pn** is planar due to its bicyclic ring structure, enforcing its anti-aromaticity. As a result, it readily dimerises above -196 °C to form two fulvene units isolated from each other by a cyclobutane linkage (Figure 1).[2]

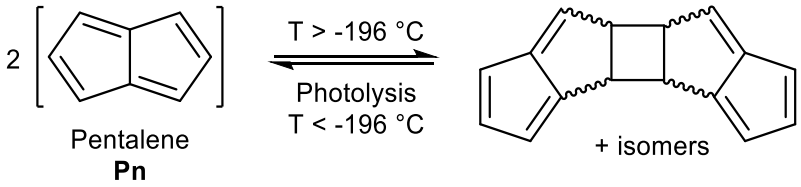

Figure 1: Reversible dimerisation of pentalene

Due to its inherent instability, **Pn** itself is of limited use for applications in synthetic chemistry. However, similar to other 8π anti-aromatics like **COT**, double reduction of **Pn** to pentalenide (**Pn^{2-}**, $C_8H_6^{2-}$) generates a stable 10π aromatic system that presents itself as a useful π ligand for organometallic chemistry.[3] Its dianionic nature makes it a stronger donor for Lewis-acidic metals than neutral 10π hydrocarbons such as naphthalene, and the two five-membered ring systems enable symmetrical charge distribution for reversible hapticity shifts of the metals bound to it (Figure 2).

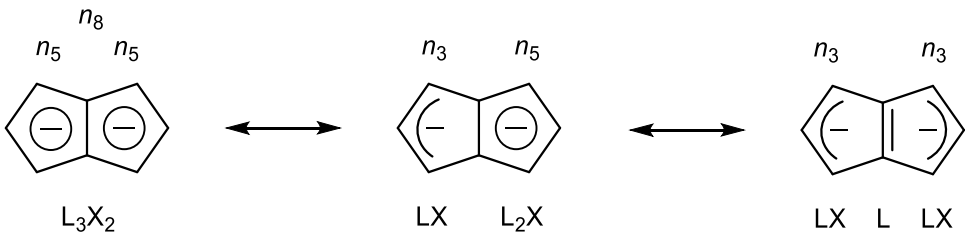

Figure 2: Charge distribution in the 10π aromatic pentalenide dianion

Due to this facile hapticity shift and a large degree of flexibility around the central C-C bridge, **Pn^{2-}** ligands exhibit some uniquely adaptive coordination abilities that neither **COT** nor naphthalene derivatives display. **Pn^{2-}** may wrap itself around large, electron-deficient metal centres in η^8 coordination mode, or form doubly η^5 / η^3 coordinated homo- and hetero-bimetallic complexes with

direct metal-metal interactions within *syn*-bimetallics and strong electronic coupling in *anti*-bimetallic systems.[4] Given these intriguing properties it may appear surprising that organometallic $\mathbf{Pn^{2-}}$ chemistry is far less explored and developed than that of its 6π congener cyclopentadienide ($\mathbf{Cp^-}$, $C_5H_5^-$), arguably the most important and most widely used organometallic ligand to date.[5] Whereas thousands of $\mathbf{Cp^-}$ complexes including almost every metal in the periodic table are known[6] and are widely used in numerous applications including sensing, electrochemistry, magnetism, material synthesis, and of course catalysis, only about 150 variously substituted $\mathbf{Pn^{2-}}$ and $\mathbf{PnH^-}$ complexes (including precursor salts) have been reported so far.

This limitation is in no small part due to the practical challenges associated with accessing suitable synthons for $\mathbf{Pn^{2-}}$ chemistry. Historically, only few dedicated organometallic labs have developed the expertise and equipment required for pentalenide chemistry, each following their own preferred synthetic method. However, a number of routes to suitable precursors have emerged in different parts of the chemical literature over the past 50 years. Here we summarise and compare various strategies for the synthesis and functionalisation of $\mathbf{Pn^{2-}}$ complexes that promise to give more facile access to a wider range of precursors, and thus hopefully allow more widespread exploration of the intriguing properties of organometallic pentalenide complexes in different areas in the future.

In the context of discussing synthetic pentalenide chemistry, it is useful to distinguish the 8π antiaromatic pentalene (**Pn**, C_8H_6), the non-aromatic dihydropentalene ($\mathbf{PnH_2}$, C_8H_8 existing as several double-bond isomers[7]), the 6π aromatic hydropentalenide ($\mathbf{PnH^-}$, $C_8H_7^-$), and the 10π aromatic pentalenide ($\mathbf{Pn^{2-}}$, $C_8H_6^{2-}$). Their structures and interconversion pathways are laid out in Figure 3.

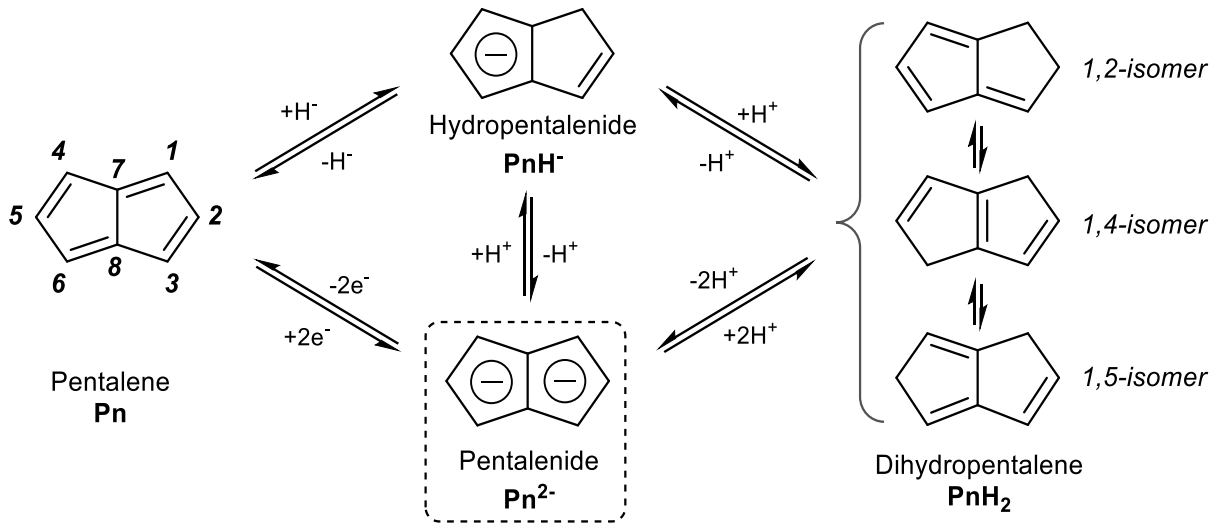

Figure 3: Nomenclature and interconversion of pentalene derivatives

1.2 Synthesis of pentalenides

1.2.1 Deprotonation of dihydropentalenes

Mono-anionic 6π **PnH**$^-$ can easily be generated by deprotonation of **PnH_2** using a weak base, as demonstrated by Katz and Mrowca.[8] They showed that an isomeric mixture of **PnH_2** would react with KOH and Tl_2SO_4 in water to furnish **TlPnH** as a precipitate in moderate yields (Figure 4). In contrast to the neutral, unsubstituted **PnH_2**, **PnH**$^-$ salts are thermally stable and can be isolated and stored at room temperature like the related **MCp** salts (M = Li, Na, K). Jones *et al.* later showed TlOEt in pentane to be equally effective in generating **TlPnH** from **PnH_2**.[9] The first pK_a of **PnH_2** must therefore be below 14, showing it to be slightly more acidic than **CpH**.[10]

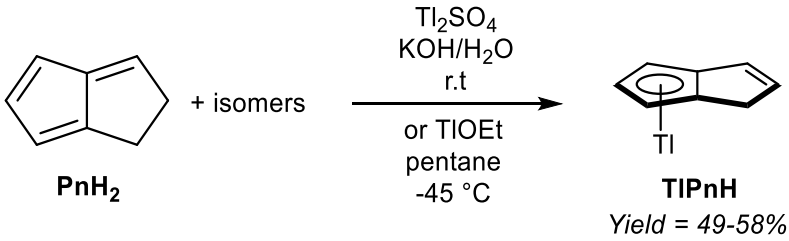

Figure 4: Synthesis of thallium hydropentalenide by deprotonation of dihydropentalenes

As a result of charge effects, deprotonation of the second ring in **PnH**$^-$ to furnish the fully 10π delocalised **Pn**$^{2-}$ requires a stronger base. In 1962 Katz *et al.* showed that **Li_2Pn** can be prepared by double deprotonation of **PnH_2** with an excess of ^{n}butyllithium at -78 °C (Figure 5).[11] Although the second pK_A value of **PnH_2** is not known with certainty, using two (or more) equivalents of bases with pK_A values >25 usually leads to quantitative double deprotonation of all **PnH_2** double-bond isomers.[1] While Katz's original preparation used heptane to precipitate **Li_2Pn**, Stezowski *et al.* later used dimethoxyethane (DME) to obtain single crystals of η^5**[Li(DME)]$_2$Pn** that showed both metals to adopt *anti*-configuration around the planar **Pn**$^{2-}$ in the solid state.[12] A recent computational study confirmed this to be the preferred geometry for all alkali-metal **Pn**$^{2-}$ complexes in solution.[13]

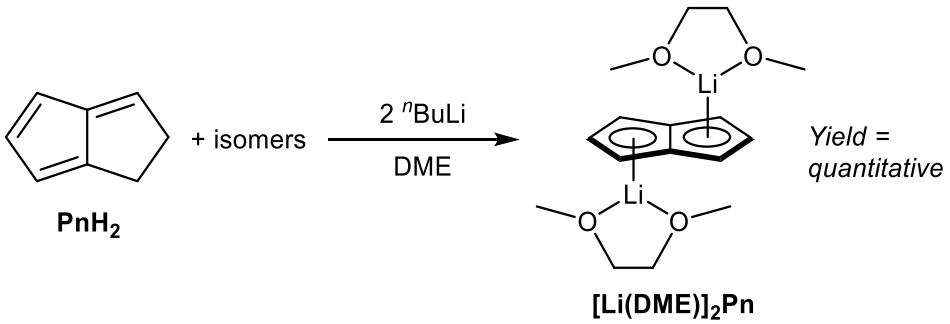

Figure 5: Synthesis of dilithium pentalenide by double deprotonation of dihydropentalenes

While these reactions look appealingly straightforward, and the utility of **PnH**$^-$ and **Pn**$^{2-}$ salts for transmetalation reactions is well documented (Section 1.3), the difficulty lies in generating the **PnH_2** starting material. In the following subsections we review the most prominent methods reported.

1.2.2 Pyrolytic routes to dihydropentalenes

PnH_2 can be obtained from controlled, anaerobic pyrolysis of suitable precursors such as isodicyclopentadiene in Katz's method (Figure 6).[14] Isodicyclopentadiene was formed by treating dihydrodicyclopentadiene (obtained from partial hydrogenation of dicyclopentadiene) with acetic anhydride and selenium dioxide, followed by dehydration of the resulting alcohol by passing over

[1] Based on the limited number of literature examples of the interconversion of **HPn**$^-$ and **Pn**$^{2-}$ reported to date, we estimate the second pK_A to be in the region of 25.

alumina at 300 °C.[15] Anaerobic pyrolysis of isodicyclopentadiene at 575 °C led to the formation of **1,4-PnH_2** (through release of ethylene) in ~30% yield, to which hydroquinoline had to be added immediately to prevent polymerisation. However, Kazennova *et al.* later reported that passing the pyrolysis distillate through a plug of solid potassium hydroxide provided pure **PnH_2** samples that were stable to polymerisation at -78 °C.[16] They also demonstrated an improved synthesis of isodicyclopentadiene, reporting a 40% overall yield of **PnH_2** starting from **CpH**.

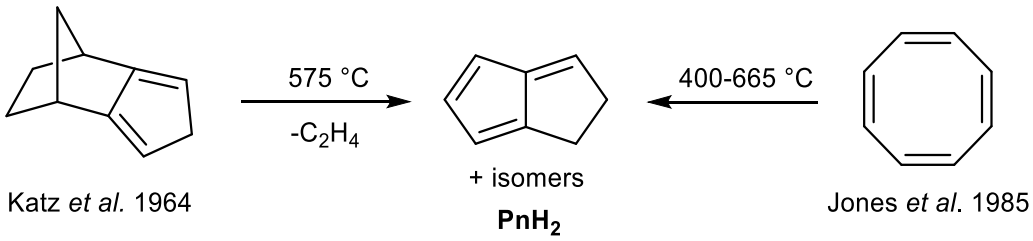

Figure 6: Synthesis of dihydropentalene by anaerobic flash vacuum pyrolysis

An alternative precursor was reported by Jones and Schwab, who showed that **COT** undergoes thermal rearrangement between 400-665 ^{o}C to give **PnH_2** (Figure 6) in addition to acetylene, benzene and styrene.[17] The selectivity to **PnH_2** was found to be highly temperature dependent, with the optimum conversion occurring between 500-600 ^{o}C. An optimised procedure was later reported by Cloke *et al*, in which a 87 % yield was achieved thanks to precise temperature and residence time control during the continuous-flow pyrolysis[18]. In this set-up, the resulting **PnH_2** were condensed into a ^{n}butyllithium solution in DME/hexane at -78 ^{o}C to be directly converted to the more stable **$[Li_2(DME)_x]Pn$** salts that precipitate to be further purified by washing with cold hexane.

While both routes are reasonably well established (with lower yields and more synthetic steps starting from inexpensive **$(CpH)_2$**, or fewer steps and higher yields starting from the more valuable **COT**), they are limited to the synthesis of the parent (unsubstituted) **PnH_2**. Substituted *iso*-**CpH** or **COT** have not been explored as pyrolysis precursors for substituted **PnH_2**, likely due to the difficulty and expense of synthesising the starting materials and/or unwanted thermal rearrangement pathways. A slightly more versatile pyrolytic method has been reported by Griesbeck, who showed the use of two

protected vinyl fulvenes, synthesised by Diels-Alder reaction of **CpH** and acroleins followed by pyrrolidine-facilitated Knoevenagel condensation with an additional equivalent of **CpH** (Figure 7).[19]

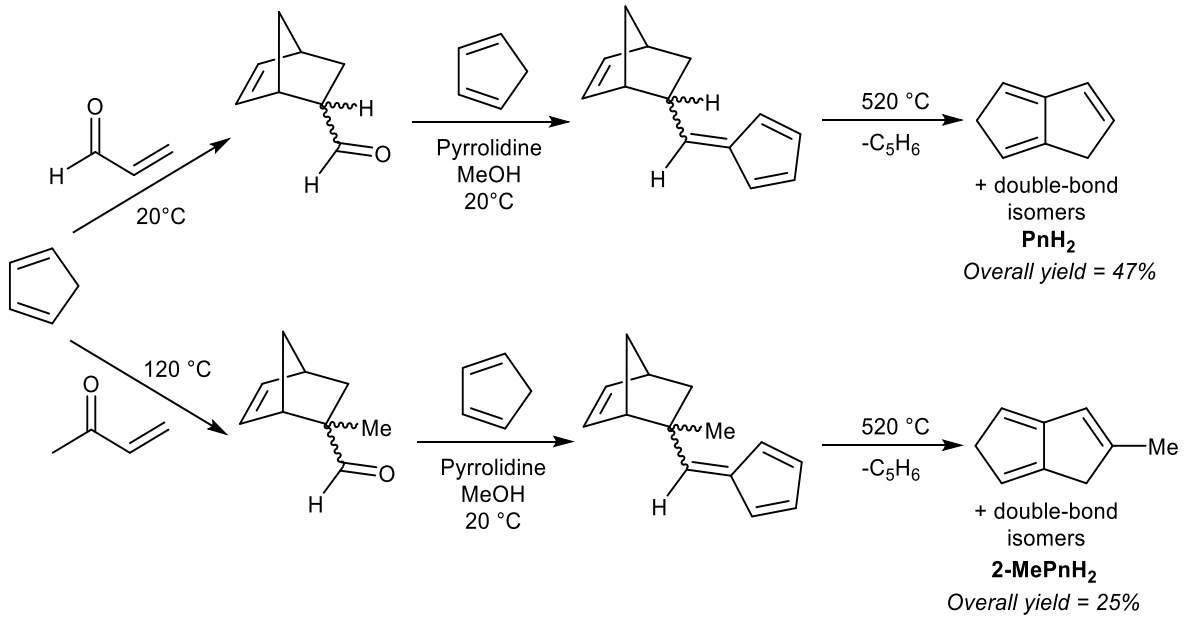

Figure 7: Flash vacuum pyrolysis of protected vinyl fulvenes derived from cyclopentadiene and acroleins

Anaerobic pyrolysis of these compounds at 520 °C furnished **PnH_2** (88 % yield) or **2-Me-PnH_2** (50% yield) through thermal cyclisation accompanied by loss of **CpH**. This methodology is appealing as the precursors are straightforward to synthesise from inexpensive starting materials, and potentially provide a route to other substituted **PnH_2** through use of substituted acroleins in the first step and/or substituted **CpH** in the second step. However, the final pyrolysis will likely require optimisation for each protected vinyl fulvene.

Another pyrolytic route to **PnH_2** and **2-MePnH_2** has been reported by Stapersma *et al.*, who showed that tetracyclo-oct-7-enes may be rearranged by anaerobic heating between 250 °C and 500 °C.[20] These starting materials, derived from photolytic rearrangements of 7-carbomethoxynorbornadienes,[21] are comparatively difficult to prepare, and their pyrolysis reactions gave relatively low **PnH_2** yields of 7-16% due to the formation of a large number of side products.

1.2.3. Thermal cyclisations of vinyl fulvenes

A mild thermal synthesis of **PnH_2** has been described by Gajewski and Cavender, who found that neat 6-vinyl fulvene will undergo thermal cyclisation at 110 °C (Figure 8).[22] This procedure gave exclusively the **1,5-PnH_2** isomer due to facile 1,5-hydride shifts occurring.

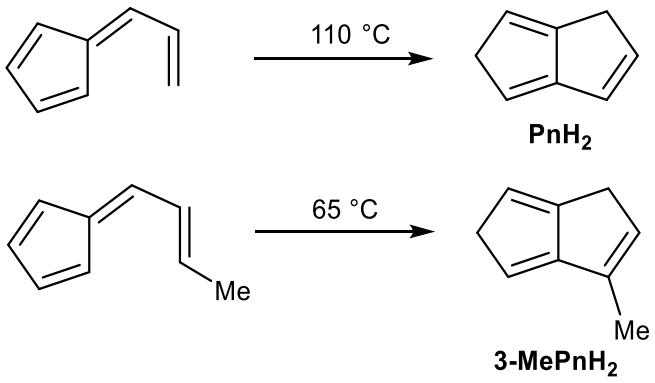

Figure 8: Thermal cyclisation of vinyl fulvenes to dihydropentalenes

6-Propenylfulvene was reported to undergo a thermal reaction at 65 °C, however, analysis of the products obtained was limited and no isolated yields were reported. The relatively low temperatures required to induce these rearrangements promise practical benefits over the higher temperature pyrolysis reactions discussed above. However, 6-vinyl fulvene is again not trivial to synthesise. Neuenschwander reported two preparations: the first reacting 1-hydroxymethyl-spiro-[2,4]-hepta-4,6-diene with HCl,[23] the second reacting **NaCp** with 3-acetoxy-3-chloro-1-propene.[24] Both routes give low yields (10% and 20%, respectively) due to significant side reactions occurring. Erden *et al.* describe an improved protocol, starting with condensation of **CpH** with 3-(methylthio)propanal, followed by oxidation with $NaIO_4$ and sulfoxide elimination with DBU. The reported yield across the three steps was 37% including a purification after each step.[25]

Kaiser and Hafner showed that 6-(2-aminovinyl)fulvenes would undergo a solution-phase thermal cyclisation and isomerisation in boiling piperidine to give **3-amino-PnH_2** in high yields (Figure 9).[26] These species could be reduced with $LiAlH_4$ to give an organoaluminium species that, upon hydrolysis, underwent amine elimination at room temperature to yield **PnH_2**. The syntheses of some mono- and

di-substituted **PnH_2** were also described, using 6-substituted amino fulvenes in the first step, and using alkyl/aryl lithiums in the following reduction/elimination step. However, purification procedures for these compounds were not described.

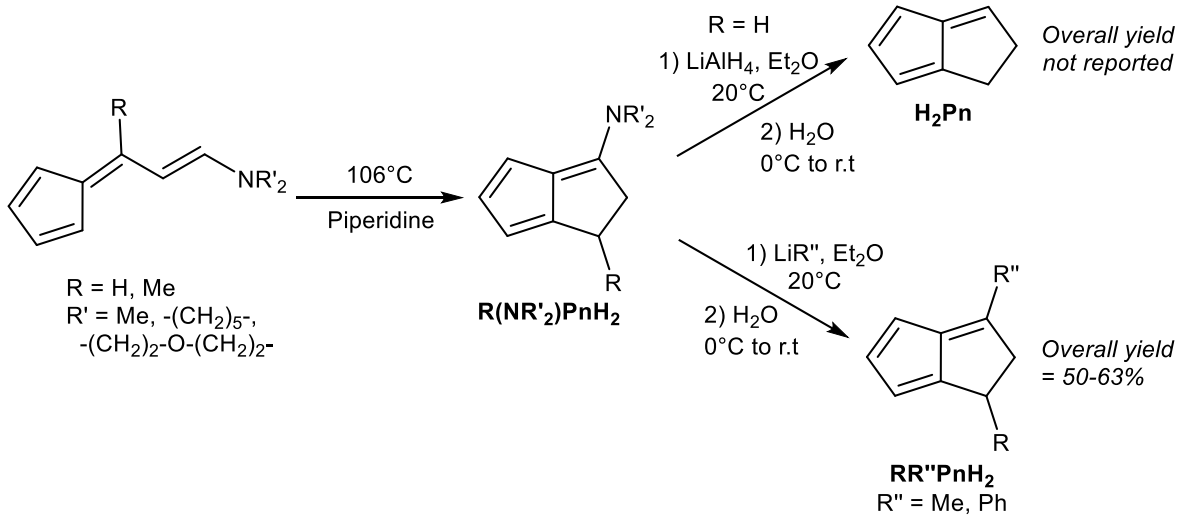

Figure 9: Thermal rearrangement of aminovinyl-fulvenes and subsequent reduction to dihydropentalenes

Similar to the above case of vinyl fulvenes, the amino-vinyl fulvene starting materials (derived from condensation of **CpH** with di(alkyl)-aminoacroleins) are difficult to handle due to their thermal instability.[27] In theory, starting from substituted **CpH** could produce more stable amino-vinyl fulvenes and provide access to more highly substituted **PnH_2**. However, it is difficult to predict whether these species would follow the same thermal rearrangement pathways.

While some of the thermal routes described above have been shown to be quite efficient in generating **PnH_2** precursors suitable for double deprotonation to **Pn^{2-}**, the limitations of these rearrangement reactions are obvious: their precursors rely on multi-step syntheses and/or utilise expensive starting materials, they often require special apparatus, conditions need to be carefully controlled and optimised, and they are rather limited in scope.

1.2.4. Solution-phase rearrangement reactions

Several solution-phase syntheses of **PnH_2** that do not involve pyrolytic steps have been described in the literature. Jones *et al.* reported the synthesis of **Li_2Pn** starting with the conversion of cycloheptatriene to 8,8-dibromobicyclo[5.1.0]octa-2,4-diene using bromoform and KO^tBu (Figure 10).[9] Reacting this species with methyllithium triggered a carbene-induced rearrangement to give **PnH_2** which was trapped with ^{n}butyllithium in DME/pentane to give **$[Li_2(DME)_x]Pn$**. Although the overall yields are quite low (<12%), this solution-phase method can be performed with standard laboratory equipment.

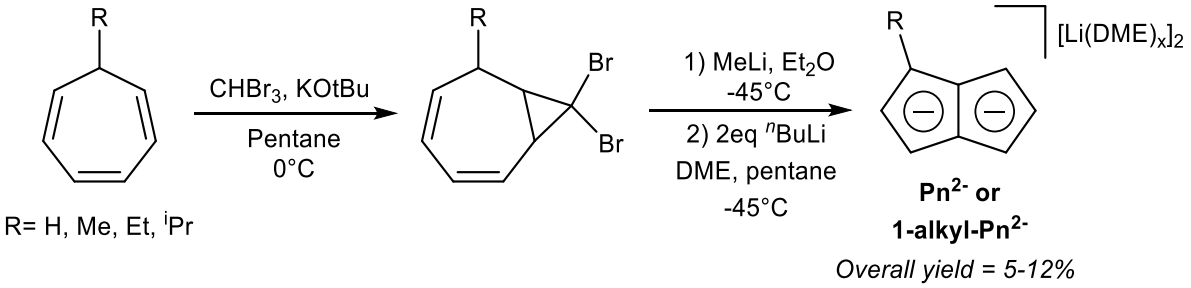

Figure 10: Synthesis of dilithium pentalenides from cycloheptatrienes

The Skattebøl rearrangement of the transient carbene generated from the geminal dihalo-cyclopropane unit allows for some variability in the substitution pattern. Cycloheptatriene can be converted to 7-alkylcycloheptatrienes through hydride abstraction, formation of the ethyl ether with EtOH and $NaHCO_3$, then finally substitution of the ether with a Grignard reagent. Although 7-tert-butyl-cycloheptatriene was found not to react with $CHBr_3$ and KO^tBu, the methyl, ethyl and isopropyl variants did undergo this transformation (albeit with low yields of 9-15%). Treating the gem-dibromo cyclopropane unit in these species with methyllithium furnished 1-alkyl substituted **PnH_2**, which gave high yields of **Li_2[1-alkyl-Pn]** upon double deprotonation with ^{n}butyllithium (53-70%).[9]

Another synthesis of **PnH_2** via carbene rearrangement has been reported by Brinker and Fleischhauer.[28] Trans-1,2-bis(2.2-dibromocyclopropyl)ethane, formed by twofold reaction of trans-1,3,5-hexatriene with $CHBr_3$ and KO^tBu, was found to rearrange to **PnH_2** when treated with

methyllithium in diethyl ether. However, significant side products were formed, and attempts to separate the mixture using vapour-phase chromatography proved unsuccessful.

Ashley *et al.* developed a solution-phase synthesis of hexamethylpentalenide, **Pn*$^{2-}$**, the pentalenide analogue of pentamethylcyclopentadienide (**Cp*$^{-}$**).[29] The starting material for this preparation is the so-called 'Weiss-H_4' compound, obtained from reaction of dimethyl-1,3-acetonedicarboxylate with glyoxal.[30]

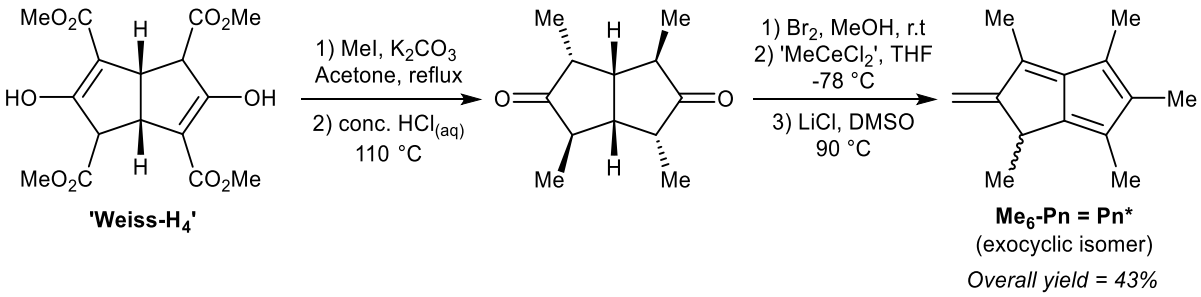

Figure 11: Synthesis of an exocyclic hexamethylpentalene isomer from 'Weiss-H_4'

Reacting the 'Weiss-H_4' compound with an excess of methyl iodide and K_2CO_3, followed by hydrolysis/decarboxylation with concentrated HCl yielded 2,4,6,8-tetramethylbicyclo[3.3.0]octane-3,7-dione (Figure 11). The so-obtained diketone could be oxidised with bromine in MeOH, then reacted with 'methylcerium dichloride' (derived from methyllithium and cerium trichloride) at -78 °C in THF. The resulting alcohol is prone to polymerisation and thus extremely sensitive to acid. The final dehydration reaction therefore required an aprotic method, and it was found that LiCl in DMSO was effective in producing 1,3,4,5,6-pentamethyl-2-methylene-1,2-dihydropentalene, **Me_6-Pn** or **Pn***, an exocyclic isomer of hexamethylpentalene. This compound is stable due to its vinylic fulvene structure preventing cyclic conjugation of an otherwise anti-aromatic 8π system and marks the only pentalenide synthon where the 8π **Pn*** is stable whereas the non-aromatic **PnH_2*** is unknown.

As outlined in Figure 3, to transform the **Pn*** into **Pn*$^{2-}$** it must be doubly reduced.[31] Direct reaction with alkali metals led to degradation of the starting material through polymerisation, but reaction with a bulky trialkyl borohydride (LS-selectride) allowed for 1,4-addition of a hydride to yield **LiPn*H** (Figure

12). Use of the less sterically demanding L-selectride resulted in a mixture of 1,2- and 1,4-addition products.

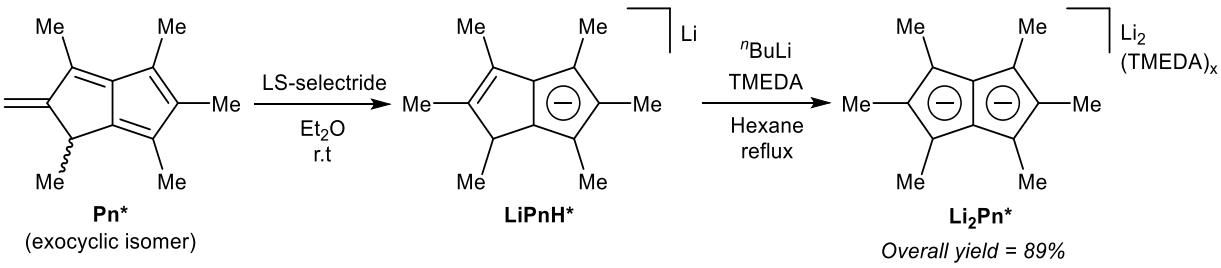

Figure 12: Reduction of hexamethyl-pentalene to lithium hexamethyl-hydropentalenide, and its subsequent deprotonation to dilithium hexamethylpentalenide

LiPn*H is reportedly insoluble in most organic solvents, requiring solubilisation with pyridine for NMR analysis. The final deprotonation of **LiPn*H** however was performed in a refluxing hexane slurry with ^{n}butyllithium and TMEDA to afford the TMEDA adduct of **Li_2Pn***. In order to obtain single crystals suitable for XRD analysis **[Li_2(TMEDA)$_x$]Pn*** had to be converted into a bis-stannyl derivative using Me_3SnCl (Figure 38, section 1.3.3), and transmetallated again using methyllithium in neat TMEDA.[31]

Despite requiring multiple steps and involving several sensitive intermediates, the overall synthesis of **[Li_2(TMEDA)$_x$]Pn*** is well developed and gives access to a valuable synthon for organometallic pentalenide chemistry without the use of special apparatus. Using different electrophiles (for example, ethyl iodide or isopropyl bromide) in the first step could in principle allow for incorporation of different substituents into these four positions, but this change would likely require downstream modification of the overall synthesis. So far there is no report of such variants.

1.2.5. Annulation reactions of cyclopentadienes

As already exemplified in some of the previous thermal rearrangement reactions, **CpH** provides a convenient starting material for the synthesis of pentalene derivatives. In the following section we review examples where selective 1,2 annulation reactions of **CpH** have been accomplished via mild solution-phase methods. An early example was provided by Hafner and Süss, who used **Li[^{t}BuCp]** to synthesise **^{t}Bu$_3$Pn** through its reaction with an iminium salt derived from 5-dimethylamino-2,2,6,6-tetramethyl-4-hepten-3-one and triethyloxonium tetrafluoroborate (Figure 13).[32]

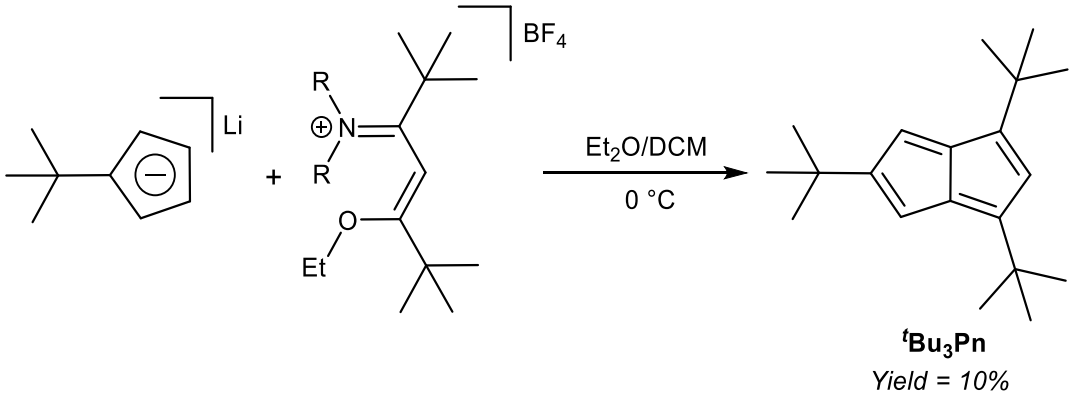

Figure 13: Synthesis of 1,3,5-tris(^{t}butyl)pentalene from lithium ^{t}butyl-cyclopentadiende

The resulting deep blue species had to be purified by chromatography on alumina at -75 °C using pentane as the eluent. Kitschke and Linder were later able to obtain crystals of **^{t}Bu$_3$Pn** for XRD analysis by recrystallisation from hexane.[33] Its stability is interesting in that although normally one would not approach the synthesis of an organometallic **Pn^{2-}** ligand via its 8π **Pn** version, this might be a viable approach in the case of sterically demanding substitution patterns such as 1,3,5-tris(tert-butyl) that are effective in blocking dimerization pathways. Ashley *et al.* have shown that a permethylated **Pn** system may be reduced using a bulky borohydride to give **PnH$^-$** and then **Pn^{2-}** upon deprotonation (Figure 11),[31] so similar chemistry might be possible with other bulky **Pn** such as Hafner's **^{t}Bu$_3$Pn**.

Due to their known stability and ease of deprotonation, routes that give access to **PnH$_2$** synthons are still preferable in most cases. Retrosynthetic analysis shows that Hafner's **CpH** annulation strategy to

synthesise ^{t}**Bu$_3$Pn** is well suited to give access to **PnH$_2$** as well: 1,4-Michael addition by a **Cp$^-$** to an electrophilic conjugated carbonyl species would yield a β-cyclopentadiene-functionalised ketone/aldehyde intermediate that is set up to undergo an intramolecular Knoevenagel condensation (Figure 14). Compatible **CpH** merely require two adjacent unsubstituted carbons in order to accommodate the final ring-closing step. Thus, a wide range of mono-, 1,2 and 1,3 di-, as well as 1,2,3-trisubstituted **CpH** may be transformed into the corresponding **PnH$_2$** pro-ligands by reaction with simple enones (chalcones).

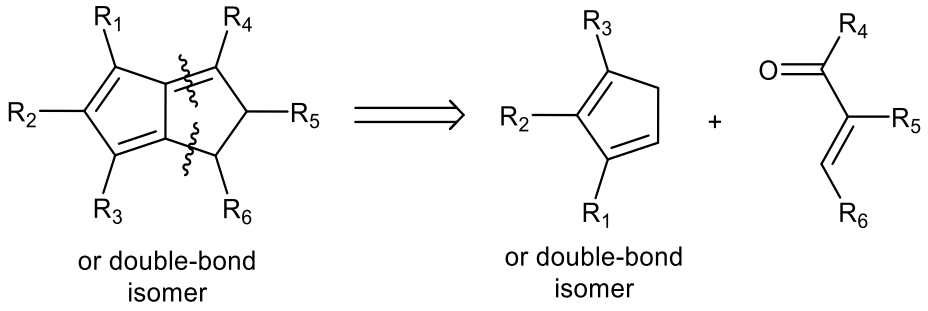

Figure 14: Retrosynthesis of substituted dihydropentalenes from cyclopentadienes and enones

The simplest unsubstituted **PnH$_2$** is currently not accessible by such a transformation, as **CpH** and acrolein are known to undergo a Diels-Alder reaction instead of the required Michael addition.[34] However, Griesbeck showed that moving to slightly higher substituted reaction partners, and using pyrrolidine to activate the chalcone towards 1,4 nucleophilic attack via its enamine, indeed furnishes substituted **PnH$_2$** in good yields from a single step reaction under mild conditions (Figure 15).[35]

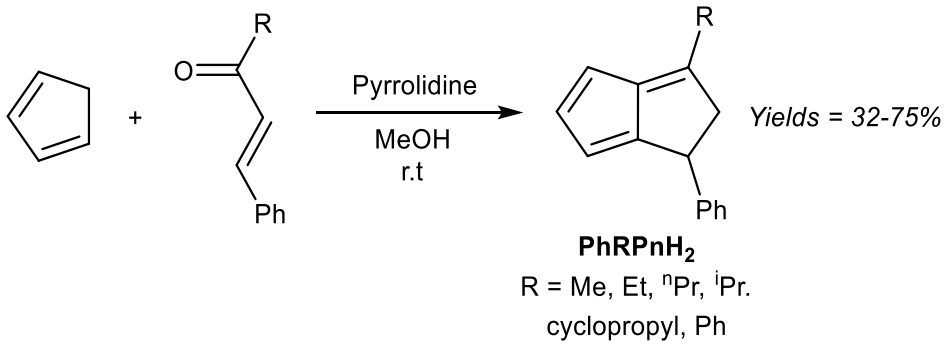

Figure 15: Synthesis of di-substituted dihydropentalenes by pyrrolidine-facilitated condensation of cyclopentadiene and substituted enones

The six different 1,3-disubstituted **PnH_2** thus prepared were air-stable compounds that did not polymerise and could be purified by high-vacuum distillation. The initially obtained 1,2 double-bond isomers were found to isomerise to the more stable 1,5 form when contacted with Brønsted acids (e.g. trifluoroacetic acid or activated alumina) or when heated above 500 °C. Curiously, none of the 1,3-disubstituted **PnH_2** reported in this study have been taken forward to the **Pn^{2-}** form by double deprotonation or used as organometallic synthons in other reports so far.

Another, more highly substituted example of this strategy has been reported by Le Goff,[36] who reported the fluoride-catalysed condensation of **1,2,3-Ph_3CpH** and 1,2,3-triphenylenone to yield **Ph_6PnH_2** (Figure 16). Oxidation with N-bromosuccinimide reportedly afforded the corresponding **Ph_6Pn** as another example of an 8π pentalene stabilised by suitable substitution pattern, as inferred from its UV-vis spectrum.

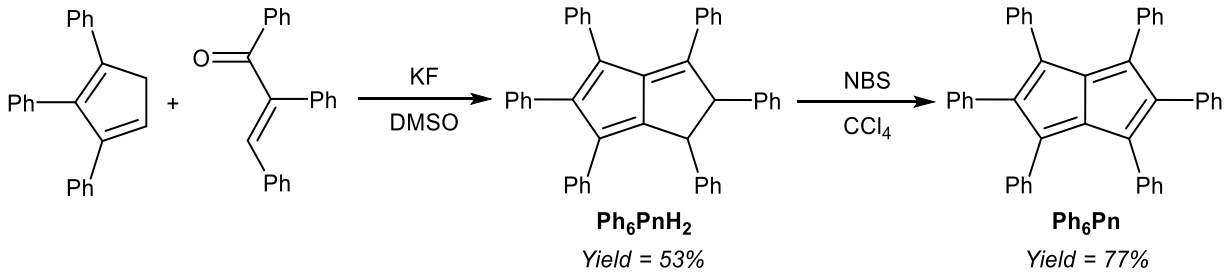

Figure 16: Synthesis of hexaphenyl-dihydropentalene and its oxidation into hexaphenylpentalene

Its corresponding **Ph_6Pn^{2-}** would make an interesting organometallic ligand, however, this two-page single-author communication does not contain any synthetic or analytical details, and the synthesis has never been replicated in later literature.

1.2.6 Annulation reactions of fulvenes

In cases where the required chalcone is either difficult to access or does not display the desired reactivity, a stepwise approach to **PnH_2** synthesis through **CpH** annulation is possible. Condensation of a **CpH** with an aldehyde yields a 6-substituted fulvene that may be attacked by an enolate to ring-close via an intramolecular Knoevenagel condensation (Figure 17). Although apparently introducing an additional reaction step, it eliminates the need for synthesising the enone in the first place.

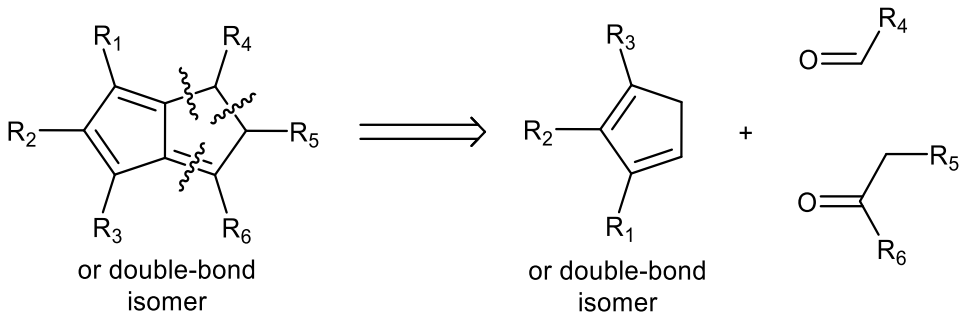

Figure 17: Retrosynthesis of substituted dihydropentalenes from cyclopentadienes, aldehydes and ketones

Formation of the fulvene intermediate from **CpH** and aldehyde follows a straightforward condensation reaction using pyrrolidine in MeOH as described by Stone and Little (Figure 18).[37]

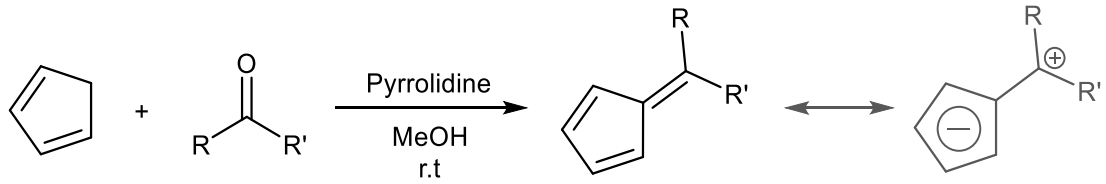

Figure 18: Synthesis of fulvenes from cyclopentadiene and carbonyl compounds and their resonance structure

6-substituted fulvenes are stable enough to be isolated, however, with their exocyclic double bond being polarised to enable nucleophilic attack by a range of nucleophiles (Figure 18).[27] Coskun *et al.*

have demonstrated the utility of this reactivity for **PnH_2** synthesis (Figure 19).[38] Reaction of **CpH** with a range of different aldehydes afforded 6-substituted fulvenes that cleanly condensed with acetone (also used as the solvent for this transformation) at room temperature in the presence of pyrrolidine to give variously substituted **1,3-RMe-PnH_2** in good yields. The air-stable products were obtained after evaporation of solvent and side products (mainly from cross-condensation of acetone) followed by flash chromatography on silica, which was found not to induce any double bond isomerisation.

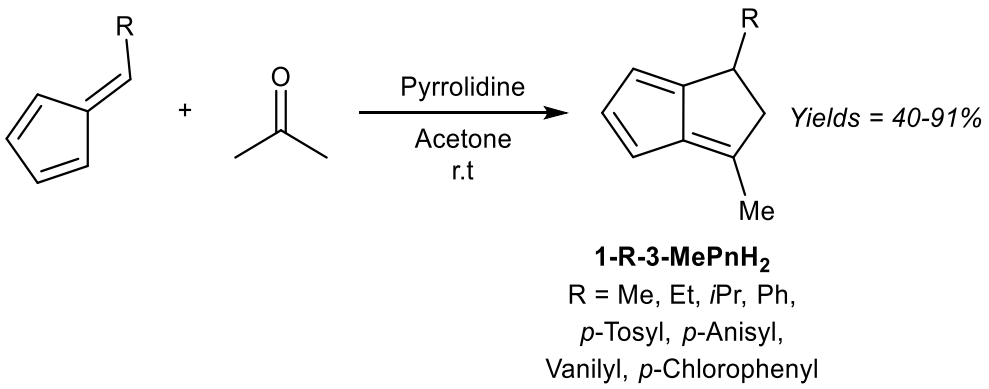

Figure 19: Synthesis of 1,3-disubstituted dihydropentalenes from 6-substituted fulvenes and acetone

Again, none of the **PnH_2** synthesised have been deprotonated to the corresponding **Pn^{2-}** in this or other studies. Coskun *et al.* only describe the reactivity of 6-methyl fulvene, but it could be supposed that fulvenes derived from substituted **CpH** and various aldehydes could be reacted in an analogous manner to give a variety of more highly substituted **PnH_2** as outlined in Figure 16. However, like the concerted double-condensation reaction using chalcones described above, the parent (unsubstituted) **PnH_2** is not likely to be accessible via this stepwise condensation method either due to the instability of its hypothetical reaction partners (unsubstituted fulvene and acetaldehyde).

1.2.7 Acetylene oligomerisation

Akin to alkyne trimerization to give variously substituted 6π aromatics (Reppe chemistry),[39] there are also some reports of alkyne oligomerisation reactions that produce pentalene scaffolds. Kuwabara *et al*.[40] and Saito *et al*.[41] reported the synthesis of bis-silylated dibenzopentalenide through reduction of phenylacetylenes with alkali metals (Figure 20). When phenyl(tris^{i}propylsilyl)acetylene was reacted with metallic lithium in Et_2O only a small amount of **$Li_2[Bn_2Pn]$** was obtained. The major product of this reaction, a 1,4-dilithio-1,3-butadiene, could be reacted with $Ba(HMDS)_2$ to give **$Ba[Bn_2Pn]$**, the hydrolysis of which yielded the silyl-substituted **Bn_2PnH_2**.[42] Reduction of phenyl(tris^{i}propylsilyl)acetylene with metallic potassium directly gave **$K_2[Bn_2Pn]$** in high yields, with other silyl-substituted phenylacetylenes reacting in the same manner (Figure 20).

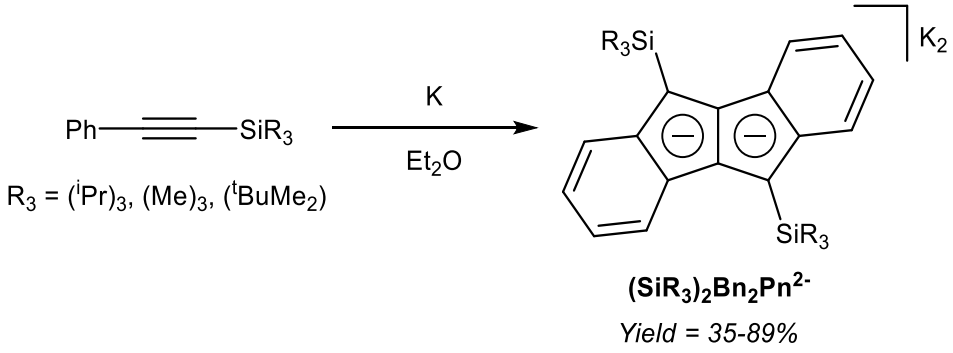

Figure 20: Formation of dibenzopentalenides by reaction of phenylsilylacetylenes with potassium

In another example, Bailey *et al*.[43] described the $PdCl_2$ catalysed cyclotetramerisation of phenylacetylene to **Ph_4PnH_2** (Figure 21). However, of the two isomeric products obtained from this reaction only one would be suitable for deprotonation into a **Ph_4Pn^{2-}**, and the report does not include methods of preparative work up and isolation.

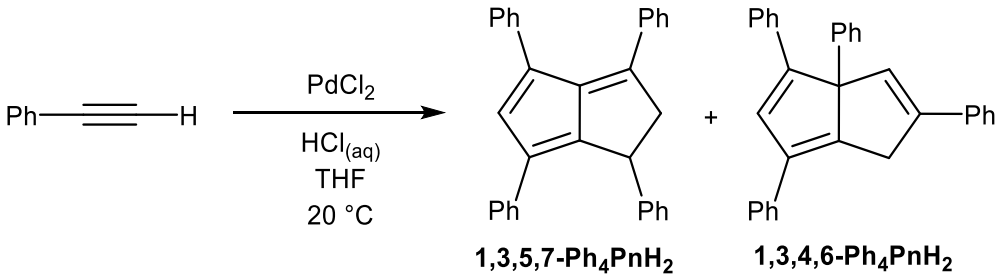

Figure 21: Palladium-mediated cyclotetramerization of phenylacetylene to tetraphenyldihydropentalenes

Although interesting examples of an alternative, potentially elegant synthetic approach of accessing **PnH_2** from simple alkyne starting materials, the generality and versatility of these methods remain to be explored more systematically.

1.2.8 Functionalisation of pentalenides

Although most solution-phase syntheses of **PnH_2** are easier for more highly substituted starting materials, the opposite is true for pyrolytic pathways. Post-synthetic functionalisation of the parent (unsubstituted) **PnH_2** obtained from e.g. FVP is also possible to some degree. Cloke *et al.* for instance demonstrated the functionalisation of **Li_2Pn** with of trialkylsilyl-groups (Figure 22), which in addition to modifying their electronic and steric parameters imparts the complexes with enhanced solubility in hydrocarbon solvents.[18]

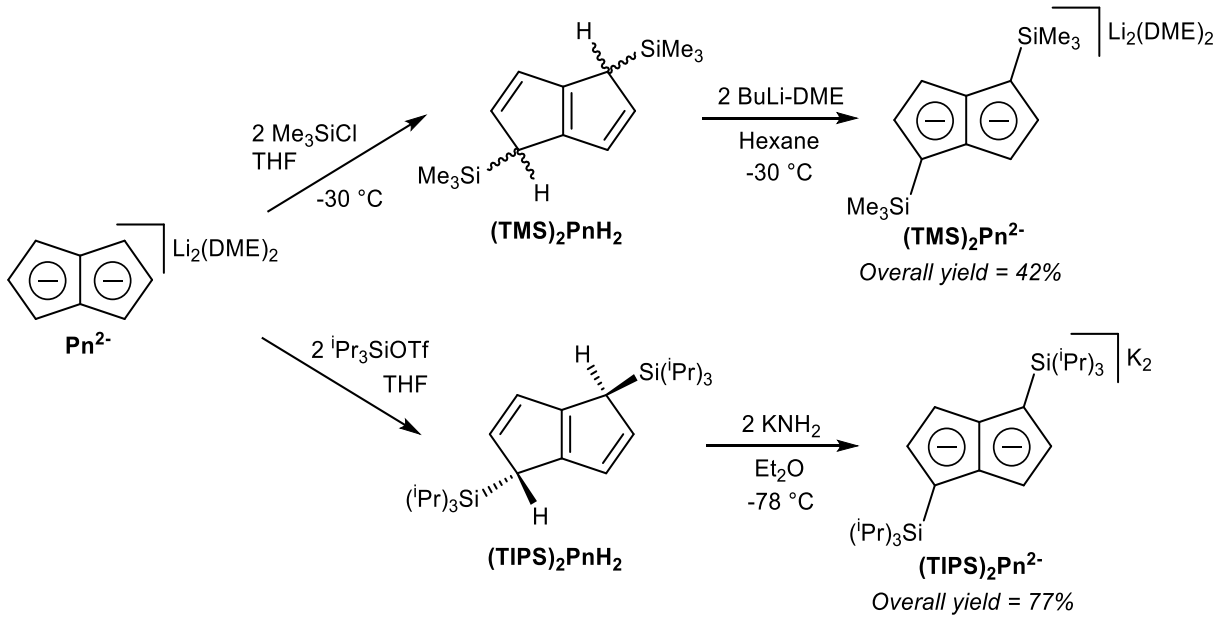

Figure 22: Reaction of dilithium pentalenide with silyl-electrophiles, and deprotonation of the resulting disilyl-dihydropentalenes

$[Li(DME)]_2Pn$ was shown to react regio-selectively with two equivalents of TMS-Cl in THF to give **1,4-TMS_2PnH_2** as a mixture of *syn* and *anti*-isomers. These could be doubly deprotonated again with

^{n}butyllithium in DME/pentane to give the corresponding **[Li(DME)]$_2$[1,4-TMS$_2$Pn]** for subsequent transmetalation reactions. When introduction of additional substituents was attempted at this stage, by further reaction of **1,4-TMS$_2$Pn^{2-}** with another two equivalents of TMS-Cl, **1,1,4,4-TMS$_4$PnH$_2$** was obtained exclusively. Due to the two bis-silylated sp^3 carbons in the 1 and 4 positions this compound cannot be converted into a **Pn^{2-}** by way of deprotonation anymore, limiting how much functionality may be introduced through this strategy. **[Li(DME)]$_2$Pn** failed to react analogously with tris(^{i}propyl)silyl chloride, but did react with the more activated tris(^{i}propyl)silyl triflate to give the corresponding **1,4-TIPS$_2$PnH$_2$**, forming the *anti*-isomer only, presumably due to steric reasons in this case. Reacting this compound with KNH_2 in Et_2O gave high yields of **K$_2$[1,4-TIPS$_2$Pn]**, a useful ligand for use in f-block chemistry where lithium salts tend to form 'ate' complexes (Section 1.3.3).[18]

The regioselectivity of the reaction of **Pn^{2-}** with hard electrophiles is a consequence of its charge distribution. In addition to the fully delocalised (aromatic) η^8 form and the partially delocalised (allylic) η^3 form that govern reactivity with soft Lewis acids, its ground state η^1 resonance structure conjugates both charges to the 1 and 4 positions (Figure 23). Thus, post-synthetic functionalisation of **Pn^{2-}** is limited to these two positions.

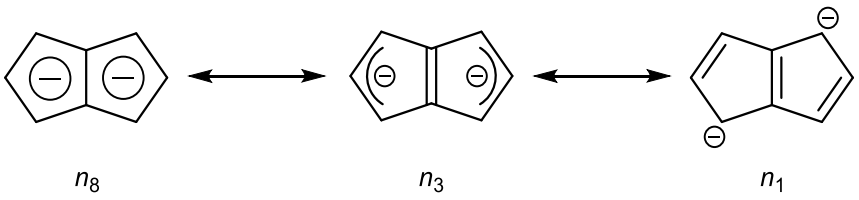

Figure 23: Resonance structures of the pentalenide dianion

1.3 Synthesis of pentalenide complexes of p-, d- and f-block metals

As mentioned in section 1.1 (Figures 4 and 5), deprotonative metalation of **PnH_2** with suitably strong bases gives straightforward access to stable **PnH^-** and **Pn^{2-}** salts that can be used for transmetalation on to p-, d-, and f-block metals in the desired oxidation state. Before we review selected cases of these in Sections 1.3.2 and 1.3.3, there are also some examples of direct metalation reactions of neutral precursors via redox reactions (as in related **CpH** chemistry) that deserve mentioning. At present these appear less generally applicable than transmetalation from **MPnH** and **M_2Pn** salts but serve to illustrate the rich coordination chemistry of pentalenide ligands.

1.3.1 Pentalenide and hydropentalenide complexes by direct metalation of neutral precursors

An early example of a direct redox metalation of **Pn** with a transition metal has been provided Hafner and Weidemüller,[44] who reported that the reaction of **Pn_2** with an iron(0) precursor produced a small amount of **$Fe_2(CO)_5Pn$** (Figure 24). According to the contemporary ionic electron counting model, and in line with the thermodynamic driving force of forming a 10π aromatic, this reaction implies a double reduction of **Pn** to **Pn^{2-}** accompanied by cleavage of the dimer and oxidation of two Fe^0 centres to Fe^I.

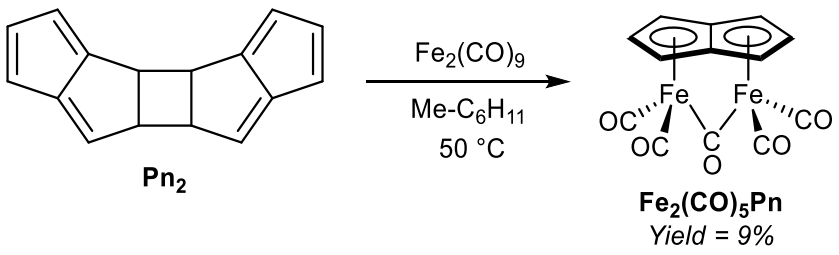

Figure 24: Reaction of pentalene dimer with diiron nonacarbonyl

Heating **Pn_2** to 50 °C in methylcyclohexane in the presence of $Fe_2(CO)_9$ resulted in the formation of a yellow crystalline solid, supposed to be the *syn*-diiron pentalenide complex shown based on its NMR spectroscopic and mass spectrometric signatures. However, no XRD analysis is available to confirm the geometry, and work up details were not provided in the original paper. A mixture of isomers of

[1,3-Me$_2$Pn]$_2$ was reacted in a similar fashion to give an unidentified green diiron complex in 21 % reported yield.[44]

In related examples of directly metalating **PnH$_2$** precursors, Hunt and Russel[45] reported that reacting **3-Me$_2$N-PnH$_2$** or **3-Ph-PnH$_2$** with $Fe(CO)_5$ would produce analogous *syn*-bimetallic **Fe$_2$(CO)$_5$Pn** complexes in similar yields (Figure 25). However, none of the geometries have been confirmed by XRD either.

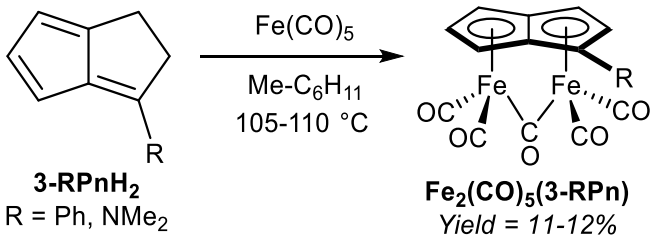

Figure 25: Reaction of mono-substituted dihydropentalenes with iron pentacarbonyl

Similar to the direct metalation reactions of **CpH** with zero-valent metal precursors to give **M(I)Cp** complexes, this conversion of a **PnH$_2$** into a bimetallic **Pn^{2-}** complex implies a double deprotonation and proton reduction to H_2 to give two Fe^{I} centres in the resulting complex.

Another redox metalation of a **Pn** has been reported by Ashley *et al.*[46] Refluxing **Pn*** (Figure 11) with an excess of $Fe_2(CO)_9$ in toluene (added in portions) furnished a brown solid upon filtration and washing. Recrystallisation from toluene/hexane produced the η^5-**Fe$_2$(CO)$_5$Pn*** complex shown in Figure 26 in good yields. In this case the *syn* geometry of the two metal centres has been established by XRD analysis. The same procedure could be applied to synthesise a related dicobalt complex using a stoichiometric amount of $Co_2(CO)_8$ (Figure 26). Notably, both compounds could be synthesised on a multigram scale.

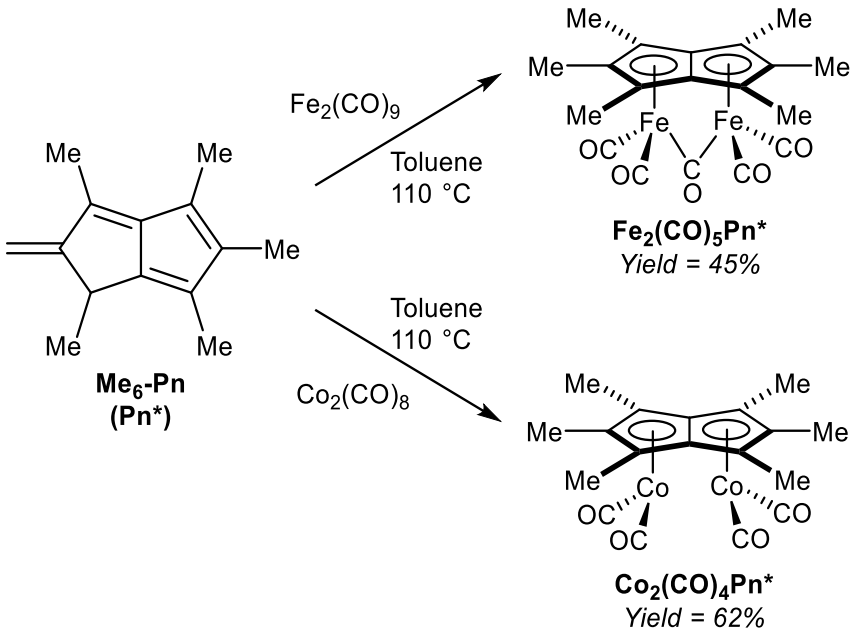

Figure 26: Reaction of hexamethylpentalene with diiron nonacarbonyl and dicobalt octacarbonyl

Both reactions involve a formal double reduction of the **Pn*** scaffold by the metal(0) precursors, accompanied by a two-bond hydrogen shift to the exocyclic methylene group. The similar reactivity but increased stability and enhanced crystallinity of these **Pn*$^{2-}$** complexes compared to the parent **Pn^{2-}** compounds are promising and provide motivation for further exploration of other substitution patterns in organometallic **Pn^{2-}** chemistry.

Redox metallations of **COT** accompanied by skeletal rearrangement to **Pn^{2-}** are also known for some d-block metal complexes. Brookes *et al*.[47] reported the reaction of *cis*-**[Ru(CO)$_4$(GeMe$_3$)$_2$]** with **COT** in refluxing heptane or octane (Figure 27). Of the several compounds produced from this reaction, a small amount of the pale yellow *syn* bimetallic **Ru$_2$Pn** complex shown in Figure 27 could be isolated and analysed by XRD.

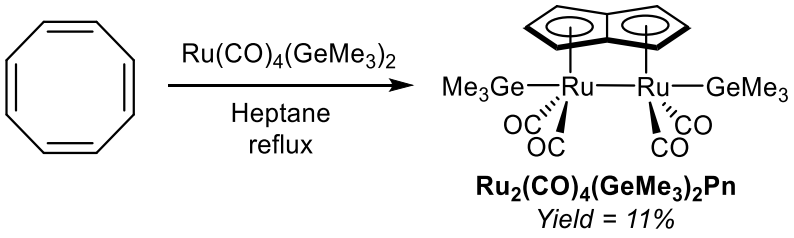

Figure 27: Rearrangement redox reaction of cyclooctatetraene with $Ru(CO)_4(GeMe_3)_2$

Similarly, Howard *et al*.[48] reported that **COT** would react with $Ru_3(CO)_{10}$ in refluxing heptane to give a trinuclear **RuPn** complex, albeit in low yields and in a mixture with various other **RuCOT** complexes. Silyl-substituted **COT** have been reported to react in an analogous manner, giving the correspondingly substituted trinuclear **RuPn** complexes.[49] All of these reactions were very low yielding and no work up procedures are available, so the synthetic utility of these transformations appears limited.

Akin to the alkali metal induced and palladium catalysed alkyne oligomerisation reactions that produce substituted **PnH_2**s (Section 1.1.7), the direct formation of **PnH^-** complexes from cyclotetramerization of acetylenes has also been reported. For example, Coffield *et al*.[50] showed that heating $Mn_2(CO)_{10}$ in THF under a pressure of acetylene resulted in the formation of η^5-**$Mn(CO)_3$[PnH]** as a viscous yellow oil that was purified by distillation (Figure 28). The same transformation could also be accomplished using $MeMn(CO)_5$ but with lower yields of 27%. Further deprotonation of the bound **PnH^-** was not attempted.

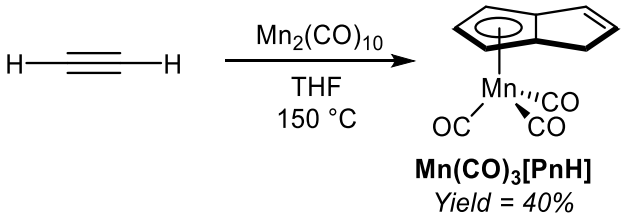

Figure 28: Reaction of acetylene with dimanganese decacarbonyl

Komatsu *et al.* reported the formation of η^5-**RPnH** complexes through Rh^I mediated tetramerisation of bulky mono-substituted alkynes (Figure 29). The reaction of *tert*-butylacetylene with $[Rh(COD)Cl]_2$

and NEt_3 in cyclohexane furnished η^5-**Rh(COD)[^{t}Bu$_4$PnH]** in 13 % yield after purification by chromatography on alumina followed by recrystallization from EtOH.[51]

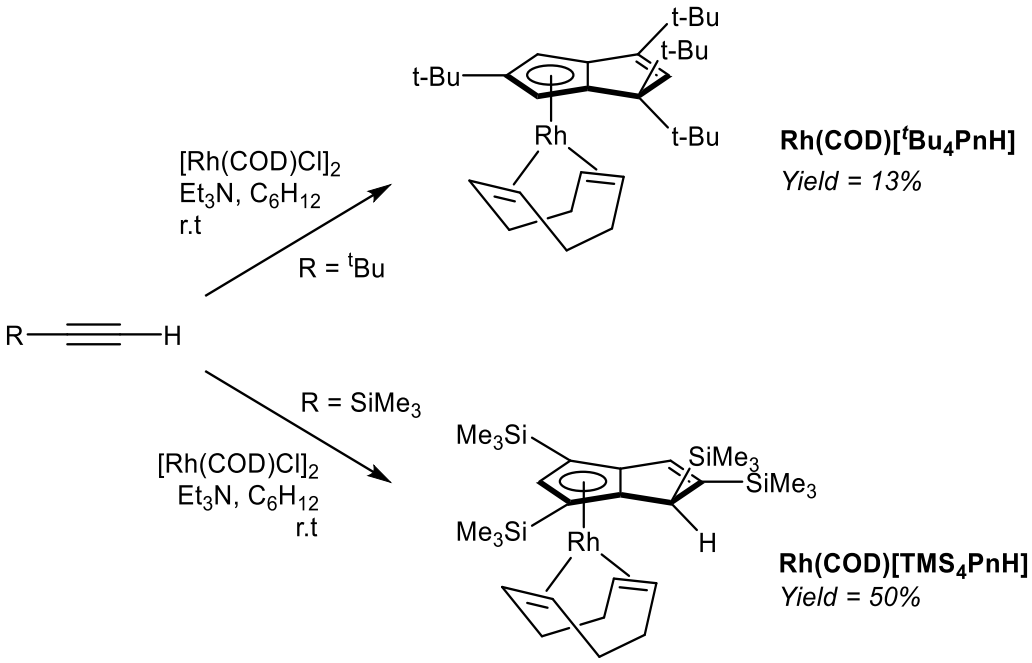

Figure 29: Reaction of substituted acetylenes with $[Rh(COD)Cl]_2$

The analogous reaction of TMS-acetylene with $[Rh(COD)Cl]_2$ gave the corresponding η^5-**Rh(COD)[TMS$_4$PnH]** complex in 50 % isolated yield. Interestingly, whereas tetramerization of ^{t}butylacetylene produced **1,1,3,5-R$_4$PnH$^-$**, TMS-acetylene yielded the **1,2,4,6-R$_4$PnH$^-$** regio-isomer. While not possible with the former, the latter could in principle allow for a second deprotonation to a **1,2,4,6-R$_4$Pn^{2-}**. However, this has not been reported yet.

1.3.2 Hydropentalenide complexes through transmetalation of hydropentalenides

As shown in Figure 3 and section 1.2.1 and illustrated in some of the examples in section 1.2.4, the monoanionic, 6π aromatic **PnH$^-$** synthon may be obtained from either hydride addition to a stable **Pn** or mono-deprotonation of **PnH$_2$**. Katz and Rosenberger provided an early demonstration of its utility as a transmetalation agent: *in situ* generation from **PnH$_2$** with 1.1 equivalents of ^{n}butyllithium in THF/hexane followed by addition of iron(II) precursors yielded the ferrocene analogue η^5 **Fe[PnH]$_2$** as

a mixture of two isomers (Figure 30).[52] The stable compound was obtained in 54 % yield after aqueous work up followed by sublimation and recrystallisation from hexane.

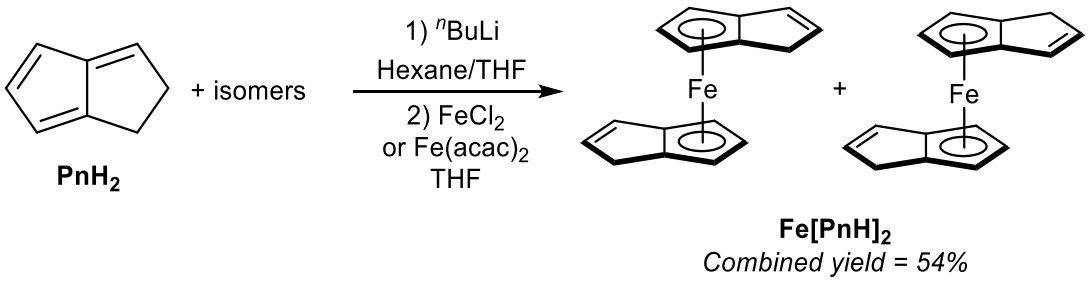

Figure 30: Synthesis of di(hydropentalenide)iron from dihydropentalene

TlCp is known to be a useful transmetalation agent in instances where alkali metal **Cp**$^-$ salts are too reducing.[53] In the same manner, **TlPnH** (Figure 4) has been shown to act as an efficient, mild transmetalating agent with d-block metal precursors: reaction with $FeCl_2$ in THF was shown to give the ferrocene derivatives shown in Figure 30 in 47% isolated yield.[8] Similarly, reaction of **TlPnH** with $[Rh(COD)Cl]_2$ in THF smoothly yielded η^5 **(COD)Rh[PnH]** (Figure 31).[8] The TlCl by-product was easily removed by filtration, and sublimation of the product gave the pure Rh^I complex in high yield. The same study also demonstrated the successful reaction of **TlPnH** with Me_3PtI, but the **Me_3Pt[PnH]** complex produced required gas-phase chromatography in order to furnish pure product.

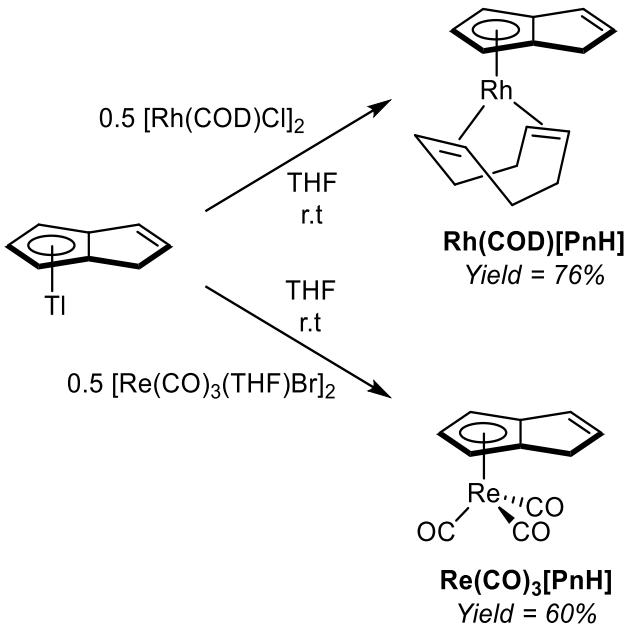

Figure 31: Transmetalation reactions of thallium hydropentalenide

Reaction of **TlPnH** with a suspension of $[Re(CO)_3(THF)Br]_2$ in THF in the absence of light gave η^5 **$(CO)_3$Re[PnH]** as a colourless solid after purification by chromatography on silica (Figure 31).[9] Recrystallisation from Et_2O yielded crystals suitable for XRD analysis. The analogous manganese complex could also be prepared through the reaction of $[Mn(CO)_3(py)_2Br]$ with **TlPnH** in THF to give the same product of the cyclotetramerisation of acetylene with $Mn_2(CO)_{10}$ (Figure 28).[4a] Reacting a mixture of **Tl[MePnH]** isomers with $[Re(CO)_3(THF)Br]_2$ in THF yielded the corresponding η^5 **$(CO)_3$Re[MePnH]** complexes as a mixture of double bond isomers.[9] Although good combined yields were obtained after purification on silica, the isomers (distinguishable by NMR) could not be separated by chromatography or fractional crystallisation.

Direct metalation reactions of **PnH_2** with other heavy p-block metal bases has also been achieved. Ustynyuk *et al.* reported the synthesis of mono- and bis-Me_3Sn derivatives of **PnH_2** using tin amides.[54] The reaction of **PnH_2** with one equivalent of $Me_3Sn(NEt_2)$ in boiling hexane produced, after distillation, a mixture of **1-** and **2-**η^1**-(Me_3Sn)PnH** (Figure 32). Higher yields were obtained by stirring the reagents in heptane at room temperature for 48 hours. According to Figure 23, the 1-isomer would be the primary reaction product from formal addition of a Me_3Sn^+ moiety to the **PnH^-** intermediate, and NMR

analysis indeed showed rapid suprafacial 1-2-3 shifts of the $Sn(Me)_3$ group within **$(Me_3Sn)PnH$** (as also observed in related η^1- $Sn(Me)_3$ **Cp** and **Ind** complexes[55]) to be responsible for formation of the 2-isomer.

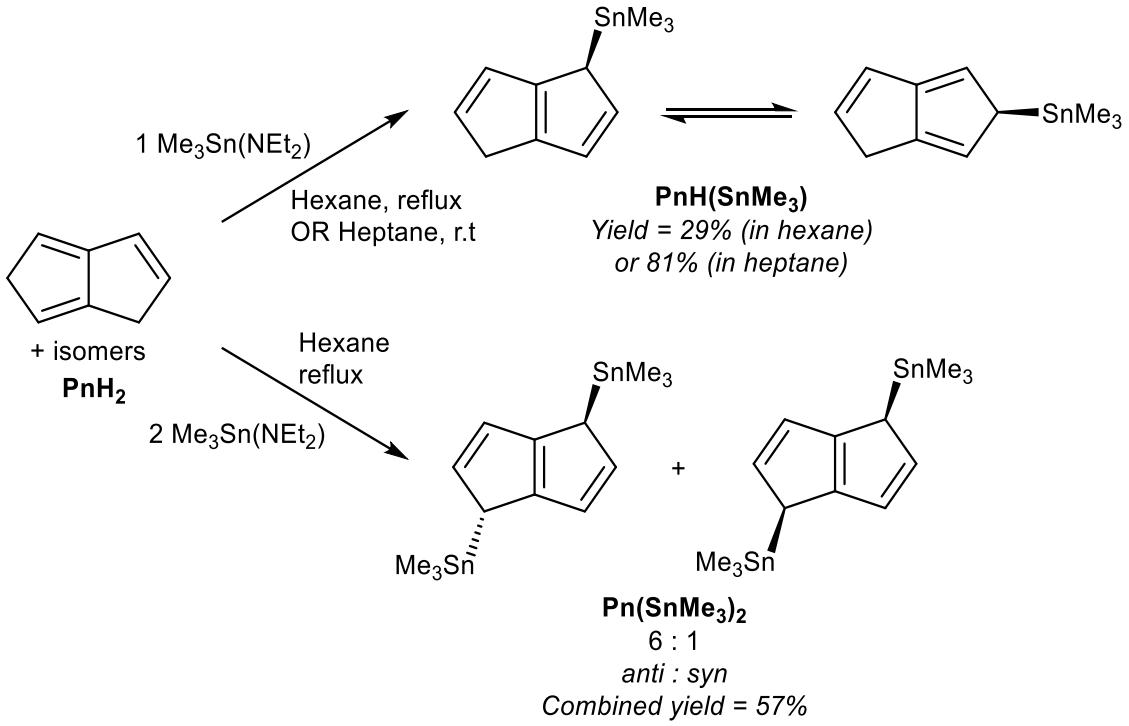

Figure 32: Reactions of dihydropentalene with trimethyltin-diethylamide

The same reaction with two equivalents of $Me_3Sn(NEt_2)$ produced **$1,4\text{-}(Me_3Sn)_2Pn$** in high yield without purification. A 6:1 mixture of *anti-* and *syn-* isomers was obtained which did not interconvert; although VT $^{13}C\{^1H\}$ NMR analysis showed suprafacial Me_3Sn shifts to be possible within each **$(Me_3Sn)_2Pn$** isomer there was no evidence for superfacial migration or intermolecular exchange. A pure sample of the *anti-* isomer could be obtained after separation by fractional distillation and crystallisation from pentane, enabling structural analysis by XRD. The authors also showed how the *anti-* and *syn-* isomers may be distinguished by their ^{119}Sn chemical shift values and assigned via characteristic ^{119}Sn-^{117}Sn coupling constants within a mixture in solution.

Similar to the η^5 thallium reagents, η^1 stannylated **Pn** act as mild transmetalation agents in cases where alkali metal **Pn^{2-}** salts are too reducing (see below). This reactivity is not seen with the structurally

related but non-fluxional η^1 silylated **Pn** derivatives discussed in Section 1.2.8 due to the strength of the covalent Si-C bond, preventing the trisalkylsily substituent from acting as a leaving group.

Turner *et al.* demonstrated the use of mono-stannylated **Pn*H**$^-$ as a ligand transfer agent for synthesising hydropentalenyl complexes of group 4 metals (Figure 33).[56] The reaction of **LiPn*H** with $SnMe_3Cl$ in pentane gave η^1 **(Me_3Sn)Pn*H** as a 1:1 mixture of *syn* and *anti* isomers in near quantitative yields after purification by filtration.

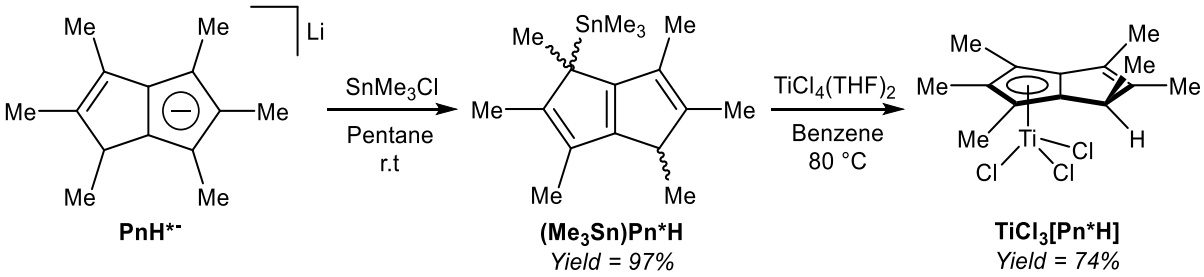

*Figure 33: Synthesis of a stannylated-derivative of Pn*H$^-$ and its reaction with a titanium(IV) precursor*

Reacting **(Me_3Sn)Pn*H** with $TiCl_4(THF)_2$ in refluxing benzene gave a single isomer of η^5 **$TiCl_3$[Pn*H]** in high yields, and single crystals for XRD analysis could be grown from diethyl ether. Chlorine-bridged, mono-nuclear zirconium and hafnium **Pn*H** dimer complexes could also be prepared from **(Me_3Sn)Pn*H**.[56] Although deprotonation of the bound **Pn*H** ligand in the Ti complex was not attempted, the reverse reaction (mono-protonation of a titanium **Pn*$^{2-}$** complex) was later reported by the same group (see Figure 40).

1.3.3 Pentalenide complexes through transmetalation of pentalenides

Due to their stability and ease of preparation, alkali metal **Pn^{2-}** salts are the most prevalent reagents for synthesising organometallic pentalenide complexes. Again similar to **MCp** chemistry, Jonas *et al.* reported that **[Li_2(DME)$_x$]Pn** would react cleanly with **Cp_2**VCl by substitution of one **Cp**$^-$ ligand and chloride.[57] The resulting [η^5-**Cp**]**V**[η^8-**Pn**] complex (Figure 34) is air sensitive but could be sublimed under vacuum to give pure product in high yields. [η^5-**Cp***]**V**[η^8-**Pn**] and [η^5-**Ind**]**V**[η^8-**Pn**] could be

prepared in the same manner, and recrystallisation from hexane at low temperatures gave samples suitable for XRD analysis.

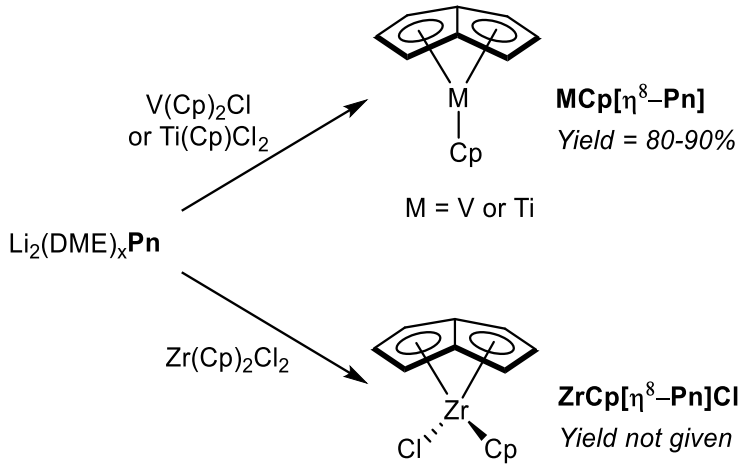

Figure 34: Transmetalation reactions of dilithium pentalenide with early d-block metals

The reaction of **Cp**$TiCl_2$ with **[Li_2(DME)$_x$]Pn** yielded **Ti[*η*^{5}-Cp][*η*-^{8}Pn]** in high yield, and the analogous reaction of **Cp**$_2ZrCl_2$ gave **Zr**[*η*^{5}-**Cp**][*η*^{8}-**Pn**]**Cl** (Figure 34).[58] However, details of solvents for these transformations is missing from these reports.

Jones *et al.* managed to access several new bimetallic group 7 carbonyl **Pn^{2-}** complexes by way of transmetalation.[59] The reaction of **[Li_2(DME)$_x$]Pn** with 2 equivalents of [$Mn(CO)_3(py)_2Br$] in THF gave exclusively the *anti*- isomer of *η*^{5}-**Mn_2(CO)$_6$Pn** (Figure 35), which after extraction and filtration in air was purified by chromatography on silica. When the analogous reaction was performed with one equivalent of [$Re(CO)_3(THF)Br]_2$, a mixture of *syn*- and *anti* *η*^{5}-**Re_2(CO)$_6$Pn** was obtained, with the ratio being dependent on the reaction temperature. The two isomers could be separated through fractional crystallisation.

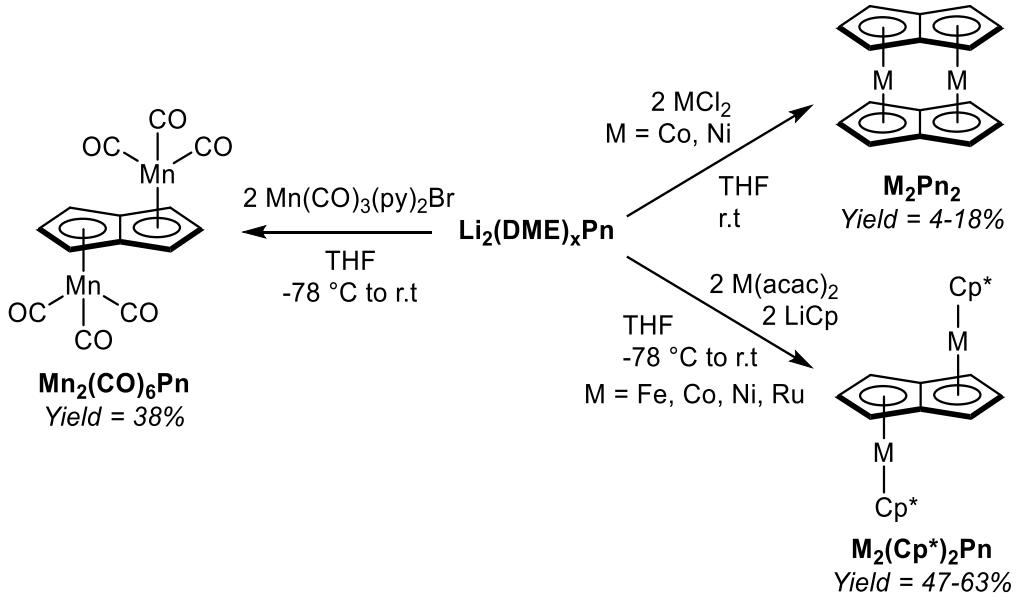

Figure 35: Transmetalation reactions of dilithium pentalenide with late d-block metals

Katz *et al.* showed that dinuclear $\mathbf{Pn^{2-}}$ sandwich complexes of cobalt and nickel could be synthesised by reacting their respective dihalide salts with $\mathbf{[Li_2(DME)_x]Pn}$ in THF (Figure 35).[60] Both compounds were obtained in low yields after purification by sublimation. The analogous reaction with $FeCl_2$ however did not produce the analogous dinuclear sandwich complex ("double ferrocene"),[60b] but a mononuclear sandwich complex with two bridging $\mathbf{PnH^-}$ ligands instead.[61] Binding *et al.* were later able to synthesise the dinuclear sandwich complex $\mathbf{[FePn^*]_2}$ by reacting $\mathbf{[Li_2(TMEDA)_x]Pn^*}$ with $Fe(acac)_2$ in THF at room temperature,[62] providing yet another example of the utility of more highly substituted pentalenide scaffolds.

Manriquez *et al.* showed that Cp*Fe(acac), generated *in situ* from LiCp* and $Fe(acac)_2$ in THF, would react smoothly with $\mathbf{[Li_2(DME)_x]Pn}$ to produce *anti* η^5**[Cp*Fe]**η^8**Pn** (Figure 35).[63] The complex was obtained in high yields after recrystallization from toluene; analogous cobalt, nickel and ruthenium complexes could be prepared in the same manner.

Exploring $\mathbf{Pn^{2-}}$ complexes of f-block metals, Cloke *at al.* successfully synthesised thorium and uranium complexes of $\mathbf{1,4\text{-}(TIPS)_2Pn^{2-}}$ by way of transmetallation.[64] The reaction of $ThCl_4$ and $\mathbf{K_2[1,4\text{-}(TIPS)_2Pn]}$ suspended in THF yielded a bright orange solid containing a mixture of staggered and eclipsed isomers

of η^8 **[1,4-(TIPS)$_2$Pn]$_2$Th** (Figure 36). The product could be purified by sublimation, and crystals for XRD analysis were grown from pentane. The same reaction with UCl_4 produced a dark green product as the analogous isomeric mixture of η^8 **[1,4-(TIPS)$_2$Pn]$_2$U** again in high yields.

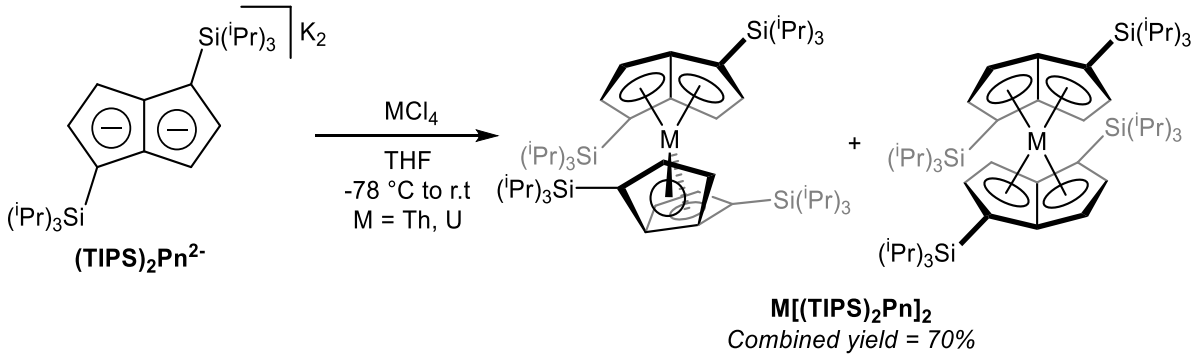

Figure 36: Transmetalation of dipotassium bis(trimethylsilyl) pentalenide with f-block metal halides

Balazs *et al.* synthesised the anionic cerium(III) sandwich complex **K[Ce(1,4-TIPS$_2$Pn)$_2$]** by reacting **K$_2$[1,4-TIPS$_2$Pn]** with $CeCl_3$ in THF at room temperature.[65] This sand-coloured species was purified by filtration and washing with pentane, and characterised crystallographically by complexing the potassium ion with 18-crown-6 and recrystallising the resulting solid from toluene. The oxidation of **K[Ce(1,4-TIPS$_2$Pn)$_2$]** was shown using a slurry of $AgBPh_4$ in THF, and the resulting cerium(IV) sandwich complex **[Ce(1,4-TIPS$_2$Pn)$_2$]** was purified by extraction with pentane and crystallisation. Ashley *et al.* showed the analogous synthesis of **CePn*$_2$** by reacting **[Li$_2$(TMEDA)$_x$]Pn*** and $CeCl_3$ in THF at room temperature, followed by oxidation of the intermediate **Li[CePn*$_2$]** using an excess of dichloroethane.[66]

In another example of a substituted **Pn^{2-}** transmetallation reaction, Cooper *et al.* described the reactivity of **Pn*$^{2-}$** with group 4 metal halides.[67] $ZrCl_4$ and $HfCl_4$ mixed with **[Li$_2$(TMEDA)$_x$]Pn*** in benzene gave, after filtration and recrystallization, halide-bridged dinuclear η^8 complexes of zirconium and hafnium as LiCl adducts (Figure 37). Attempts to remove coordinated THF via high vacuum led to decomposition.

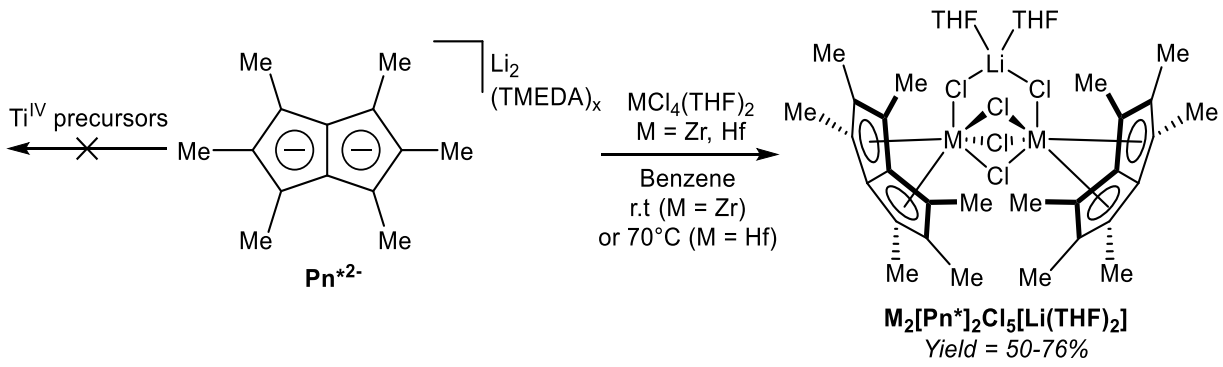

Figure 37: Reactions of dilithium hexamethylpentalenide with group IV metal halides

When the analogous reaction was performed with titanium(IV) precursors, no titanium complex could be obtained but ligand degradation was observed instead. Reaction of **[Li_2(TMEDA)$_x$]Pn*** with $TiCl_3$ and subsequent oxidation with $PbCl_2$ did give a dinuclear Ti^{IV} complex, however, only in 8 % yield.

In order to access **Ti^{IV}_2Pn*** complexes, less reducing transmetalation agents were required. **[Li_2(TMEDA)$_x$]Pn*** was thus reacted with two equivalents of Me_3SnCl to give η^1 **(Me_3Sn)$_2$Pn*** derivatives (Figure 38), analogous to those reported for the parent **PnH_2** (section 1.3.2, Figure 32), in an extension to the η^1 **(Me_3Sn)Pn*H** shown in Figure 33.[67]

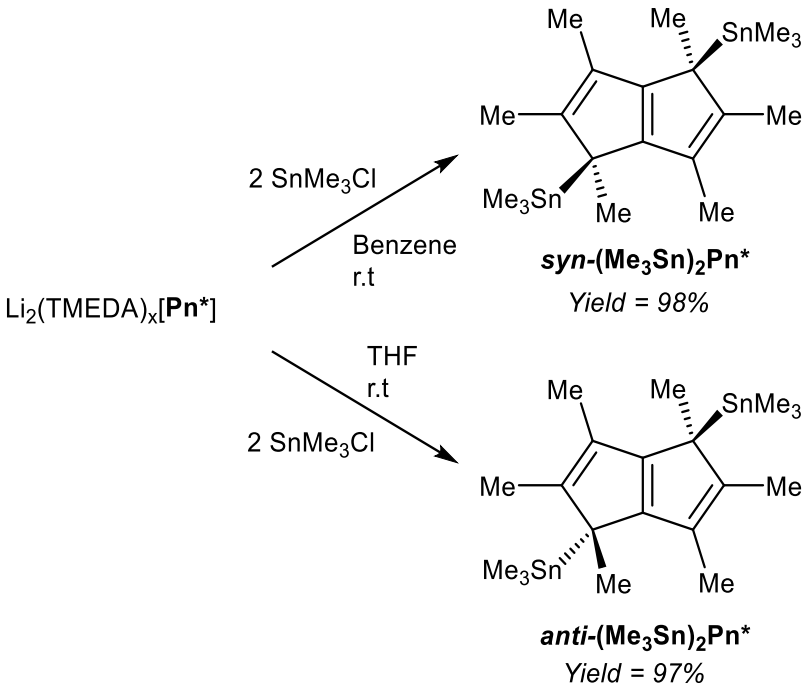

Figure 38: Synthesis of bis-stannylated hexamethylpentalenides

Interestingly, the use of a non-polar solvent such as benzene led to formation of the *syn* product, whereas the use of THF exclusively gave the *anti*-isomer. Both could be isolated in very high yields after filtration and recrystallisation from toluene or pentane. It was proposed that the second lithiation step in the synthesis of **[Li$_2$(TMEDA)$_x$]Pn*** initially precipitated the *syn*-dilithio complex as the kinetic product, which when reacted further in a benzene slurry produced *syn*-Sn(Me)$_3$ derivatives, whereas the use of THF allowed interconversion to the thermodynamic *anti*-dilithio configuration during the dissolution, producing *anti*-Sn(Me)$_3$ derivatives. This represents an interesting opportunity to steer the face selectivity of **M$_2$Pn** reagents in transmetalation reactions in general, but remains to be explored for other pentalenide reagents than **[Li$_2$(TMEDA)$_x$]Pn***.

In terms of transmetalation ability, reaction of *syn* η^1 **(Me$_3$Sn)$_2$Pn*** with $TiCl_4$ in toluene indeed smoothly produced η^8 **[TiCl$_2$Pn*]$_2$** in high yields after recrystallization (Figure 39).[67] The analogous reactions with $ZrCl_4$ and $HfCl_4$ failed to produce the desired complexes, suggesting the presence of LiCl is required to stabilise the Zr/Hf **Pn*** complexes shown in Figure 37.

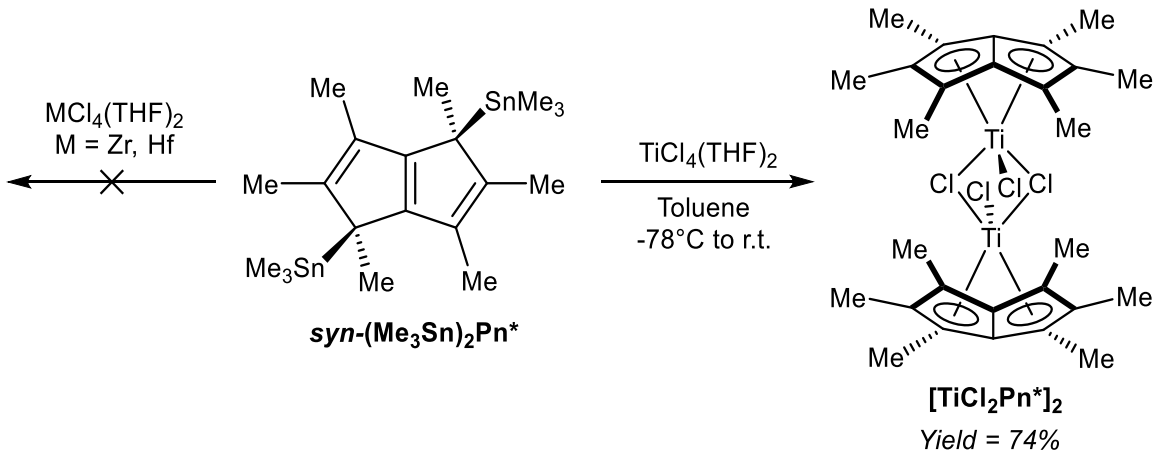

Figure 39: Reactions of bis(trimethylstannyl)-hexamethylpentalenide with group IV metal halides

In a controlled hydrolysis experiment, Clement *et al.* showed that reacting **[TiCl$_2$Pn*]$_2$** with one equivalent of 2,6-xylenol (pK_A ~10) in toluene resulted in clean mono-protonation of the bound **Pn*** ligand and cleavage of the dimer by coordination of the aryloxide (Figure 40), giving a single isomer of the mono-nuclear hydropentalenide complex **Ti(OR)Cl$_2$[Pn*H]** in 68% yield.[68] This transformation

represents an interesting example of accessing a **PnH**$^{-}$ complex via protonation of a **Pn**$^{2-}$ complex, but on its own does not allow commenting on the reversibility of the reaction.

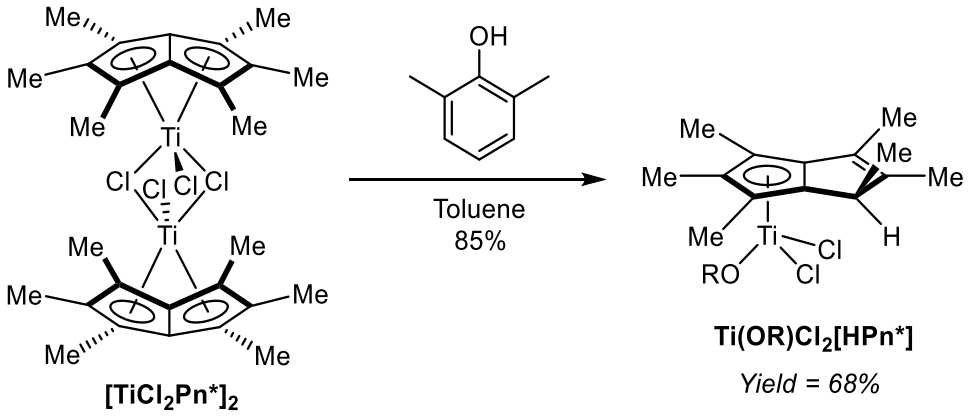

Figure 40: Partial hydrolysis of a titanium(IV) Pn complex with 2,6-xylenol*

In a further demonstration of the usefulness of **(Me$_3$Sn)$_2$Pn*** as a mild transmetalation agent, Chadwick *et al.* successfully synthesised dinuclear **Pn*$^{2-}$** complexes of easily reducible rhodium(I) and iridium(I) precursors.[69] Reactions of $[M(CO)_2Cl]_2$ (M = Rh, Ir) with *syn* η^1 **(Me$_3$Sn)$_2$Pn*** (generated *in situ*) selectively produced the corresponding *syn* η^5 **[(CO)$_2$M]$_2$Pn*** complexes (Figure 41). Both the rhodium and iridium complexes have been analysed by XRD, with suitable crystal samples grown from hexane at low temperatures.

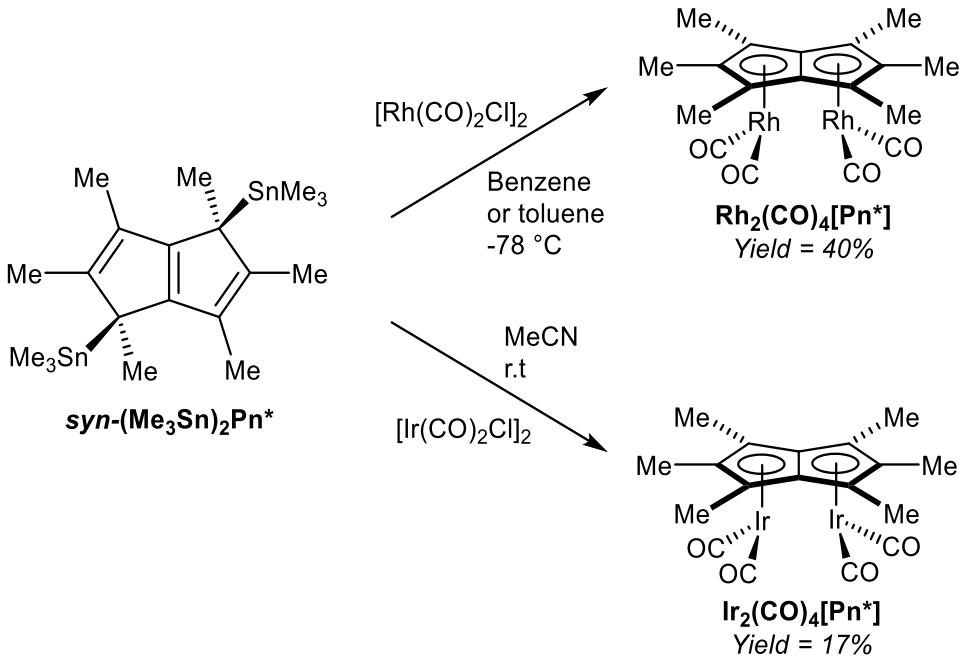

Figure 41: Reactions of bis(trimethylstannyl)-hexamethylpentalenide with group IX metal carbonyl dimers

Whether the observed *syn* selectivity of the transmetalation was a result of using *syn* **(Me$_3$Sn)$_2$Pn*** or due to the dimeric nature of the metal precursor is not clear, however.

1.4 Conclusion

From the selected examples reviewed it is clear that a number of different synthetic routes to pentalenide complexes exist. Unsubstituted **PnH_2** is mostly synthesised by controlled anaerobic pyrolysis of various starting materials, whereas several relatively straightforward solution-phase methods for substituted **PnH_2** exist. It is interesting that not all of these, mostly developed in the realm of organic synthesis, have been put to use in organometallic pentalenide chemistry yet.

Symmetrically substituted **PnH_2** appear most desirable to reduce the number of possible isomers, which may be hard to separate or transform selectively from a mixture. Given that their reactivity is mostly governed by their core π electronic system, it is not unreasonable to expect that most new substituted **PnH_2** would be amenable to the same deprotonation, functionalisation and transmetalation methods developed for the two archetypical synthons, unsubstituted **PnH_2** and permethylated **Pn***. This would allow a wider range of novel **Pn^{2-}** complexes to be synthesised for a more systematic study of **Pn^{2-}** ligand effects on their electronic structure and reactivity. Thallium salts and Me_3Sn derivatives have proven to be mild and effective transmetalation agents in addition to the alkali metal salts, but the development of less toxic alternatives would be desirable for practical reasons.

The prospect of controlling the face selectivity of **Pn^{2-}** double metalation via either kinetically controlled deprotonation or installation of *syn*-configured leaving groups represents an exciting opportunity for selectively synthesising *syn*-dinuclear half-sandwich complexes with interesting properties for binding and activating various ligands across the two metal sites. The stability of mono-deprotonated **PnH^-** and its metal complexes may even allow consecutive installation of different metals to synthesise heterodinuclear compounds in a controlled manner. In general, the flexible and adaptive nature of **Pn^{2-}** to bind a range of different metals together with the ability of bringing two metals together in close proximity with electronic coupling hold great potential for future applications in sensing, electrochemistry, and homogeneous catalysis.

1.5 Bibliography

1. Linder, H. J., Pentalene und Dihydropentalene. In *Houben-Weyl Methods of Organic Chemistry*, 4th ed.; Georg Thieme Verlag: Stuttgart, 1985; Vol. 5: Carbocyclic p-Electron Systems, pp 103-122.

2. Bally, T.; Chai, S.; Neuenschwander, M.; Zhu, Z., Pentalene: Formation, Electronic, and Vibrational Structure. *J Am Chem Soc* **1997,** *119* (8), 1869-1875.

3. Knox, S. A. R.; Stone, F. G. A., Approaches to the synthesis of pentalene via metal complexes. *Accounts of Chemical Research* **1974,** *7* (10), 321-328.

4. (a) Summerscales, O. T.; Cloke, F. G. N., The organometallic chemistry of pentalene. *Coordin Chem Rev* **2006,** *250* (9-10), 1122-1140; (b) Cloke, F. G. N.; Green, J. C.; Kilpatrick, A. F. R.; O'Hare, D., Bonding in pentalene complexes and their recent applications. *Coordin Chem Rev* **2017,** *344*, 238-262.

5. Crabtree, R. H., The Organometallic Chemistry of the Transition Metals, 6th Edition. *The Organometallic Chemistry of the Transition Metals, 6th Edition* **2014**, 1-504.

6. Hartwig, J. F., *Organotransition Metal Chemistry : From Bonding To Catalysis*. University Science Books: Sausalito, California, 2010; 1127.

7. Pauli, A.; Kolshorn, H.; Meier, H., Isomerisierung der Dihydropentalene und Umsetzung mit Tetracyanethylen. *Chem Ber* **1987,** *120* (10), 1611-1616.

8. Katz, T. J.; Mrowca, J. J., The Pentalenylcycloocta-1,5-dienerhodium Anion and Hydropentalenyl Complexes of Thallium, Platinum, and Rhodium. *J Am Chem Soc* **1967,** *89* (5), 1105-1111.

9. Jones, S. C.; Roussel, P.; Hascall, T.; O'Hare, D., Convenient solution route to alkylated pentalene ligands: New metal monoalkylpentalenyl complexes. *Organometallics* **2006,** *25* (1), 221-229.

10. Bandura, A. V.; Lvov, S. N., The ionization constant of water over wide ranges of temperature and density. *J Phys Chem Ref Data* **2006,** *35* (1), 15-30.

11. Katz, T. J.; Rosenberg, M., Pentalenyl Dianion. *J Am Chem Soc* **1962,** *84* (5), 865-&.

12. Stezowski, J. J.; Hoier, H.; Wilhelm, D.; Clark, T.; Schleyer, P. V., The Structure of an Aromatic 10-Pi Electron Dianion - Dilithium Pentalenide. *J Chem Soc Chem Comm* **1985,** (18), 1263-1264.

13. Barroso, J.; Mondal, S.; Cabellos, J. L.; Osorio, E.; Pan, S.; Merino, G., Structure and Bonding of Alkali-Metal Pentalenides. *Organometallics* **2017,** *36* (2), 310-317.

14. Katz, T. J.; Ohara, R. K.; Rosenberg, M., Pentalenyl Dianion. *J Am Chem Soc* **1964,** *86* (2), 249

15. Alder, K.; Flock, F. H.; Janssen, P., Uber Das Iso-Dicyclopentadien Und Das Dehydro-Iso-Dicyclopentadien. *Chem Ber-Recl* **1956,** *89* (12), 2689-2697.

16. Kazennova, N. B.; Shestakova, A. K.; Chertkov, V. A.; Ustynyuk, N. A.; Ustynyuk, Y. A., Convenient Preparation Method for the 1,5-Dihydropentalene Synthesis. *Zh Org Khim,* **1986,** *22* (10), 2108-2111.

17. Jones, M.; Schwab, L. O., Cyclooctatetraene-Dihydropentalene Rearrangement. *J Am Chem Soc* **1968,** *90* (23), 6549-&.

18. Cloke, F. G. N.; Kuchta, M. C.; Harker, R. M.; Hitchcock, P. B.; Parry, J. S., Trialkylsilyl-substituted pentalene ligands. *Organometallics* **2000,** *19* (26), 5795-5798.

19. Griesbeck, A. G., Efficient Preparation of 1,5-Dihydropentalene and 2-Methyl-1,5-Dihydropentalene from Acrolein and Methacrolein. *Synthesis-Stuttgart* **1990,** (2), 144-147.

20. Stapersma, J.; Rood, I. D. C.; Klumpp, G. W., Mechanism of the Thermal-Conversion of Tetracyclo[3.3.0.0-2,4.0-3,6]Oct-7-Ene into Dihydropentalenes. *Tetrahedron* **1982,** *38* (14), 2201-2211.

21. Stapersma, J.; Rood, I. D. C.; Klumpp, G. W., Synthesis of Tetracyclo[3.3.0.02,4.03,6]Oct-7-Ene and Some of Its Derivatives. *Tetrahedron* **1982,** *38* (1), 191-199.

22. Gajewski, J. J.; Cavender, C. J., Facile Thermal Cyclization of 6-Vinylfulvene to Dihydropentalene. *Tetrahedron Lett* **1971,** (16), 1057.

23. Neuenschwander, M.; Schaltegger, H.; Meuche, D., 6-Vinylfulven. *Helv Chim Acta* **1963,** *46* (5), 1760.

24. Kyburz, R.; Schaltegger, H.; Neuenschwander, M., Eine neue Fulvensynthese. 4. Mitteilung. *Helv Chim Acta* **1971,** *54* (4), 1037-1046.

25. Erden, I.; Sabol, J.; Gubeladze, A.; Ruiz, A., An expedient synthesis of 6-Vinylfulvene. *Turk J Chem* **2013,** *37* (4), 519-524.

26. Kaiser, R.; Hafner, K., Simple Synthesis of 1,2-Dihydropentalene and Its Substitution Products. *Angew Chem Int Ed* **1970,** *9* (11), 892.

27. Hafner, K.; Häfner, K. H.; König, C.; Kreuder, M.; Ploss, G.; Schulz, G.; Sturm, E.; Vöpel, K. H., Fulvenes as Isomers of Benzenoid Compounds. *Angew Chem Int Ed* **1963,** *2* (3), 123-134.

28. Brinker, U. H.; Fleischhauer, I., Carbene Rearrangements .8. Carbene-Carbene Rearrangements as a Route to 1,5-Dihydropentalene. *Tetrahedron* **1981,** *37* (25), 4495-4502.

29. Ashley, A. E.; Cowley, A. R.; O'Hare, D., Permethylpentalene chemistry. *Eur J Org Chem* **2007,** (14), 2239-2242.

30. S. H. Bertz, J. M. C., A. Gawish, U.Weiss, Condensation of Dimethyl 1,3-Acetonedicarboxylate with 1,2-Dicarbonyl Compounds: cis-bicyclo[3.3.0]octane-3,7-diones. In *Org Synth*, 1986; Vol. 64, pp 27-38.

31. Ashley, A. E.; Cowley, A. R.; O'Hare, D., The hexamethylpentalene dianion and other reagents for organometallic pentalene chemistry. *Chem Commun* **2007,** (15), 1512-1514.

32. Hafner, K.; Suss, H. U., 1,3,5-Tri Tert Butylpentalene - Stabilized Planar 8pi-Electron System. *Angew Chem Int Edit* **1973,** *12* (7), 575-577.

33. Kitschke, B.; Lindner, H. J., The crystal and molecular structures of two substituted pentalenes. *Tetrahedron Lett* **1977,** *18* (29), 2511-2514.

34. Griesbeck, A. G., Pyrrolidine-Catalyzed Reactions between Alpha,Beta-Unsaturated Carbonyl-Compounds and Cyclopentadiene - a Convenient Approach to 1,2-Dihydropentalenes and 1,5-Dihydropentalenes. *J Org Chem* **1989,** *54* (21), 4981-4982.

35. Griesbeck, A. G., Synthesis of 1-Phenyl-1,2-Dihydropentalenes and 4-Phenyl-1,5-Dihydropentalenes. *Chem Ber* **1991,** *124* (2), 403-405.

36. Le Goff, E., Synthesis of Hexaphenylpentalene. *J Am Chem Soc* **1962,** *84* (20), 3975.

37. Stone, K. J.; Little, R. D., An exceptionally simple and efficient method for the preparation of a wide variety of fulvenes. *The Journal of Organic Chemistry* **1984,** *49* (11), 1849-1853.

38. Coskun, N.; Ma, J. X.; Azimi, S.; Gartner, C.; Erden, I., 1,2-Dihydropentalenes from Fulvenes by [6+2] Cycloadditions with 1-Isopropenylpyrrolidine. *Org Lett* **2011,** *13* (22), 5952-5955.

39. Schore, N. E., Transition metal-mediated cycloaddition reactions of alkynes in organic synthesis. *Chem Rev* **1988,** *88* (7), 1081-1119.

40. Kuwabara, T.; Ishimura, K.; Sasamori, T.; Tokitoh, N.; Saito, M., Facile Synthesis of Dibenzopentalene Dianions and Their Application as New pi-Extended Ligands. *Chem-Eur J* **2014,** *20* (25), 7571-7575.

41. Saito, M.; Nakamura, M.; Tajima, T.; Yoshioka, M., Reduction of Phenyl Silyl Acetylenes with Lithium: Unexpected Formation of a Dilithium Dibenzopentalenide. *Angew Chem Int Ed* **2007,** *46* (9), 1504-1507.

42. Li, H.; Wei, B.; Xu, L.; Zhang, W.-X.; Xi, Z., Barium Dibenzopentalenide as a Main-Group Metal η^8-Complex: Facile Synthesis from 1,4-Dilithio-1,3-butadienes and $Ba[N(SiMe_3)_2]_2$, Structural Characterization, and Reaction Chemistry. *Angew Chem Int Ed* **2013,** *52* (41), 10822-10825.

43. Bailey, P. M.; Mann, B. E.; Brown, I. D.; Maitlis, P. M., Dihydropentalenes from Palladium(Ii)-Induced Cyclotetramerisation of Acetylenes - X-Ray Crystal-Structures of 2 Dihydropentalenes. *J Chem Soc Chem Comm* **1976,** (7), 238-239.

44. Weidemüller, W.; Hafner, K., Synthesis of Carbonyliron Complexes of Pentalene and Its Derivatives. *Angew Chem Int Ed* **1973,** *12* (11), 925-925.

45. (a) Hunt, D. F.; Russell, J. W., Stable Transition-Metal Pi Complex of Dimethylaminopentalene. *J Am Chem Soc* **1972,** *94* (20), 7198; (b) Hunt, D. F.; Russell, J. W., Phenylpentalenediiron Pentacarbonyl. *J Organomet Chem* **1972,** *46* (1), C22

46. Ashley, A. E.; Balazs, G.; Cowley, A. R.; Green, J. C.; O'Hare, D., syn-Permethylpentalene iron and cobalt carbonyl complexes: Proximity bimetallics lacking metal-metal bonding. *Organometallics* **2007,** *26* (23), 5517-5521.

47. Brookes, A.; Gordon, F.; Howard, J.; Knox, S. A. R.; Woodward, P., Transition-Metal Carbonyl Complex of Pentalene. *J Chem Soc Chem Comm* **1973,** (16), 587-589.

48. Howard, J. A. K.; Knox, S. A. R.; Riera, V.; Stone, F. G. A.; Woodward, P., Pentalene Complexes from Cyclo-Octatetrenes - Crystal-Structure of $Ru_3(Co)_8(C_8H_6)$. *J Chem Soc Chem Comm* **1974,** (11), 452-453.

49. Howard, J. A. K.; Knox, S. A. R.; Stone, F. G. A.; Szary, A. C.; Woodward, P., Pentalene Complexes from Cyclo-Octatrienes - Crystal-Structure of Eta-(1,5-Bistrimethylsilyl)Pentalene-1,1,2,2,3,3,3,3-Octacarbonyl-Triangulo-Triruthenium, $Ru_3(Co)_8[C_8H_4(SiMe_3)_2]$. *J Chem Soc Chem Comm* **1974,** (19), 788-789.

50. Coffield, T. H.; Ihrman, K. G.; Burns, W., Pi-Dihydropentalenylmanganese Tricarbonyl. *J Am Chem Soc* **1960,** *82* (16), 4209-4210.

51. Komatsu, H.; Suzuki, Y.; Yamazaki, H., Unprecedented rhodium-mediated tetramerization of bulky terminal alkynes leading to hydropentalenylrhodium complexes. *Chem Lett* **2001,** (10), 998-999.

52. Katz, T. J.; Rosenberger, M., Ferrocene Derivatives of Pentalene: Dipentalenyliron Dianion and Hydrodipentalenyliron Anion. *J Am Chem Soc* **1963,** *85* (13), 2030-2031.

53. Janiak, C., (Organo)thallium (I) and (II) chemistry: syntheses, structures, properties and applications of subvalent thallium complexes with alkyl, cyclopentadienyl, arene or hydrotris(pyrazolyl)borate ligands. *Coordin Chem Rev* **1997,** *163*, 107-216.

54. Ustynyuk, Y. A.; Shestakova, A. K.; Chertkov, V. A.; Zemlyansky, N. N.; Borisova, I. V.; Gusev, A. I.; Tchuklanova, E. B.; Chernyshev, E. A., Synthesis, Structure and Fluxional Behavior of Isomeric Bis(Trimethylstannyl)Dihydropentalenes. *J Organomet Chem* **1987,** *335* (1), 43-57.

55. Sergeyev, N. M., Nuclear magnetic resonance spectroscopy of cyclopentadienyl compounds. *Progress in Nuclear Magnetic Resonance Spectroscopy* **1973,** *9* (2), 71-144.

56. Turner, Z. R.; Buffet, J.-C.; O'Hare, D., Chiral Group 4 Cyclopentadienyl Complexes and Their Use in Polymerization of Lactide Monomers. *Organometallics* **2014,** *33* (14), 3891-3903.

57. Jonas, K.; Gabor, B.; Mynott, R.; Angermund, K.; Heinemann, O.; Kruger, C., Novel mononuclear vanadium complexes having pentalene ligands eta(8)-bonded to a single metal atom - A new type of coordination in organometallic chemistry. *Angew Chem Int Edit* **1997,** *36* (16), 1712-1714.

58. Jonas, K.; Korb, P.; Kollbach, G.; Gabor, B.; Mynott, R.; Angermund, K.; Heinemann, O.; Kruger, C., Mononuclear pentalene and methylpentalene complexes of titanium, zirconium, and hafnium. *Angew Chem Int Edit* **1997,** *36* (16), 1714-1718.

59. Jones, S. C.; Hascall, T.; Barlow, S.; O'Hare, D., Pentalene complexes of group 7 metal carbonyls: An organometallic mixed-valence system with very large metal-metal electronic coupling. *J Am Chem Soc* **2002,** *124* (39), 11610-11611.

60. (a) Katz, T. J.; Acton, N., Bis(Pentalenylnickel). *J Am Chem Soc* **1972,** *94* (9), 3281; (b) Katz, T. J.; Acton, N.; Mcginnis, J., Sandwiches of Iron and Cobalt with Pentalene. *J Am Chem Soc* **1972,** *94* (17), 6205.

61. Churchill, M. R.; Lin, K. K. G., Crystallographic elucidation of the molecular geometry of bis(pentalenyl)iron, including the location and refinement of hydrogen atoms. *Inorg Chem* **1973,** *12* (10), 2274-2279.

62. Binding, S. C.; Green, J. C.; Myers, W. K.; O'Hare, D., Synthesis, Structure, and Bonding for Bis(permethylpentalene)diiron. *Inorg Chem* **2015,** *54* (24), 11935-11940.

63. Manriquez, J. M.; Ward, M. D.; Reiff, W. M.; Calabrese, J. C.; Jones, N. L.; Carroll, P. J.; Bunel, E. E.; Miller, J. S., Structural-Properties and Physical-Properties of Delocalized Mixed-Valent [Cp*M(Pentalene)M'Cp*](N+) and [Cp*M(Indacene)M'Cp*](N+) (M, M'=Fe, Co, Ni, N=0, 1, 2) Complexes. *J Am Chem Soc* **1995,** *117* (23), 6182-6193.

64. (a) Cloke, F. G. N.; Green, J. C.; Jardine, C. N., Electronic structure and photoelectron spectra of bispentalene complexes of thorium and uranium. *Organometallics* **1999,** *18* (6), 1080-1086; (b) Cloke, F. G. N.; Hitchcock, P. B., A New Class of Actinide "Sandwich" Complexes: Synthesis and

Molecular Structure of a Thorium Bis(η^8-pentalene) Complex. *J Am Chem Soc* **1997,** *119* (33), 7899-7900.

65. Balazs, G.; Cloke, F. G. N.; Green, J. C.; Harker, R. M.; Harrison, A.; Hitchcock, P. B.; Jardine, C. N.; Walton, R., Cerium(III) and Cerium(IV) Bis(η^8-pentalene) Sandwich Complexes: Synthetic, Structural, Spectroscopic, and Theoretical Studies. *Organometallics* **2007,** *26* (13), 3111-3119.

66. Ashley, A.; Balazs, G.; Cowley, A.; Green, J.; Booth, C. H.; O'Hare, D., Bis(permethylpentalene)cerium - another ambiguity in lanthanide oxidation state. *Chem Commun* **2007,** (15), 1515-1517.

67. Cooper, R. T.; Chadwick, F. M.; Ashley, A. E.; O'Hare, D., Synthesis and Characterization of Group 4 Permethylpentalene Dichloride Complexes. *Organometallics* **2013,** *32* (7), 2228-2233.

68. Clement, D. D.; Binding, S. C.; Arnold, T. A. Q.; Chadwick, F. M.; Casely, I. J.; Turner, Z. R.; Buffet, J.-C.; O'Hare, D., Synthesis and characterization of permethylpentalene titanium aryloxide and alkoxide complexes. *Polyhedron* **2019,** *157*, 146-151.

69. Chadwick, F. M.; Ashley, A. E.; Cooper, R. T.; Bennett, L. A.; Green, J. C.; O'Hare, D. M., Group 9 bimetallic carbonyl permethylpentalene complexes. *Dalton Trans* **2015,** *44* (46), 20147-20153.

Chapter 2: Synthesis of phenyl-substituted dihydropentalenes

2.1 Introduction

2.1.1 Phenyl substituents

In pentalenide (**Pn^{2-}**) and hydropentalenide (**PnH^{-}**) complexes the metal-ligand bonding is strongly affected by the substituents attached to the ligand core.[1] The steric effects, orientation and electronic properties attached groups all affect the properties of the resulting complexes. For this reason, the incorporation of phenyl groups, as well as substituted aryl groups, into **Pn^{2-}** and **PnH^{-}** ligands provide interesting possibilities for the tuning the properties of derived metal complexes.

Phenyl groups are bulky compared to hydrogen, so steric effects play a large role in the stability and reactivity of phenyl substituted ligands.[2] Conformational analysis of substituted cyclohexanes allows this steric demand to be quantified though the so-called 'A' value. This is a measure of the difference in energy between the equatorial and axial conformation for a particular mono-substituted cyclohexane arising from 1,3-diaxial repulsion (Figure 1).

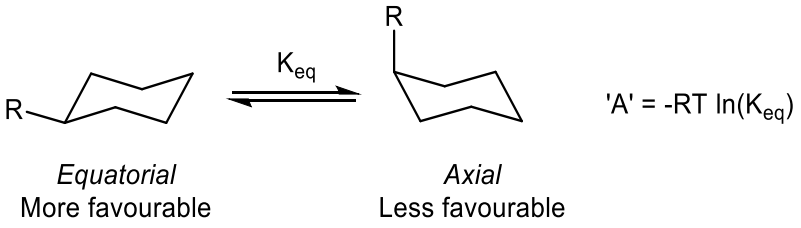

Figure 1: Defining 'A' values by conformational analysis of substituted cyclohexanes

Phenyl groups are shown to have a high A value of 3.0 kcal mol^{-1}.[3] This can be compared to the 'A' values of 2.15 kcal mol^{-1} for isopropyl and cyclohexyl groups, and 4.50 kcal mol^{-1} for *tert*-butyl groups. Other conformation analysis techniques also demonstrate this high steric demand. For example, Boiadjiev and Lightner[4] used circular dichroism spectroscopy on substituted bilirubins to determine

steric demand of different functional groups. In this system the relative demand of phenyl and isopropyl is reversed, but phenyl is still shown to exert a high steric influence. In phenyl-substituted **PnH**$^{-}$ and **Pn**$^{2-}$ derivatives the high steric demand will act to shield the negative charge in the ligand core, and in complexes of these ligands the steric influence may be able to shield reactive metal centres.

The inductive and resonance effects of phenyl substituents can be demonstrated by quantitative structure-activity relationship (QSAR) analysis. The Hammett equation uses the ionisation of meta- and para-substituted benzoic acids to quantify the electron-donating/withdrawing properties of a substituent through the Hammett constants σ_m, for meta-substitution, and σ_p, for para-substitution (Figure 2).[5]

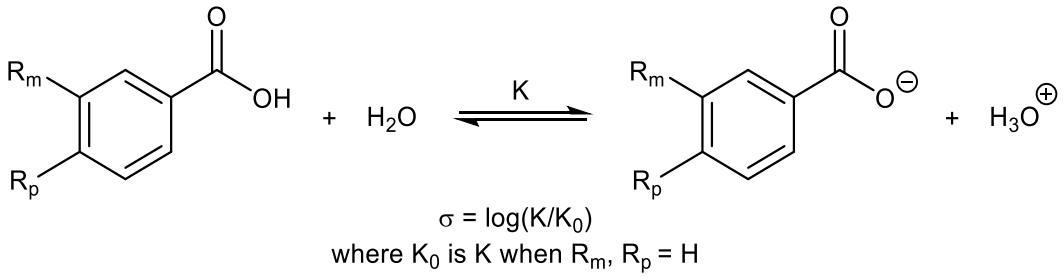

Figure 2: Defining σ parameters from the ionisation of substituted benzoic acids

Electron-withdrawing groups have positive values for these constants, and electron-donating have negative values. For example, a strongly electron-withdrawing group such as CF_3 has a σ_m of 0.43 and a σ_p of 0.56. The σ_m value, which reflects inductive effects[6], for a phenyl group is 0.06 and its σ_p value, which reflects both inductive and resonance effects, is -0.01. This shows that phenyl groups are weakly electron-withdrawing through induction. For anionic species such as **PnH**$^{-}$s and **Pn**$^{2-}$s phenyl substituents can be expected to stabilise the negative charge through inductive effects. Delocalization of the negative charge into the phenyl rings through resonance will also help to stabilise these anions (Figure 3).

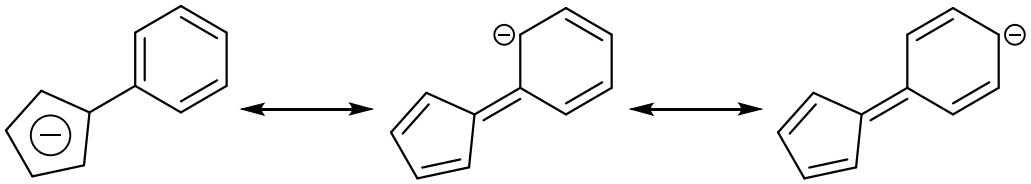

Figure 3: Delocalisation of negative charge in a phenyl-cyclopentadienide by resonance

This combination of steric and electronic effects will determine the properties of phenyl-substituted **Pn**$^{2-}$ and **PnH**$^{-}$ ligands (see chapter 3) but will also affect the formation and properties of the phenyl-substituted **PnH$_2$** species that act as precursors for these ligands.

2.1.2. Aryl-substituted cyclopentadienes

These steric and electronic effects of phenyl groups are demonstrated by the chemistry of phenyl substituted **CpH**s. Aryl-substituted **CpH**s have been thoroughly explored, with the synthesis of mono-[7], di-[8], tri-[9] , tetra[9c, 10] and penta-aryl[11] **CpH**s having been described.

An important example is pentaphenylcyclopentadiene (**Ph$_5$CpH**). This species is a colourless crystalline solid which melts at 259-260 °C,[12] compared to **CpH** and **Cp*H** which are volatile liquids. Like **Cp*H**, **Ph$_5$CpH** is resistant to the dimerization typical of low-substitution **CpH**s.[13] It is typically synthesised by the reaction of tetraphenylcyclopentadienone, with phenylmagnesiumbromide (PhMgBr), followed by reduction of the alcohol, either directly or via the bromo-derivative (Figure 3).

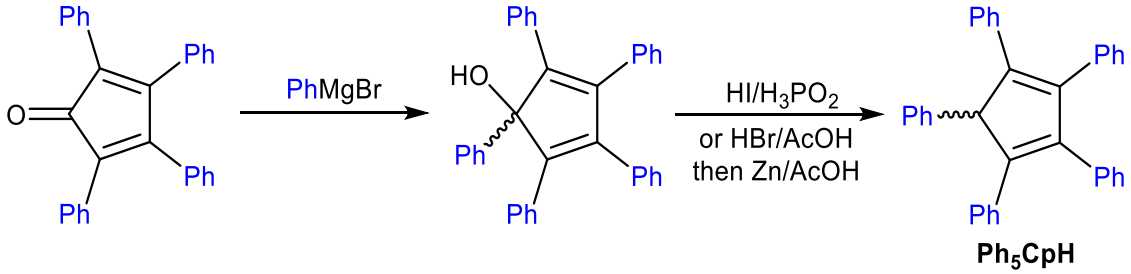

Figure 3: Synthesis of pentaphenylcyclopentadiene from tetraphenylcyclopentadienone

Field *et al.*[14] characterised the structure of **Ph$_5$CpH** crystallographically using crystals isolated in the synthesis of Cr(CO)$_3$(Ph$_5$CpH) (Figure 4). This analysis shows that, due to steric demand, the 4 phenyl

rings attached to sp^2-carbons in the central ring are rotated out of the plane of that ring (either 30.8-32.2° or 65.2-70.4°). The molecule contains a mirror plane through the sp^3-carbon, meaning 4 of the phenyl rings exist as two equivalent pairs. This structure is also reflected in the $^{13}C\{^1H\}$-NMR of **Ph_5CpH** which shows 12 resonances for the phenyl groups and 3 resonances for the C_5-ring, consistent with a mirror plane symmetric structure in solution.[15]

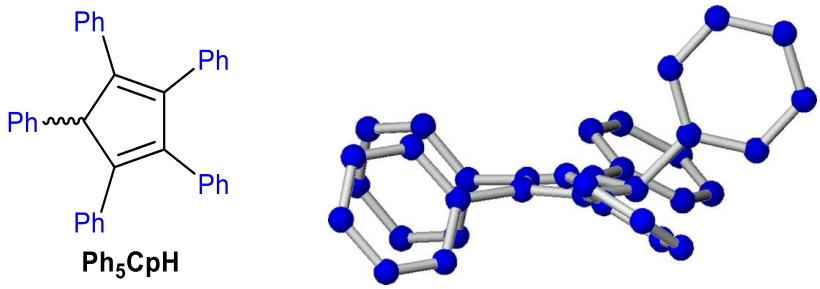

Figure 4: Crystal structure of pentaphenylcyclopentadiene [2]

Ph_5CpH has a pK_a of 12.5 in DMSO, making it considerably more acidic than **CpH** (pK_a = 18.0) and **Cp*H** (pK_a = 26.1).[16] This is due to the electron-withdrawing phenyl groups stabilising the conjugate anion (Section 3.1.1) through inductive effects. Steric crowding prevents the phenyl rings from achieving a co-planar arrangement with the central C_5-ring, so the negative charge cannot be stabilised by resonance. It has been shown that increasing the number of phenyl substituents increases the acidity of the **CpH** derivative, as **2,5-Ph_2CpH** has a pK_a of 14.3[17] and **2,3,4,5-Ph_4CpH** has a pK_a of 13.2.[18] However, for the tri- and tetra-phenyl substituted **CpH**s the increase in acidity is not as large as might be expected due to the increased steric crowding.[2]

For other cyclopentadiene derivatives, such as indenyl and fluorenyl, arylated-derivatives have been synthesised[19] and some of their organometallic chemistry explored.[19d, 20]

2.1.3. Phenyl-substituted dihydropentalenes

Kaiser and Hafner [21] described the thermal cyclisations of amino-vinyl fulvenes (Section 1.2.3). (**6-NMe_2-vinyl)Fv** cyclised in boiling piperidine to give **3-(NMe_2)PnH_2**, which reacted with PhLi to give, after amine elimination, **3-PhPnH_2** (Figure 5). Whereas **PnH_2** is a thermolabile oil, **3-PhPnH_2** is a stable solid that melts at 61-62 °C. This stability is likely due to steric shielding preventing polymerisation, and the deactivating effect of the phenyl group on the reactive fulvene-like double-bond. The higher melting point **3-PhPnH_2** can be attributed to π-stacking of phenyl rings leading to an increase in lattice energy for this species.

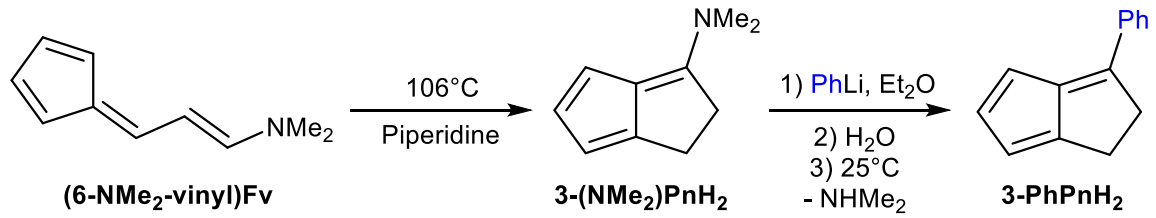

Figure 5: Synthesis of 3-phenyl-dihydropentalene from 6-diemethylamino-vinylfulvene

Griesbeck[22] reported the pyrrolidine-facilitated reactions of **CpH** with enones (Section 1.2.5). The condensation of **CpH** with 1,3-diphenylprop-2-en-1-one was reported to give the 1,2-H_2 isomer of **1,3-Ph_2PnH_2** (Figure 6). This was then isomerised to the 1,5-H_2 isomer either by treatment with trifluoracetic acid or by chromatography on alumina. This species is reported as a stable solid that melts at 142-144 °C, with the additional phenyl substitution compared to **3-PhPnH_2** contributing to an 80 °C increase in melting point.

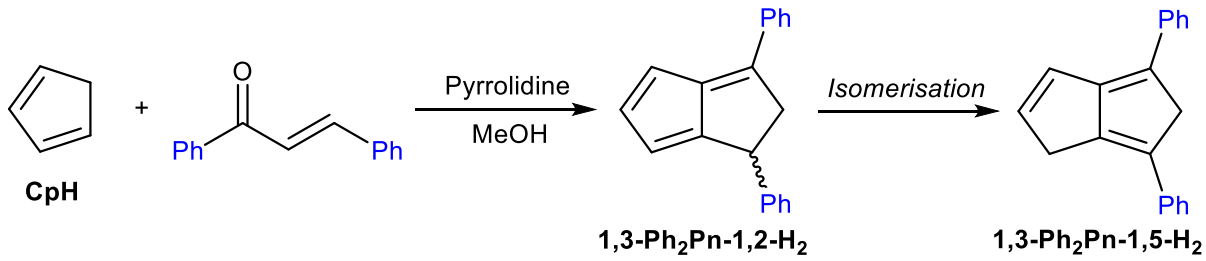

Figure 6: Synthesis of 1,3-diphenyldihydropentalenes from cyclopentadiene and 1,3-diphenylprop-2-en-1-one

2.1.4. Aims

Our aim was to explore the chemistry of arylated **Pn**$^{2-}$ species with a view to creating ligands that would stabilise metal complexes through the presence of the bulky, inductively electron-withdrawing phenyl groups. More highly-aryl substituted pentalenides could also possess planar chirality (depending on the barrier to rotation), and therefore could be useful ligands for stereoselective catalysts.

Dihydropentalenes have been demonstrated as convenient precursors for both hydropentalenides and pentalenides (Chapter 1). It was supposed that phenyl-substitution would make the **PnH$_2$**s less volatile and easier to purify, as well as stabilising them against degradation and polymerisation, allowing long term storage of these precursors. Increasing aryl substitution should also make these derivatives more acidic, potentially allowing weaker bases to be used to generate the respective **PnH**$^-$ and **Pn**$^{2-}$ species.

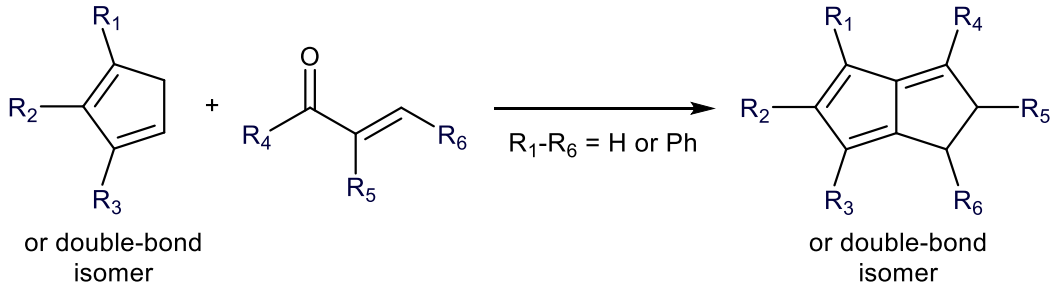

Figure 7: Synthesis of phenyl-substituted dihydropentalenes from phenyl-substituted cyclopentadienes and phenyl-substituted enones

As described in chapter 1 annulation reactions of **CpH**s provides a route to accessing **PnH$_2$** derivatives. This strategy was used to investigate the synthesis of a series of novel phenyl-substituted **PnH$_2$**s from cheap and readily available organic precursors. Through this it was hoped that a more modular approach to synthesis of **PnH$_2$**s can be devised, allowing incorporation of different substituents at varied positions around the central core. Access to a wide range of **PnH$_2$**s will allow a wider investigation on the chemistry of **PnH**$^-$ and **Pn**$^{2-}$ ligands.

2.2 Synthesis of 1,3-diphenyldihydropentalenes

2.2.1. Formation of 1,3-diphenyldihydropentalene from cyclopentadiene

Griesbeck[22-23] describes the synthesis of synthesis of **Ph_2PnH_2** from **CpH** (see above). The reaction is facilitated by pyrrolidine, a cyclic amine which has been shown to be an effective reagent for condensing **CpH** derivatives with carbonyl species[24]. Interestingly using diethylamine, the acyclic analogue of pyrrolidine, for these transformations results in much slower and lower-yielding reactions. It was decided to attempt to replicate Griesbeck's procedure in order to obtain **1,3-Ph_2PnH_2** which would serve as a precursor for **1,3-Ph_2Pn^{2-}** (Figure 8), a ligand that could provide two different η^5-binding sites for late transition metals.

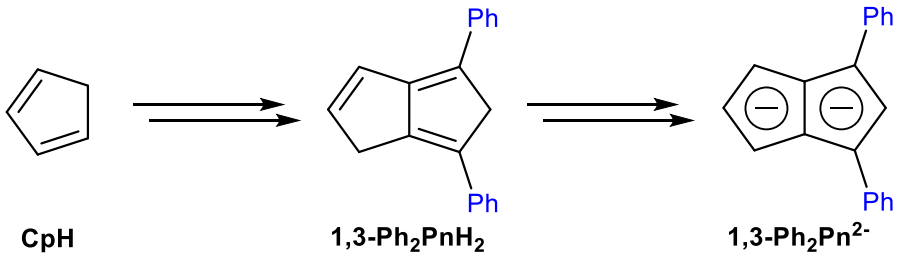

Figure 8: 1,3- Diphenyldihydropentalene as a precursor for 1,3-diphenylpentaleneide

Freshly cracked **CpH** was reacted with 1,3-diphenylprop-2-en-1-one using pyrrolidine in methanol (Section 2.1.3), before treating the reaction mixture with acetic acid and extracting the product with ethyl acetate. In Griesbeck's report upon removing the ethyl acetate under reduced pressure pure **1,3-PhPn-1,2-H_2** is obtained without any further workup.

However, in our hands we observed the 1,5-H_2 isomer by NMR, and our samples contained many by-products as identified by NMR and TLC. Griesbeck's preparation uses three equivalents of **CpH**, but we found this led to large amounts of **$(CpH)_2$** in our crude samples. Reducing the stoichiometry to one and a half equivalents greatly reduced the amount of **$(CpH)_2$** formed, but there were still many by-products present. The low solubility of the products meant crude samples could not be purified using chromatography on silica or alumina, even if the material is passed through multiple columns.

Attempts to recrystallise the crude material after passing through a silica column also failed to yield pure product.

2.2.2. Formation of 1,3-diphenyldihydropentalene from the cyclopentadienide anion

Because the procedure described by Griesbeck failed to give a pure sample of **1,3-Ph_2PnH_2** it was decided to develop an alternate synthesis. Whereas pyrrolidine promotes the condensation reaction by making the enone more electrophilic through formation of the enamine derivative, an alternate strategy is to activate the **CpH** to enhance its nucleophilicity. We supposed that using alkali-metal alkoxides would lead to partial deprotonation of the **CpH** *in situ*, greatly enhancing its nucleophilicity. Additionally, deprotonating the CpH will 'trap' it as the **Cp^-** anion and prevent it dimerising into **$(CpH)_2$**, limiting the amount of that by-product that needs to be removed from the crude material.

The reaction of freshly cracked **CpH** with 1,3-diphenylprop-2-en-1-one was performed using sodium methoxide in methanol (Figure 9). The crude reaction mixture was found to contain the 1,5-H_2 isomer of **1,3-Ph_2PnH_2**, alongside several unidentified by-products. After a biphasic workup the product mixture was found to contain much less **$(CpH)_2$** than the pyrrolidine method above, but still was found to contain many by-products by NMR and TLC. Once again, the products could not be sufficiently separated by chromatography. When the reaction was performed with sodium *tert*-butoxide in *tert*-butanol we observed no **Ph_2PnH_2** in the crude reaction mixture, which consisted of mostly insoluble organic material.

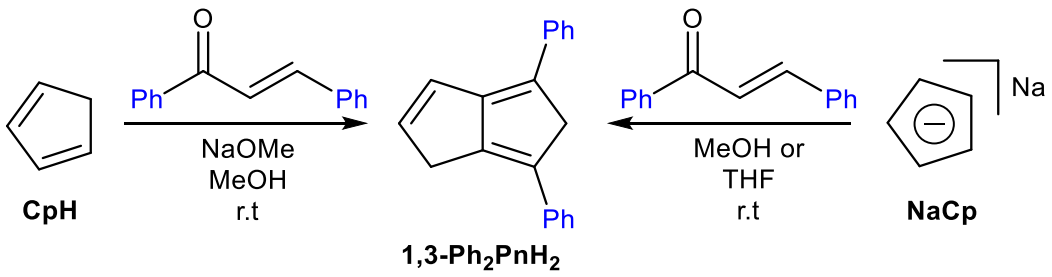

Figure 9: Synthesis of 1,3-diphenylcyclopentadiene from sodium cyclopentadieneide

It was supposed that sodium methoxide might only be partially forming **NaCp** leading to alternative reaction pathways occurring. Therefore, it was decided to use a pre-prepared sample of **NaCp** in the synthesis of **1,3-Ph_2PnH_2**. **NaCp** was synthesised by Panda *et al.*'s method[25] using molten sodium and **$(CpH)_2$**. When this reagent was reacted with 1,3-diphenylprop-2-en-1-one in either methanol or THF (Figure 9) the same reactivity was observed as for the sodium methoxide method, and therefore we were unable to obtain a pure sample of either isomer of **1,3-Ph_2PnH_2** via this method.

Although the methods tested did lead to formation of the 1,5-isomer of **1,3-Ph_2PnH_2** (we did not observe the 1,2-isomer), neither the methods described by Griesbeck or modified routes gave access to a pure sample of this dihydropentalene. Attempts to form **1,3-Ph_2PnH^-** and **1,3-Ph_2Pn^{2-}** from impure samples of **1,3-Ph_2PnH_2** failed, suggesting the formation of these anionic species is sensitive to the impurities present in these samples. This prevented the exploration of the chemistry of these ligands.

2.3 Synthesis of triphenyl-dihydropentalenes from phenyl-cyclopentadiene

It was supposed that replacing **CpH** with **PhCpH** in the condensation with 1,3-diphenylprop-2-en-1-one described by Griesbeck[22] would allow access to **Ph_3PnH_2** (Figure 10). The regioselectivity of fulvene synthesis would suggest that in **PnH_2** synthesis the first addition occurs at the 3-position of a **1-RCpH**, with the second condensation occurring at the 4-position. This would suggest in the case of **Ph_3PnH_2** the **1,3,5-Ph_3PnH_2** isomer would be the major product, with the **1,3,6-Ph_3PnH_2** isomer either being the minor product or not forming at all.

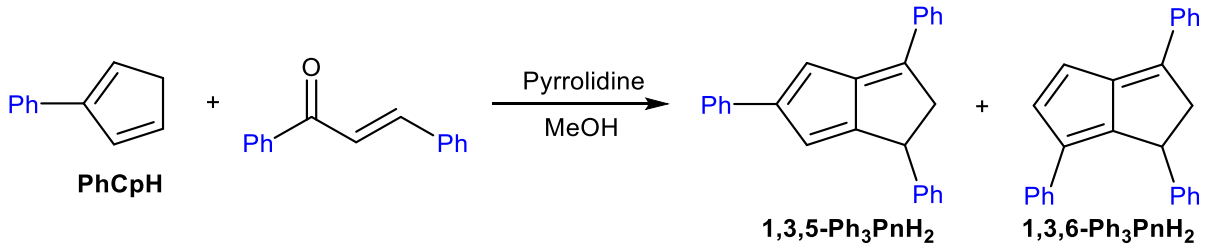

Figure 10: Phenylcyclopentadiene as a precursor for triphenyldihydropentalenes

However, whereas **CpH** is commercially available as its dimer, **PhCpH** is not and must be synthesised. There are only a limited number of reported syntheses for **PhCpH**. The most apparently straightforward is reacting 2-cyclopentenone, which is commercially available, with a source of the phenyl anion to form 1-phenylcyclopent-2-en-1ol, and then performing a dehydration reaction to generate the diene (Figure 11). Riemschneider *et al.*[26] describe using PhLi for this reaction, whereas Singh *et al.*[27] describe using PhMgBr.

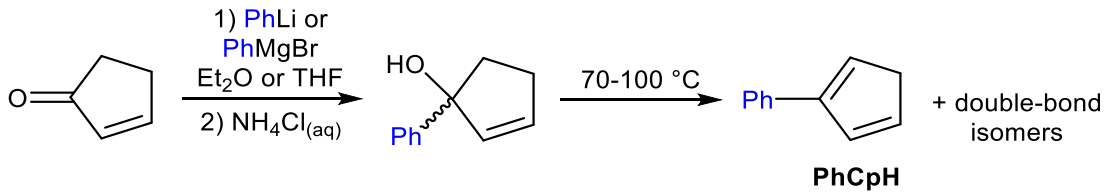

Figure 11: Synthesis of phenylcyclopentadiene from 2-cyclopentenone

We reacted freshly distilled 2-cyclopentenone with freshly prepared PhLi or PhMgBr in either THF or diethyl ether. In all cases what was observed, after quenching with the reactions with ammonium chloride, was a complex mixture of products presumably containing some amount of 1-phenylcyclopent-2-en-1ol. In Singh *et* al.'s preparation the crude alcohol is not purified further and is instead subjected to vacuum distillation. Heating to 70-100 °C under high vacuum is reported to cause the dehydration, and distillation purified the product **PhCpH** at the same time. However, in our hands we observed only a little formation of a waxy solid, and this was found to be a mixture of products and heavily contaminated with water. Attempts to perform the dehydration either by stirring the crude alcohol in dry THF over 3 Å molecular sieves, or by passing it through silica using ethyl acetate or diethyl ether, failed to give any of the desired **PhCpH**.

The failure of this procedure is in line with what is described by Nifant'ev *et al.*[28] who report that the low thermal stability and oxidisability of **PhCpH** made it difficult to isolate by this route. They instead described an alternative synthetic route (Section 2.6) that could provide access to samples of **PhCpH** of suitable purity in order to test its utility in the formation of **PnH$_2$**s.

2.4 Synthesis of dihydropentalenes derived from 1,4-diphenylcyclopentadiene

2,4.1. Synthesis of 1,4-diphenylcyclopentadiene

1,4-diphenylcyclopenta-1,3-diene (**1,4-Ph_2CpH**) was identified as a suitable starting material for several **PnH_2** derivatives. In addition, this species, unlike **PhCpH**, is described as a thermally stable material which would enable us to gain high purity samples of **1,4-Ph_2CpH** and to store them for long periods. [8b]

Several syntheses of **Ph_2CpH** have been described, such as addition of PhMgBr to 3-phenylcyclopent-2-enone followed by dehydration[17], ruthenium-catalysed cycloisomerization of ethynylphenylbenzenepropanol[29] or tin(II) chloride facilitated deoxygenation of 1,4-diphenylcyclopent-2-ene-1,4-peroxide.[30] However, these routes require difficult to obtain starting material or suffer from poor yields.

Drake and Adams[8b] describe the synthesis of **1,4-Ph_2CpH** from benzoylethylpropionate and acetophenone (Figure 12), and this route was selected due to the cheapness of the starting material and the small number of synthetic steps. We found the synthetic procedure as reported to give inconsistent results, so this was modified in order to improve the reliability.

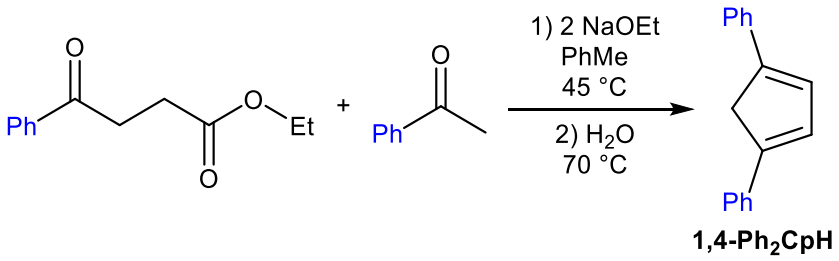

Figure 12: Synthesis of 1,4-diphenylcyclopentadiene from benzoylethylpropionate

Benzoylethylpropionate was prepared by acid-catalysed esterification of benzoylpropionic acid,[31] and it was found that the ester should be distilled from CaH_2 before use in order to achieve consistent yields of **1,4-Ph_2CpH**. The ester was treated with sodium ethoxide in the toluene at 0 °C, and then

freshly-distilled acetophenone was added. Upon heating at 45 °C for 3 days, a dark red solution was produced, supposedly containing diphenylcyclopentadiene ethyl ester.[17] This intermediate is extracted with water, and then heated to 70 °C which results in decarboxylation and precipitation of **1,4-Ph_2CpH**. High purity material was acquired through recrystallization from ethanol. The yield of this procedure is only moderate (42%), but this is a considerable improvement over the >15 % yield previously reported.[8b, 17]

Greifenstein *et al.* [17] reported that this synthetic route can be used with substituted acetophenones to give **1-Ar-3-PhCpH**'s. The aryl substituents reported include PhMe, PhOMe, biphenyl, and halogen-substituted phenyl groups. However, the synthesis was reported to fail for acetophenones with strongly electron-withdrawing substituents such as NO_2. Access to these **CpH** derivatives could allow them to be used for synthesising **PnH_2**s with different aryl-substituents and different degrees of symmetry.

2.4.2. Synthesis of 1,3,4,6-tetraphenyl-1,2-dihydropentalene

1,4-Ph_2CpH was used to synthesise 1,3,4,6-tetraphenyl-1,2-dihydropentalene (**1,3,4,6-Ph_4PnH_2**) through a pyrrolidine-facilitated condensation with 1,3-diphenylprop-2-en-1-one (Figure 13). As for Griesbeck's synthesis of **1,3-Ph_2PnH_2** [22-23] methanol was used as the solvent. However, it was found that addition of toluene (in a 1:1 ratio with methanol) to solubilise the starting materials improved the yields by suppressing the formation of by-products. Although the synthesis of **1,3-Ph_2PnH_2** is performed at room temperature it was found that heating at 70 °C was required to achieve high yields of **1,3,5,6-Ph_4PnH_2**, possibly due to the decreased nucleophilicity and increased steric demand of **1,4-Ph_2CpH** compared to **CpH**. When the reaction was conducted in air using 'wet' methanol and toluene some product formation was observed, but this procedure produced a large amount of by-products so anhydrous, air-free conditions are required for high yields.

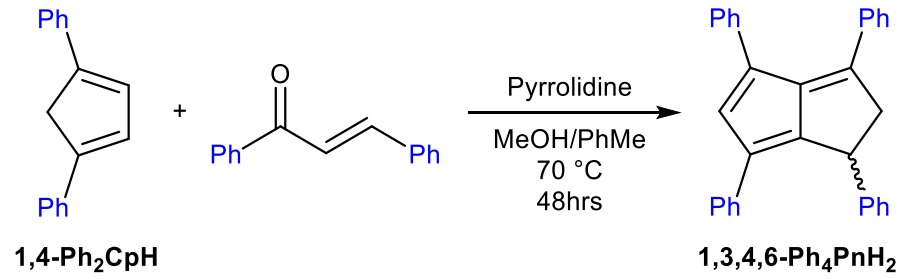

Figure 13: Synthesis of 1,3,4,6-tetraphenyldihydropentalene by the pyrrolidine-facilitated condensation of 1,4-diphenylcyclopentadiene and 1,3-diphenylprop-2-en-1-one

After 48 hours of stirring the reaction mixture at 70 °C crude **1,3,4,6-Ph_4PnH_2** was obtained by quenching with acetic acid and performing a biphasic workup. Pure product was obtained by filtration through silica followed by recrystallisation from ethanol, giving **1,3,4,6-Ph_4PnH_2** in 83% yield as a dark red crystalline solid which melts at 180-181 °C. The extra phenyl-substitution compared to **Ph_2PnH_2** raises the melting point by 38 °C, likely because of increased π-π interactions between molecules.

1,3,4,6-Ph_4PnH_2 formed as exclusively the 1,2-H_2 isomer (see below), and our attempts to induce isomerisation to the 1,5-H_2 isomer (as Griesbeck described for **1,3-Ph_2PnH_2**[22]) either through prolonged heating (up to 200 °C) or through chromatography on silica or alumina were not successful. **1,3,4,6-Ph_4PnH_2** contains a single stereocentre and presumably exists as a racemic mixture. The two enantiomers could potentially be separated using an enantioseparation technique[32] such as chiral chromatography[33] or selective crystallisation[34] presuming the enantiomers don't readily interconvert. This could be useful for instances that would require an optically pure **PnH_2**, such as synthesising optically pure **PnH^-** ligands.

The ^{1}H-NMR spectrum clearly shows the 1,2-H_2 nature of **1,3,4,6-Ph_4PnH_2**, with a characteristic set of resonances at 4.55, 4.10 and 3.50 ppm (Figure 14). The shifts at 4.10 and 3.50 ppm correspond to the 2 hydrogens attached to the C-2 carbon, and these peaks show partial 'roofing' due to the large $^2J_{HH}$-coupling (19.5 Hz) between them. These hydrogens attached the C-2 carbon can be differentiated by the upfield shift of the hydrogen that is 'cis' to the phenyl group attached to the C-1 carbon, with proximity to the π-system of the phenyl ring resulting in greater shielding of this proton.

This assignment is confirmed by the Karplus relationship between the C-2 hydrogens and the hydrogen attached to C-1. The Karplus equation relates dihedral angels between hydrogens and the resulting $^{3}J_{HH}$-coupling between them, with the angles 0° and 180° giving the largest coupling values and 90° giving the smallest.[35] From the XRD structure the dihedral angle between the two hydrogens 'cis' to each other is 15.7°, which gives a $^{3}J_{HH}$-coupling constant of 6.85 Hz. The hydrogens 'trans' to each other have a dihedral angle of 135.84°, which produces a smaller coupling constant of 1.75 Hz.

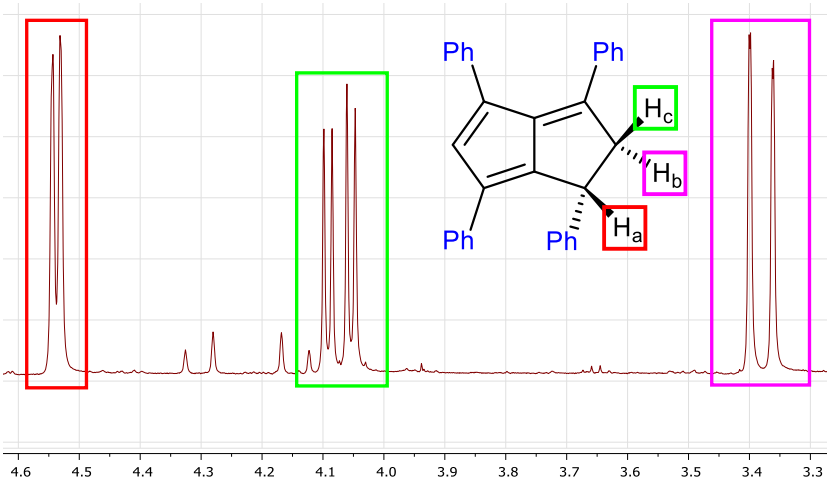

Figure 14: ^{1}H-NMR spectrum of 1,3,4,6-tetraphenyldihydropentalene

Bailey *et al.* [36] described the crystal structure of **1,3,4,6-Ph_4PnH_2** formed by cyclotetramisation of phenyl acetylene (Section 1.2.7). The product of the condensation reaction described above was analysed by XRD in order to confirm its structure. Crystals suitable for diffraction measurements were grown from ethanol at -15 °C.

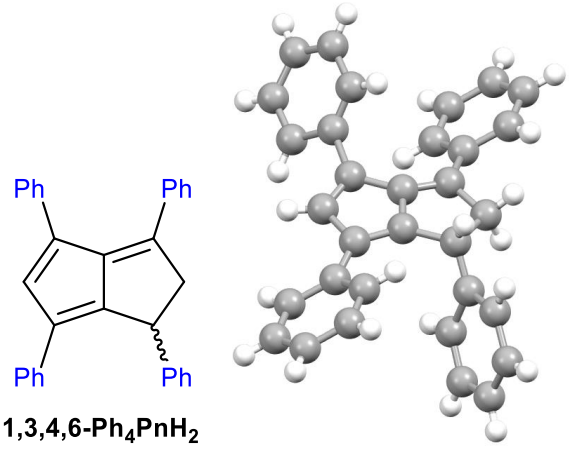

Figure 15: XRD structure of 1,3,4,6-tetraphenyldihydropentalene – asymmetric unit displayed

The crystal analysed showed an overlaid structure of the *R*- and *S*-enantiomers of **1,3,4,6-Ph$_4$PnH$_2$**, meaning the two isomers crystallised together. The XRD analysis of **1,3,4,6-Ph$_4$PnH$_2$** demonstrated its fulvene-like structure (Figure 15). Peloquin *et al.*[8a] reported the crystal structure **1,3,6-Ph$_3$Fv**, and it was found the that the fulvene 'core' of **1,3,4,6-Ph$_4$PnH$_2$** is similar to this species.

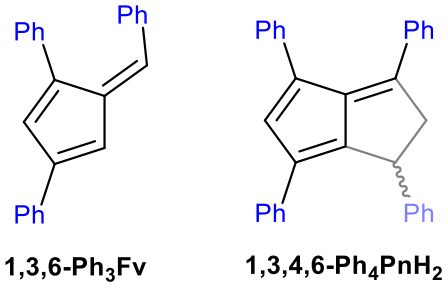

Figure 16: Fulvene-like structure of 1,3,4,6-tetraphenyldihydropentalene

For example, the exocyclic C-C double bond in **1,3,6-Ph$_3$Fv** is 1.354 Å,[8a] and the analogous C-C bond in **1,3,4,6-Ph$_4$PnH$_2$** was found to be 1.357(6) Å. The C-C bond lengths in the diene ring of **1,3,6-Ph$_3$Fv** are 1.355-1.360 Å and 1.460-1.466 Å, and in **1,3,4,6-Ph$_4$PnH$_2$** they are 1.365(11)-1.370(17) Å and 1.448(6)-1.476(12) Å with the shorter C-C single bond being the between the 'bridgehead' carbons. One key difference was in the C-C bond length for the phenyl group attached to the fulvene double bond, with the quaternary phenyl carbon-fulvene carbon distance being 8% longer in **1,3,4,6-Ph$_4$PnH$_2$**

than in **1,3,6-Ph$_3$Fv**. This could be due to the having a neighbouring -CH$_2$- group, as opposed to just having a hydrogen atom in the case of **1,3,6-Ph$_3$Fv**.

The UV/vis spectrum of **Ph$_4$PnH$_2$** was acquired using a 1.01x10^{-5} mol dm^{-3} THF solution of this species. The spectrum shows three distinct absorbances – two in the UV range with λ_{max} at 300 nm and 338 nm, and one broad absorbance in the visible range with λ_{max} centred at 465 nm. The absorbances at 300 nm and 338 nm have molar extinction coefficients (ε) of 34964 dm^3 mol^{-1} cm^{-1} and 27855 dm^3 mol^{-1} cm^{-1} respectively. The wavelengths of these absorbances and the magnitude of their extinction coefficients suggest these features are arising from fully spin-, symmetry- and orbital-allowed transitions. These are likely π-π* transitions involving the conjugated system in the diene-ring of **1,3,4,6-Ph$_4$PnH$_2$**, as a similar absorbance at 355 nm is observed in the UV/vis spectrum of **1,4-Ph$_2$CpH**.

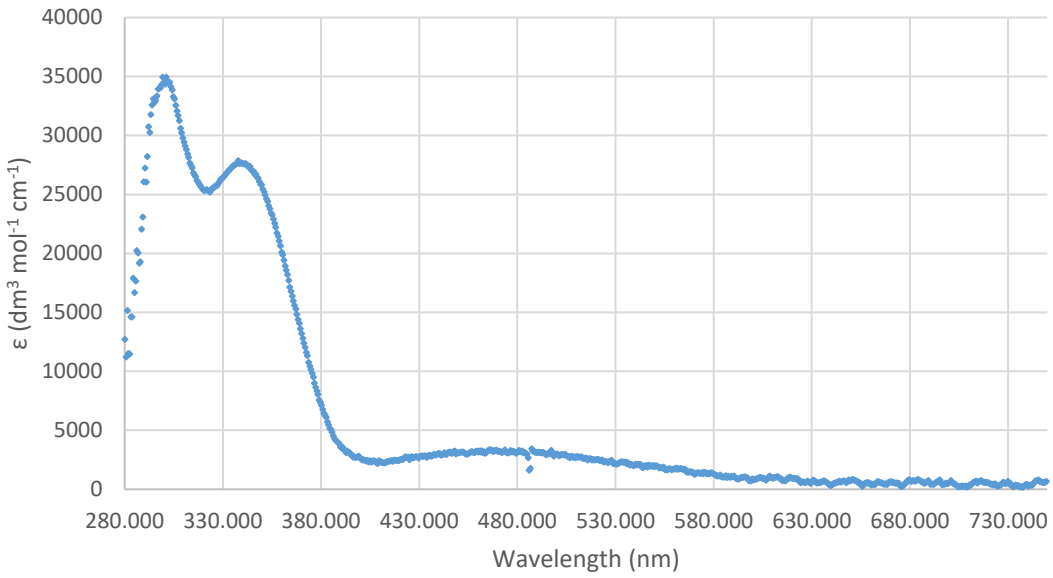

Figure 17: UV/vis spectrum of 1,3,4,6-teteraphenyldihydropentalene in THF

The absorbance at 465 nm has an ε value of 3432 dm^3 mol^{-1} cm^{-1}, and this magnitude of ε suggests this feature is arising from a spin-allowed but symmetry- or orbital-forbidden transition, likely a π-π* transition. An analogous absorbance is present in the UV/vis spectrum of **1,3,6-Ph$_3$Fv** but is not present in the spectrum of **1,4-Ph$_2$CpH**, suggesting that the fulvene-like bond is the structural feature that gives rise to this absorbance. This absorbance is likely the cause of the intense red colour

observed for **1,3,4,6-Ph_4PnH_2** and **1,3,6-Ph_3Fv**, as **1,4-Ph_2CpH** lacks this absorbance and is pale yellow in colour.

Pyrrolidine facilitates the formation of **1,3,4,6-Ph_4PnH_2** by enhancing the electrophilicity of the enone through formation of an enamine. An alternative strategy is to enhance the nucleophilicity of the **Ph_2CpH**. In Le Goff's synthesis of **1,2,3,4,5,6-Ph_6PnH_2** the weak base potassium fluoride is used to 'catalyse' the reaction between **1,2,3-Ph_3CpH** and the relevant enone through partial acidification of the **CpH**.[37]

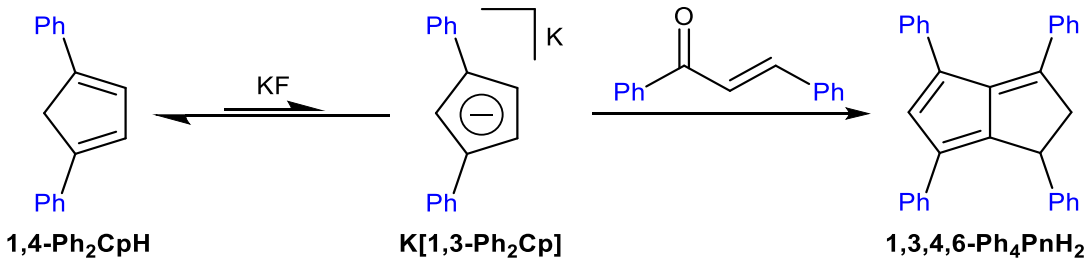

Figure 18: Synthesis of 1,3,4,6-tetraphenyldihydropentalene by potassium fluoride activation of 1,4-diphenylcyclopentadiene

In our hands anhydrous KF was shown to facilitate the condensation of **1,4-Ph_2CpH** and 1,3-diphenylprop-2-en-1-one (Figure 18) in 1:1 methanol and toluene. However, the yield was 35%, considerably lower than using pyrrolidine. KF mounted on alumina has been shown to have enhanced activity for a variety of transformations including condensations.[38] However, using 40% KF on Al_2O_3 did not lead to an improvement in the yield of **1,3,4,6-Ph_4PnH_2**.

Potassium fluoride has limited solubility in organic solvents, and the heterogeneous nature of the reaction above could have contributed to the low yield of **1,3,4,6-Ph_4PnH_2**. This solubility issue can be overcome by the addition of 18-crown-6 which allows potassium fluoride to be dissolved in even apolar solvents such as benzene.[39] Complexation of the potassium cation by the crown ether also enhances the reactivity of the fluoride anion. Therefore, the synthesis of **1,3,4,6-Ph_4PnH_2** was carried out using potassium fluoride and a stoichiometric amount of 18-crown-6. While a slight increase in

the yield, up to 41 %, was observed with the addition of crown ether, the yield is still considerably lower than with pyrrolidine.

While KF partially activates **1,4-Ph$_2$CpH**, the use of a stronger base would result in complete conversion of **1,4-Ph$_2$CpH** into the nucleophilic **1,3-Ph$_2$Cp$^-$** anion, which should react with the relevant Michael acceptor. The pK_a of **1,4-Ph$_2$CpH** is 14.3,[17] so alkoxide bases are suitably strong facilitate this deprotonation (Figure 19).

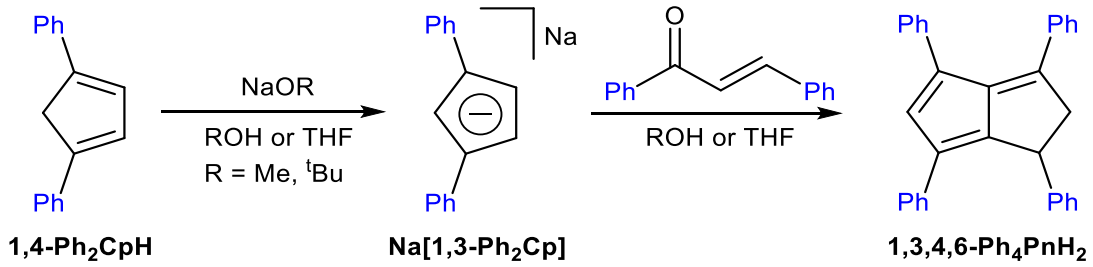

Figure 19: Synthesis of 1,3,4,6-tetraphenyldihydropentalene from sodium 1,3-diphenylcyclopentadienide

Addition of **1,4-Ph$_2$CpH** to sodium methoxide (pK_a = 15.5) in methanol, followed by addition of 1,3-diphenylprop-2-en-1-one resulted in the formation of **1,3,4,6-Ph$_4$PnH$_2$** after heating at 70 °C for 40 hours. Crude material was obtained by a diethyl ether:water workup. The crude product was stripped through silica (using 50:50 diethyl ether:hexane as the eluent) and recrystallised from ethanol to give **1,3,4,6-Ph$_4$PnH$_2$** in 65% yield. This is a higher yield than given by KF, showing complete deprotonation to be superior to the equilibrium process in the case of the weak base.

The use of sodium *tert*-butoxide (pK_a = 17.0) to facilitate the condensation was investigated to determine if using a stronger base resulted in higher yields. Reacting **1,4-Ph$_2$CpH** with sodium *tert*-butoxide in *tert*-butanol resulted in the formation of a large amount of precipitate forming, presumably **Na[1,3-Ph$_2$Cp]**. Addition of 1,3-diphenylprop-2-en-1-one followed by heating did result in some formation of **1,3,4,6-Ph$_4$PnH$_2$**, but only in low amounts, alongside a large amount of unidentified by-products. We suppose that the insolubility of the **Na[1,3-Ph$_2$Cp]** in *tert*-butanol means that the reaction is occurring heterogeneously and leading to undesired reaction pathways.

To address this the reaction with sodium *tert*-butoxide was performed in THF, in which **Na[1,3-Ph_2Cp]** is soluble. In this case the reaction was more successful, and after work-up (a similar work-up to that described for the sodium methoxide reaction) **1,3,4,6-Ph_4PnH_2** was obtained in 53% yield. This is less than that observed using sodium methoxide, so increasing base strength did not increase the yield. We suppose that the higher yield in the case of the methoxide reaction is due to the presence of methanol which, as the proton-transfer is suggested to part of the mechanism of **PnH_2** formation[40] and methanol, being more acidic than *tert*-butanol, is likely better facilitate these reaction steps.

Base	**Solvent**	**Yield (%)**
Pyrrolidine	Methanol:toluene (1:1)	83
KF	Methanol:toluene (1:1)	35
KF + 18-crown-6	Methanol:toluene (1:1)	41
NaOMe	MeOH	65
NaO^tBu	^tBuOH	>10
NaO^tBu	THF	53

Figure 20: Table of reagents used to synthesise 1,3,4,6-tetraphenyldihydropentalene

It has been shown that the alkali-metal counter-ion affects conjugate additions of anionic nucleophiles, exemplified by different reactivity of enolates with Michael acceptors. Lithium enolates are found to undergo 1,2-addition to conjugate carbonyls due to the high affinity of the hard lithium counter ion for oxygen donors, whereas sodium and potassium enolates, with a softer, more dissociated cation undergo 1,4-addition. As formation of **Ph_4PnH_2** begins with a conjugate addition it was decided to investigate the effect of cations on **PnH_2** synthesis.

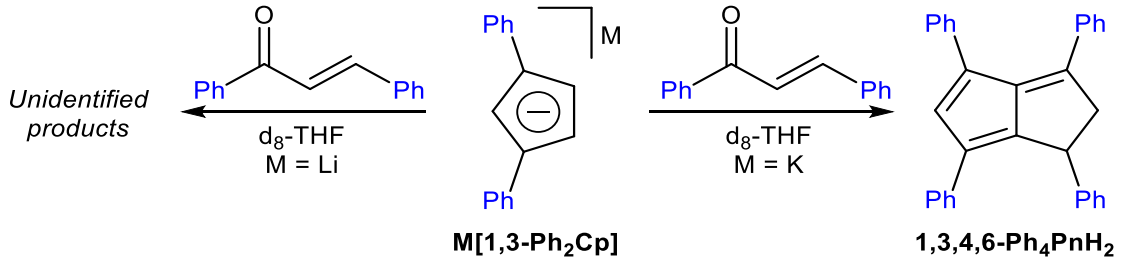

Figure 21: Reactions of lithium and potassium 1,3-diphenylcyclopentadienide with 1,3-diphenylprop-2-en-1-one

Li[Ph$_2$Cp] and **K[Ph$_2$Cp]** were prepared with treating **1,4-Ph$_2$CpH** with the relevant MHMDS base in d_8-THF to ensure complete, irreversible deprotonation (Figure 21). To these species were added 1,3-diphenylprop-2-en-1-one, and the reaction monitored with NMR. In the case of **K[Ph$_2$Cp]** rapid formation of **Ph$_4$PnH$_2$** was observed. However, in the case of the **Li[Ph$_2$Cp]** reaction no **Ph$_4$PnH$_2$** formation was observed, and instead alternate species were observed. Over time the NMR signals disappeared, and the formation of a brown precipitate was observed. This precipitate could not be re-dissolved in d_8-THF, C_6D_6 or $CDCl_3$ to analyse it by NMR, so we suppose it is one or more degradation products. With these results we conclude that **Li[Ph$_2$Cp]** (and potentially other **LiCp** derivatives) is inappropriate for the formation of **PnH$_2$**s by Michael-addition pathways.

Another synthetic approach to accessing **1,3,5,6-Ph$_4$PnH$_2$** from **1,4-Ph$_2$CpH** is by first converting it to 1,3,6-triphenylfulvene (**1,3,6-Ph$_3$Fv)**, and then condensing this species with acetophenone in a manner analogous to the method described by Coskum *et al.*[40a] **1,3,6-Ph$_3$Fv** was synthesised by condensing **1,4-Ph$_2$CpH** with benzaldehyde using pyrrolidine in methanol (Figure 22),[8a, 24] and worked up by filtration, washing with cold methanol and recrystallisation from ethanol. This procedure is high-yielding (95%) and straightforward.

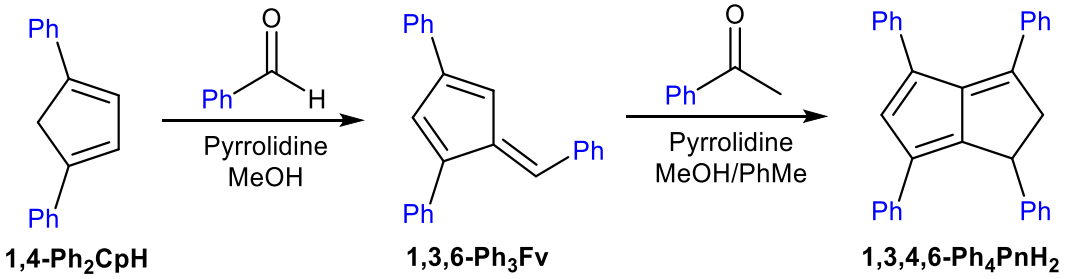

Figure 22: Synthesis of 1,3,4,6-tetraphenyldihydropentalene from 1,3,6-triphenylfulvene

This stepwise strategy uses two Knoevenagel condensations and results in elimination of two equivalents of water, and it was supposed this would provide a higher thermodynamic driving force than the reaction with the enone, which only eliminates 1 equivalent of water. Reacting the fulvene with acetophenone using pyrrolidine in toluene and methanol (Figure 22) gave **1,3,5,6-Ph_4PnH_2** in 72% yield, meaning the combined yield across the two steps is 68%. This a lower conversion of **1,4-Ph_2CpH** into **1,3,5,6-Ph_4PnH_2** than the reaction with 1,3-diphenylprop-2-en-1-one, and requires and additional reaction step, so is less useful as a synthetic strategy. However, it does show the enamine of acetophenone will react with a hindered fulvene, so this could provide access to other substituted dihydropentalenes using other fulvenes.

2.5. Synthesis of dihydropentalenes from 1,2,3-triphenylcyclopentadiene

2.5.1 Synthesis of 1,2,3-triphenylcyclopentadiene

In order to replicate Le Goff's synthesis of **1,2,3,4,5,6-Ph_6PnH_2** [37] a reliable, gram-scale synthesis of 1,2,3-triphenylcyclopentadiene (**1,2,3-Ph_3CpH**) was required. The method described by Lee *et al.*[41] was appealing in that it was reported to be high yielding and could also provide access to a range of 1,2,3-trisubstituted cyclopentadienes in addition to **1,2,3-Ph_3CpH**. The first step of this synthesis is a dicobalt octacarbonyl ($Co_2(CO)_8$) facilitated Pauson-Khand reaction between diphenylacetylene and norbornadiene (Figure 23).

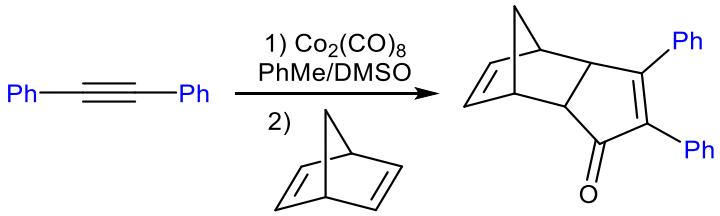

Figure 23: Cobalt octacarbonyl facilitated Pauson-Khand reaction of diphenylacetylene and norbornadiene

Diphenyl acetylene was stirred with a stochiometric amount of $Co_2(CO)_8$ in toluene at room temperature, resulting in formation of a black solution of (diphenylacetylene)hexacarbonyldicobalt. To this solution was added norbornadiene and DMSO as a promotor,[42] and the reaction stirred for five days. In our hands stirring at 50 °C as reported produced a low (>10%) yield of the desired norbornene-fused cyclopentenone derivative, however performing the reaction at 80 °C increased the yield to 37%. The product is purified by filtering the reaction mixture through silica to remove cobalt salts and recrystallising the resulting solid from ethyl acetate.

$Co_2(CO)_8$ is an expensive and highly-toxic material so replacement of the stoichiometric loading of this species with a catalytic one was attempted, as it has been demonstrated that performing Pauson-Khand reactions under an atmosphere of carbon monoxide enables use of sub-stoichiometric amounts of metal species[43]. However, when the reaction was attempted with a 10% loading of Co_2CO_8 under 5atm of CO little (>5%) yield of product was obtained. In both the stochiometric and sub-stochiometric reactions precipitates formed, and these toluene-insoluble species where shown to be the cobalt species $Co_2(CO)_4(NBD)_2$ and $[Co(DMSO)_6][Co(CO)_4]$ by XRD, and the precipitation of the cobalt from the reaction could be responsible for limiting the yield and preventing a catalytic regime from being adopted. This could perhaps be overcome by using super-stochiometric amounts of $Co_2(CO)_8$ but that is undesirable for the reasons mentioned above.

Installation of the third phenyl-substituent was achieved by Grignard addition (Figure 24). Addition of the Pauson-Khand product to an ether solution of PhMgBr, freshly prepared by reacting

bromobenzene with Mg turnings, produced, after quenching with ammonium chloride, the alcohol derivative in 56% yield.

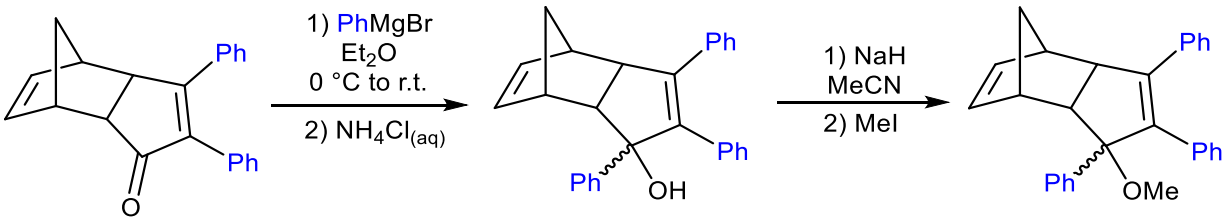

Figure 24: Conversion of Pauson-Khand product into methyl ester derivative

The next step was to convert the alcohol into the methoxy-ester. Attempts to directly form the ester by quenching the Grignard reaction with methyl iodide fails. Instead the synthesis was achieved by deprotonation of the worked-up alcohol using sodium hydride in dry acetonitrile, followed by addition of methyl iodide. The product is purified through addition of ether and washing with water, followed by chromatography on silica using hexane:ethyl acetate as the eluent.

The final step of Lee *et al.*'s synthesis is a retro-Diels-Alder, a reaction that usually requires high temperatures but has been shown to occur at lower temperatures when ionic intermediates are involved.[44]

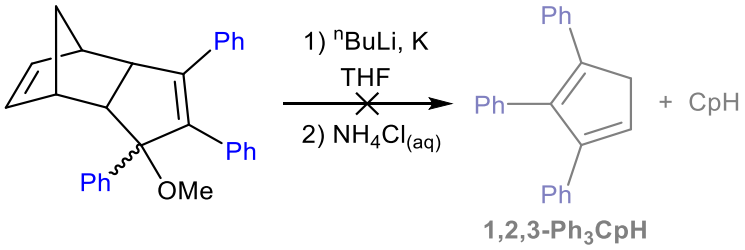

Figure 25: Retro Diels-Alder reaction of methyl ester derived from Pauson-Khand product

In this case the rearrangement was reported to be induced by reduction of the ester functionality with potassium and trapping of the produced cyclopentadienes by deprotonation with *n*-BuLi moving the equilibrium towards the products (Figure 25). Quenching the Cp salts with ammonium chloride was reported to furnish **1,2,3-Ph$_3$CpH** in high yields. However, in our hands no product formation was

observed either by TLC or NMR over multiple attempts, and instead only destruction of the starting material occurred.

Because of this an alternative synthetic route was required. Pauson [45] described the synthesis of **1,2,3-Ph_3CpH** through acid-catalysed dehydration of 1,2,3-triphenylpentan-1,2-diol, which is formed by the intramolecular-pinacol coupling of 1,2,5-triphenylpentan-1,5-dione (Figure 26). A similar synthetic route is used to synthesise **1,2,3,4-Ph_4PnH** from 1,2,4,5-tetraphenylpentan-1,5-dione.[46]

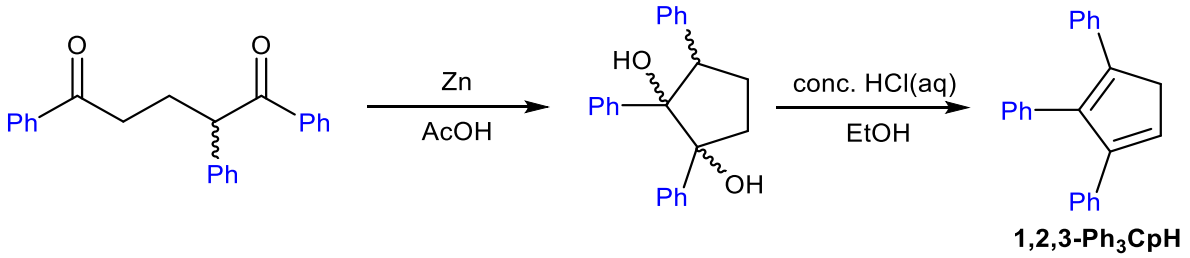

Figure 26: Synthesis of 1,2,3-triphenylcyclopentadiene through pinacol coupling of 1,2,5-triphenylpentan-1,5-dione followed by acid-catalysed dehydration

In Pauson's report 1,2,5-triphenylpentan-1,5-dione is synthesised from (2-benzoylethyl)trimethylammonium iodide and deoxybenzoin. The ammonium salt is synthesised in 2 steps, the first being an acid catalysed Mannich reaction with acetophenone, dimethylamine (handled as its hydrochloride salt) and paraformaldehyde (Figure 27).[47] After refluxing the substrates in ethanol with a small amount of aqueous HCl for 96 hours the solvent is removed to give the crude product as the hydrochloride salt on the desired amine. The crude sample is treated with saturated Na_2CO_3 solution, and the neutral amine extracted with diethyl ether. After removing the solvent under reduced pressure (2-benzoylethyl)dimethylamine was obtained in high yields (70%).

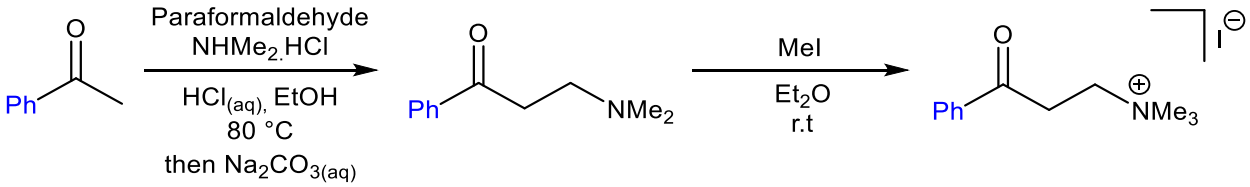

Figure 27: Synthesis of (2-benzoylethyl)trimethylammonium iodide

Reacting the Mannich product with an excess of methyl iodide in diethyl ether forms (2-benzoylethyl)trimethylammonium iodide which precipitates from the ether solution, allowing it be easily isolated by filtration. This procedure is straightforward and high yielding (92%). However, it does require large volumes of highly toxic methyl iodide.

As described by Pauson[45] (2-benzoylethyl)trimethylammonium iodide is reacted with deoxybenzoin by heating in a methanolic solution of NaOH (Figure 28). After an acidic workup the crude product is obtained, and can be purified by recrystallization to give 1,2,5-triphenylpentan-1,5-dione. However, the samples were frequently contaminated by amines, primarily trimethylamine, and these proved difficulty to fully remove and would likely requiring careful washing and chromatography.

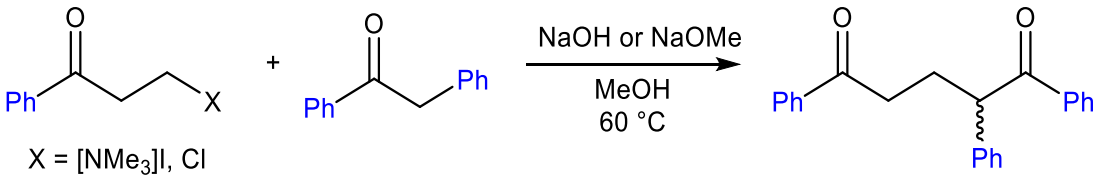

Figure 28: Synthesis of 1,2,5-triphenylpentan-1,5-dione

Because of this the ammonium reagent was replaced with the commercially available reagent 3-chloropropiophenone, chosen because the by-product of the enolate addition would be sodium chloride, which would be easy to remove. Reacting 3-chloropropiophenone and deoxybenzoin with methanolic NaOH gave (Figure 28), after a biphasic workup, 1,2,5-triphenylpentan-1,5-dione. This was purified by recrystallization from ethanol to give the product in high yield. Replacing the sodium hydroxide in 'wet' methanol with sodium methoxide in anhydrous methanol resulted in a higher yield (80%), likely to due to lower occurrence of side products.

The next step is cyclisation through coupling of the two ketone functionalities within the 1,2,5-triphenylpentan-1,5-dione (Figure 29). Pinacol coupling is a reductive, free radical reaction of carbonyl species which leads to formation of 1,2-diols.[48] In the case of our diketone each carbonyl functionality will undergo a single electron reduction to form ketyl radicals templated by coordination to the oxides

form of the reductant. Intramolecular combination of the two radicals then leads to ring-closing C-C bond formation.

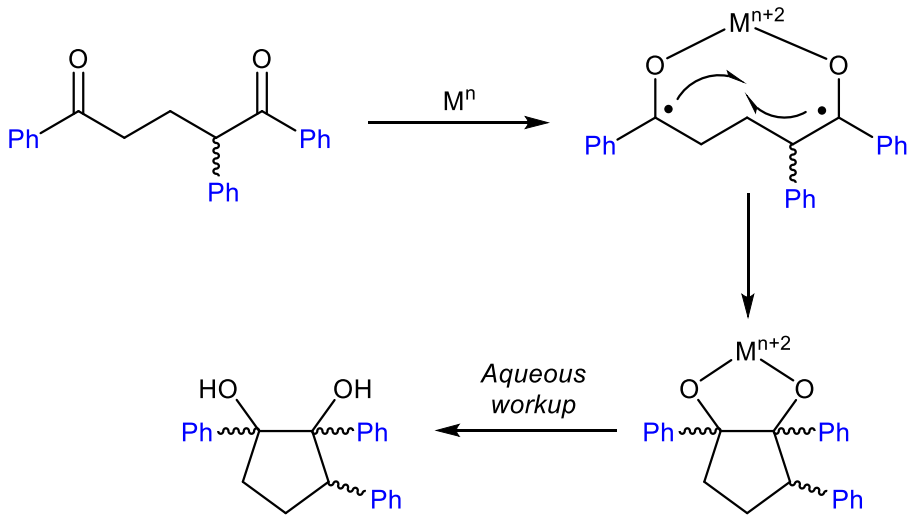

Figure 29: General scheme of a metal-promoted pinacol coupling of 1,2,5-triphenylpentan-1,5-dione

In Pauson's report the reducing agent is metallic zinc, with the reaction being carried out in acetic acid.[45] Pauson reported a yield of 1,2,3-triphenylpentan-1,2-diol of 30%. However, in our hands the use of zinc proved unreliable, either giving small yields (>10%) or failing completely, with most of what was isolated after work up being unreacted starting material. We supposed that because zinc is oxidised in air, our samples of zinc were being rendered inert by a layer of zinc oxide. To amend this fresh samples of zinc were kept under an argon atmosphere before use, and the reaction carried out in deoxygenated acetic acid. However, this did not improve the yields, and neither did mechanical grinding of the zinc powder under argon or by ultrasound irradiation of the reaction mixture. Attempts to activate the zinc powder using hydrochloric acid [49] also did not lead to increased activity.

Because of this an alternative reducing agent was sought. Alkali metals are potential one-electron reductants for radical coupling reactions,[50] but attempts to react 1,2,5-triphenylpentan-1,5-dione by stirring in THF over a sodium mirror resulted in destruction of the starting material (Figure 30). Magnesium has been demonstrated to perform pinacol couplings,[51] so the reaction of the diketone with magnesium in both THF and water[52] was attempted. However, no reaction was observed in either

case. Attempts to activate the magnesium with either iodine or ultrasound irradiation did not lead to any product formation either.

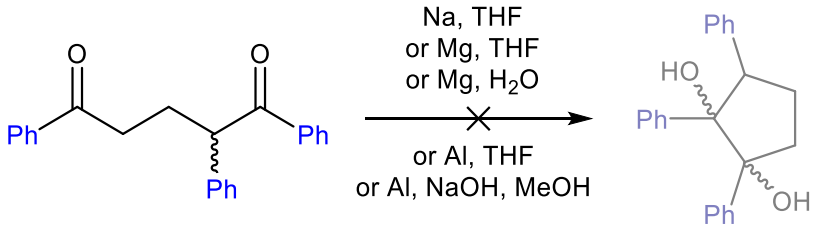

Figure 30: Attempted pinacol coupling of 1,2,5-triphenylpentan-1,5-dione using sodium, magnesium or aluminium

Aluminium powder has also been shown to be a reductant for pinacol couplings (Figure 30)[53], but attempts to use this reagent in either THF or a methanolic sodium hydroxide solution[52] gave only unreacted starting material, even with prolonged ultrasound irradiation. Potentially the use or highly reactive magnesium or aluminium powders prepared by the Rieke method[54] could lead to the desired reactivity but the lack of any product formation in our screening attempts meant this was not investigated.

Reductant	**Solvent**	**Yield of Ph_3CpH (%)**	**Success rate**
Zn	AcOH	9	1/10
Na	THF	<1%	0/2
Mg	THF	<1%	0/2
Mg	H_2O	<1%	0/1
Al	THF	<1%	0/2
Al	NaOH/MeOH	<1%	0/1

Figure 31: Table of metal (0) reagents used to attempt the pinacol coupling of 1,2,5-triphenylpentan-1,5-dione

Titanium reagents have been shown to facilitate a wide range of reductive coupling reactions, most famously exemplified by the McMurry coupling, a reaction closely related to pinacol couplings (Figure

32).[55] In titanium-induced pinacol and McMurray couplings an intermediate titanium diolate is formed[56] with protonation of this species leading to diol formation in pinacol couplings, whereas deoxygenation of this intermediate leads to alkene formation in the McMurray reaction[57]. The active reagent in these transformations in 'low-valent titanium' (LVT), generated *in situ* by reduction of titanium(III) or titanium(IV) species, typically titanium halides.[58] While a range of reducing agents are reported for generating LVT, McMurray *et al.* [59] reported that zinc is a suitable reductant when used alongside $TiCl_3$.

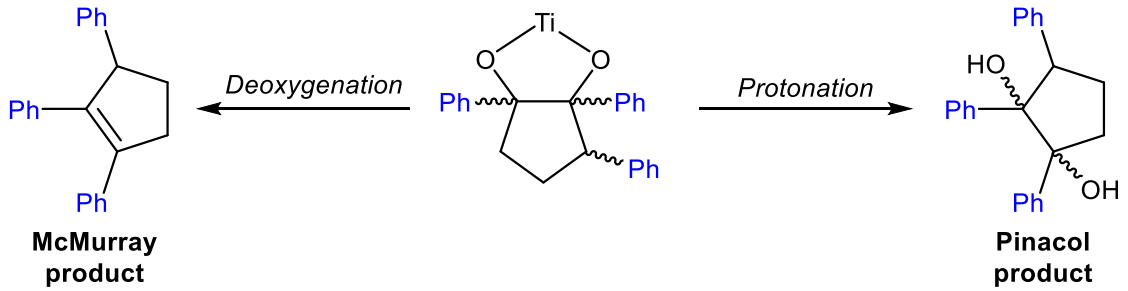

Figure 32: Formation of McMurray and pinacol products from titanium diolate intermediate

$TiCl_3$ is commercially available as a solution in aqueous HCl, and when this solution was added to zinc powder in THF under argon a dark grey suspension was formed, indicative of LVT formation (Figure 33). Presumably the acid solution 'activates' the zinc powder as intense bubbling is observed as the HCl solution, likely due to formation of hydrogen. This activation will accelerate the reaction of the $TiCl_3$ with the zinc surface. Slow addition of 1,2,5-triphenylpentan-1,5-dione dissolved in THF, followed by prolonged heating leads to the reaction mixture forming a dark blue suspension, likely due to formation of inorganic zinc-titanium species. After filtering out these solids the reaction is quenched with saturated Na_2CO_3 and extracted with ethyl acetate. This reaction produced the target diol and did not produce any of the McMurray product. The diol is difficult to purify, so instead the crude material is carried forward to the next step. Heating the material with HCl in ethanol leads to formation of **1,2,3-Ph_3CpH**. The workup is straightforward, and high purity samples can be obtained by silica filtration followed by recrystallisation from ethanol.

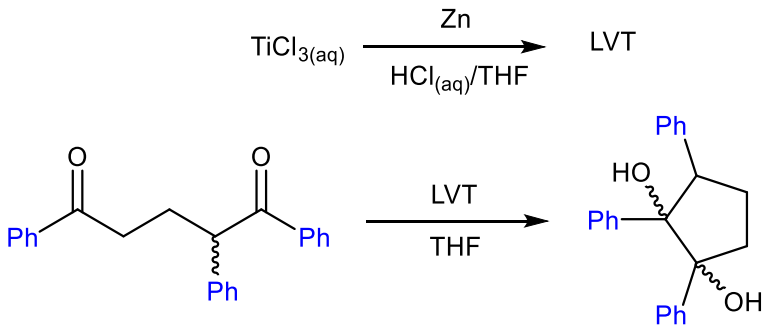

Figure 33: Formation of low-valent titanium (top) and its use for the pinacol coupling of 1,2,5-triphenylpentan-1,5-dione (bottom)

In our hands the best yield of **1,2,3-Ph$_3$CpH** from 1,2,5-triphenylpentan-1,5-dione achieved using commercial $TiCl_3$ solution (Figure 35) was 33% across the two steps. However, this procedure was found to be unreliable, and frequently failed to give any product. It has been shown that solutions of $TiCl_3$ degrade over time, especially in the presence of oxygen, but storing $TiCl_3$ solutions under argon or using freshly obtained batches did not improve the reliability of the reaction, so a high purity source of $TiCl_3$ was sought.

Commercial solid $TiCl_3$ is expensive but Jones *et al.* [60] showed that high purity $TiCl_3(THF)_3$ adduct could be made from cheap, commercially-available $3TiCl_3.AlCl_3$ powder. A slurry of $3TiCl_3.AlCl_3$ in toluene was treated with THF at low temperature, and then refluxed for 14 hours, and upon cooling a pale blue crystalline solid forms, which is worked-up by filtration and washing with hexane (Figure 34).

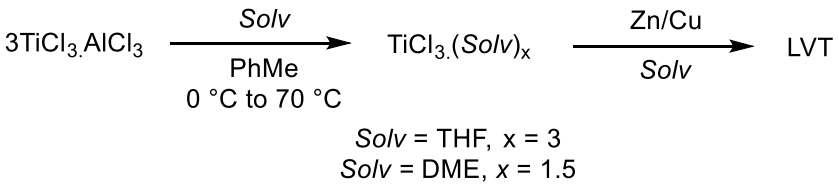

Figure 34: Synthesis of titanium trichloride adducts and their use as precursors for low-valent titanium

McMurry *et al.* [59] showed that zinc/copper couple[61] was superior to zinc for the reduction of $TiCl_3$ adducts. In our hands refluxing our $TiCl_3(THF)_3$ with an excess of commercial zinc/copper couple in THF led to formation of a black suspension (Figure 35). 1,2,5-triphenylpentan-1,5-dione in THF was added slowly to this suspension at room temperature, and the resulting mixture refluxed (Figure 35). However, monitoring this reaction by TLC and NMR showed that, no matter how long this reaction was heated, the starting material remained unreacted.

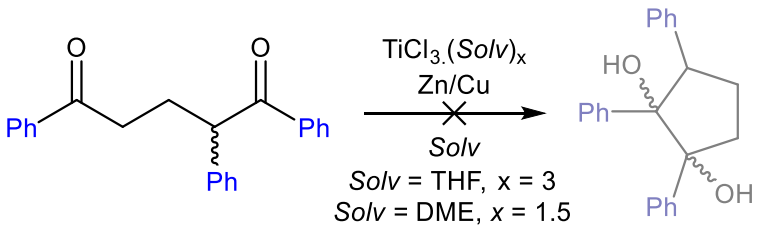

Figure 35: Attempted pinacol coupling of 1,2,5-triphenylpentan-1,5-dione using titanium trichloride adducts

In McMurray *et al.*'s [59] optimised preparations the DME adduct of titanium is described as the most effective titanium source for LVT generation, and DME to be the superior solvent for the coupling reaction. Because of this $TiCl_3(DME)_{1.5}$ was prepared from $3TiCl_3.AlCl_3$ powder in the same manner as the THF adduct. Refluxing the DME adduct with an excess of commercial zinc/copper couple in DME also led to formation of a black suspension visually identical to that formed from the THF adduct. 1,2,5-triphenylpentan-1,5-dione in DME was added to this suspension and heated at 80 °C for 38 hours (Figure 35). Once again, the starting material remained unreacted.

This result was surprising as the more rigorous procedures, using freshly distilled solvents, pure titanium reagents and reactive zinc/copper powder completely failed to generate the desired pinacol product, whereas the less rigorous procedure was shown to give the desired diol, albeit unreliably. Freshly prepared zinc-copper couple[61a] is likely to be more active than the commercial sources we used, but because we visually observed it reacting to form the desired LVT we suppose this reagent is not the primary source of the lack of observed reaction. The lack of a proton donor in our $TiCl_3(L)_x$ reactions could the reason for the lack of reactivity if proton-transfer is a required step in the pathway

towards our desired product. However, it was decided to pursue an alternative reductant for our pinacol coupling so the use of protic additives was not explored.

Samarium(II) diiodide (SmI_2) has been shown to perform a wide range of reductions and reductive couplings.[62] The ability of SmI_2 to perform pinacol couplings has been demonstrated for a variety of substrates, so its use in the synthesis of **1,2,3-Ph$_3$CpH** was investigated. Using the method described by Szostak *et al.* [63] a SmI_2 solution was prepared by first stirring samarium metal under argon to grind the solid up, then suspending the metal in THF and adding a THF solution of iodine at room temperature, leaving a small excess of solid samarium to stabilise the solution (Figure 36). The resulting mixture is heated at 65 °C for 20 hours resulting in the formation of a dark blue solution.

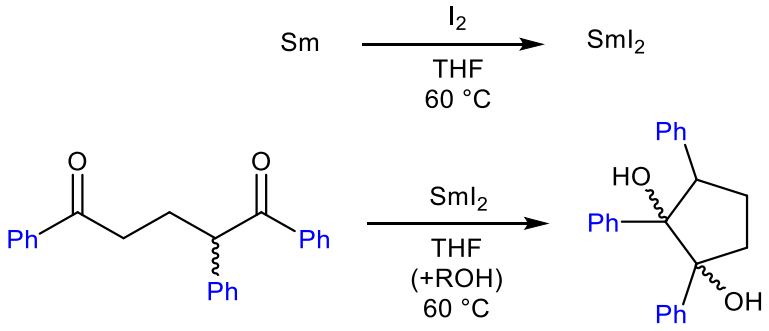

Figure 36: Formation of samarium diiodide (top) and its use for the pinacol coupling of 1,2,5-triphenylpentan-1,5-dione (bottom)

1,2,5-triphenylpentan-1,5-dione was slowly added to the SmI_2 solution at room temperature before heating the resulting mixture at 65 °C for 40 hours (Figure 36). The mixture was filtered, quenched with aqueous Na_2CO_3 and extracted with ethyl acetate. The organic fraction was washed with aqueous $Na_2S_2O_3$ to remove excess iodine during workup. The crude diol was heated with HCl in ethanol for 20 hours, before purifying **1,2,3-Ph$_3$CpH** in the same manner as described for the $TiCl_3$ synthesis. The yield of **1,2,3-Ph$_3$CpH** from 1,2,5-triphenylpentan-1,5-dione was 42% across the two steps, and although this is only moderate yield the use of SmI_2 was found to give consistent results.

The addition of a protic solvent has been found to improve the yields of reductive couplings using SmI_2 through rapid protonation of charged reaction intermediates.[62a] The addition of five equivalents of

tert-butanol to the pinacol coupling of 1,2,5-triphenylpentan-1,5-dione did not lead to an improvement in the yield of **1,2,3-Ph_3CpH**. However, it was found that the addition of 5 equivalents of methanol to the pinacol coupling (Figure 36) increased the final yield of **1,2,3-Ph_3CpH** to 60%. This preparation provides a high-yielding, reproducible synthetic route to this species and is the method of choice for accessing this **CpH** derivative. It could also provide access to other substituted-**CpH**'s starting from variously substituted pentan-1,5-diones. The main drawback of this route is the use of expensive samarium metal, which must be used with at least two equivalents per diketone. In our hands using 2.01g samarium furnished 1.08 g of 1,2,3-Ph_3CpH from 2.00 g 1,2,5-triphenylpentan-1,5-dione. Catalytic amounts of SmI_2 have been shown to perform couplings in the presence of a sacrificial reductant,[64] so using a regime like this could reduce the expense associated with this reaction.

Reductant	**Solvent**	**Yield of Ph_3CpH (%)**	**Success rate**
$TiCl_3$, Zn	THF/$HCl_{(aq)}$	33	3/17
$TiCl_3(THF)_3$, Zn/Cu	THF	<1%	0/2
$TiCl_3(DME)_3$, Zn/Cu	DME	<1%	0/2
SmI_2	THF	42	3/3
SmI_2	THF/MeOH	60	2/2

Figure 37: Table of titanium and samarium regents used to facilitate the pinacol coupling of 1,2,5-triphenylpentan-1,5-dione

2.5.2 Synthesis of 1,3,4,5,6-pentaphenyl-1,2-dihydropentalene

1,2,3-Ph_3CpH was reacted with 1,3-diphenylprop-2-en-1-one using pyrrolidine in 1:1 toluene and methanol. After working the reaction mixture up a yellow solid was obtained. NMR analysis of this material showed it to contain both the 1,2-H_2 and 1,5-H_2 isomer of **Ph_5PnH_2**, (Figure 38) alongside a third unidentified by-product. This species seems to readily isomerise, perhaps existing in equilibrium between the two isomers as a mixture is always observed. This contrasts with **Ph_4PnH_2**, which could not be induced to isomerise even in 'forcing' conditions (see above).

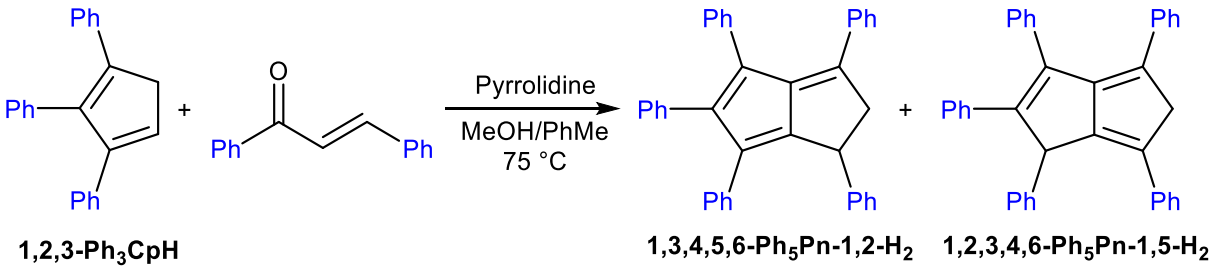

Figure 38: Synthesis of pentaphenyldihydropentalenes from 1,2,3-triphenylcyclopentadiene

The 1,5-H_2 isomer of **Ph_5PnH_2** was identified by three ^{1}H NMR signals at 5.13, 4.35 and 4.01 ppm. The singlet at 5.13 corresponded to its C1-hydrogen, and the doublets at 4.35 and 4.01 ppm corresponded to the two C5-hydrogens. The 1,2-H_2 isomer was identified by ^{1}H NMR signals at 4.48 ppm for its C1 hydrogen and at 4.00 (overlaid with signal for 1,5-H_2 C5-hydrogen) and 3.40 ppm. The shifts and coupling pattern for the 1,2-H_2 isomer of **Ph_5PnH_2** were comparable to those observed for the **1,3,4,6-Ph_4PnH_2**, which exists exclusively as its 1,2-H_2 isomer.

Attempts to separate these species were unsuccessful. Chromatography on silica did not allow separation as the components had very similar R_f values in all the solvent systems tried. Recrystallisation from a variety of solvents gave solids with the same composition as the 'crude' material.

2.5.3 Attempted synthesis of 1,2,3,4,5,6-hexaphenyl-1,2-dihydropentalene

Le Goff [37] reported the synthesis of **1,2,3,4,5,6-Ph_6PnH_2** from **1,2,3-Ph_3CpH** and 1,2,3-triphenyl-2-propen1-one using KF in DMSO. We sought to synthesise this **PnH_2** derivative as double deprotonation of it would yield **1,2,3,4,5,6-Ph_6Pn^{2-}**, the pentalenide analogue of the **Ph_5Cp^-** ligand. Le Goff's report lacks any experimental details, so a synthetic procedure needed to be devised.

1,2,3-Ph_3CpH and 1,2,3-triphenyl-2-propen1-one were refluxed in DMSO with an excess of KF (Figure 39), then the solvent was removed under reduced pressure. Analysis of the crude material by NMR showed that the **1,2,3-Ph_3CpH** was unreacted, with unidentified organic by-products present in the mixture, presumably arising from degradation of the enone. Using toluene, methanol or a 50:50 mixture of the two as the solvent also left the **1,2,3-Ph_3CpH** unreacted.

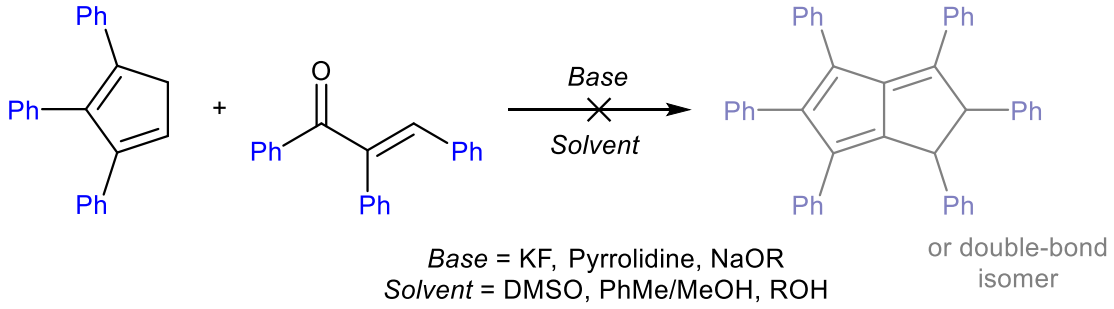

Figure 39: Attempted synthesis of 1,2,3,4,5,6-hexaphenyldihydropentalene from 1,2,3-triphenylcyclopentadiene

Pyrrolidine has been shown to be effective for forming **Ph_4PnH_2**, so it was hoped that it would also facilitate the synthesis of **Ph_6PnH_2**. **1,2,3-Ph_3CpH** and 1,2,3-triphenyl-2-propen-1-one were heated in 50:50 methanol and toluene with an excess of pyrrolidine (Figure 39) for 3 days, then the solvent was removed under reduced pressure. Once again NMR analysis of the crude material showed the **1,2,3-Ph_3CpH** was unreacted and that the pyrrolidine had degraded the enone.

Alkali metal alkoxides were also shown to facilitate the synthesis of **Ph_4PnH_2**, so the use of these bases for synthesising **Ph_6PnH_2** was investigated. **1,2,3-Ph_3CpH** and 1,2,3-triphenyl-2-propen1-one were

refluxed in methanol with an excess of sodium methoxide (Figure 39) for 2 days, and the solvent removed under reduced pressure. No reaction was observed by NMR analysis of the crude material. Potassium *tert*-butoxide in *tert*-butanol also failed to facilitate the desired condensation.

The inability to react **1,2,3-Ph$_3$CpH** with the triphenyl-enone led us to investigate an alternative. The condensation of 6-substituted fulvenes with ketones has been shown to furnish **PnH$_2$** species,[40a] including **Ph$_4$PnH$_2$** (Section 2.4.2). We supposed that the reaction of **1,2,3,6-Ph$_4$Fv** with deoxybenzoin could provide access to **Ph$_6$PnH$_2$**.

1,2,3,6-Ph$_4$Fv was prepared according to the method described by Pauson and Williams.[65] **1,2,3-Ph$_3$CpH** was heated for 20 hours with benzaldehyde and sodium methoxide in methanol. Upon cooling, the resulting solid was collected by filtration, washed with cold methanol and recrystallised from ethanol to give **1,2,3,6-Ph$_4$Fv** as a light orange solid in 60% yield.

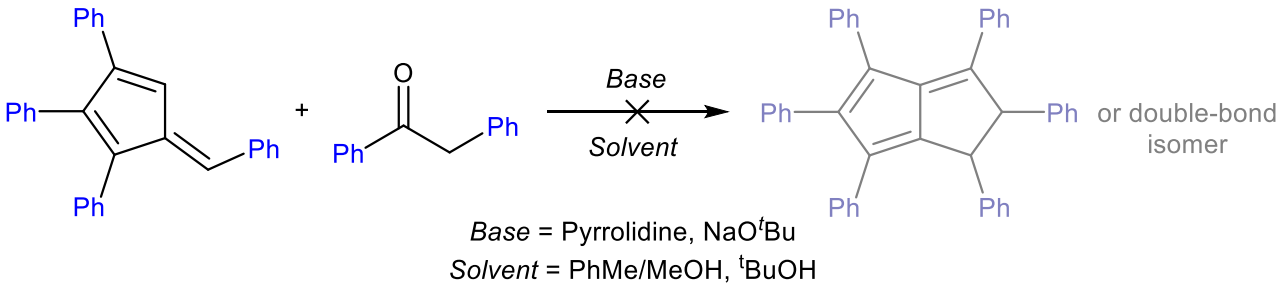

Figure 40: Attempted synthesis of 1,2,3,4,5,6-hexaphenyldihydropentalene from 1,2,3,6-tetraphenylfulvene

1,2,3,6-Ph$_4$Fv and deoxybenzoin were dissolved in 50:50 toluene and methanol, and pyrrolidine was added (Figure 40) and the reaction mixture heated at 70 °C for 40 hours. After removing the solvent, the crude material was analysed by NMR, which showed that the fulvene had not reacted and that the deoxybenzoin was decomposed into unidentified organic products. Similarly the reaction using sodium methoxide in 50:50 methanol:toluene or using potassium *tert*-butoxide in *tert*-butanol failed to cause the fulvene to react.

2.6 Conclusion and future work

In this chapter the synthesis of several **PnH_2** derivatives from **CpH**s has been described. A range of bases were shown to facilitate the reaction of **CpH** with the relevant carbonyl compounds. The gram-scale synthesis of **Ph_4PnH_2** was demonstrated, using cheap, commercially available reagents. The literature synthesis of **Ph_2CpH** was improved, providing large quantities of starting material for synthesising **Ph_4PnH_2**. Unlike the **PnH_2** species formed by pyrolysis (Section 1.2.2), **Ph_4PnH_2** forms in relatively mild conditions without the need for specialised equipment. This species was found to not be thermolabile like the parent **PnH_2** species, allowing it to be stored without degradation. Access to large amounts of this material allowed exploration of its deprotonation chemistry (Chapter 3).

Difficulties were encountered synthesising the more highly-arylated **PnH_2** derivatives. Literature preparations of the **Ph_3CpH** starting material failed to give this species in suitable quantities. However, a high-yielding, reliable synthetic procedure was devised, utilising the SmI_2-facilitated pinacol coupling of 1,2,5-pentan-1,5-dione. This pinacol coupling strategy could potentially be used to access other 1,2,3-trisbustituted **CpH**s for **PnH_2** synthesis (Section 4.5).

A pure sample of **Ph_5PnH_2** was not obtained. This formation of the 1,2-H_2 and 1,5-H_2 isomer of this **PnH_2** was observed by NMR, but these isomers could not be separated from each other or from an unidentified by-product. The presence of the two isomers is comparable to the reported isomerisation of **Ph_2PnH_2**, even though in our hands only the 1,5-H_2 isomer of **Ph_2PnH_2** was observed. However, the reason **Ph_5PnH_2** forms as two isomers when **Ph_4PnH_2** does not is not clear.

Ph_6PnH_2 was reportedly synthesised by Le Goff,[37] but this synthesis could not be replicated using a variety of approaches. Using potassium fluoride as described in Le Goff's preparation did not result in any reaction occurring. A range of bases were shown to facilitate the formation of **Ph_4PnH_2** but attempts to apply these reagents to the synthesis of **Ph_6PnH_2** all failed. Further work could find a suitable system for the synthesis of this **PnH_2** derivative. However, issues of solubility found for **Ph_4Pn^{2-}** (chapter 3), and the reported issues of solubility for highly-arylated **Cp^-** derivatives, means that further

investigation of the highly phenyl-substituted species **Ph_5PnH_2 and Ph_6PnH_2** may not be worth pursuing for use in organometallic chemistry. .

Future work would focus on obtaining pure samples of some of the the **PnH_2**s that were not appropriately isolated. While **Ph_2PnH_2**, was formed in the reactions conducted, it could not be sufficiently purified in order to carry it forwards into deprotonation reactions. Further investigation would look at modifying reaction conditions, such as temperature, solvent and the bases used, in order to suppress the formation of by-products, allowing easier purification of the crude product. If this is not successful then the current synthesis conditions could be used with modified work-up procedures - for example, altering the chromatography procedures, using distillation/sublimations or by separating the components of the crude material by careful fractional crystallisations.

Because a suitable sample of **PhCpH** could not be obtained from 2-cyclopentenone using either PhLi or PhMgBr, the synthesis of **1,3,5-Ph_3PnH_2** could not be attempted**.** Nifant'ev *et al.*[28] reported difficulties with this synthetic route leading them devise an alternative preparation. 3-phenylcyclopent-2-en-1-one[17] is converted to a hydrazine through its reaction with tosylhydrazide (Figure 41). This species then undergoes a Shapiro reaction[66] when treated with BuLi in ether to give, upon quenching with NH_4Cl, **PhCpH** in 31% yield across the 2 steps. If this procedure could be replicated it would provide starting material to attempt the synthesis of **1,3,5-Ph_3PnH_2.** Additionally, Riemschneider and Nerin[26] report that 3-phenyl-2-cyclopenten-1-one could be converted directly into **PhCpH** by reacting it with aluminium isopropoxide, so this route could also potentially provide the desired **CpH** derivative.

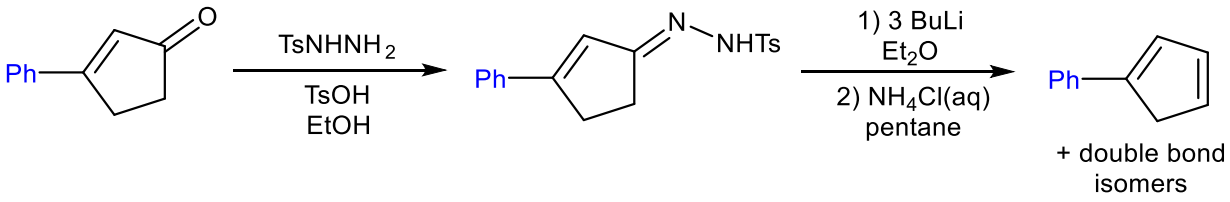

Figure 41: Synthesis of phenylcyclopentadiene from 3-phenylcyclopent-2-en-1-one

Because it has been shown that **1,4-Ph$_2$CpH** condenses successfully with 1,3-diphenylprop-2-en-1-one to give **1,3,4,6-Ph$_4$PnH$_2$**, we suppose that **1,2-Ph$_2$CpH** could be used to synthesise the structural isomer **1,3,5,6-Ph$_4$PnH$_2$** (Figure 42). This could potentially be used to form **1,3,5,6-Ph$_4$Pn^{2-}**, a ligand with two binding sites that would display similar electronic properties but different steric environments.

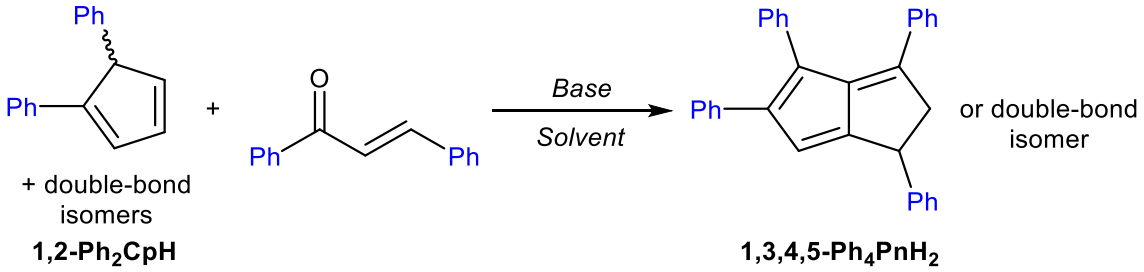

Figure 42: Synthesis of 1,3,5,6-tetraphenyldihydropentalene from 1,2-diphenylcyclopentadiene

Several syntheses of **1,2-Ph$_2$CpH** have been reported. As for the synthesis of **Ph$_3$CpH** the pinacol coupling of 1,5-pentan-1,5-dione gives a cyclopentan-1,2-diol derivative that, upon treating with acid, dehydrates to give **1,2-Ph$_2$CpH** (Figure 43). This pinacol coupling has been reported using several reagents,[67] including $SmBr_2$.[68] It has been demonstrated in this chapter that SmI_2 is a useful reagent for their transformation and could potentially be applied to this synthesis.

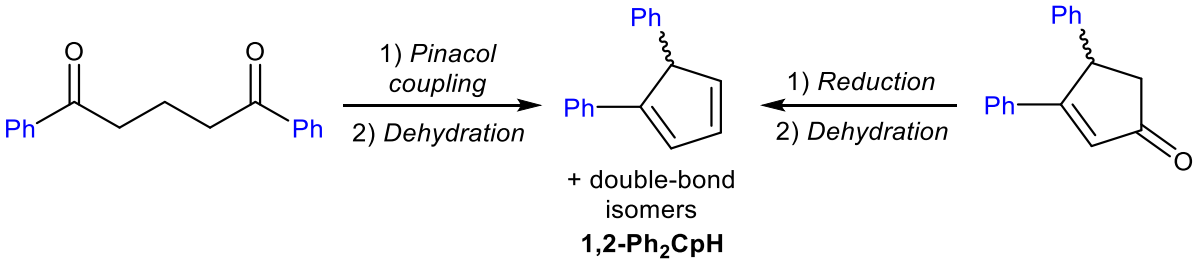

Figure 43: Synthesis of 1,2-diphenylcyclopentadiene

Zhang *et al.* [55] reported that **1,2-Ph$_2$CpH** could be synthesised from 3,4-diphenyl-2-cyclopenten-1-one (Figure 43).[69] The reaction of sodium borohydride with 3,4-diphenyl-2-cyclopenten-1-one gives an alcohol that can be treated with concentrated HCl to give **1,2-Ph$_2$CpH**. If this **CpH** derivative could be obtained in suitable amounts and purity the synthesis of **1,3,4,5-Ph$_4$PnH$_2$** could be attempted using the methods described for **1,3,4,6-Ph$_4$PnH$_2$**.

2.7 Experimental

General: All reactions and workups were carried out in air unless specified otherwise. Reactions under argon were performed using standard Schlenk techniques or an MBraun Unilab Plus glovebox. NMR spectroscopy was conducted using a 500 MHz Bruker Avance III at 25 °C. Chemical shifts (δ) are reported in ppm. Mass spectrometry was carried out at the EPSRC UK National Mass Spectrometry Facility in Swansea. Single crystal X-ray diffraction analysis was carried out by Dr Gabriele Kociok-Köhn at the University of Bath using a RIGAKU SuperNova Dual. UV/Vis spectroscopy was conducted using an Avantes AvaLight-DH-S-BAL light source and an Avantes AvaSpec-2048L spectrometer. Commercially available materials were obtained from Sigma Aldrich, Fisher or Acros. Methanol was dried by distillation from magnesium. Toluene was dried by distillation from sodium. THF, Et_2O and hexane were dried by distillation from potassium. d_8-THF was dried by distillation from potassium and stored over a sodium mirror. *Tert*-butanol and acetonitrile were dried by distillation from calcium hydride and stored over 4 Å molecular sieves. Dicyclopentadiene was dried over sodium prior to use. 1,3-diphenylprop-2-en-1-one and deoxybenzoin were purified by recrystallisation from ethanol. 2-cyclopentenone was purified by distillation. Bromobenzene, acetophenone, benzaldehyde and benzoylethylpropionate were purified by distillation from calcium hydride. Pyrrolidine was purified by drying over sodium followed by distillation. 18-crown-6 was purified by recrystallization from dry acetonitrile. $TiCl_3(THF)_3$ and $TiCl_3(DME)_{1.5}$ were prepared according to literature procedures.[60]

1,4-Diphenyl-1,3-cyclopentadiene: Under argon, benzoylethylpropionate (7.20 g, 35.0 mmol) in 10 ml dry toluene was added dropwise to sodium ethoxide (5.00 g, 73.5 mmol) in 40 ml dry toluene at 0 °C, and the solution was allowed to warm to room temperature. To this red solution was added acetophenone (4.20 g, 35.0 mmol), and the resulting solution was stirred at 45 °C for 72 hours. The solution was cooled to 0 °C, and in air 150 ml water was slowly added. The solution is warmed to room temperature and stirred for 1 hr. 150 ml diethyl ether was added, the aqueous fraction was collected

and warmed to 70 °C for 2 hours. The resulting yellow solid is filtered, washed with 2x50 ml water and recrystallized from ethanol to give a yellow crystalline solid (3.55 g, 16.3 mmol, 47%);

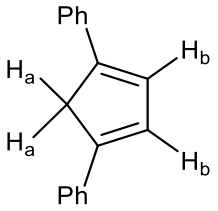

^{1}H NMR (500 MHz, C_6D_6): δ = 7.48 (***o*-Ph,** d, 4H, $^3J_{HH}$ = 7.33Hz), 7.26 (***m*-Ph,** t, 4H, $^3J_{HH}$ = 7.90 Hz), 7.13 (***p*-Ph,** t, 2H, $^3J_{HH}$ = 7.33 Hz), 6.86 (**H_b**, s, 2H), 3.70 (**H_a**, s, 2H); these data agree with those previously reported [17]

1,3,6-Triphenylfulvene: As described by Peloquin *et al.*[8a] 1,4-Diphenyl-1,3-cyclopentadiene (1.00 g, 4.58 mmol) and benzaldehyde (0.52 ml, 5.04 mmol) were dissolved in 20 ml dry methanol under argon, and to this was added pyrrolidine (0.48 ml, 4.58 mmol). The resulting mixture was stirred at room temperature for 20 hours leading to formation of a dark red precipitate. The mixture was filtered in air, and the precipitate washed with 3x10 ml cold methanol. The solid was recrystallised from ethanol to give a dark red crystalline solid (1.33 g, 4.35 mmol, 95%);

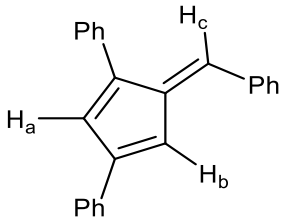

^{1}H NMR (500 MHz, $CDCl_3$): δ = 7.63 (***o*-Ph**, d, 2H, $^3J_{HH}$ = 7.75 Hz), 7.56 (***o*-Ph**, d, 2H, $^3J_{HH}$ = 7.59 Hz), 7.17-7.42 (***o*-Ph**, ***m*-Ph**, ***p*-Ph**, **H_c**, m, 12H), 6.97 (**H_a**, s, 1H), 6.93 (**H_b**, d, 1H, $^4J_{HH}$ = 1.54 Hz); these data agree with those previously reported [8a]

1,3,4,6-tetraphenyl-1,2-dihydropentalene:

Method A: 1,4-diphenyl-1,3-cyclopentadiene (1.00 g, 4.58 mmol) and 1,3-diphenylprop-2-en-1-one (1.05 g, 5.04 mmol) were dissolved in 20 ml dry methanol and 20ml dry toluene under argon.

Pyrrolidine (0.40 ml, 5.04 mmol) was added, and the resulting solution was stirred for 40 hours at 70 °C. To the dark red solution was added 5 ml acetic acid in air, and the solvent was removed under reduced pressure. The crude material was dissolved in 150 ml diethyl ether and washed with 3x150 ml water then 150 ml aqueous Na_2CO_3, 100 ml water and 150 ml brine. The ether fraction was dried over $MgSO_4$ and the solvent volume reduced to 30ml under reduced pressure. The fraction was then filtered through silica using 1:1 diethyl ether:hexane as the eluent, and the solvent removed under reduced pressure. The resulting dark red solid was recrystallized from ethanol to give the dark red crystalline solid (1.55 g, 3.80 mmol, 83%).

Method B: 1,4-diphenyl-1,3-cyclopentadiene (1.00 g, 4.58 mmol) and 1,3-diphenylprop-2-en-1-one (1.05 g, 5.04 mmol) were dissolved in 20 ml dry methanol and 20 ml dry toluene under argon. To this was added a solution of potassium fluoride (0.47 g, 4.58 mmol) and 18-crown-6 (1.20 g, 4.58 mmol) in 10 ml dry toluene and 10 ml dry methanol. The resulting solution was stirred for 48 hours at 70 °C. The solvent was removed under reduced pressure. In air the crude material was dissolved in 150 ml diethyl ether and washed with 3x150 ml water and 150 ml brine. The ether fraction was dried over $MgSO_4$ and the solvent the solvent removed reduced pressure. The fraction was then filtered through silica using 1:1 diethyl ether:hexane as the eluent, and the solvent removed under reduced pressure. The resulting dark red solid is recrystallized from ethanol to give the dark red crystalline solid (0.77 g, 1.88 mmol, 41%).

Method C: 1,4-diphenyl-1,3-cyclopentadiene (1.00 g, 4.58 mmol) and 1,3-diphenylprop-2-en-1-one (1.05 g, 5.04 mmol) were dissolved in 20 ml dry methanol under argon. To this was added sodium methoxide (0.25 g, 4.58 mmol) in 20 ml dry methanol, and to the resulting solution was stirred for 48 hours at 70 °C. The solvent was removed under reduced pressure. In air the crude material was dissolved in 150 ml diethyl ether and washed with 3x150 ml water and 150 ml brine. The ether fraction was dried over $MgSO_4$ and the solvent the solvent removed reduced pressure. The fraction was then filtered through silica using 1:1 diethyl ether:hexane as the eluent, and the solvent removed under

reduced pressure. The resulting dark red solid is recrystallized from ethanol to give the dark red crystalline solid (1.21 g, 2.98 mmol, 65%).

Method D: 1,4-diphenyl-1,3-cyclopentadiene (1.00 g, 4.58 mmol) and 1,3-diphenylprop-2-en-1-one (1.05 g, 5.04 mmol) were dissolved in 20 ml dry THF under argon. To this was added sodium *tert*-butoxide (0.44 g, 4.58 mmol) in 20 ml dry THF, and to the resulting solution was stirred for 44 hours at 70 °C. The solvent was removed under reduced pressure. In air the crude material was dissolved in 150 ml diethyl ether and washed with 3x150 ml water and 150 ml brine. The ether fraction was dried over $MgSO_4$ and the solvent the solvent removed reduced pressure. The fraction was then filtered through silica using 1:1 diethyl ether:hexane as the eluent, and the solvent removed under reduced pressure. The resulting dark red solid is recrystallized from ethanol to give the dark red crystalline solid (0.99 g, 2.43 mmol, 53%).

Method E: 1,3,6-Triphenylfulvene (0.50 g, 1.63 mmol) and acetophenone (0.21 ml, 1.80 mmol) were dissolved in 10 ml methanol and 10 ml toluene under argon, and to this was added pyrrolidine (0.14 ml, 1.63 mmol). The resulting mixture was stirred at 70 °C for 42 hours. The solvent was removed under reduced pressure. In air the crude material was dissolved in 150 ml diethyl ether and washed with 3x150 ml water and 150 ml brine. The ether fraction was dried over $MgSO_4$ and the solvent the solvent removed reduced pressure. The fraction was then filtered through silica using 1:1 diethyl ether:hexane as the eluent, and the solvent removed under reduced pressure. The resulting dark red solid is recrystallized from ethanol to give the dark red crystalline solid (0.48 g, 1.17 mmol, 72%);

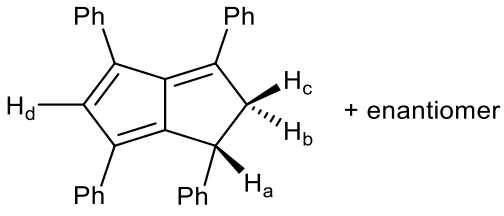

+ enantiomer

^{1}H NMR (500 MHz, C_6D_6): δ = 6.98-7.32 (**H_d, Ph,** m, 21H), 4.52 (**H_a**, dd, 1H, $^3J_{HH}$ = 6.85 Hz, $^3J_{HH}$ = 1.75 Hz), 4.05 (**H_c**, dd, 1H, $^3J_{HH}$ = 6.85 Hz, $^2J_{HH}$ = 18.59 Hz), 3.37 (**H_b**, dd, 1H, $^3J_{HH}$ = 1.75 Hz, $^2J_{HH}$ = 18.82 Hz);

$^{13}C\{^{1}H\}$ NMR (125 MHz, C_6D_6): δ = 154.51, 148.29, 146.57, 144.21, 139.19, 136.59, 135.19, 135.03, 130.43, 130.05, 130.00, 129.48, 128.71, 128.32, 128.22, 127.95, 127.84, 127.35, 126.36, 126.12, 55.14, 42.71;

HR ASAP-MS (+): m/z (expected) = 409.1956 [M+H]; (found) = 409.1953 [M+H]

UV/vis: $\lambda_{max}(\varepsilon)$ = 300 nm (34964 dm^3 mol^{-1} cm^{-1}), 338 nm (27855 dm^3 mol^{-1}), 465 nm (3432 dm^3 mol^{-1} cm^{-1})

Melting point: 180-181 °C

(2-benzoylethyl)trimethylammonium iodide: As described by Abid *et al*.[47b] acetophenone (13 ml, 111 mmol), dimethyl amine hydrochloride (10 g, 123 mmol) and paraformaldehyde (3.69 g. 123 mmol) were dissolved in 100 ml ethanol with 5 ml concentrated hydrochloric acid, and the resulting solution refluxed for 3 days. The ethanol was removed under reduced pressure, and the resulting slurry washed with 100 ml acetone and filtered. The solid was dissolved in 50 ml saturated $NaHCO_3$ solution and extracted with 3x50 ml ethyl acetate. The solvent was removed under reduced pressure to give a yellow oil. This oil as dissolved in 100 ml diethyl ether, and methyl iodide (4.98 ml, 0.111mol) was added. The resulting solution was stirred for 16 hours at room temperature. The solution was filtered, and the solid washed with 2x50 ml diethyl ether and dried under reduced pressure to give a white solid (13.52 g, 70.5 mmol, 64%);

^{1}H NMR (500MHz, D_2O): δ = 7.97 (d, 2H, $^{3}J_{HH}$ = 7.82 Hz), 7.60 (t, J_{HH} = 7.63Hz, 1H), 7.51 (t, 2H, $^{3}J_{HH}$ = 7.82 Hz), 4.70 (s, 9H), 3.20 (s, 2H), 2.88 (s, 6H); this data agree with that previously reported.[47b]

1,2,5-Triphenylpentan-1,5-dione: 3-chloropropiophenone (5.00 g, 29.65 mmol) and deoxybenzoin (5.82 g, 29.65 mmol) were dissolved in 40 ml dry methanol under argon, and to this was added sodium methoxide (1.60 g, 29.65 mmol) in 20 ml dry methanol. The resulting solution was stirred at 60 °C for 40 hours. 5 ml acetic acid was added in air, and then the solvent was removed under reduced pressure. The residue was dissolved in 150 ml diethyl ether and washed with 4 x 100ml water and 100 ml brine.

The organic fraction was dried over $MgSO_4$ and the solvent removed under reduced pressure. The solid was recrystallized from ethanol to give a pale cream solid (7.78g, 23.72 mmol, 80%)

^{1}H NMR (500 MHz, $CDCl_3$): δ = 7.91 (d, 2H, J_{HH} = 7.65 Hz), 7.83 (d, 2H, J_{HH} = 8.51 Hz), 7.47 (t, 1H, J_{HH} = 6.80 Hz) 7.42-7.27 (m, 5H), 7.25-7.10 (m, 5H), 4.70 (t, 1H, J_{HH} = 7.49 Hz), 2.90 (m, 2H) 2.51 (quintet, 1H, J_{HH} = 6.98 Hz), 2.22 (quintet, 1H, J_{HH} = 6.90 Hz); these data agree with those previously reported.[70]

3a,4,7,7a-tetrahydro-2,3-diphenyl-7-methano-1H-inden-1-one: As described by Lee *et al*.[41] diphenylacetylene (1.78 g, 10.00 mmol) and dicobalt octacarbonyl (3.42 g, 10.00 mmol) were dissolved in 50 ml dry toluene under argon and stirred at room temperature for 2 hours. To this solution was added norbornadiene (5.5 ml, 50 mmol) and 2 ml dry DMSO, and the resulting solution stirred at 50 °C for 120 hours. The reaction solution is filtered through silica in air, washed with 2x50 ml brine, dried over $MgSO_4$ and the solvent removed under reduced pressure to give a yellow solid. The product is recrystallized in ethyl acetate to give a white solid (1.81 g, 6.07 mmol, 37%);

^{1}H NMR (500MHz, $CDCl_3$): δ = 7.64-6.96 (m, 10H), 6.40-6.06 (m, 2H), 3.41 (q, 1H, $^3J_{HH}$ = 7.90 Hz) 3.29 (d, 1H $^3J_{HH}$ = 5.62 Hz), 3.06 (s, 1H), 2.55 (d, 2H, $^3J_{HH}$ = 5.87 Hz); these data agree with those previously reported.[41]

3a,4,7,7a-tetrahydro-1-methoxy-1,2,3-triphenyl-4,7-methano-1H-indene: As described by Lee *et al*.[41] 3a,4,7,7a-tetrahydro-2,3-diphenyl-7-methano-1H-inden-1-one (2.50 g, 8.30 mmol) was dissolved in 20 ml diethyl ether under argon and to this was added phenyl magnesium bromide (generated *in situ* by stirring 1.67 ml bromobenzene over magnesium, 0.125 mol) in 20 ml diethyl ether at 0 °C. The solution was allowed to warm to room temperature and was stirred for 18 hours. In air 20 ml saturated ammonium chloride solution was added, and the organic fraction collected, dried over $MgSO_4$ and the solvent removed under reduced pressure to give a dark yellow oil. The Grignard reaction product was dissolved in 20 ml acetonitrile under argon, and to this was added sodium hydride (0.22 g, 9.36 mmol) in 20 ml acetonitrile at 0 °C. The solution was allowed to warm to room temperature and was stirred for 2 hours. Methyl iodide (0.780 ml, 0.011 mol) was added dropwise, and the resulting solution stirred

for 16 hours. In air 50 ml diethyl ether and 50 ml water were added, and the ether fraction collected. The aqueous phase was extracted with 50 ml ether, and the combined organic phases were dried over $MgSO_4$ and the solvent removed under reduced pressure to give a yellow oil (1.10 g, 2.82 mmol, 34%);

^{1}H NMR (500MHz, $CDCl_3$): δ = 7.30 (d, 2H, $^3J_{HH}$ = 7.83 Hz), 7.24-6.98 (m, 8H), 6.94 (d, 2H $^3J_{HH}$ = 5.59 Hz), 6.88 (d, 1H, $^3J_{HH}$ = 8.69 Hz), 6.05 (dq, 1H, $^3J_{HH}$ = 14.22 Hz, $^3J_{HH}$ = 2.80 Hz), 3.59 (s, 1H), 1.68 (quintet, 1H, $^3J_{HH}$ = 4.42 Hz); these data agree with those previously reported.[41]

1,2,3-Triphenyl-1,3-cyclopentadiene:

Method A: Zinc dust (1.98 g, 30.47 mmol) was suspended in 20 ml acetic acid under argon. To this was added dropwise 1,2,5-triphenylpentan-1,5-dione (2.00 g, 6.10 mmol) in 30 ml acetic acid, and the resulting mixture heated at 100 °C for 24 hours. The resulting solution was cooled and then in air was poured into 50 ml water at 0 °C. This resulted in the formation of a cream solid that was collected by filtration. The solid was washed with 20 ml water and 20 ml cold methanol. The resulting oil was dissolved in 100 ml ethanol, and to this was added 1 ml concentrated HCl. The resulting solution was heated at 80 °C for 20 hours. The solvent was removed under reduced pressure, and the residue dissolved in 150 ml diethyl ether. The solution was washed with 100 ml saturated Na_2CO_3 solution and 3x100 ml water. The ether fraction was dried over $MgSO_4$ and the solvent removed under reduced pressure. The resulting solid was recrystallised from ethanol to give a yellow crystalline solid (0.16 g, 0.55 mmol, 9%);

Method B: Low-valent titanium was prepared by first suspending zinc powder (0.88 g, 13.4 mmol) in dry THF under argon. To this mixture 20% $TiCl_3$ in 2N HCl solution (10.33 ml, 13.4 mmol) was slowly added at 0 °C. The solution was allowed to room temperature and stirred for 2 hours, giving a dark grey LVT suspension. To this suspension was added dropwise 1,2,5-triphenylpentan-1,5-dione (2.00 g, 6.10 mmol) in 10ml dry THF, and the resulting mixture was heated at 70 °C for 44 hours. The resulting purple suspension was filtered in air, and the solids extracted 3x50 ml ethyl acetate. The combined organic fractions were washed with 2x100 ml saturated Na_2CO_3 solution and 2x100 ml water. The

organic fraction was dried over $MgSO_4$ and the solvent removed under reduced pressure. The resulting oil was dissolved in 100 ml ethanol, and to this was added 1 ml concentrated HCl. The resulting solution was heated at 80 °C for 20 hours. The solvent was removed under reduced pressure, and the residue dissolved in 150 ml diethyl ether. The solution was washed with 100 ml saturated Na_2CO_3 solution and 3x100 ml water. The ether fraction was dried over $MgSO_4$ and the solvent removed under reduced pressure. The resulting solid was recrystallised from ethanol to give a yellow crystalline solid (0.59 g, 2.01 mmol, 33%)

Method C: A SmI_2 solution was prepared according to the procedure described by Szostak *et al.*[63] Sm (2.01 g, 13.41 mmol) was stirred under argon for 20 hours. To the finely ground Sm was added 20ml dry THF, followed by iodine (3.40 g, 26.81 mmol) dissolved in 10ml THF. The resulting solution was heated at 60 °C for 24 hours to give a dark blue SmI_2 solution. To the solution was added 1,2,5-triphenylpentan-1,5-dione (2.00 g, 6.10 mmol) and methanol (2.5 ml, 60.95 mmol) dissolved in 10ml dry THF, and the resulting mixture was heated at 60 °C for 40 hours. The solution was cooled to room temperature and in air was added to 50 ml saturated Na_2CO_3 solution. The mixture was extracted with 100 ml ethyl acetate, and the organic fraction washed with 50 ml saturated $Na_2S_2O_3$ solution and 3 x 50 ml water. The organic fraction was dried over $MgSO_4$ and the solvent removed under reduced pressure. The resulting oil was dissolved in 100 ml ethanol, and to this was added 1 ml concentrated HCl. The resulting solution was heated at 80 °C for 20 hours. The solvent was removed under reduced pressure, and the residue dissolved in 150 ml diethyl ether. The solution was washed with 100 ml saturated Na_2CO_3 solution and 3 x 100 ml water. The ether fraction was dried over $MgSO_4$ and the solvent removed under reduced pressure. The resulting solid was recrystallised from ethanol to give a yellow crystalline solid (1.08 g, 3.66 mmol, 60%);

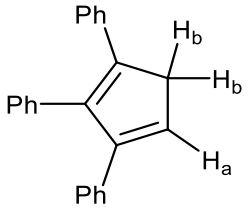

^{1}H NMR (500 MHz, C_6D_6): δ = 7.24-6.90 (***o*-Ph, *m*-Ph, *p*-Ph**, m, 15H), 6.35 (**H_a**, t, 1H, $^4J_{HH}$ = 1.91 Hz), 3.29 (**H_b**, d, 2H, $^4J_{HH}$= 1.91 Hz); these data agree with those previously reported.[41]

1,2,3-triphenylprop-2-en-1-one: As described by Lu *et al.*[71] deoxybenzoin (3.90 g, 20.00 mmol) and benzaldehyde (2.34 g, 22.00 mmol) were dissolved in 80 ml ethanol, and to this was added 80 ml 0.1 M potassium hydroxide solution. The resulting solution was stirred at room temperature for 96 hours. The ethanol is removed under reduced pressure, and the solution extracted with 3x50 ml ethyl acetate. The combined organic phases were washed with 100 ml 1M HCl solution, 2x100 ml water and 100 ml brine, dried over $MgSO_4$ and the solvent removed under reduced pressure. The resulting solid is recrystallized from ethanol 3 times to give a white solid (2.23 g, 7.85 mmol 40%);

^{1}H NMR (500MHz, $CDCl_3$): δ = 7.95 (d, 2H, $^3J_{HH}$ = 7.29 Hz), 7.47 (t, 1H, $^3J_{HH}$ = 7.29 Hz), 7.37 (t, 2H, J_{HH} = 8.02 Hz), 7.21-7.45 (m, 8H), 7.10 (m, 2H); these data agree with those previously reported.[71]

1,2,3,6-Tetraphenylfulvene: As described by Pauson and Williams,[65] 1,2,3-triphenylcyclopentadiene (0.50 g, 1.70 mmol) and benzaldehyde (0.19 ml, 1.87 mmol) were dissolved in 30 ml dry methanol under argon. To this was added sodium methoxide (0.09 g, 1.70 mmol) in 10 ml dry methanol, and the resulting solution heated at 60 °C for 20 hours. The reaction mixture was cooled to room temperature, and the precipitate collected by filtration in air. The precipitate was washed with 10 ml cold water and 3 x 10 ml cold methanol. The solid was recrystallised from ethanol to give an orange crystalline solid (0.39 g, 1.02 mmol, 60%).

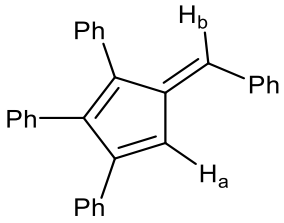

^{1}H NMR (500 MHz, $CDCl_3$): δ = 7.54 (***o*-Ph**, d, 2H, $^{3}J_{HH}$ = 8.21 Hz), 7.35, (***m*-Ph**, t, 2H, $^{3}J_{HH}$ = 7.74 Hz), 7.29 (***p*-Ph**, t, 1H, $^{3}J_{HH}$ = 7.34 Hz), 7.02-7.25 (***o*-Ph**, ***m*-Ph**, ***p*-Ph**, **H_b**, m, 14H), 6.88 (***p*-Ph**, **H_a**, m, 3H); these data agree with those previously reported.[65]

2.8 Bibliography

1. Cloke, F. G. N.; Green, J. C.; Kilpatrick, A. F. R.; O'Hare, D., Bonding in pentalene complexes and their recent applications. *Coordin Chem Rev* **2017,** *344*, 238-262.

2. Field, L. D.; Lindall, C. M.; Masters, A. F.; Clentsmith, G. K. B., Penta-arylcyclopentadienyl complexes. *Coordin Chem Rev* **2011,** *255* (15), 1733-1790.

3. A. Hirsch, J., Table of Conformational Energies—1967. 2007; Vol. 1, pp 199-222.

4. Boiadjiev, S. E.; Lightner, D. A., Steric Size in Conformational Analysis. Steric Compression Analyzed by Circular Dichroism Spectroscopy. *J Am Chem Soc* **2000,** *122* (46), 11328-11339.

5. Hammett, L. P., The Effect of Structure upon the Reactions of Organic Compounds. Benzene Derivatives. *J Am Chem Soc* **1937,** *59* (1), 96-103.

6. Lewis, M.; Bagwill, C.; Hardebeck, L. K. E.; Wireduaah, S., The Use Of Hammett Constants To Understand The Non-Covalent Binding Of Aromatics. *Computational and Structural Biotechnology Journal* **2012,** *1* (1), e201204004.

7. Schumann, H.; Janiak, C.; Khani, H., Cyclopentadienylthallium(I) compounds with bulky cyclopentadienyl ligands. *J Organomet Chem* **1987,** *330* (3), 347-355.

8. (a) Peloquin, A. J.; Stone, R. L.; Avila, S. E.; Rudico, E. R.; Horn, C. B.; Gardner, K. A.; Ball, D. W.; Johnson, J. E. B.; Iacono, S. T.; Balaich, G. J., Synthesis of 1,3-Diphenyl-6-alkyl/aryl-Substituted Fulvene Chromophores: Observation of π–π Interactions in a 6-Pyrene-Substituted 1,3-Diphenylfulvene. *J Org Chem* **2012,** *77* (14), 6371-6376; (b) Drake, N. L.; Adams, J. R., Some 1,4-Diaryl-1,3-cyclopentadienes. *J Am Chem Soc* **1939,** *61* (6), 1326-1329.

9. (a) Pauson, P. L., Ferrocene Derivatives .1. The Direct Synthesis of Substituted Ferrocenes. *J Am Chem Soc* **1954,** *76* (8), 2187-2191; (b) Zhang, X.; Ye, J.; Xu, L.; Yang, L.; Deng, D.; Ning, G., Synthesis, crystal Structures and aggregation-induced emission enhancement of aryl-substituted cyclopentadiene derivatives. *J Lumin* **2013,** *139*, 28-34; (c) Hirsch, S. S.; Bailey, W. J., Base-Catalyzed Alkylation of Cyclopentadiene Rings with Alcohols and Amines. *J Org Chem* **1978,** *43* (21), 4090-4094.

10. Cava, M. P.; Narasimhan, K., Synthesis of tetraphenylcyclopentadiene from tetracyclone. *J Org Chem* **1969,** *34* (11), 3641-3642.

11. (a) Product Class 3: Cyclopentadienyl Anions, Cyclopentadienones, and Heteroatom Analogues. In *Category 6, Compounds with All-Carbon Functions*, 1st Edition ed.; Siegel, J. S.; Tobe, Y.; Shinkai, I., Eds. Georg Thieme Verlag: Stuttgart, 2009; Vol. 45a; (b) Dyker, G.; Heiermann, J.; Miura, M.; Inoh, J.-I.; Pivsa-Art, S.; Satoh, T.; Nomura, M., Palladium-Catalyzed Arylation of Cyclopentadienes. *Chem-Eur J* **2000,** *6* (18), 3426-3433.

12. Ziegler, K.; Schnell, B., Zur Kenntnis des ”dreiwertigen„ Kohlenstoffs: III. Über das Penta-phenyl-cyclo-pentadienyl. *Justus Liebigs Annalen der Chemie* **1925,** *445* (1), 266-282.

13. Wilson, P. J.; Wells, J. H., The Chemistry and Utilization of Cyclopentadiene. *Chem Rev* **1944,** *34* (1), 1-50.

14. Field, L. D.; Hambley, T. W.; Lindall, C. M.; Masters, A. F., Crystal and molecular structures of pentaphenylcyclopentadiene and of an isomer, 4,8-diphenyltribenzo[b,f,i]tricyclo[6.2.1.01,5]undecane, the product of a novel metal-assisted photoreaction. *Inorg Chem* **1992,** *31* (12), 2366-2370.

15. Zhang, R.; Tsutsui, M.; E. Bergbreiter, D., Alkali metal salts of pentaphenylcyclopentadienide. *J Organomet Chem* **1982,** *229* (2), 109-112.

16. Bordwell, F. G.; Bausch, M. J., Methyl effects on the basicities of cyclopentadienide and indenide ions and on the chemistry of their transition metal complexes. *J Am Chem Soc* **1983,** *105* (19), 6188-6189.

17. Greifenstein, L. G.; Lambert, J. B.; Nienhuis, R. J.; Drucker, G. E.; Pagani, G. A., Response of Acidity and Magnetic-Resonance Properties to Aryl Substitution in Carbon Acids and Derived Carbanions - 1-Aryl-4-Phenylcyclopenta-1,3-Dienes - Dependence of Ionic Structure on Aryl Substitution. *J Am Chem Soc* **1981,** *103* (26), 7753-7761.

18. Bordwell, F. G.; Cheng, J. P.; Bausch, M. J., Acidities of radical cations derived from cyclopentadienes and 3-aryl-1,1,5,5-tetraphenyl-1,4-pentadienes. *J Am Chem Soc* **1988,** *110* (9), 2872-2877.

19. (a) Mylavarapu, S.; Yadav, M.; Bhanuchandra, M., KHMDS mediated synthesis of 9-arylfluorenes from dibenzothiophene dioxides and arylacetonitriles by tandem SNAr-decyanation-based arylation. *Org Biomol Chem* **2018,** *16* (42), 7815-7819; (b) Ji, X.; Huang, T.; Wu, W.; Liang, F.; Cao, S., LDA-Mediated Synthesis of Triarylmethanes by Arylation of Diarylmethanes with Fluoroarenes at Room Temperature. *Org Lett* **2015,** *17* (20), 5096-5099; (c) Kimiaki, Y.; Hideyoshi, M.; Akira, S., Formation of 2-Substituted 1,3-Diphenylindenes by an N-Bromosuccinimide Prompted Dehydrocyclization of 2-Substituted 1,3,3-Triphenyl-1-propenes. *B Chem Soc Jpn* **1986,** *59* (11), 3699-3701; (d) Xi, Q.; Zhang, W.; Zhang, X., (η^5-Triphenylindenyl)$Ru(CO)_2Cl$: A New Ruthenium Catalyst for the Highly Efficient Racemization of Chiral 1-Phenylethanol at Room Temperature. *Synlett* **2006,** *2006* (06), 945-947.

20. (a) Ma, Z.; Zhang, X.; Wang, H.; Han, Z.; Zheng, X.; Lin, J., Syntheses, structures and catalytic activity for Friedel-Crafts reactions of substituted indenyl rhenium carbonyl complexes. *J Coord Chem* **2017,** *70* (4), 709-721; (b) Honzíček, J.; Romão, C. C.; Calhorda, M. J.; Mukhopadhyay, A.; Vinklárek, J.; Padělková, Z., Reaction of Spiro[2.4]hepta-4,6-diene with Molybdenum(II) Indenyl Compounds: Effects of Substitution in the Indenyl Ligand. *Organometallics* **2011,** *30* (4), 717-725.

21. Kaiser, R.; Hafner, K., A Simple Synthesis of 1,2-Dihydropentalene and its Substitution Products. *Angew Chem Int Ed Eng* **1970,** *9* (11), 892-893.

22. Griesbeck, A. G., Notizen/Notes Synthesis of 1-Phenyl-1,2- and 4-Phenyl-1,5-dihydropentalenes. *Chem Ber* **1991,** *124* (2), 403-405.

23. Griesbeck, A. G., Pyrrolidine-catalyzed reactions between .alpha.,.beta.-unsaturated carbonyl compounds and cyclopentadiene: a convenient approach to 1,2- and 1,5-dihydropentalenes. *J Org Chem* **1989,** *54* (21), 4981-4982.

24. Stone, K. J.; Little, R. D., An exceptionally simple and efficient method for the preparation of a wide variety of fulvenes. *J Org Chem* **1984,** *49* (11), 1849-1853.

25. Panda, T. K.; Gamer, M. T.; Roesky, P. W., An Improved Synthesis of Sodium and Potassium Cyclopentadienide. *Organometallics* **2003,** *22* (4), 877-878.

26. Riemschneider, R.; Nerin, R., Substitutionsprodukte des Cyclopentadiens, 9. Mitt.: Phenylcyclopentadien. *Monatshefte für Chemie und verwandte Teile anderer Wissenschaften* **1960,** *91* (5), 829-835.

27. Singh, P.; Rausch, M. D.; Bitterwolf, T. E., Formation and Synthetic Utility of Benzyl-Cyclopentadienylthallium and Phenyl-Cyclopentadienylthallium. *J Organomet Chem* **1988,** *352* (3), 273-282.

28. Nifant'ev, I. E.; Vinogradov, A. A.; Vinogradov, A. A.; Ivchenko, P. V., Zirconocene-catalyzed dimerization of 1-hexene: Two-stage activation and structure-catalytic performance relationship. *Catal Commun* **2016,** *79*, 6-10.

29. Datta, S.; Odedra, A.; Liu, R.-S., Ruthenium-Catalyzed Cycloisomerization of cis-3-En-1-ynes to Cyclopentadiene and Related Derivatives through a 1,5-Sigmatropic Hydrogen Shift of Ruthenium−Vinylidene Intermediates. *J Am Chem Soc* **2005,** *127* (33), 11606-11607.

30. Shigeo, K.; Satoru, K.; Makoto, Y.; Kazutoshi, Y., Deoxygenat ion of 1,3-Diene 1,4-Endoperoxides by Tin(II) Chloride. *Chem Lett* **1988,** *17* (9), 1477-1478.

31. Lin, Z.; Li, J.; Huang, Q.; Huang, Q.; Wang, Q.; Tang, L.; Gong, D.; Yang, J.; Zhu, J.; Deng, J., Chiral Surfactant-Type Catalyst: Enantioselective Reduction of Long-Chain Aliphatic Ketoesters in Water. *J Org Chem* **2015,** *80* (9), 4419-4429.

32. Ward, T. J.; Ward, K. D., Chiral Separations: A Review of Current Topics and Trends. *Anal Chem* **2012,** *84* (2), 626-635.

33. (a) Aboul-Enein, H., *A Practical Approach to Chiral Separations by Liquid Chromatography*. 1996; Vol. 8, p 351-351; (b) Okamoto, Y.; Ikai, T., Chiral HPLC for efficient resolution of enantiomers. *Chem Soc Rev* **2008,** *37* (12), 2593-2608.

34. (a) Wang, Y.; Chen, A. M., Enantioenrichment by Crystallization. *Org Process Res Dev* **2008,** *12* (2), 282-290; (b) Lorenz, H.; Perlberg, A.; Sapoundjiev, D.; Elsner, M. P.; Seidel-Morgenstern, A., Crystallization of enantiomers. *Chem Eng Process: Process Inten* **2006,** *45* (10), 863-873.

35. Minch, M. J., Orientational dependence of vicinal proton-proton NMR coupling constants: The Karplus relationship. *Concepts Magnetic Res* **1994,** *6* (1), 41-56.

36. Bailey, P. M.; Mann, B. E.; Brown, I. D.; Maitlis, P. M., Dihydropentalenes from the palladium(II)-induced cyclotetramerisation of acetylenes; X-ray crystal structures of two dihydropentalenes. *J Chem Soc, Chem Comm* **1976,** (7), 238-239.

37. Le Goff, E., The Synthesis of Hexaphenylpentalene. *J Am Chem Soc* **1962,** *84* (20), 3975-3976.

38. Blass, B. E., KF/Al_2O_3-Mediated Organic Synthesis. *Chem Inform* **2003,** *34* (3).

39. Liotta, C. L.; Harris, H. P., Chemistry of naked anions. I. Reactions of the 18-crown-6 complex of potassium fluoride with organic substrates in aprotic organic solvents. *Journal of the American Chemical Society* **1974,** *96* (7), 2250-2252.

40. (a) Coskun, N.; Çetin, M.; Gronert, S.; Ma, J.; Erden, I., Pyrrolidine catalyzed reactions of cyclopentadiene with α,β-unsaturated carbonyl compounds: 1,2- versus 1,4-additions. *Tetrahedron* **2015,** *71* (18), 2636-2642; (b) Erden, I.; Xu, F.-P.; Sadoun, A.; Smith, W.; Sheff, G.; Ossun, M., Scope and Limitations of Fulvene Syntheses. Preparation of 6-Vinyl-Substituted and -Functionalized Fulvenes. First Examples of Nucleophilic Substitution on a 6-(Chloromethyl)fulvene. *J Org Chem* **1995,** *60* (4), 813-820.

41. Lee, B. Y.; Moon, H.; Chung, Y. K.; Jeong, N., Generation of Cyclopentadienyl Ligands via the Pauson-Khand and Retro-Diels-Alder Reactions. *J Am Chem Soc* **1994,** *116* (5), 2163-2164.

42. Chung, Y. K.; Lee, B. Y.; Jeong, N.; Hudecek, M.; Pauson, P. L., Promoters for the (alkyne) hexacarbonyldicobalt-based cyclopentenone synthesis. *Organometallics* **1993,** *12* (1), 220-223.

43. Shibata, T., Recent Advances in the Catalytic Pauson–Khand-Type Reaction. *Adv Synth Cat* **2006,** *348* (16-17), 2328-2336.

44. (a) RajanBabu, T. V.; Eaton, D. F.; Fukunaga, T., Chemistry of bridged aromatics. A study of the substituent effect on the course of bond cleavage of 9,10-dihydro-9,10-ethanoanthracenes and an oxyanion-assisted retro-Diels-Alder reaction. *J Org Chem* **1983,** *48* (5), 652-657; (b) Bunnelle, W. H.; Randall Shangraw, W., Acid catalysis of the retro-diels alder reaction. Formation and electrophilic reactivity of 2-methylene-1,3-cyclopentanedione. *Tetrahedron* **1987,** *43* (9), 2005-2011.

45. Pauson, P. L., Ferrocene Derivatives. Part I. The Direct Synthesis of Substituted Ferrocenes. *J Am Chem Soc* **1954,** *76* (8), 2187-2191.

46. Ye, J.; Zhang, X.; Deng, D.; Ning, G.; Liu, T.; Zhuang, M.; Yang, L.; Gong, W.; Lin, Y., Selective C–C bond cleavage of cyclopentadiene rings assisted by ferric chloride to synthesize water-soluble pyrylium salts. *RSC Adv* **2013,** *3* (22), 8232-8235.

47. (a) Mannich, C., Eine Synthese von β-Ketonbasen. *Archiv der Pharmazie* **1917,** *255* (2-4), 261-276; (b) Abid, M.; Azam, A., Synthesis and antiamoebic activities of 1-N-substituted cyclised pyrazoline analogues of thiosemicarbazones. *Bioorg Med Chem* **2005,** *13* (6), 2213-2220.

48. Chatterjee, A.; Joshi, N. N., Evolution of the stereoselective pinacol coupling reaction. *Tetrahedron* **2006,** *62* (52), 12137-12158.

49. Yamamura, S.; Toda, M.; Hirata, Y., Modified Clemmensen Reduction - Cholestane. *Org Synth* **1988,** *50-9*, 289-292.

50. Robertson, G. M., 2.6 - Pinacol Coupling Reactions. In *Comprehensive Organic Synthesis*, Trost, B. M.; Fleming, I., Eds. Pergamon: Oxford, 1991; pp 563-611.

51. Zhang, W.-C.; Li, C.-J., Magnesium-Mediated Carbon−Carbon Bond Formation in Aqueous Media: Barbier−Grignard Allylation and Pinacol Coupling of Aldehydes. *J Org Chem* **1999,** *64* (9), 3230-3236.

52. Bhar, S.; Panja, C., Pinacol coupling of aromatic aldehydes and ketones. An improved method in an aqueous medium. *Green Chem* **1999,** *1* (6), 253-255.

53. Bian, Y. J.; Liu, S. M.; Li, J. T.; Li, T. S., Pinacol coupling of aromatic aldehydes using aluminium under ultrasound irradiation. *Synthetic Commun* **2002,** *32* (8), 1169-1173.

54. (a) Rieke, R. D., Preparation of Organometallic Compounds from Highly Reactive Metal Powders. *Science* **1989,** *246* (4935), 1260-1264; (b) Rieke, R. D.; Bales, S. E.; Hudnall, P. M.; Burns, T. P.; Poindexter, G. S., Highly Reactive Magnesium for the Preparation of Grignard-Reagents - 1-Norbornanecarboxylic Acid. *Org Synth* **1988,** *50-9*, 845-852.

55. Zhang, F.; Mu, Y.; Zhao, L.; Zhang, Y.; Bu, W.; Chen, C.; Zhai, H.; Hong, H., New sterically hindered unbridged zirconocene complexes with 1,2-diphenylcyclopentadienyl ligands: synthesis, structure and properties as olefin polymerization catalysts. *J Organomet Chem* **2000,** *613* (1), 68-76.

56. Villiers, C.; Ephritikhine, M., New Insights into the Mechanism of the McMurry Reaction. *Angew Chem Int Ed Eng* **1997,** *36* (21), 2380-2382.

57. Ephritikhine, M., A new look at the McMurry reaction. *Chem Commun* **1998,** (23), 2549-2554.

58. McMurry, J. E., Carbonyl-coupling reactions using low-valent titanium. *Chem Rev* **1989,** *89* (7), 1513-1524.

59. McMurry, J. E.; Lectka, T.; Rico, J. G., An optimized procedure for titanium-induced carbonyl coupling. *J Org Chem* **1989,** *54* (15), 3748-3749.

60. Jones, N. A.; Liddle, S. T.; Wilson, C.; Arnold, P. L., Titanium(III) Alkoxy-N-heterocyclic Carbenes and a Safe, Low-Cost Route to $TiCl_3(THF)_3$. *Organometallics* **2007,** *26* (3), 755-757.

61. (a) LeGoff, E., Cyclopropanes from an Easily Prepared, Highly Active Zinc—Copper Couple, Dibromomethane, and Olefins. *J Org Chem* **1964,** *29* (7), 2048-2050; (b) Shank, R.; Shechter, H., Notes: Simplified Zinc-Copper Couple for Use in Preparing Cyclopropanes from Methylene Iodide and Olefins. *J Org Chem* **1959,** *24* (11), 1825-1826.

62. (a) Szostak, M.; Fazakerley, N. J.; Parmar, D.; Procter, D. J., Cross-Coupling Reactions Using Samarium(II) Iodide. *Chem Rev* **2014,** *114* (11), 5959-6039; (b) Nicolaou, K. C.; Ellery, S. P.; Chen, J. S., Samarium Diiodide Mediated Reactions in Total Synthesis. *Angew Chem Int Ed* **2009,** *48* (39), 7140-7165.

63. Szostak, M.; Spain, M.; Procter, D. J., Preparation of Samarium(II) Iodide: Quantitative Evaluation of the Effect of Water, Oxygen, and Peroxide Content, Preparative Methods, and the Activation of Samarium Metal. *J Org Chem* **2012,** *77* (7), 3049-3059.

64. Corey, E. J.; Zheng, G. Z., Catalytic reactions of samarium (II) iodide. *Tetrahedron Lett* **1997,** *38* (12), 2045-2048.

65. Pauson, P. L.; Williams, B. J., Cyclopentadienes, Fulvenes, and Fulvalenes .3. 2,3,4-Triphenylcyclopentadienone and Related Products. *J Chem Soc* **1961,** (Sep), 4162-&.

66. Adlington, R. M.; Barrett, A. G. M., Recent Applications of the Shapiro Reaction. *Accounts Chem Res* **1983,** *16* (2), 55-59.

67. (a) Ogawa, A.; Takeuchi, H.; Hirao, T., Diastereoselective pinacol coupling of alkyl aryl ketones with rare earth metals in the presence of chlorosilanes. *Tetrahedron Lett* **1999,** *40* (39), 7113-7114; (b) Clerici, A.; Pastori, N.; Porta, O., Facile reduction of aromatic aldehydes, ketones, diketones and oxo aldehydes to alcohols by an aqueous $TiCl_3/NH_3$ system: Selectivity and scope. *Eur J Org Chem* **2002,** (19), 3326-3335.

68. Hélion, F.; Lannou, M.-I.; Namy, J.-L., A new preparation of samarium dibromide and its use in stoichiometric and catalytic pinacol coupling reactions. *Tetrahedron Lett* **2003,** *44* (29), 5507-5510.

69. Polo, E.; Barbieri, A.; Traverso, O., The Effect of Phenyl Substituents on the Activity of Some Zirconocene Photoinitiators. *Eur J Inorg Chem* **2003,** *2003* (2), 324-330.

70. Martinez-Haya, R.; Marzo, L.; König, B., Reinventing the De Mayo reaction: synthesis of 1,5-diketones or 1,5-ketoesters via visible light [2+2] cycloaddition of β-diketones or β-ketoesters with styrenes. *Chem Commun* **2018,** *54* (82), 11602-11605.

71. Lu, S.-M.; Bolm, C., Highly Enantioselective Synthesis of Optically Active Ketones by Iridium-Catalyzed Asymmetric Hydrogenation. *Angew Chem Int Ed* **2008,** *47* (46), 8920-8923.

Chapter 3: Reactions of phenyl-substituted dihydropentalenes

3.1 Introduction

3.1.1 Alkali-metal salts of phenyl-substituted cyclopentadienides

With access to $\mathbf{Ph_xPnH_2}$ species (Chapter 2), suitable reagents for generating anionic ligands from these precursors were required. The synthesis of phenyl-substituted $\mathbf{Pn^{2-}}$s and $\mathbf{HPn^-}$s should resemble that of the analogous phenyl-substituted $\mathbf{Cp^-}$s (Figure 1). Anionic **Cp** derivatives are generated either by deprotonation with a suitable base, or by reductive metalation using a suitable metal species.

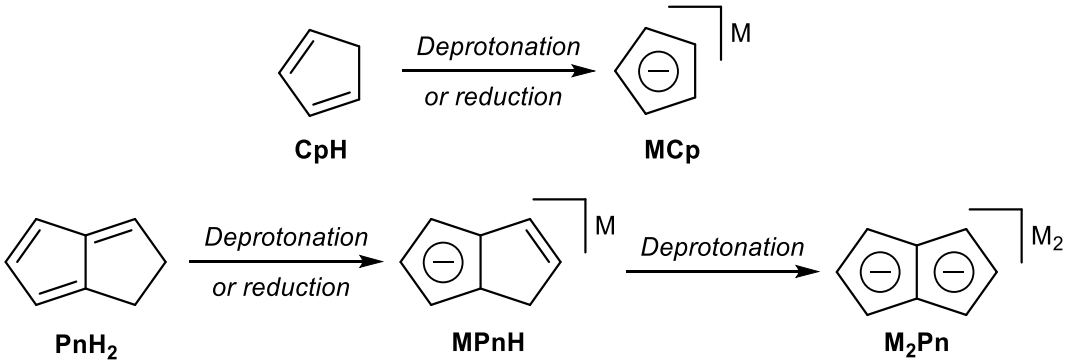

Figure 1: Formation of cyclopentadienides, hydropentalenides and pentalenides

Alkali-metal salts of $\mathbf{Cp^-}$ are commonly employed as transmetalation agents for synthesis of p-, d- and f-block **Cp** complexes. Zhang *et al.* [1] showed that $\mathbf{LiPh_5Cp}$ could be generated by treating $\mathbf{Ph_5CpH}$ with ^{n}BuLi (pK_a = 50) at 100 °C in toluene (Figure 2), with the product being isolated after cooling by centrifugation, removal of the supernatant and drying under vacuum.[2]

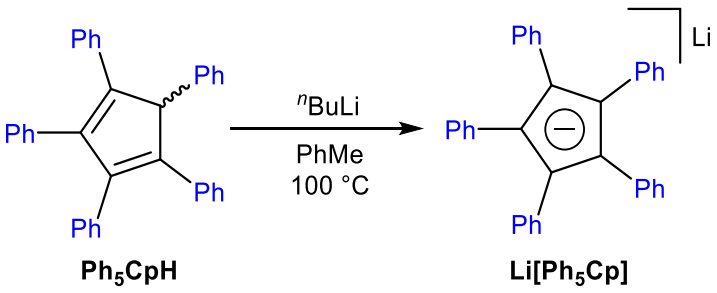

Figure 2: Synthesis of lithium pentaphenylcyclopentadienide

It has been shown that **NaPh$_5$Cp** can be generated using NaH (pK_a = 35) in THF [3] or $NaNH_2$ (pK_a = 35) [4] in toluene, and also that KH (pK_a = 35) is suitable for generating potassium salts of arylated **Cp** derivatives.[5] The synthesis of **TlPh$_5$Cp** using TlOEt[6] (pK_a = 16) demonstrates that using a weak alkoxide base is sufficient to deprotonate **Ph$_5$CpH**, as would be expected by its pK_a (section 2.1.2). Perhaps due to the low solubility of **Ph$_5$CpH** all these preparations require high temperatures. It is also possible that there is a high kinetic barrier to deprotonation due to the large amount of steric crowding around the acidic hydrogen atom.

Ph$_x$Cp$^-$ can be also be generated through the reaction of **Ph$_x$CpH** with alkali metals, analogous to the synthesis of alkali metal salts of **Cp**$^-$.[7] Zhang *et al.* [1] prepared the sodium, potassium and caesium salts of **Ph$_5$Cp**$^-$ by heating a suspension of **Ph$_5$CpH** and the corresponding alkali metal in toluene (Figure 3). Tabner and Walker[8] showed that for the reaction of **Ph$_4$CpH** with alkali metals initially the radical anion is formed, and then elevated temperatures cause this to decay into the **Ph$_4$Cp**$^-$ anion. It could be inferred that this would be the case for **Ph$_5$CpH** and other phenyl substituted **CpH**s.

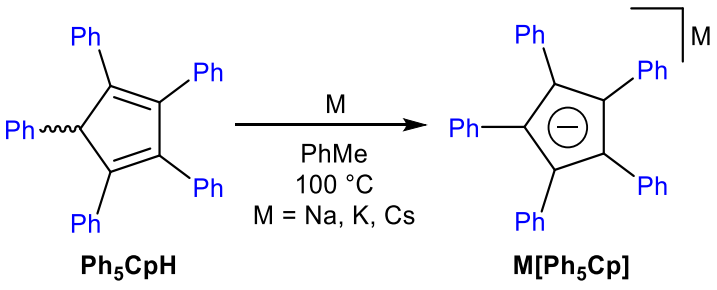

Figure 3: Synthesis of alkali-metal salts of pentaphenylcyclopentadienide

The resulting **MPh$_5$Cp** species are reported to be more soluble than **Ph$_5$CpH,** allowing them to easily purified by recrystallisation from THF. **MPh$_5$Cp** are less air-sensitive than the analogous **MCp**'s due to the presence of phenyl groups (Section 2.1.1), and these salts can be handled briefly outside of an inert atmosphere without appreciable decomposition.[1]

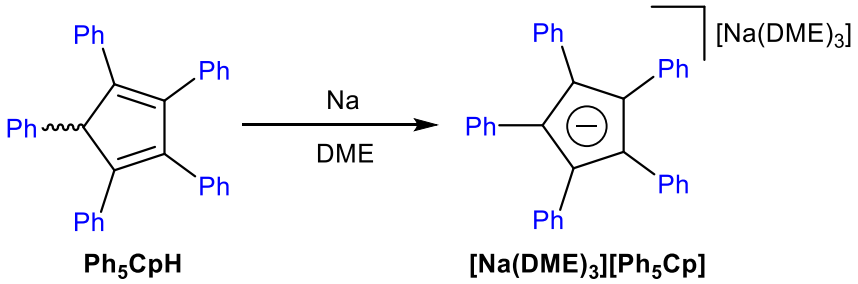

Figure 4: Synthesis of the DME-adducted sodium salt of pentaphenylcyclopentadienide

The **Ph$_5$Cp**$^-$ anion has been crystallographically characterised by Holl *et al.*[9] as its [Na(DME)$_3$] salt, which was synthesised by stirring **Ph$_5$CpH** in DME over a sodium mirror (Figure 4). Layering the reaction solution with hexane and leaving it to stand allowed growth of white prisms that were suitable for XRD analysis. This species was shown to exist in the solid state as a solvent-separated ion pair with the sodium cation fully complexed by DME ligands.

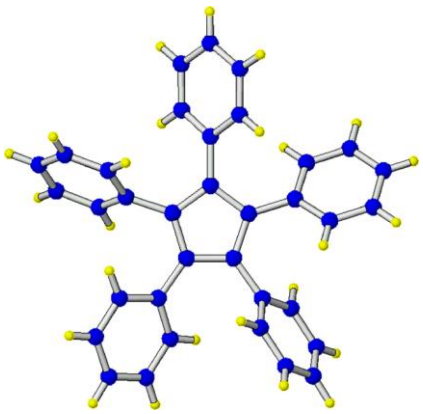

Figure 5: Crystal structure of pentaphenylcyclopentadiende (cation omitted) [10]

The XRD structure of **Ph$_5$Cp**$^-$ (Figure 5) shows all the phenyl-rings are rotated out of the plane with respect to the Cp ring with angles between 33.3° and 62.0°, meaning there is little π-delocalisation of the negative charge into the phenyl rings.[1] The high degree of steric crowding creates a high barrier

to rotation for the phenyl rings. This leads to **Ph_5Cp^-** possessing planar chirality, with the ligand being described as a 'five-blade chiral propeller'.[5, 11] This allows **Ph_5Cp^-** and other **Ar_5Cp^-** ligands to impart planar chirality once bonded to metals.[12]

3.1.2 Structure of substituted-hydropentalenides

The **PnH^-** anion structurally resembles a fused-ring vinyl **Cp^-** anion with the negative charge localised in one of the rings as an aromatic 6π system. This allows it to act as a η^5-ligand in monometallic complexes (Section 1.3.2).

When metal-bound the different positioning of the double bond within the unbound ring of **PnH^-** results in it possessing planar chirality.[13] **PnH^-**s substituted at the 1-position also contain a stereocentre, leading to four possible diastereomers (Figure 6). Highly phenyl-substituted **PnH^-**s might also possess the 'propeller' chirality shown for **Ph_5Cp^-** if the barrier to rotation for the phenyl rings is high enough, but this has not been demonstrated.

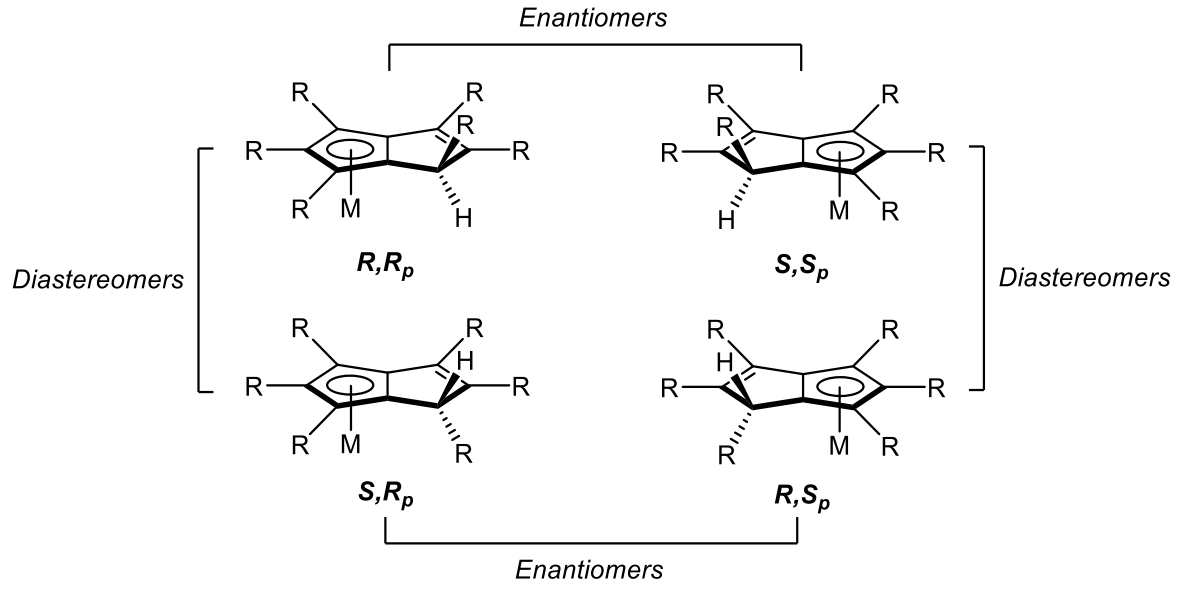

Figure 6: Stereoisomers of substituted hydropentalenides

Less symmetrical hydropentalenides can show additional positional isomerisation. Jones *et al.* [14] report that **$Re[MePnH](CO)_3$** formed as 1:1 mixture of the 1-methyl and 3-methyl isomer (Figure 7).

The 1-isomer has four diastereomers, two which have the methyl group orientated *syn* to the metal centre and two orientated *anti.*

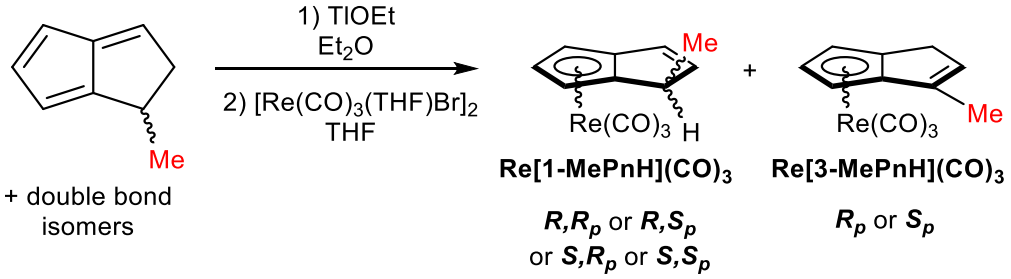

Figure 7: Formation of rhenium tricarbonyl derivatives of methylhydropentalenide

The 3-isomer, lacking a stereocentre, has just the two enantiomers arising from planar chirality, giving six total configurations for **Re[MePnH](CO)$_3$**. While the 1-methyl and 3-methyl isomers were differentiated by NMR, the *syn* and *anti*-configured diastereomers of the 1-methyl configuration could not be distinguished. With a larger substituent than methyl the chemical shift difference of the C1-hydrogen between the *syn*- and *anti*-diastereomers might be more pronounced and distinguishable by NMR.

Turner *et al*.[13] showed **Pn*H** could be used as a ligand in chiral group 4 complexes. Single diastereomers of derived Ti (Figure 8), Zr and Hf complexes were obtained by fractional crystallisation, and in each of these cases the methyl group at the stereocentre is oriented *anti* to the metal centre. The preference for the *anti*-configuration may be expected to be more pronounced with bulkier substituents.

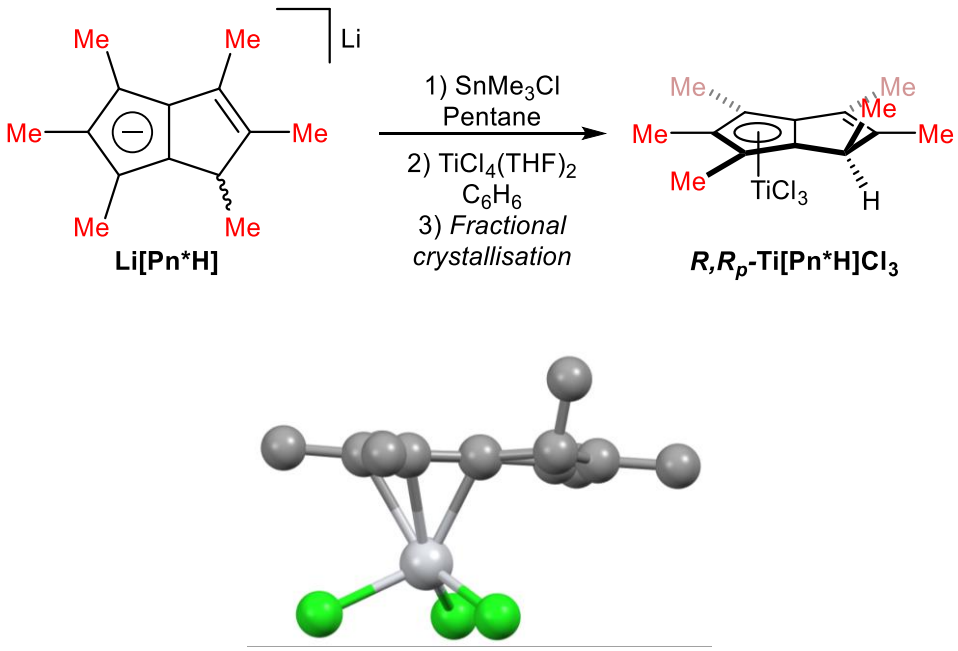

Figure 8: Synthesis of a chiral titanium(IV) hexamethylhydropentalenyl complex (above) and its crystal structure [13] (below)

These group 4 **Pn*H** complexes were shown to act as polymerisation catalysts for the formation polylactide. However, the nature of the chiral complexes did not affect the tacticity of the resulting polymers potentially due to the methyl group at the chiral centre being too small to induce chirality in the resulting polymer. Bulkier substituents could potentially affect these polymerisation reactions through increased steric interactions.

3.1.3 Structure of alkali-metal pentalenides

The $\mathbf{Pn^{2-}}$ dianion contains two '**Cp**' sites for η^5-binding to metals. Stezowski *et al.*[15] discussed several potential structures which the dilithium salt of $\mathbf{Pn^{2-}}$ could adopt (Figure 9) and used modified neglect of diatomic overlap (MNDO) calculations to determine the most stable configuration. Structures with η^5-binding of the two lithium atoms were calculated to be much more stable than those with η^3-edge-lithiated arrangements.

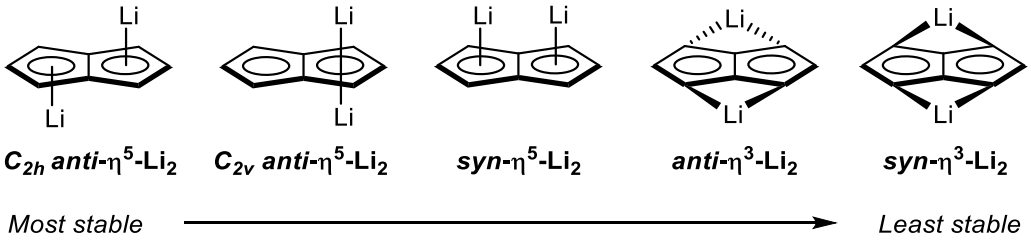

Figure 9: Potential structures of dilithium pentalenide as calculated by Stezowski et al.[15]

Arranging the two lithium atoms on the same face of the $\mathbf{Pn^{2-}}$ ligand (syn-Li_2) leads to unfavourable electrostatic interactions between the two cations. Binding of the lithiums to the same ring (C_{2v} *anti*-Li_2) leaves several carbon atoms without a neighbouring cation to stabilise their share of the delocalised negative charge. Because of this the structure with the two lithiums bound to different rings on the opposite faces of the ligand (C_{2h} *anti*-Li_2) is calculated to be the most stable arrangement. Density functional theory (DFT) computations by Barroso *et al*.[16] also calculated the C_{2h} inverted sandwich arrangement to be the lowest energy configuration.

Barroso *et al.*[16] also performed DFT calculations for the heavier alkali-metal salts of $\mathbf{Pn^{2-}}$, and reported that *anti*-M_2 arrangements were the most stable configurations in each case. However, the positioning of the metal cation above the ring varies along the series (Figure 10). In $\mathbf{Na_2Pn}$ the positions of the sodium atoms were shown to be closer to the bridgehead carbons than C1/C2/C3, reflected in a larger C2-centroid-M angle than in the lithium analogue, and in $\mathbf{K_2Pn}$ this angle is even larger. The calculated structures of $\mathbf{Rb_2Pn}$ and $\mathbf{Cs_2Pn}$ showed each of the cations to be sat directly above the bridging carbons in an η^8-like fashion.

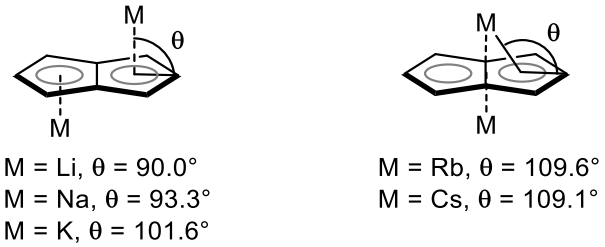

Figure 10: Calculated cation positions in M_2Pn species[16]

Stezowski [15] was able to grow crystals of **Li_2[Pn]** by performing the dilithation of **PnH_2** in DME (chapter 1, section 2.1). XRD analysis showed that this species adopts the predicted C_{2h} *anti*-Li_2 structure, with each lithium atom complexed by one chelating DME molecule (Figure 11). The carbon atoms in the Pn^{2-} core are all co-planar as would be anticipated for a fully delocalised 10π aromatic system. The C-C bond lengths of 1.42-1.44 Å are close to those found in lithium cyclopentadienide.[17] The C2-centroid-Li angle is 87.9°, smaller than the value calculated by Barroso *et al.* [16] (see above). The lithium-carbon bond distances for the two central 'bridgehead' carbons, 2.31 Å, are longer than for C1/C2/C3, which average 2.22 Å. However, this difference is small enough to still classify the binding as η^5.

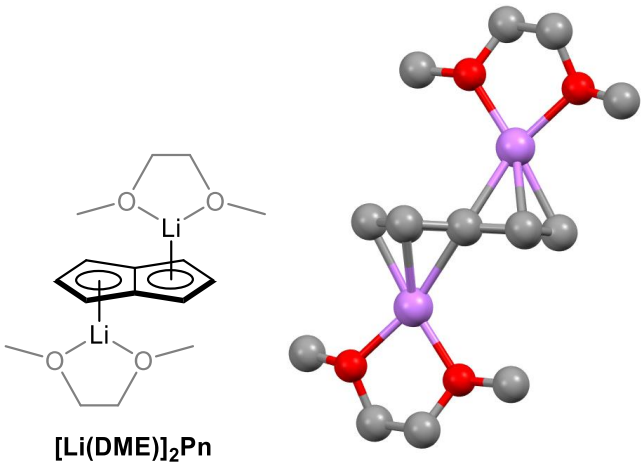

Figure 11: Crystal structure of $[Li(DME)]_2Pn$[15]

Ashely *et al.* [18] were able to grow crystals of **Li_2[Pn*]** as its TMEDA adduct (Section 1.2.4). XRD analysis of this species (Figure 12) showed the ligand is planar and the C-C bond lengths within the **Pn^{2-}** core are almost identical to those in **$[Li(DME)]_2Pn$**. The C-Li bonds lengths in **$[Li(TMEDA)]_2Pn$*** are shorter than in **$[Li(DME)]_2Pn$** due to the increased electron density in the **Pn^{*2-}** ligand bestowed by methyl

subsitution. This is analagous to the shortened lithium-ligand bonds observed for **LiCp*** as compared to **LiCp**.[17, 19]

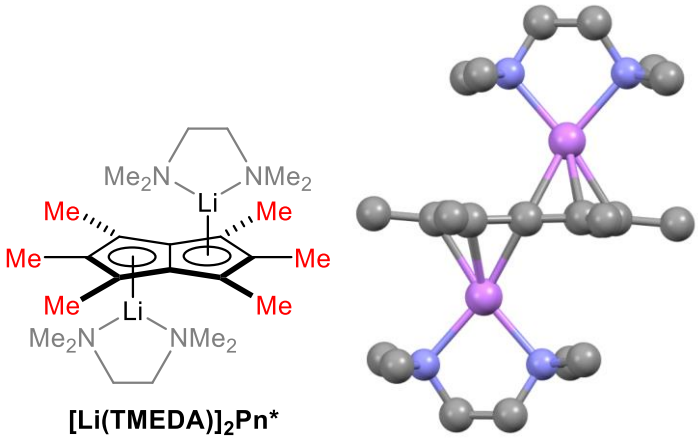

Figure 12: Crystal structure of [Li(TMEDA)]$_2$Pn[18]*

Currently there are no examples of sodium, rubidium or caesium pentalenides reported. The single example of a potassium pentalenide is provided by Cloke *et al.* [20], who have synthesised the bispotassium salt of **1,4-TIPS-Pn^{2-}** (Section 1.2.8). Recrystallisation of this species from benzene gave crystals suitable for analysis by XRD. This species was shown to crystallise as a benzene-complexed coordination polymer, with the crystal structure consisting of alternating **K$_2$[1,4-TIPS-Pn]$_2$** and $K_2[C_6H_6]$ units (Figure 13).

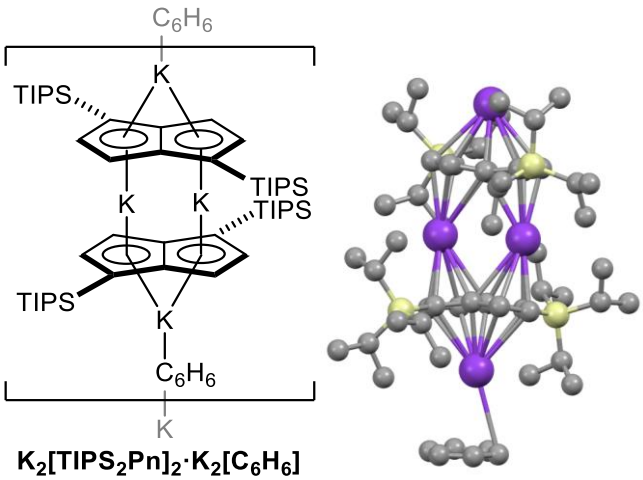

Figure 13: Crystal structure of the benzene-adducted potassium salt of TIPS$_2$Pn^{2-}

3.1.4 Aims

In Section 2.4.2 the gram scale synthesis of **Ph_4PnH_2** was described, and access to high purity samples of this species allowed investigation of its viability as a ligand precursor. In this chapter the use of **Ph_4PnH_2** for the synthesis of **Ph_4PnH^-** and **Ph_4Pn^{2-}** species (Figure 14) is described. As there are currently only a small number of **PnH^-** and **Pn^{2-}** species reported, successful synthesis of the desired phenyl-derivatives will be a useful addition to the field of pentalenide chemistry.

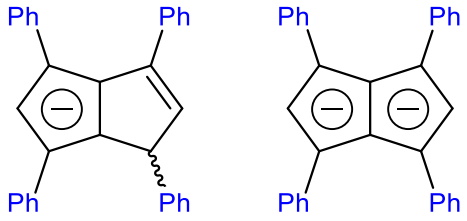

Ph_4PnH^- **Ph_4Pn^{2-}**

Figure 14: Structures of 1,3,4,6-tetraphenylhydropentalenide (left) and 1,3,4,6-tetraphenylpentalenide (right)

Ph_4PnH^- is a species that could function as a chiral **Cp^-** derivative, hence complexes containing this ligand could be used in stereoselective catalysis. Alkali-metal salts of **Cp^-** derivatives are the most common ligand transfer agents for these species. Therefore, alkali-metal salts of **Ph_4PnH^-** could be a useful precursors for the synthesis of d-, p- and f-block complexes containing this ligand. The synthesis of these salts was therefore investigated. For instances where the alkali-metal salts are too reducing, 'softer' ligand transfer-agents would be required (chapter 1, section 3.2). Tin(IV) and thallium(I) derivatives were identified as potentially fulfilling this role and therefore the synthesis of **$Tl[Ph_4PnH]$** and **$Ph_4PnH(SnR_3)$** was attempted.

Pn^{2-}s are ligands that offer a range of binding-modes for both mono- and bi-metallic complexes (chapter 1). The phenyl groups of **Ph_4Pn^{2-}** could provide steric shielding to bound metals, and this could potentially stabilise reactive metal centres in a manner that the parent **Pn^{2-}** or **Pn^{*2-}** cannot. Alkali-metals salts of **Ph_4Pn^{2-}**, which could function as precursors for transition-metal complexes, were

synthesised either directly from **Ph_4PnH_2** or via **Ph_4PnH^-**. Tin(IV) derivatives of **Ph_4Pn^{2-}** are also investigated as less reducing ligand transfer agents.

The reactions described in this chapter are all carried out in J.Young NMR tubes in order to ensure that water and oxygen are excluded.

3.2 Synthesis of 1,3,4,6-tetraphenyl-1-hydropentalenide

3.2.1 Synthesis of lithium 1,3,4,6-tetraphenylhydropentalenide

To generate **Ph_4PnH^-** from **Ph_4PnH_2** a suitable base is required. The parent **PnH_2** has a pK_a below 14 (Section 1.2.1), and **Ph_4PnH_2** is likely to have a lower pK_a due the presence of electron-withdrawing substituents (section 2.1.1). Therefore, a wide range of bases were likely to facilitate the required deprotonation.

Initially it was decided to investigate the use of LiHMDS, as this species has a pK_a of 25 so would be strong enough to cause fast, irreversible deprotonation of **Ph_4PnH_2**. Silyl amides display low nucleophilicity, meaning that HMDS would be less likely to undergo undesired nucleophilic addition reactions. In addition, the conjugate acid, (H)HMDS shows ^{1}H-NMR signals with shifts at 0.01 and 1.44 ppm. These signals were unlikely to overlap with signals from the target **Ph_4PnH^-**, and this allowed accurate characterisation of product peaks.

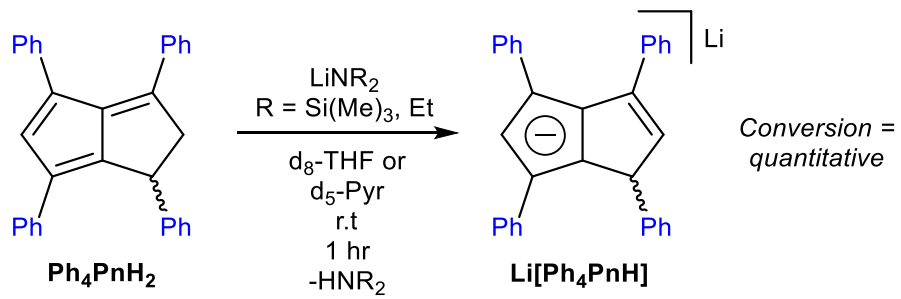

Figure 15: Formation of lithium 1,3,4,6-tetraphenylhydropentalenide

Treating **Ph_4PnH_2** with one equivalent of LiHMDS in d_8-THF led to rapid formation of a bright orange solution, identified by ^{1}H-NMR spectroscopy as containing **Li[Ph_4PnH]** (Figure 15). The disappearance of the ^{1}H-NMR signals for **Ph_4PnH_2**, particularly those at 4.55, 4.10 and 3.50 ppm, showed that the starting material was consumed. This coincided with the appearance of two signals at 5.68 and 4.47 ppm, corresponding to the C1 and C2 hydrogens in **Li[Ph_4PnH]** (Figure 16).

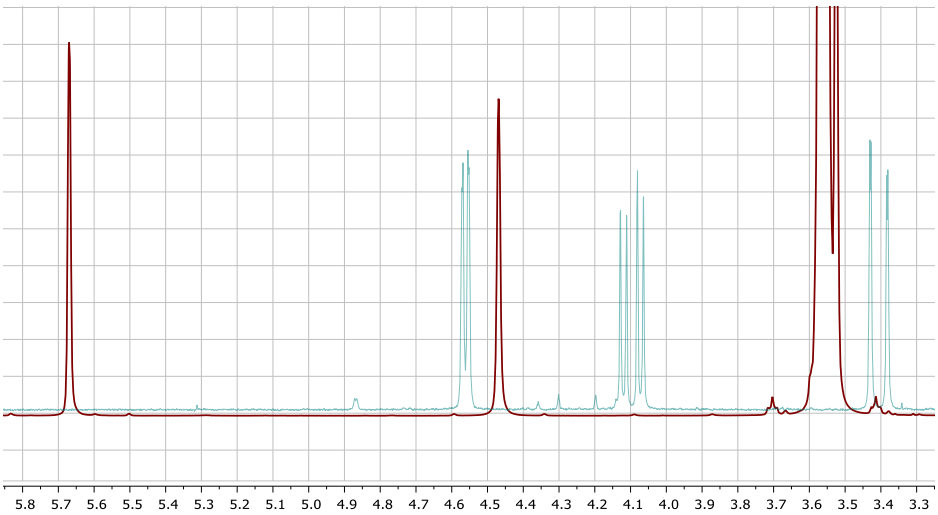

Figure 16: Overlaid ^{1}H-NMR (500 MHz) spectra of 1,3,4,6-tetraphenyldihydropentalene (blue) and lithium 1,3,4,6-tetraphenylhydropentalenide with THF peak at 3.56 ppm (red)

The ^{1}H-signal at 5.70 ppm showed the sp^3-hybridised C2 carbon in the precursor had been converted into a highly deshielded sp^2-hybridised carbon. The ^{13}C{^{1}H}-spectrum confirms this, as the dC2 signal was shifted from 55.2 to 130.3 ppm. This low-field shift is likely due to conjugation of the C2-C3 double bond π-system with the aromatic π-system in the anionic ring. The four phenyl groups were shown to be inequivalent. At 25 °C several of the ^{1}H-signals were overlaid but the use of VT-NMR allowed the four sets of *ortho*-, *meta*- and *para*-hydrogens to be distinguished (Figure 17). Acquiring the ^{1}H-spectrum at higher temperatures also allowed a singlet at 6.43 ppm, which was overlaid with a *para*-hydrogen signal at 25 °C to be distinguished. This singlet corresponded to the C5 ring-bound hydrogen.

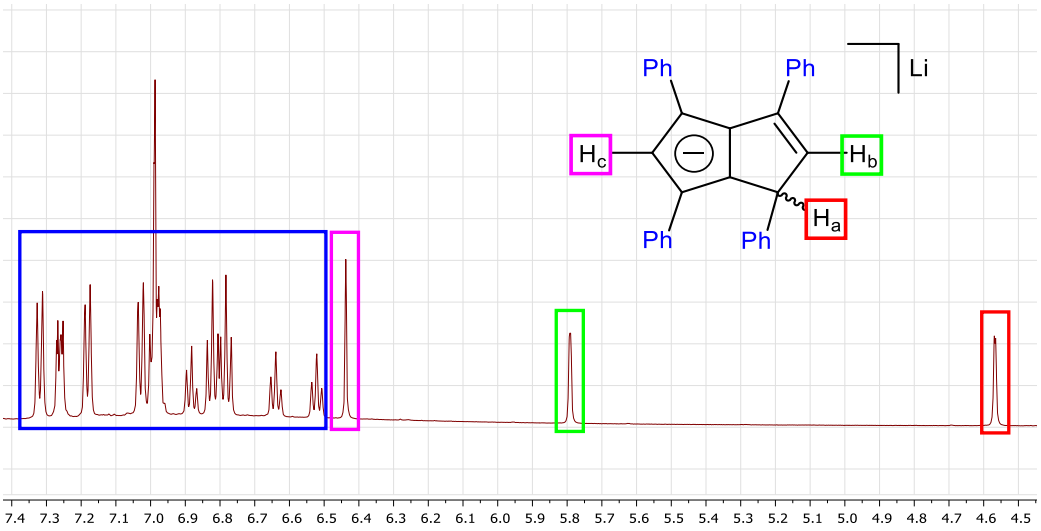

Figure 17: ^{1}H-NMR (500 MHz) spectrum of lithium 1,3,4,6-tetraphenylhydropentalenide in d_8-THF at 55 °C

The $^{13}C\{^{1}H\}$ shift for the C5 carbon was 103.7 ppm, comparable to the signal observed for the analogous carbon in **Li[Ph$_2$Cp]** which had a shift of 97.4 ppm. The analogous carbon in **Ph$_4$PnH$_2$** had a $^{13}C\{^{1}H\}$-shift of 139.2 ppm, meaning that the signal is shifted 35.5 ppm upfield in the anion as compared to the neutral precursor. For phenyl-substituted **Cp**$^-$ derivatives the $^{13}C\{^{1}H\}$ signal for the *para*-carbon of the phenyl substituents is a useful probe for the degree of delocalisation of the negative charge.[10] In **Li[Ph$_4$PnH]** these carbons had $^{13}C\{^{1}H\}$ signals between 118.4 and 125.2 ppm, compared to those in **Ph$_4$PnH$_2$** which had signals at 126.2 to 127.9 ppm. This suggests that there could be some delocalisation of charge into the phenyls attached to the anionic ring of **Ph$_4$PnH**$^-$, producing the chemical shift of 118.4 ppm which is 7.8 ppm upfield as compared to **Ph$_4$PnH$_2$**. DFT calculations could be used to determine the exact degree of delocalisation, but that is beyond the scope of this investigation.

This reaction leads to rapid, quantitative conversion of the **Ph$_4$PnH$_2$** even if performed at -40 °C, but the reaction can be performed at room temperature without detection of any by-products by ^{1}H-NMR. **Li[Ph$_4$PnH]** was found to be stable in THF up to 80 °C, and solutions remain unchanged over weeks when stored at room temperature under argon. However, this species was found to be extremely sensitive to air with THF solutions rapidly discolouring upon exposure to air, with the formation of a

range of unidentified organic products shown by NMR. Decomposition presumably occurs either through oxidation or partial protonation.

In contrast to **Li[Pn*H]**, which Ashley *et al.*[18] reported to be only sparingly soluble in THF, **Li[Ph_4PnH]** was found to be very soluble in THF as well as DME. TMEDA is often used to solubilise organolithium species, but addition of TMEDA to this reaction did not appreciably alter the solubility of **Li[Ph_4PnH]** or the speed of its formation. d_5-pyridine was reported to solubilise **Li[Pn*H]** sufficiently to analyse by NMR. Deprotonating **Ph_4PnH_2** with one equivalent of LiHMDS in d_5-pyridine led to formation of a dark red solution, shown by ^{1}H-NMR to contain **Li[Ph_4PnH]**.

$LiNEt_2$ (pK_a = 35) was identified as a base for forming **Ph_4Pn^{2-}** (see section 3.3.1), but first it was necessary to show that this base could form the monoanion without the occurrence of side-reactions. Treating **Ph_4PnH_2** with one equivalent of $LiNEt_2$ in d_8-THF led to quantitative formation of **Li[Ph_4PnH]** without formation of by-products detectable by NMR. Crystals of **Li[Ph_4PnH]** could not be obtained from any of the preparations described, so this species could not be analysed by XRD.

3.2.2 Synthesis of sodium 1,3,4,6-tetraphenylhydropentalenide

As the pK_a of **Ph_4PnH_2** is expected to be below 14, alkali metal alkoxides were expected to be strong enough to perform this deprotonation. Also, these bases should be insufficiently strong to facilitate the second deprotonation to the **Pn^{2-}**, so an excess of the alkoxide could be used without risk of partial **Pn^2** formation. Therefore, the use of sodium *tert*-butoxide and ethoxide was investigated to determine the viability of these bases, and to determine if the sodium salt of **Ph_4PnH^-** could be obtained.

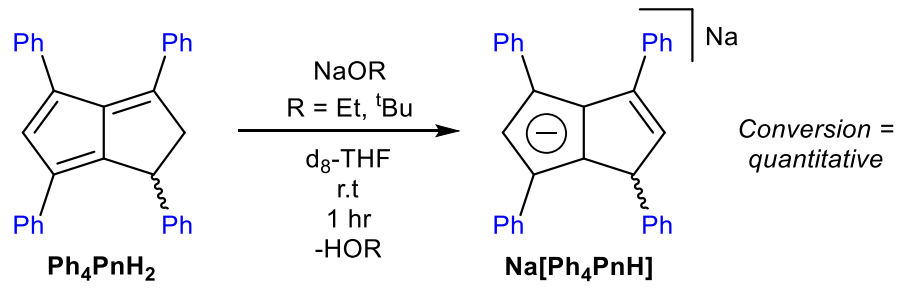

Figure 18: Formation of sodium 1,3,4,6-tetraphenylhydropentalenide

Reacting **Ph_4PnH_2** with sodium *tert*-butoxide (pK_a = 17) or ethoxide (pK_a = 16) in d_8-THF led to the formation of a dark red solution, shown to contain **Na[Ph_4PnH]** (Figure 18) by ^{1}H-NMR. The deprotonation was found to proceed slowly at -40 °C but occurred rapidly at room temperature without significant formation of by-products. **Na[Ph_4PnH]** was found to be very soluble in THF and stable over weeks when stored at room temperature under argon. Like **Li[Ph_4PnH]**, **Na[Ph_4PnH]** was found to be very sensitive to air. The ^{1}H-NMR spectrum of **Na[Ph_4PnH]** (Figure 19) was almost identical to that of the lithium salt, showing that in solution the structure and charge distribution of the **Ph_4PnH** anion are not significantly affected by the cation. This suggests a degree of solvent separation between the **Ph_4PnH^-** and the alkali-metal counterion. As with the lithium salt crystals of this species could not be grown in order to conduct XRD analysis.

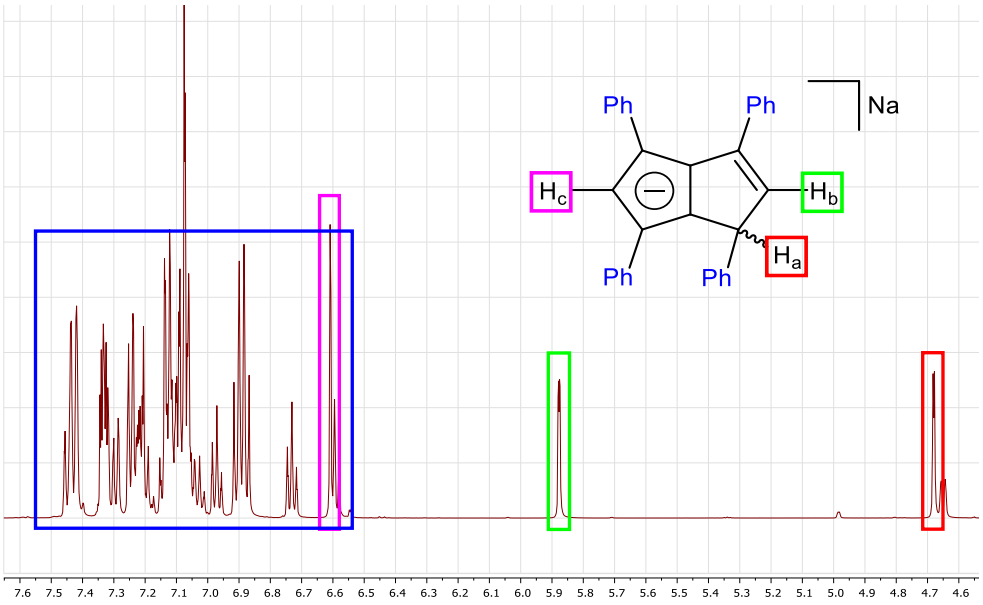

Figure 19: ^{1}H-NMR (500 MHz) spectrum of sodium 1,3,4,6-tetraphenylhydropentalenide in d_8-THF at 25 °C

It was supposed that $NaNH_2$ (pK_a = 35) would be sufficiently strong to doubly-deprotonate **Ph_4PnH_2**, but first it was necessary to test if it could form **Na[Ph_4PnH]** without side-reactions occurring. $NaNH_2$ is more prone to undergo addition reactions than the more sterically hindered amide bases, so this possibility needed to be tested.

Addition of **Ph_4PnH_2** to a slurry of one equivalent of $NaNH_2$ in d_8-THF led to formation of a dark red precipitate. The reaction mixture was filtered before analysing by NMR, and the solution was shown to contain only unreacted **Ph_4PnH_2**. The solids could not be dissolved in d_8-THF or d_5-pyridine in order to analyse them by NMR. The failure of this reaction is attributed to the heterogeneous nature of $NaNH_2$ in THF due to its low solubility. Reactions using more equivalents of $NaNH_2$ (Section 3.3.2) suggest that in the case of the 1:1 reaction, half the sample of **Ph_4PnH_2** underwent double-deprotonation at the surface of the $NaNH_2$ solid to form insoluble **$Na_2[Ph_4Pn]$**, leaving the unreacted half of the **Ph_4PnH_2** sample in solution to be observed by NMR. Using ammonia as the solvent for this reaction could led to the desired reactivity by solubilising the $NaNH_2$, but as a suitable base for forming **$Na[Ph_4PnH]$** in THF had already been determined this was not investigated.

3.2.3 Synthesis of potassium 1,3,4,6-tetraphenylhydropentalenide

Potassium **HPn^-** and **Pn^-** salts have been shown to be useful in situations when the lithium salts are too reducing or when they form 'ate' complexes rather than undergoing complete transmetalation.[20] While **$Na[Ph_4PnH]$** should serve as a less reducing source of **Ph_4PnH^-**, it was also decided to synthesise the potassium analogue. As sodium and potassium halide salts (which would be formed by reactions with metal halide precursors) are less soluble in organic solvents than lithium halides the precipitation of these salts would provide additional driving force for transmetalation reactions, and also further reduce the risk of forming 'ate' complexes.

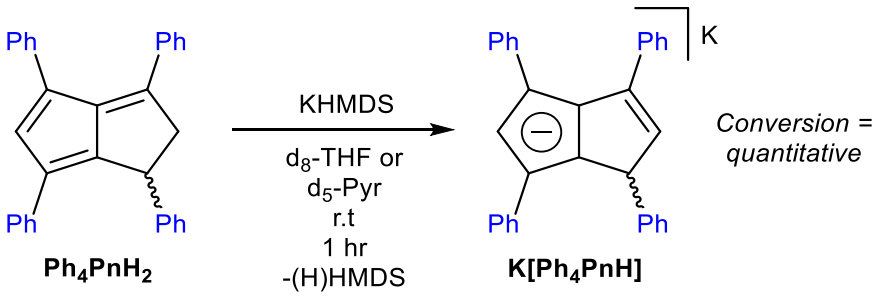

Figure 20: Formation of potassium 1,3,4,6-tetraphenylhydropentalenide

Reacting **Ph_4PnH_2** with one equivalent of KHMDS in d_8-THF at room temperature led to formation of a cherry red solution, shown by ^{1}H-NMR to contain **K[Ph_4PnH]** (Figure 20). It can also be synthesised in d_5-pyridine using KHMDS and gives the same species in solution as in d_8-THF. **K[Ph_4PnH]** is extremely insoluble in C_6D_6 or toluene, and if the deprotonation with KHMDS is performed in these solvents the product precipitates from the reaction mixture as a non-crystalline red solid.

While this species in moderately soluble in THF and pyridine, if solutions are allowed to stand for several the salt with slowly precipitate out (and the relevant signals will disappear from the NMR spectrum). This decreased solubility compared to the lithium and sodium salts is comparable to the difference in solubilities observed for alkali metal **Cp**$^-$ salts.[21] The ^{1}H- and ^{13}C{^{1}H}-NMR signals for the **Ph_4PnH^-** anion (Figure 21) in the potassium salt are almost identical to those in the lithium and sodium salts.

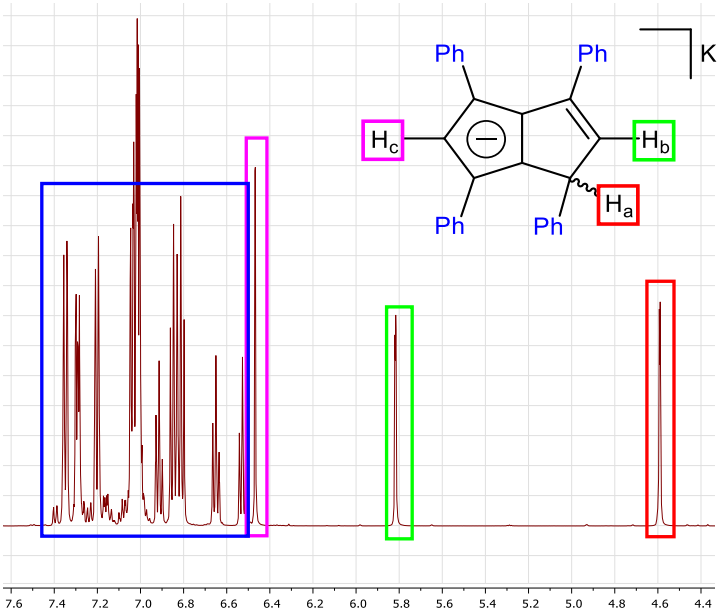

Figure 21: ^{1}H-NMR (500 MHz) spectrum of potassium 1,3,4,6-tetraphenylhydropentalenide d_8-THF at 25 °C

The use of KH (pK_a = 35) for forming **K[Ph_4PnH]** was also investigated. **Ph_4PnH_2** was added to suspension of 1 equivalent in d_8-THF, then after stirring overnight the mixture was filtered and analysed by NMR. Like with the reaction with 1 equivalent of $NaNH_2$ only unreacted **Ph_4PnH_2** was observed in solution. This is presumably because, like $NaNH_2$, KH is insoluble in THF so the

heterogeneous nature of the deprotonation leads to half the sample undergoing double deprotonation to the insoluble **K_2[Ph_4Pn]** (see section 3.3.3) and half remaining unreacted in solution.

As with the other **Ph_4PnH^-** salts, crystals of **K[Ph_4PnH]** could not be obtained to analyse it by XRD. This is potentially due to the high solubility of these salts in the coordinating solvents tested. Using different coordinating solvents, such as diethyl ether, could promote solid formation. However, the presence of multiple stereoisomers of this anion (section 3.1.2) could disfavour packing of the molecules in the solid state and prevent crystallisation from any solvent system. If the cation can dynamically shift from the faces of the **PnH** core, this would mean that the planar diastereomers interconvert and would further disfavour crystal formation.

3.2.4 Attempted synthesis of thallium 1,3,4,6-tetraphenylhydropentalenide

Thallium **Cp** species have been found to be useful ligand transfer agents in instances when the alkali metal salts are too reducing.[22] Likewise **Tl[PnH]** has been shown to a useful precursor for **PnH^-** complexes. For example, it is able to smoothly react with easily reduced Rh(I) precursors to give **Rh[PnH]** derivatives.[23] It was hoped that forming **Tl[Ph_4PnH]** would allow this to be used as alternative precursor to the alkali metal salts described above.

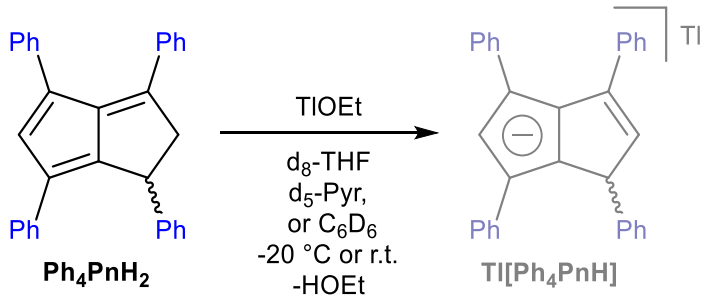

Figure 22: Attempted synthesis thallium 1,3,4,6-tetraphenylhydropentalenide

TlOEt has been shown to be a suitable regent for forming **Tl[PnH]** derivatives (chapter 1, section 3.1), and it has been shown that ethoxide is a suitably strong base for deprotonating **Ph_4PnH_2** (section 3.2.2). **Ph_4PnH_2** was treated with an excess of TlOEt in d_8-THF (Figure 22) with the exclusion of light, as

Tl[PnH] species have been shown to be light sensitive.[14] This reaction led to the formation of an insoluble brown precipitate. NMR analysis of the solution showed that the **Ph_4PnH_2** had been consumed, but only a small amount of **Ph_4PnH^-** was detectable. Performing the reaction in d_5-pyridine or C_6D_6 produced the same result, suggesting that if **Tl[Ph_4PnH]** does form it is insufficiently soluble to characterise by ^{1}H-NMR.

3.2.5 Attempted synthesis of stannylated 1,3,4,6-tetraphenyl-1-hydropentalenides

Another alternative to alkali-metal **PnH^-**s is provided by tin(IV) derivatives of **PnH^-**, which have been shown to provide access to high-valent early transition-metal complexes of **PnH^-**s (Section 1.3.3). These 'soft' ligand transfer agents react with metal halides via metathesis reaction, produce tin(IV) halides as a by-products. It was hoped that accessing **$Ph_4PnH(SnMe_3)$** would allow this to be used as a precursor for **Ph_4PnH^-** complexes.

Ustynyuk *et al*.[24] showed $SnMe_3$ derivatives of **PnH^-** and **Pn^{2-}** could be prepared by reacting PnH_2 with either one or two equivalents $SnMe_3(NEt_2)$ respectively. It was hoped that a similar approach could be applied to **Ph_4PnH_2**. It had been shown that alkali-metal HMDS bases are suitable for forming **Ph_4PnH^-** (Section 3.2.1), so it was supposed that $SnMe_3$(HMDS) could allow synthesis of **$Ph_4PnH(SnMe_3)$**.

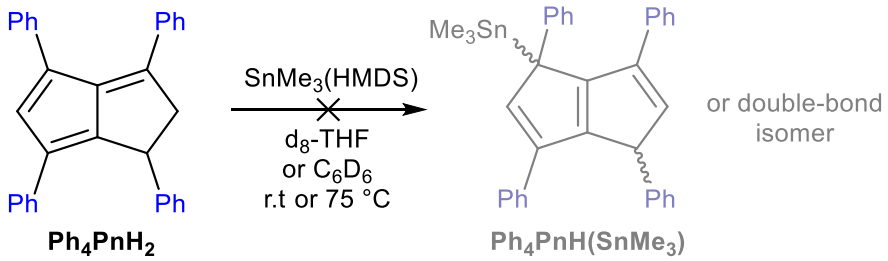

Figure 23: Attempted reaction of 1,3,4,6-tetraphenyldihydropentalene with trimethyltin(trimethylsilyl)amide

$SnMe_3$(HMDS) was prepared *in situ* by reacting $SnMe_3Cl$ with KHMDS in d_8-THF, with its formation confirmed by ^{119}Sn NMR. To this species was added one equivalent of **Ph_4PnH_2** (Figure 23). However, after two days at room temperature no reaction was observed either by ^{1}H or ^{119}Sn NMR and heating

the reaction mixture to 75 °C for two days also did not lead to any reaction. Performing this reaction in C_6D_6 also produced no reaction.

Turner *et al.*[13] reported the synthesis of **Pn*H(SnMe$_3$)** by reacting **Li[Pn*H]** with $SnMe_3Cl$. Therefore it was supposed that treating **Ph$_4$PnH$^-$** with $SnMe_3Cl$ could provide access to **Ph$_4$PnH(SnMe$_3$)**.

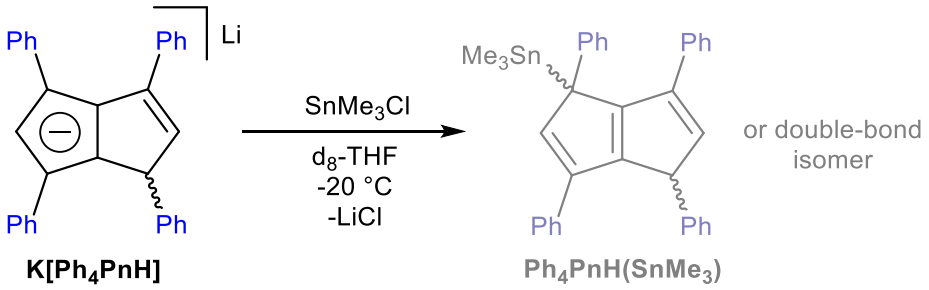

Figure 24: Attempted reaction of 1,3,4,6-tetraphenyl-1-hydropentalenide with trimethyltin chloride

When **Li[Ph4PnH]**, generated *in situ* by treating Ph_4PnH_2 with LiHMDS, was reacted with $SnMe_3Cl$ in d_8-THF a bright yellow solution was formed. The ^{1}H-NMR showed that the **Li[Ph4PnH]** had been consumed, but little product could be detected in solution. This could be due to poor solubility of **Ph$_4$PnH(SnMe$_3$)** as precipitates are observed to form over time. ^{119}Sn-NMR showed a new signal at 41.97 ppm which could correspond to **Ph$_4$PnH(SnMe$_3$)**, but further investigation would be required to confirm this (Section 3.4).

3.2.6 Oxidation of 1,3,4,6-tetraphenyldihydropentalene

Le Goff [25] reported that **1,2,3,4,5,6-Ph$_6$PnH$_2$** could be used a precursor for the anti-aromatic species **1,2,3,4,5,6-Ph$_6$Pn**. It was therefore supposed that **1,3,4,6-Ph$_4$PnH$_2$** could be used to synthesise **1,3,4,6-Ph$_4$Pn**. **1,2,3,4,5,6-Ph$_6$Pn** was generated by reacting **1,2,3,4,5,6-Ph$_6$PnH$_2$** with NBS in refluxing CCl_4. Therefore **1,3,4,6-Ph$_4$PnH$_2$** was treated with NBS in $CDCl_3$ (Figure 25) due to lack of availability of CCl_4. Combining the reagents at room temperature produced no reaction as observed by ^{1}H-NMR. Heating the mixture overnight led to the destruction of the starting material and the formation of insoluble brown solids. The solution was shown by ^{1}H-NMR to contain unidentified organic products in low concentrations. When this reaction was carried out in d_8-THF the same result was observed.

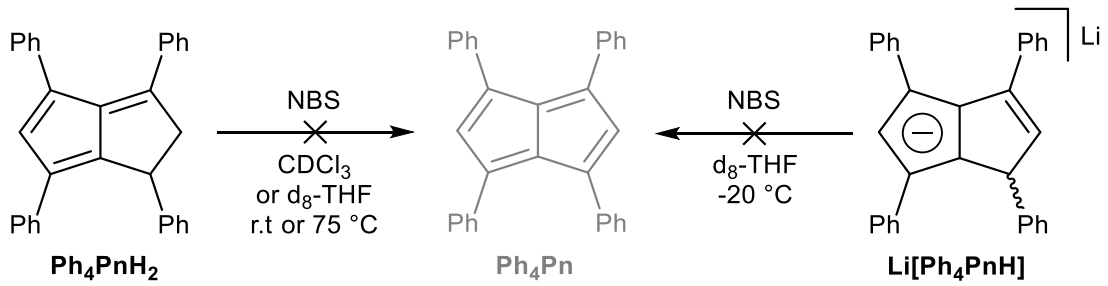

Figure 25: Attempted synthesis of 1,3,4,6-tetraphenylpentalene

Le Goff [25] also reported that **1,2,3,4,5,6-Ph_6Pn** could be prepared by treating **1,2,3,4,5,6-Ph_6PnH_2** with ^{n}BuLi then oxidising the lithium salt with iodine. **Li[Ph_4PnH]** was prepared *in situ* reacting **1,3,4,6-Ph_4PnH_2** with LiHMDS in d_8-THF, and it was then treated with NBS (Figure 25). This led to the destruction of the lithium salt and the formation of insoluble brown precipitates. The solution was shown by ^{1}H-NMR to contain unidentified organic products in low concentrations.

The failure to detect the anti-aromatic **Ph_4Pn** derivative potentially suggests that **1,3,4,6-Ph_4Pn** is unstable and degrades under the reaction conditions tested. The decreased steric protection of the **Pn** core as compared to **1,2,3,4,5,6-Ph_6Pn** could be the cause of this decreased stability. However, it is also possible that NBS is not suitable for generating **1,3,4,6-Ph_4Pn** and is instead producing the wrong reactivity and leads to the destruction of the starting material. As the **Pn** derivative is less useful in the context of organometallic chemistry than the anionic species, no further investigation of the anti-aromatic species was carried out.

3.3 Synthesis of 1,3,4,6-tetraphenylpentalenide

3.3.1 Synthesis of dilithium 1,3,4,6-tetraphenylpentalenide

In metal pentalenide chemistry the dillithium salts are often employed as transmetalation reagents; for example. the reactions of **Li_2Pn** and **Li_2Pn^*** with a variety of metal precursors have been reported (Section 1.3.3). Therefore, it was desirable to synthesise the dilithium salt of **Ph_4Pn^{2-}** for use as a precursor for organometallic **Ph_4Pn^{2-}** complexes.

BuLi is used to synthesise **Li_2Pn** from **PnH_2** and **Li_2Pn^*** from **Li[Pn*H]**. It is appealing as its high pK_a leads to rapid, irreversible deprotonation, with the formed butane bubbling from solution. However, when **Ph_4PnH_2** was treated with two equivalents of ^{n}BuLi in either THF, DME or hexane with TMEDA at either 0 °C or -78 °C formation of an insoluble brown solid was observed. This solid could not be dissolved in order to characterise them by NMR. This contrasts with **Ph_5CpH**, which can be smoothly deprotonated with BuLi at high temperatures (section 3.1.1).

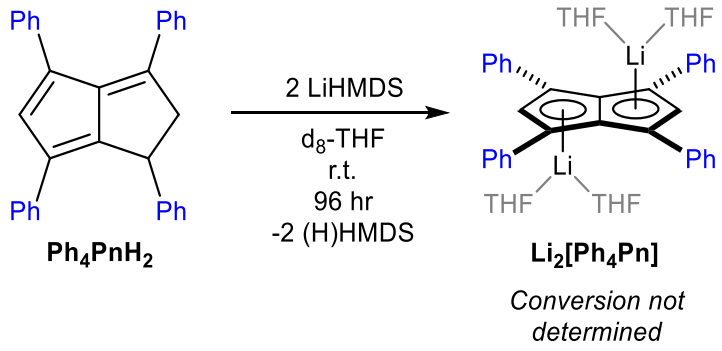

Ph_4PnH_2

$Li_2[Ph_4Pn]$

Conversion not determined

Figure 26: Formation of dilithium 1,3,4,6-tetraphenylpentalenide from 1,3,4,6-tetraphenyldihydropentalene

When a sample of **Ph_4PnH_2** was treated with two (or more) equivalents of LiHMDS (Figure 26) in d_8-THF the quantitative formation of **Li[Ph_4PnH]** was observed after 1 hour, but no **$Li_2[Ph_4Pn]$** was observed by ^{1}H-NMR. However, if the sample is left for several days the ^{1}H-NMR signals of **Li[Ph_4PnH]** slowly disappear and a light orange, crystalline precipitate formed. This crystalline material was found to be suitable for analysis by XRD, and was confirmed to be **$[Li(THF)_2]_2[Ph_4Pn]$** (Section 3.3.4). While

each lithium atom is solvated by two THF molecules in the solid state, the degree of cation solvation in the solution phase could not be determined.

The XRD analysis confirmed that LiHMDS was sufficiently strong to form **$Li_2[Ph_4Pn]$** to some extent, but the conversion of **$Li[Ph_4PnH]$** to **$Li_2[Ph_4Pn]$** could not be determined due to precipitation of the product preventing NMR analysis. The deprotonation of **$Li[Ph_4PnH]$** by LiHMDS at room temperature was shown to be very slow by monitoring the disappearance of the **$Li[Ph_4PnH]$** ^{1}H-NMR signals. This is possibly because the pK_a of **$Li[Ph_4PnH]$** is close to 25, although the actual pK_a has not been determined. However, there could also be a different kinetic barrier to the second deprotonation, such as steric hindrance from the phenyl rings. If the reaction mixture was heated at 60 °C for six hours the formation of a dark, powdery precipitate was observed, and **$Li[Ph_4PnH]$** disappeared more rapidly, suggesting the formation of **$Li_2[Ph_4Pn]$** was being accelerated. However, this powdery solid could not be analysed to confirm this, due to the low solubility in all solvents tested (see below).

The sample from which the crystal for XRD analysis was harvested could not be sufficiently re-dissolved in even large volumes of d_8-THF in order to analyse by NMR. Additionally, this material could not be dissolved in d_5-pyridine, DME, 12-crown-4, C_6D_6 or a 50:50 mixture of C_6D_6 and 12-crown-4. When the reaction of **Ph_4PnH_2** with two equivalents of LiHMDS in d_8-THF was performed in the presence of an excess of TMEDA the same, slow precipitation of what is likely **$Li_2[Ph_4Pn]$** is observed, with the TMEDA failing to keep the product in solution. If an excess of 12-crown-4 is used as additive for the reaction with two equivalents LiHMDS precipitation of what is assumed to be **$[Li(12\text{-crown-}4)]_2[Ph_4Pn]$** occurs more rapidly (over the course of 24 hours), likely due to the crown ether enhancing reactivity of the LiHMDS. However, the 12-crown-4 does not solubilise **$Li_2[Ph_4Pn]$** as would be expected from the behaviour of **Cp^-** salts with crown ethers.[21]

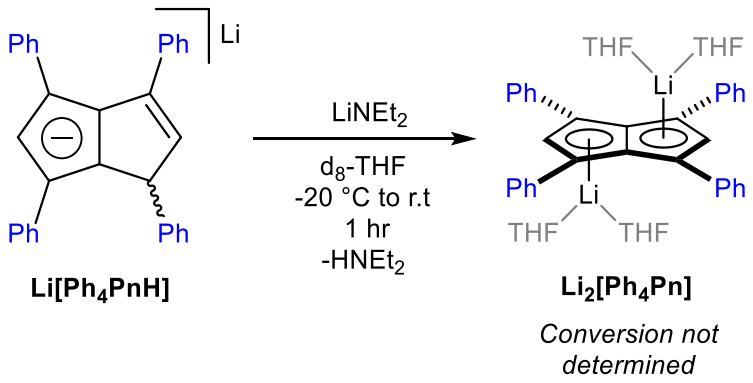

Figure 27: Formation of dilithium 1,3,4,6-tetraphenylpentalenide from 1,3,4,6-tetraphenylhydropentalenide

It was found that treating **Ph_4PnH_2** with one equivalent of $LiNEt_2$ in d_8-THF would rapidly form **Li[Ph_4PnH]** (section 3.2.1). Adding a second equivalent of $LiNEt_2$ (Figure 27) led to the rapid disappearance of the **Li[Ph_4PnH]** NMR signals, and the formation of a light orange precipitate. This was assumed to be **$Li_2[Ph_4Pn]$** due to visual similarities to the solid formed in the reaction with two equivalents of LiHMDS. However, once again the product could not be sufficiently re-dissolved in order to analyse it with NMR and confirm this structure.

3.3.2 Synthesis of disodium 1,3,4,6-tetraphenylpentalenide

As **$Li_2[Ph_4Pn]$** was found to be insoluble in the organic solvents tested it was not possible to analyse it using solution-phase NMR. The inability to form homogeneous solutions of the **Pn^{2-}** species would likely affect its ability to cleanly transmetalate when reacted with metal precursors. It was decided to investigate whether changing the lithium cations, which are hard and more covalent in their binding, for either sodium or potassium, which are softer and more ionic in their binding, would affect the solubility of the **Ph_4Pn^{2-}** salt.

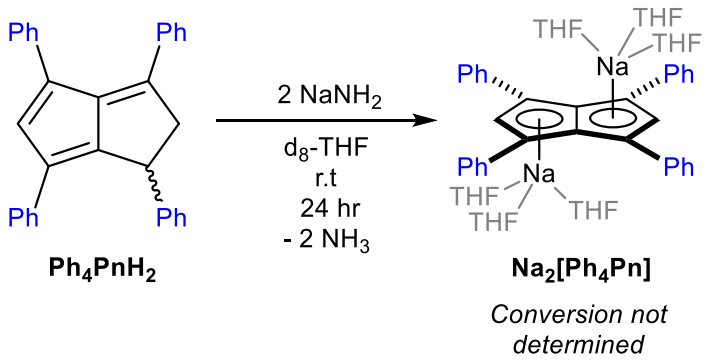

Figure 28: Formation of disodium 1,3,4,6-tetraphenylpentalenide from 1,3,4,6-tetraphenyldihydropentalene

Treating **Ph_4PnH_2** with two equivalents of $NaNH_2$ suspended in d_8-THF (Figure 28) led to slow formation of a dark red crystalline solid. This material proved suitable for analysis by XRD, and was shown to be **$[Na(THF)_3]_2[Ph_4Pn]$** (Section 3.3.4). However, this species was insufficiently soluble in THF to detect in solution by ^{1}H-NMR. When the filtered reaction mixture was analysed by NMR only a small amount of **$Na[Ph_4PnH]$** was present. Performing deprotonation with $NaNH_2$ in d_5-pyridine also led to formation of an insoluble solid, with no **$Na_2[Ph_4Pn]$** detected in solution.

3.3.3 Synthesis of dipotassium 1,3,4,6-tetraphenylpentalenide

Reacting **Ph_4PnH_2** with two (or more) equivalents of KHMDS in d_8-THF (Figure 29) led to rapid formation of **$K[Ph_4PnH]$**. Upon standing for several days a crystalline red precipitate forms and the ^{1}H-NMR signals for **$K[Ph_4PnH]$** disappear. This crystalline material was suitable for analysis by XRD and was found to be **$[K(THF)_3]_2[Ph_4Pn]$** as a THF-bridged polymer (Section 3.3.4). This species was again insufficiently soluble in d_8-THF or d_5-pyridine to analyse by NMR so DOSY techniques could not be used to determine if this species adopts a polymeric structure in solution.

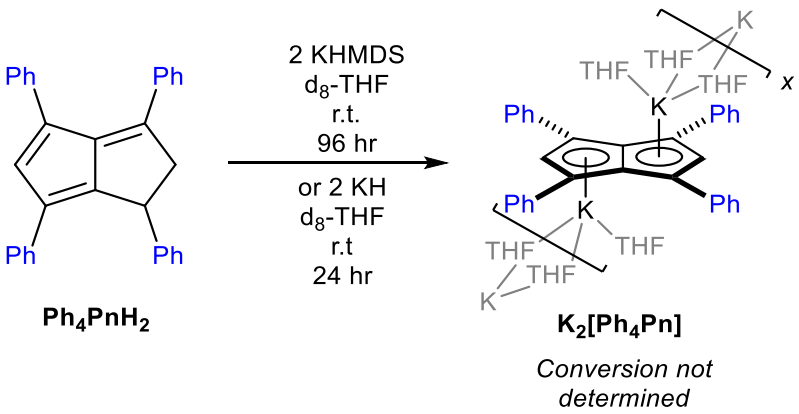

Figure 29: Formation of dipotassium 1,3,4,6-tetraphenylpentalenide from 1,3,4,6-tetraphenyldihydropentalene

Reacting **Ph_4PnH_2** with a suspension of two equivalents of KH in THF (Figure 29) led to the formation of the same red precipitate, assumed to be **$K_2[Ph_4Pn]$**. This solid could not be dissolved sufficiently in THF, d_5-pyridine, DME or C_6D_6 in order to analyse it by NMR. Adding TMEDA or 18-crown-6 to the reaction mixtures also did not solubilise **$K_2[Ph_4Pn]$** in order to detect in solution by NMR.

3.3.4 X-ray structures of 1,3,4,6-tetraphenylpentalenides

Previously reported **Pn^{2-}** species have only been characterised as a single alkali metal salt – for example, the dilithium salt for the parent **Pn^{2-}** and **Pn^{*2-}**, and dipotassium for **1,4-TIPS-Pn^{2-}**. However, in this investigation the dilithium, disodium and dipotassium salts of **Ph_4Pn^{2-}** have all been synthesised and characterised by XRD.

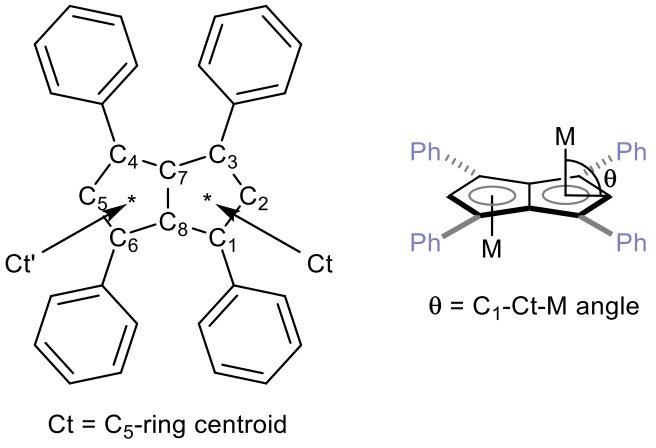

Figure 30: Definitions for positions and angles in 1,3,4,6-tetraphenylpentalenide

Light orange crystals of **[Li(THF)$_2$]$_2$[Ph$_4$Pn]** (Figure 31) were grown by allowing the reaction mixture of **Ph$_4$PnH$_2$** and two equivalents of LiHMDS in THF to stand at -20 °C. XRD showed this species adopted the *anti*-Li$_2$ structure that would be expected based on the crystal structures of **[Li(DME)]$_2$Pn** and **[Li(TMEDA)]$_2$Pn***. Each lithium was solvated by two THF molecules, analogous to how the lithiums in **[Li(DME)]$_2$Pn** were complexed by two oxygen donor atoms from the chelating DME.

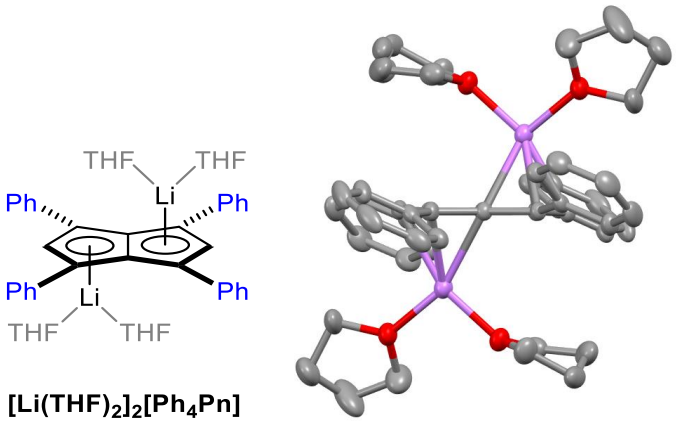

Figure 31: Crystal structure of THF-adducted dilithium 1,3,4,6-tetraphenylpentalenide (hydrogens omitted)

The C2-centroid-Li angle in **[Li(THF)$_2$]$_2$[Ph$_4$Pn]** is 90.04(9)°, meaning the lithium atom was positioned centrally above the C$_5$-ring, consistent with η^5-binding without any η^3-allyl character. The Li-centroid distance was 1.98(3) Å, longer than the distances observed in **[Li(DME)]$_2$Pn** and **[Li(TMEDA)]$_2$Pn*** at 1.89 Å and 1.87 Å respectively. This suggests that the phenyl-substitution leads to decreased electron-density in the **Pn^{2-}** rings, and therefore there is less donation to the lithium atoms leading to longer bond lengths. The phenyl rings were rotated out of the plane of the central ring system by either 35.77(2)° or 29.26(2)°, meaning that in the solid state the negative charges cannot be fully delocalised into the π-system of the phenyl groups by resonance. Therefore, it would be mostly inductive effects that are responsible for affecting the electron density in the central rings (see section 2.1.1).

The phenyl groups were bent towards the lithium atoms, with the C1-phenyl and C-3-phenyl bonds bent away from the plane of the central rings by either 4.25(1)° or 10.98(1)°, suggesting some influence of the cation over the orientation of these groups. However, the shortest C-Li distances for

the phenyl groups were 3.13(3) Å and 3.35(3) Å for the quaternary phenyl carbons, too long to ascribe a degree of covalent C-Li bonding.

Dark red crystals of **[Na(THF)$_3$]$_2$[Ph$_4$Pn]** (Figure 32) were obtained by standing a THF solution of **Ph$_4$PnH$_2$** over an excess of sodium amide at -20 °C. The disodium salts adopted the same *anti*-configuration as the Li_2 salt, with the larger sodium atoms being solvated by three THF molecules instead of two. With bidentate donors such as DME or TMEDA this species salt might adopt a solvent-bridged polymeric structure, but this had not yet been demonstrated.

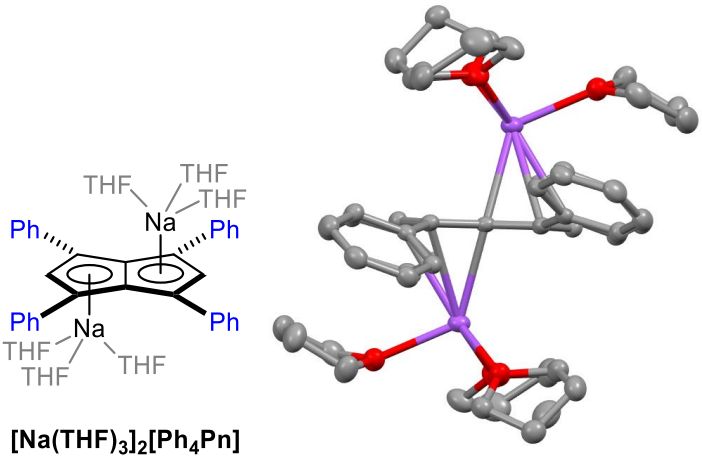

Figure 32: Crystal structure of THF-adducted disodium 1,3,4,6-tetraphenylpentalenide (hydrogens omitted)

The Na-centroid distance in **[Na(THF)$_3$]$_2$[Ph$_4$Pn]** was 2.49(1) Å, longer than the metal-centroid distance in the lithium salt due to the increased ionic radius of a sodium cation compared to lithium. The bonding of the **Ph$_4$Pn^{2-}** to the sodium is likely to be more ionic in character than for lithium, which would also contribute to longer metal-carbon bond lengths. The C2-centroid-Na angle in **[Na(THF)$_3$]$_2$[Ph$_4$Pn]** was 100.68(6)°, larger than observed in the lithium analogue. The sodium atoms were positioned closer to the central bridgehead carbons than the end carbons, with the C7/C8-Na bond lengths being 2.61(1)-2.63(1) Å compared to the C1/C2/C3-Na lengths of 2.81(1)-2.95(1) Å. This observed difference in cation positioning between the lithium and sodium salts agrees with the computations of the **Li$_2$Pn** and **Na$_2$Pn** structures reported by Barroso *et al.* [16]

Dark orange crystals of **$[K_2(THF)_4(Ph_4Pn)]_x$** (Figure 33) were grown by allowing a THF solution of **Ph_4PnH_2** with two equivalents of KHMDS to stand at -20 °C. XRD analysis showed a polymeric structure, consisting of THF-bridged anti-**$K_2[Ph_4Pn]$** units. Pairs of K atoms are bridged by two THF-molecules and are each solvated by an additional non-bridging THF.

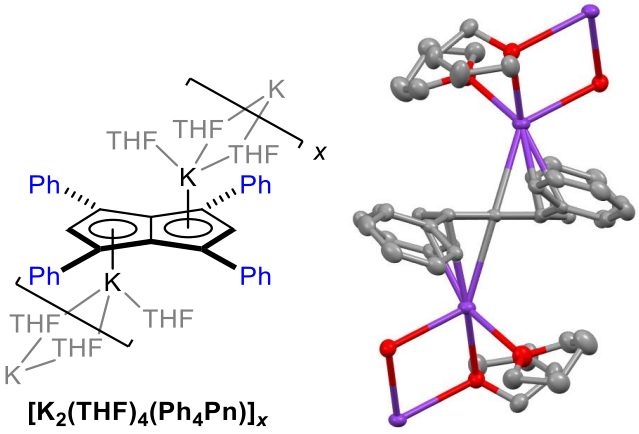

Figure 33: Crystal structure of THF-adducted dipotassium 1,3,4,6-tetraphenylpentalenide (hydrogens omitted)

The K-centroid distance in **$[K_2(THF)_4(Ph_4Pn)]_x$** was 2.69(2) Å, longer than the equivalent distance in **$[Na(THF)_3]_2[Ph_4Pn]$**, likely due to increasing ionic character in the M-Pn bonding. However, the difference in M-centroid distances between the Na and K salts was smaller than between the Na and Li salts, as the larger alkali-metals are more similar in their bonding character.

The C2-centroid-K angle in **$[K_2(THF)_4(Ph_4Pn)]_x$** was 95.17(8)°, larger than the in the lithium salt. However, it is a smaller angle than observed in the sodium salt, meaning the K atoms are positioned more centrally above the C_5-ring than the Na atoms are. This is in contrast to the calculated **K_2Pn** structure reported by Barosso *et al.*[16] It is possible the bridged structure of this crystal influences the positioning of K atoms. The presence of phenyl groups could result in different cation positioning than in the parent **K_2Pn,** but this species has not been experimentally characterised in order to compare XRD structures. The shortest C-K for the phenyl groups was 3.45(2) Å, too long to ascribe a degree of C-K bonding, so it is unclear how much the phenyl rings influence the cation positioning.

3.3.5 Mixed alkali-metal salts of 1,3,4,6-tetraphenylpentalenide

The three **$M_2[Ph_4Pn]$** that were investigated were found to be insoluble in all the tested solvents, meaning that ^{1}H- and ^{13}C{^{1}H}-NMR spectra of these species could not be obtained. In order to use NMR spectroscopy to analyse this dianion a soluble source of **Ph_4Pn^{2-}** was required. The XRD structures of the **$M_2[Ph_4Pn]$** species (Section 3.3.4) showed that the ligand-metal distances are quite different in the lithium and potassium species, so a **Ph_4Pn^{2-}** salt with one lithium cation and one potassium cation would have asymmetrical metal-ligand environments. It was supposed that this asymmetry would disrupt the packing within the solid form of the salt, and therefore would decrease the lattice energy and increase the solubility.

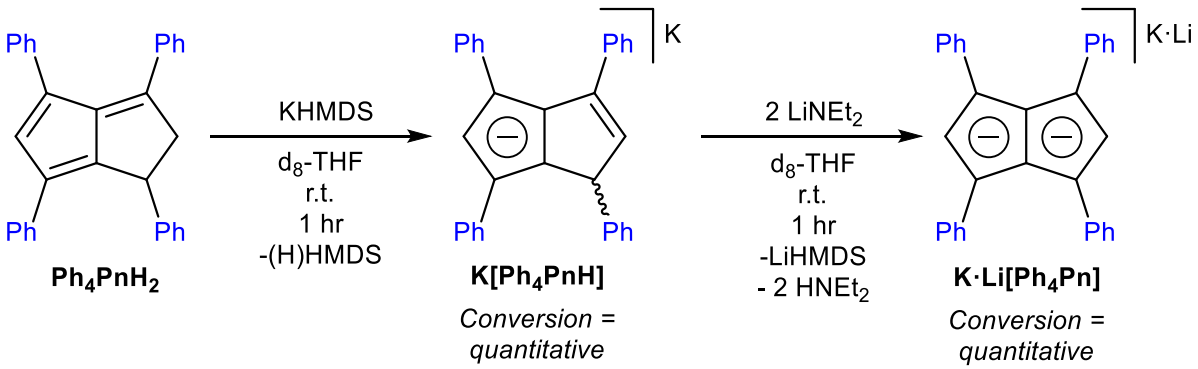

Figure 34: Formation of lithium potassium 1,3,4,6-tetraphenylpentalenide from potassium 1,3,4,6-tetraphenylhydropentalenide

$K[Ph_4PnH]$ was generated *in situ* by treating **Ph_4PnH_2** with one equivalent of KHMDS in d_8-THF. This solution was added to two equivalents of $LiNEt_2$ in d_8-THF (Figure 34) leading to formation of an orange solution. An additional equivalent of is $LiNEt_2$ required in order to first deprotonate the (H)HMDS present in solution. This solution remained homogeneous initially and was shown by ^{1}H-NMR to contain **Ph_4Pn^{2-}**, presumably existing as **$K{\cdot}Li[Ph_4Pn]$**. Leaving the sample to stand for several weeks led to the formation of precipitates along with the disappearance of the NMR signals for **Ph_4Pn^{2-}**. These precipitates could not be re-dissolved to analyse this material by NMR, and the solids were not suitable for XRD analysis. It was supposed that these solids are **$Li_2[Ph_4Pn]$** and **$K_2[Ph_4Pn]$** forming by slow cation

exchange in solution (see below). This means that solutions of **K·Li[Ph$_4$Pn]** cannot be stored indefinitely.

The ^{1}H-NMR spectrum of **K·Li[Ph$_4$Pn]** (Figure 35) showed only four signals - three at 7.08, 6.95 and 6.53 ppm for the phenyl groups, and one at 6.81 ppm for the H-atoms bound to the **Pn^{2-}** core. This shows that in solution all four phenyl groups are equivalent and that the two halves of the molecule are equivalent. As the phenyl groups only display one signal for *ortho*-Hs and one for *meta*-Hs, this suggests that at 25 °C the rings can rotate making these hydrogens equivalent on an NMR time scale. The C2/C5 ring bound hydrogen signals at 6.81 ppm are comparable to the analogous hydrogen in **Li[Ph$_2$Cp]**, which showed a ^{1}H signal at 6.56 ppm.

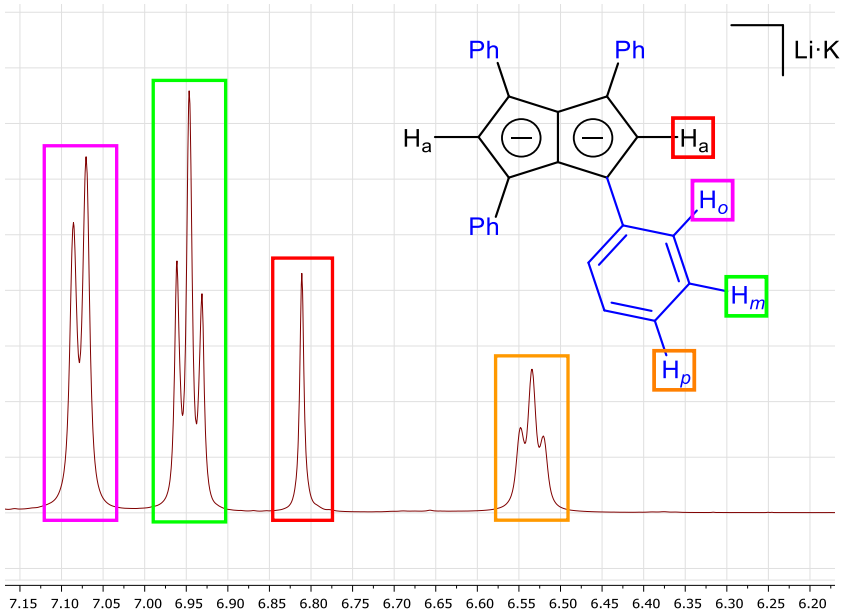

Figure 35: ^{1}H-NMR (500 MHz) spectrum of lithium potassium 1,3,4,6-tetraphenylpentalenide

The ^{13}C{^{1}H}-NMR spectrum of **K·Li[Ph$_4$Pn]** (Figure 36) was similarly symmetrical. Only six signals were observed in this spectrum, with an additional signal observed as a cross-peak in the HMBC spectrum. This high degree of symmetry would not be predicted if the two different cations were tightly bound to the two C$_5$-rings of the ligand, as the different electronic influence of the cations would cause differences in the chemical shifts for the two halves of the molecule. This means there was likely a

degree of solvent separation for this species in solution, keeping the cations too distant from the ligand to significantly affect the chemical shifts.

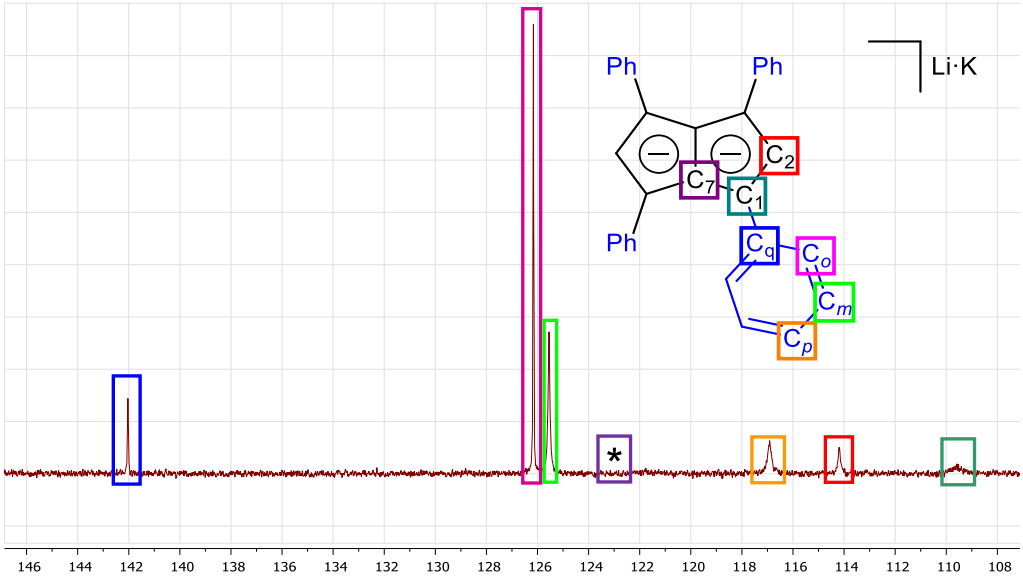

*Figure 36: $^{13}C\{^{1}H\}$-NMR (125 MHz) spectrum of lithium potassium 1,3,4,6-tetraphenylpentalenide; * cross-peak observed at 123.0 ppm on HMBC*

The ^{13}C-signal for the *para*-hydrogens of the phenyls in **K·Li[Ph$_4$Pn]** had a chemical shift of 116.9 ppm. This is 9.3-11.0 ppm upfield of the equivalent carbons in **Ph$_4$PnH$_2$**, suggesting that the negative charges in the **Ph$_4$Pn^{2-}** are causing extra shielding for the *para*-carbons. This is comparable to the change in *para*-carbons signals observed for **Ph$_2$CpH** and **Li[Ph$_2$Cp]**, with the signal shifted upfield by 8.20 ppm for **Ph$_2$Cp$^-$**. This could be due to π-delocalisation of the negative charges into the phenyl rings, as in solution the phenyls should be able to adopt a coplanar arrangement with the ligand core through rotation around the C-C axis. However, DFT calculations would be required to determine the degree of this delocalisation.

When this stepwise deprotonation with two different alkali metal bases is performed in d$_5$-pyridine the formation of the same species was observed by NMR, and the species also remained in solution initially. However, as with the THF solution, over the course of weeks crystalline precipitates formed from the solution. In this case, a crystal suitable for XRD analysis was obtained. It was shown to be

[K(Pyr)$_3$]$_2$[Ph$_4$Pn] (Figure 37), which presumably forms by cation exchange occurring in solution. This crystalline material could not be sufficiently re-dissolved to analyse by NMR.

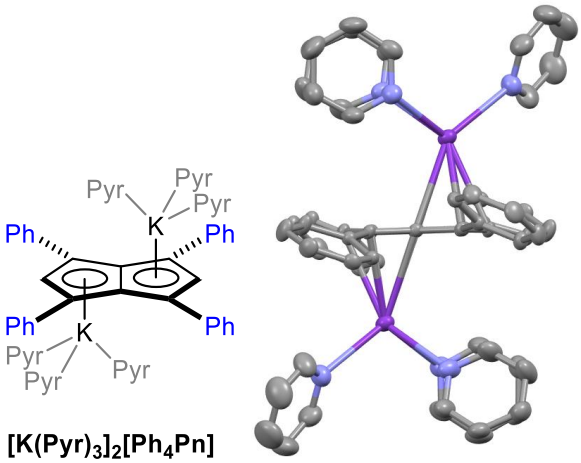

Figure 37: Crystal structure of pyridine-adducted dipotassium 1,3,4,6-tetraphenylpentalenide (hydrogens omitted)

The crystal structure **[K(Pyr)$_3$]$_2$[Ph$_4$Pn]** had each K atom solvated by three pyridine atoms and does not adopt the solvent-bridged polymer structure of the THF-adduct (Section 3.3.4). The centroid-K distance was 2.75(1) Å, longer than observed in the THF-adduct. This is likely due to increased donation from the solvent leading to weaker bonding with the **Ph$_4$Pn^{2-}**. The C2-centroid-K angle was 91.0(6)°, meaning the K atoms are aligned more centrally above the ring than in the THF-adduct. This small angle contrasts with the calculated positioning of K atoms in **K$_2$Pn** reported by Barroso *et al.*[16] (Section 3.1.3)

These results show that **Ph$_4$Pn^{2-}** salts with two different cations are more soluble in co-ordinating solvents than those with two identical cations. This also demonstrates that $LiNEt_2$ is a suitable base for deprotonating **Ph$_4$PnH$^-$** to form **Ph$_4$Pn^{2-}**. However, the mixed system must undergo slow cation exchange, so solutions of this species would need to be generated shortly before use in transmetalation reactions.

Similarly, stirring a d_8-THF solution of **Li[Ph$_4$PnH]**, generated *in situ* by reacting **Ph$_4$PnH$_2$** with one equivalent of LiHMDS, with two equivalents of KH led to quantitative conversion of the monoanion

into **K·Li[Ph$_4$Pn]** over the course of 24 hours (Figure 38). Dianion formation is slower than using diethylamide, presumably because of the heterogeneous nature of KH in THF. However, this result shows that hydride is a suitable base for forming **Ph$_4$Pn^{2-}**, and this base has the benefit of having a volatile conjugate acid that easily leaves the solution and would not interfere with subsequent transmetalation reactions.

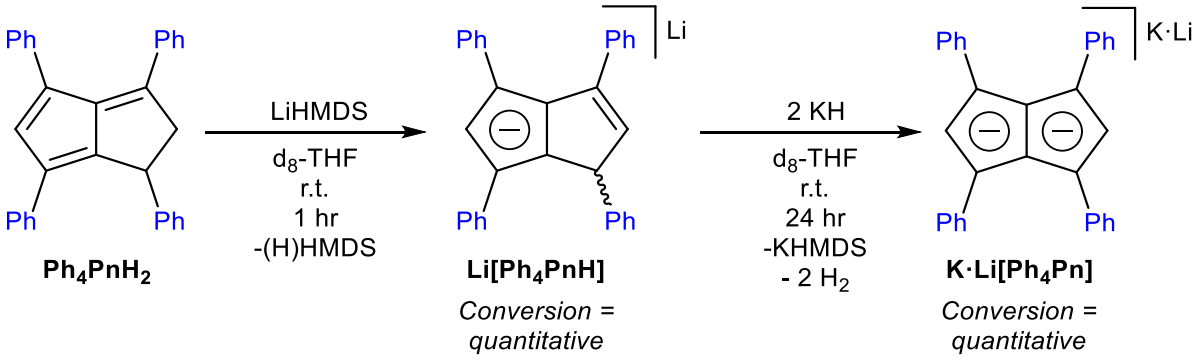

Figure 38: Formation of lithium potassium 1,3,4,6-tetraphenylpentalenide from lithium 1,3,4,6-tetraphenylhydropentalenide

While the solution remained homogeneous initially, allowing the THF solution to stand for several weeks led to precipitation of a crystalline solid. XRD analysis of one of these crystals showed it to be a mixture of **Li$_2$[Ph$_4$Pn]** and **K$_2$[Ph$_4$Pn]** units in the ratio of 1:3. In this crystal structure the C2-centroid-K angle is 100.21(2)°, larger than the equivalent angle in the polymeric **K$_2$[Ph$_4$Pn]** structure described in Section 3.3.4. This is closer to the calculated positioning of K atom in **K$_2$Pn** as reported by Barroso *et al.*[16] The K-centroid distance is 2.64(2) Å, 0.05 Å shorter than in the polymeric structure. Because the of the overlay of the metal atom the Li-ligand bond distances and angles could not be determined for this crystal structure.

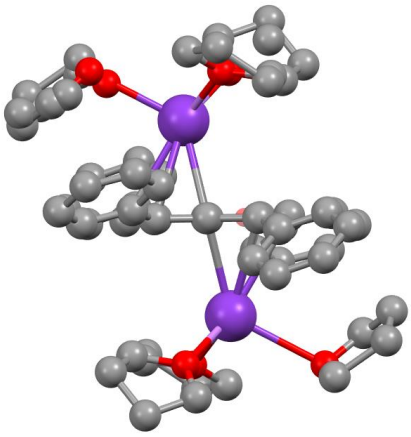

Figure: XRD structure of a mixed $Li_2[Ph_4Pn]$ and $K_2[Ph_4Pn]$ crystal (hydrogens omitted)

While **K·Li[Ph$_4$Pn]** is a soluble source of the **Ph$_4$Pn^{2-}**, it contains a '**LiCp**'-like unit within it which could be too reducing for use with high-valent metal precursors. [20, 26] Replacing the lithium cation with a sodium cation would potentially prevent this unwanted reactivity and widen the range of complexes that could be formed with this ligand.

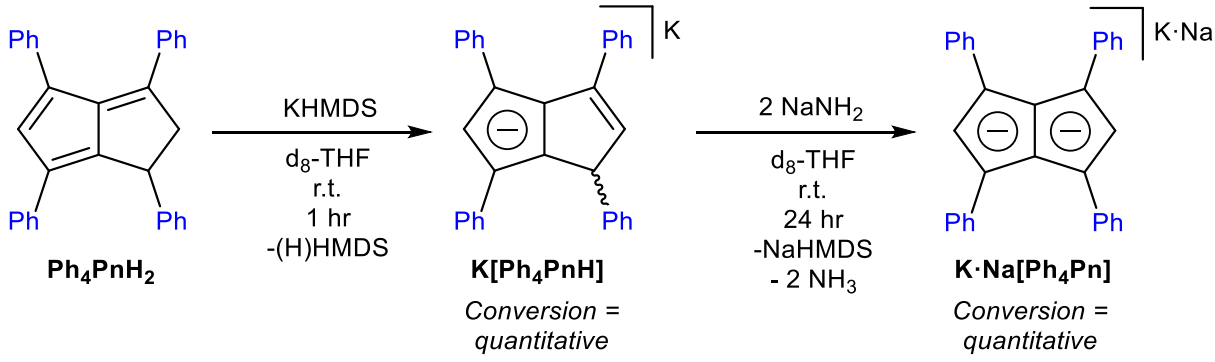

Figure 39: Formation of potassium sodium 1,3,4,6-tetraphenylpentalenide from potassium 1,3,4,6-tetraphenylhydropentalenide

Reacting **K[Ph$_4$PnH]**, formed *in situ* by reacting **Ph$_4$PnH$_2$** with one equivalent of KHMDS in d$_8$-THF, with two equivalents of $NaNH_2$ in d$_8$-THF led to quantitative conversion of the mono-anion into **Ph$_4$Pn^{2-}**, presumably existing in solution as **K·Na[Ph$_4$Pn]** (Figure 39). The ^{1}H- (Figure 40) and $^{13}C\{^1H\}$-NMR spectra for this species were almost identical to that of **K·Li[Ph$_4$Pn]**, suggesting a degree of solvent separation between the alkali-metal cations and the **Ph$_4$Pn^{2-}** anion in both cases. Crystals of this species could not be grown, so it could not be analysed by XRD.

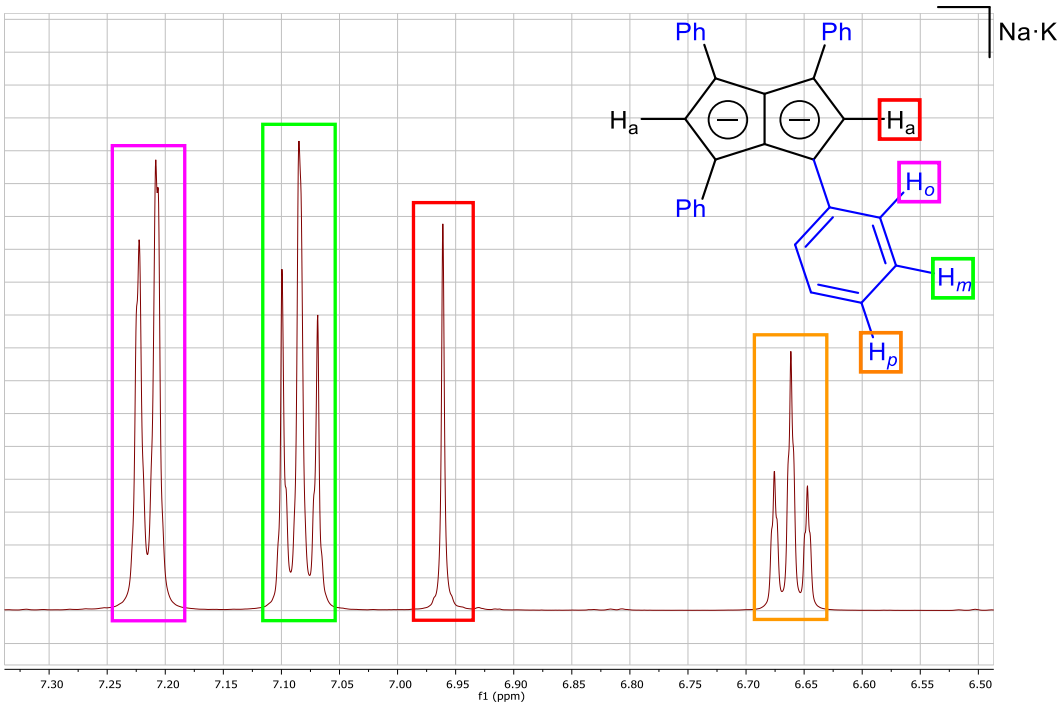

Figure 40: ^{1}H-NMR (500MHz) spectrum of sodium potassium 1,3,4,6-tetraphenylpentalenide

3.3.6 Attempted synthesis of stannylated derivatives of 1,3,4,6-tetraphenylpentalenide

Cooper *et al.*[26] reported that **Pn*(SnMe$_3$)$_2$** could be synthesised by reacting **Li$_2$Pn*** with two equivalents of SnMe$_3$Cl. They showed that this stannylted derivative could react cleanly with Ti(IV),[26] Rh(I) and Ir(I)[27] precursors that the dilithium salt is incompatible with. It was supposed that reacting a soluble **Ph$_4$Pn^{2-}** salt with two equivalents of SnMe$_3$Cl could furnish **Ph$_4$Pn(SnMe$_3$)$_2$**, a soft ligand transfer agent for synthesising **Ph$_4$Pn^{2-}** complexes.

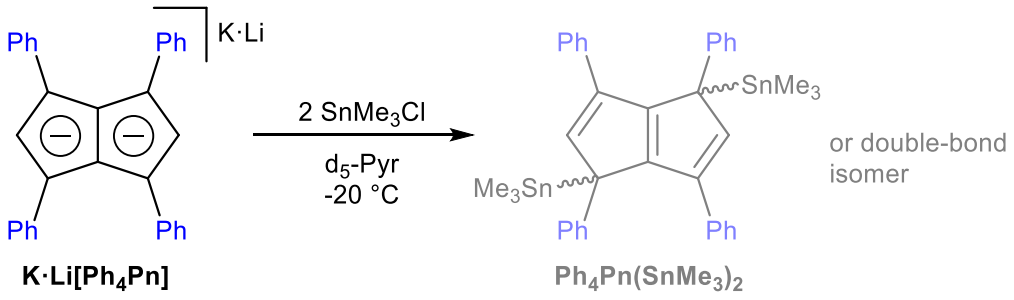

Figure:

When **K·Li[Ph$_4$Pn]** was reacted with two equivalents of SnMe$_3$Cl in d$_5$-pyridine, the dark red solution was transformed into a bright yellow one. The ^{1}H-NMR spectrum showed the **Ph$_4$Pn^{2-}** had been

consumed, but little product could be detected in solution. It could be that **$Ph_4Pn(SnMe_3)_2$** is too insoluble in pyridine to analyse this species by NMR. The ^{119}Sn showed two new signals arising at 51.82 and 47.51 ppm, either or both from **$Ph_4Pn(SnMe_3)_2$** or a different stannylated derivative. However, these results are so far inconclusive and would require further investigation (Section 4).

3.4 Conclusion and future work

In this chapter the formation of novel **PnH^-** and **Pn^{2-}** derivatives has been described. The lithium, sodium and potassium salts of **Ph_4PnH^-** were synthesised. This is the first **PnH^-** anion to be characterised as salts with different alkali metals. HMDS bases were shown to be suitable for cleanly forming these salts, so it could be supposed that RbHMDS[28] and CsHMDS[29] would be suitable for forming the heavier alkali-metal salts of **Ph_4PnH^-**. In the literature there are no reported alkali-metal **PnH^-** species that have been characterised by XRD, and similarly crystals of the synthesised **Ph_4PnH^-** salts could not be grown. Due to time constraints UV/Vis spectra of these **PnH^-**s were not measured, and future work would include acquiring these spectra. As these salts were found to be air sensitive inert conditions for these measurements would be required. These UV/Vis spectra could provide information about the electronic structure of the **Ph_4PnH^-** ligand, and then could be compared to UV/Vis spectra of transition metal complexes derived from this ligand.

The dilithium, disodium and dipotassium salts of **Ph_4Pn^{2-}** were synthesised and characterised by XRD. This is the first **Pn^{2-}** to be characterised for different alkali-metals, and **$Na_2[Ph_4Pn]$** is the first disodium salt of a **Pn^{2-}** species to be reported. However, these homobimetallic species were all insufficiently soluble to be characterised by NMR. This poor solubility might also limit their potential utility as ligand-transfer agents. This problem was overcome by synthesising **Ph_4Pn^{2-}** salts with two different alkali-metals. **$K{\cdot}Li[Ph_4Pn]$** and **$K{\cdot}Na[Ph_4Pn]$** were both found to be highly soluble in both THF and pyridine and could be analysed by ^{1}H- and ^{13}C{^{1}H}-NMR. However, these mixed species could not be analysed by XRD, as cation exchange occurring in solution led to formation and crystallisation of the

homobimetallic salts. Successfully solubilising the **Ph_4Pn^{2-}** ligand would allow this species to be analysed by UV/Vis spectroscopy. These spectra could then be compared to transition-metal complexes of **Ph_4Pn^{2-}** if they could be successfully synthesised. However, due to time constraints meant these UV/vis measurements were not performed and would be conducted in future work.

Thallium and tin derivatives of **Ph_4PnH^-** and **Ph_4Pn^{2-}** could not be successfully synthesised. Further investigation could be conducted to devise suitable conditions for synthesising these derivatives so they could be used as softer transmetalation agents. However, as the phenyl-substituted **Pn** derivatives have been shown to suffer solubility issues, future work would focus instead on synthesising thallium and tin derivatives of functionalised variants of **Ph_4Pn^{2-}** (see below).

While mixed cations were shown to solubilise **Ph_4Pn^{2-}** species, an alternate approach to the problem of insolubility is to synthesise derivatives with functionalised phenyl groups. While **Ph_5Cp^-** species typically suffer from issues of solubility, the analogous **$(p\text{-Tol})_5Cp^-$** species have shown to be more soluble in many solvents.[10] Another example of this is provided by Harder and Ruspic,[5] who report the utility of **$(p\text{-}^n\text{BuPh})_5Cp^-$** ($Cp^{BIG}$) as a soluble penta-aryl **Cp^-** derivative. This species can be used to synthesise deca-aryl metallocenes for a wide range of metals that are soluble even in apolar solvents such as hexane.[11a, 12]

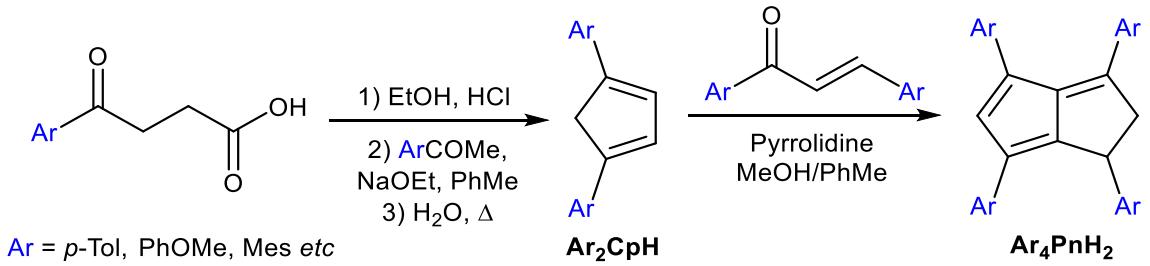

Figure 41: Synthetic route to 1,3,4,6-tetraaryldihydropentalenes

$1,3,4,6\text{-}Ar_4PnH^-$ and **$1,3,4,6\text{-}Ar_4Pn^{2-}$** would be derived from **$1,3,4,6\text{-}Ar_4PnH_2$,** and these could be synthesised from **Ar_2CpH** derivatives (Figure 41). The method describe by Drake and Adams,[30] which is used to synthesise **$1,4\text{-}Ph_2CpH$** (section 2.4.1), can also be used to synthesise **1-Ar-4-PhCpH** species.[31] Clennan and Mehrsheikh-Mohammadi[32] report that **$1,4\text{-}(p\text{-Tol})_2CpH$** can be also be accessed

by this method. It is supposed that a range of **Ar$_2$CpH**s could be accessed from the relevant substituted benzoyl-propionic acids and substituted acetophenones. These **CpH** derivatives could then be condensed with the relevant enone, which would be derived from a substituted acetophenone and a substituted benzaldehyde, and pyrrolidine is likely to be the reagent of choice to facilitate this reaction (section 2.4.2).

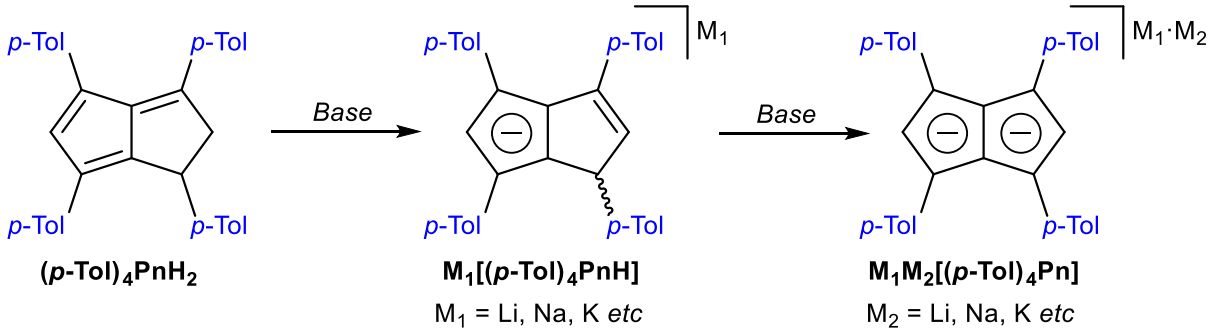

Figure 42: Synthesis of 1,3,4,6-(p-Tolyl)hydropentalenide and 1,3,4,6-(p-Tolyl)pentalenide

The initial target of the future work would be **(*p*-Tol)$_4$PnH$_2$** (Figure 42). It is supposed that this species would provide access to **(*p*-Tol)$_4$Pn^{2-}** salts, which would potentially be more soluble that the analogous **Ph$_4$Pn^{2-}** salts. This would enable the homobimetallic salts to be characterised by NMR and find greater utility in transmetalation chemistry. Other aryl derivatives would hopefully be accessible via this route, as would asymmetrically substituted variants. Different aryl-substituents will exert different amounts of steric shielding on metals bound to these ligands, and the different electronic properties of these aryl groups could allow tuning of the metal-ligand bonding.

With soluble sources of **Ph$_4$PnH$^-$** and **Ph$_4$Pn^{2-}** synthesised, future work would look at exploring their organometallic chemistry. There are a range of metal precursors that have been shown to react with **PnH$^-$** and **Pn^{2-}** species (chapter 1), and the steric stabilisation of the multiple phenyl groups might allow reactivity for **Ph$_4$PnH$^-$** and **Ph$_4$Pn^{2-}** that is not accessible for the unsubstituted and methyl-substituted derivatives. In instances where the phenyl-substituted complexes are not soluble enough to be analysed the substituted-aryl ligands described above could be used in their place.

3.5 Experimental

General: All reactions were carried out under argon using standard Schlenk techniques or an MBraun Unilab Plus glovebox. NMR spectroscopy was conducted using a 500 MHz Bruker Avance III at 25 °C. Chemical shifts (δ) are reported in ppm. Single crystal X-ray diffraction analysis was carried out by Dr Gabriele Kociok-Köhn at the University of Bath using a RIGAKU SuperNova Dual. Commercially available materials were obtained from Sigma Aldrich, Fisher or Acros. d_8-THF was dried by distillation from potassium and was stored over a sodium mirror. C_6D_6 and DME were dried by distillation from sodium and stored over a sodium mirror. d_5-pyridine and TMEDA were dried by distillation from calcium hydride and stored over 4 Å molecular sieves. 12-crown-4 was purified by distillation. 18-crown-6 was purified by recrystallistion from dry acetonitrile.

Lithium 1,3,4,6-tetraphenylhydropentalenide: 1,3,4,6-Ph_4PnH_2 (10 mg, 0.025 mmol) dissolved in 0.2 ml d_8-THF was added dropwise to LiHMDS (4.1 mg, 0.025 mmol) or $LiNEt_2$ (2.0 mg, 0.025 mmol) in 0.2 ml d_8-THF. The bright orange solution was allowed to stand for 30 mins, and then was filtered into a J. Young NMR tube. The ^{1}H-NMR spectrum showed quantitative conversion of the starting material into **Li[Ph_4PnH]**.

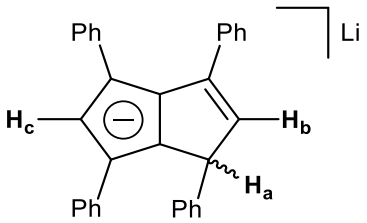

^{1}H NMR (500 MHz, d_8-THF): δ (ppm) = 7.49 (***o*-Ph**, m, 4H), 7.41 (***o*-Ph**, d, 2H, $^3J_{HH}$ = 7.40 Hz), 7.19 (***o*-Ph**, ***m*-Ph**, m, 6H), 7.07 (***p*-Ph**, t, 1H, $^3J_{HH}$ = 7.42 Hz), 6.96 (***m*-Ph**, ***p*-Ph**, m, 5H), 6.76 (***p*-Ph**, t, 1H, $^3J_{HH}$ = 7.28 Hz), 6.63 (***p*-Ph**, **H_C**, m, 2H), 5.90, (**H_b**, d, 1H, $^3J_{HH}$ = 1.57 Hz), 4.71 (**H_a**, d, 1H, $^3J_{HH}$ = 1.57 Hz);

^{13}C{^{1}H} NMR (125 MHz, d_8-THF): δ (ppm) = 141.9, 139.6, 138.8, 137.9, 129.8, 126.6, 126.2, 125.9, 125.5, 125.2, 124.8, 123.9, 123.06, 122.1, 119.6, 118.7, 50.6;

Sodium 1,3,4,6-tetraphenylhydropentalenide: 1,3,4,6-Ph_4PnH_2 (10 mg, 0.025 mmol) dissolved in 0.2 ml d_8-THF was added dropwise to NaOEt (1.7 mg, 0.025 mmol) in 0.2 ml d_8-THF. The dark red solution was allowed to stand for 20 hours, and then was filtered into a J. Young NMR tube. The ^{1}H-NMR spectrum showed quantitative conversion of the starting material into **Na[Ph_4PnH]**.

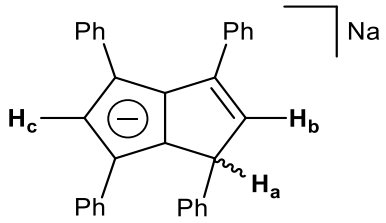

^{1}H NMR (500 MHz, d_8-THF): δ = 7.58 (***o*-Ph**, m, 2H) 7.47 (***o*-Ph**, m, 2H) 7.37 (***o*-Ph**, m, 2H), 7.20-7.28 (***o*-Ph**, ***m*-Ph**, ***p*-Ph**, m, 7H), 7.11 (***p*-Ph**, t, 1H, $^3J_{HH}$ = 7.24 Hz), 7.03 (***m*-Ph**, m, 4H), 6.87 (***p*-Ph**, t, 1H, $^3J_{HH}$ = 7.26 Hz), 6.73 (***p*-Ph**, **H_c**, m, 2H), 6.02 (**H_b**, d, 1H, $^3J_{HH}$ = 2.20 Hz, $^6J_{HH}$ = 0.76 Hz), 4.82 (**H_a**, d, 1H, $^3J_{HH}$ = 2.20 Hz);

^{13}C{^{1}H} NMR (125 MHz, d_8-THF): δ = 142.0, 139.3, 138.5, 133.4, 130.4, 125.7, 125.5, 123.9, 122.9, 121.5, 119.4, 118.2, 114.0, 112.4, 103.1, 50.5;

Potassium 1,3,4,6-tetraphenylhydropentalenide: 1,3,4,6-Ph_4PnH_2 (10.0 mg, 0.025 mmol) dissolved in 0.2 ml d_8-THF was added dropwise to KHMDS (4.9 mg, 0.025 mmol) in 0.2 ml d_8-THF. The bright red solution was allowed to stand for 30 mins, and then was filtered into a J. Young NMR tube. The ^{1}H-NMR spectrum showed quantitative conversion of the starting material into **K[Ph_4PnH]**. The analogous reaction in d_5-pyridine produces a dark purple solution, shown by ^{1}H-NMR to contain **K[Ph_4PnH]**.

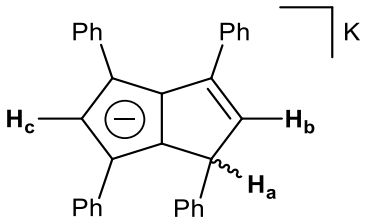

^{1}H NMR (500 MHz, d_8-THF): δ = 7.54 (***o*-Ph**, d, 2H, $^3J_{HH}$ = 8.53 Hz), 7.49 (***o*-Ph**, m, 2H), 7.39, (***o*-Ph**, d, 2H, $^3J_{HH}$ = 8.05 Hz), 7.22 (***o*-Ph**, ***m*-Ph**, ***p*-Ph**, m, 7H), 7.11, (***p*-Ph**, t, 1H, $^3J_{HH}$ = 7.32 Hz), 7.02, (***m*-Ph**, m, 4H),

6.84, (***p*-Ph**, t, 1H, $^{3}J_{HH}$ = 7.27 Hz), 6.66 (**H_c**, d, 1H, $^{6}J_{HH}$ = 0.64 Hz), 6.01 (**H_b**, dd, 1H, $^{3}J_{HH}$ = 2.19 Hz, $^{6}J_{HH}$ = 0.64 Hz), 4.78 (**H_a**, d, 1H, $^{3}J_{HH}$ = 2.19 Hz);

$^{13}C\{^{1}H\}$ NMR (125 MHz, d_8-THF): δ = 144.1, 140.3, 139.5, 137.4, 134.4, 130.1, 129.5, 127.9, 125.9, 125.5, 123.7, 122.1, 118.0, 116.3, 107.6, 52.1;

Dilithium 1,3,4,6-tetraphenylpentalenide: 1,3,4,6-Ph_4PnH_2 (10.0 mg, 0.025 mmol) dissolved in 0.2 ml d_8-THF was added to LiHMDS (8.2 mg, 0.050 mmol) in 0.2 ml d_8-THF. The resulting solution was allowed to stand for 1 week at room temperature and then cooled to -20 °C for 2 weeks. A light orange crystalline solid was formed which provided a sample suitable for XRD analysis and was shown to be **$[Li(THF)_2]_2[Ph_4Pn]$**. The ^{1}H spectrum of the filtered reaction solution showed quantitative consumption of the starting material, but the product was insufficiently soluble to analyse by NMR.

Disodium 1,3,4,6-tetraphenylpentalenide: 1,3,4,6-Ph_4PnH_2 (10.0 mg, 0.025 mmol) dissolved in 0.2 ml d_8-THF was added to $NaNH_2$ (2.0 mg, 0.050 mmol) in 0.2 ml d_8-THF. The resulting solution was allowed to stand for 1 week at room temperature and then cooled to -20 °C for 3 weeks. A red crystalline solid was formed which provided a sample suitable for XRD analysis and was shown to be **$[Na(THF)_3]_2[Ph_4Pn]$**. The ^{1}H spectrum of the filtered reaction solution showed quantitative consumption of the starting material, but the product was insufficiently soluble to analyse by NMR.

Dipotassium 1,3,4,6-tetraphenylpentalenide: 1,3,4,6-Ph_4PnH_2 (10.0 mg, 0.025 mmol) dissolved in 0.2 ml d_8-THF was added to KHMDS (10.0 mg, 0.050 mmol) in 0.2 ml d_8-THF. The resulting solution was allowed to stand for 1 week at room temperature and then cooled to -20 °C for 2 weeks. An orange crystalline solid was formed which provided a sample suitable for XRD analysis and was shown to be **$[K_2(THF)_4(Ph_4Pn)]_x$**. The ^{1}H spectrum of the filtered reaction solution showed quantitative consumption of the starting material, but the product was insufficiently soluble to analyse by NMR.

Lithium potassium 1,3,4,6-tetraphenylpentalenide:

Method A: **1,3,4,6-Ph_4PnH_2** (10.0 mg, 0.025 mmol) dissolved in 0.2 ml d_8-THF was added to KHMDS (4.9 mg, 0.025 mmol) in 0.2 ml d_8-THF. The reaction mixture was allowed to stand for 30 minutes at room temperature, and then was added to $LiNEt_2$ (3.0 mg, 0.050 mmol) in 0.1 ml d_8-THF. The mixture was allowed to stand overnight for 1 hour and was then filtered into a J. Young NMR tube. The ^{1}H-spectrum of the reaction solution showed quantitative conversion of the starting material into **K·Li[Ph_4Pn]**.

Performing the analogous reaction in d_5-pyridine produces a purple solution shown by ^{1}H-NMR to contain **K·Li[Ph_4Pn]** with quantitative conversion of starting material. Allowing the pyridine solution to stand for 3 weeks at -20 °C produced crystals of **[K(Pyr)$_3$]$_2$[Ph_4Pn]** which could not be redissolved.

Method B: **1,3,4,6-Ph_4PnH_2** (10.0 mg, 0.025 mmol) dissolved in 0.2 ml d_8-THF was added to LiHMDS (4.1 mg, 0.025 mmol) in 0.2 ml d_8-THF. The reaction mixture was allowed to stand for 30 minutes at room temperature, and then was added to KH (4.0 mg, 0.10mmol) in 0.1 ml d_8-THF. The mixture was allowed to stand overnight and then was filtered into a J. Young NMR tube. The ^{1}H-NMR spectrum of the reaction solution showed quantitative conversion of the starting material into **K·Li[Ph_4Pn]**.

Allowing the reaction mixture to stand at -20 °C for 4 weeks produced crystals found to contain a mixture of **K_2[Ph_4Pn]** and **Li_2[Ph_4Pn]** which could not be redissolved. Performing the analogous reaction in d_5-pyridine produces a purple solution shown by ^{1}H-NMR to contain **K·Li[Ph_4Pn]** with quantitative conversion of starting material.

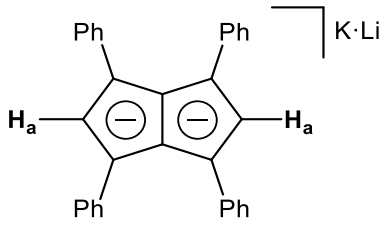

^{1}H NMR (500 MHz, d_8-THF): δ = 7.08 (***o*-Ph,** d, 8H , $^3J_{HH}$ = 7.70 Hz), 6.95 (***m*-Ph,** t, 8H, $^3J_{HH}$ = 7.67 Hz), 6.81 (**H_a**, s, 2H), 6.53 (***p*-Ph**, t, 4H, $^3J_{HH}$ = 6.97 Hz);

$^{13}C\{^{1}H\}$ NMR (125 MHz, d_8-THF): δ = 142.0, 126.2, 125.6, 116.9, 114.2, 109.5 (Note: a peak at 123.0 is observed as a cross-peak in the HMBC spectrum)

Sodium potassium 1,3,4,6-tetraphenylpentalenide: 1,3,4,6-Ph_4PnH_2 (10.0 mg, 0.025 mmol) dissolved in 0.2 ml d_8-THF was added to KHMDS (4.9 mg, 0.025 mmol) in 0.2 ml d_8-THF. The reaction mixture was allowed to stand for 30 minutes at room temperature, and then was added to $NaNH_2$ (2.0 mg, 0.050 mmol) in 0.1 ml d_8-THF. The mixture was allowed to stand overnight and then was filtered into a J. Young NMR tube. The ^{1}H-NMR spectrum of the reaction solution showed quantitative conversion of the starting material into **K·Na[Ph_4Pn]**.

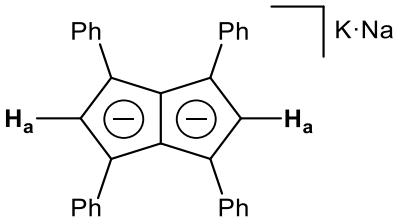

^{1}H NMR (500 MHz, d_8-THF): δ = 7.03 (***o*-Ph,** d, 8H, $^{3}J_{HH}$ = 8.28 Hz), 6.90 (***m*-Ph,** t, 8H, $^{3}J_{HH}$ = 7.31 Hz), 6.78 (**H_a**, s, 2H), 6.48 (***p*-Ph**, t, 4H, $^{3}J_{HH}$ = 7.24 Hz);

$^{13}C\{^{1}H\}$ NMR (125 MHz, d_8-THF): δ = 143.3, 127.3, 126.6, 117.8, 115.4, 111.1 (Note: a peak at 123.2 is observed as a cross-peak in the HMBC spectrum);

3.6 Bibliography

1. Zhang, R.; Tsutsui, M.; E. Bergbreiter, D., Alkali metal salts of pentaphenylcyclopentadienide. *J Organomet Chem* **1982,** *229* (2), 109-112.

2. Giesbrecht, G. R.; Gordon, J. C.; Clark, D. L.; Scott, B. L., Synthesis, structure and solution dynamics of lithium salts of superbulky cyclopentadienyl ligands. *Dalton Trans* **2003,** (13), 2658-2665.

3. (a) Anderson, Q. T.; Erkizia, E.; Conry, R. R., Synthesis and Characterization of the First Pentaphenylcyclopentadienyl Copper(I) Complex, (Ph_5Cp)Cu(PPh_3). *Organometallics* **1998,** *17* (22), 4917-4920; (b) Hoobler, R. J.; Hutton, M. A.; Dillard, M. M.; Castellani, M. P.; Rheingold, A. L.; Rieger, A. L.; Rieger, P. H.; Richards, T. C.; Geiger, W. E., Synthesis, characterization, and crystal structure of the chromium complex (η^5-C_5Ph_5)$Cr(CO)_3$ radical. *Organometallics* **1993,** *12* (1), 116-123.

4. Chambers, J. W.; Baskar, A. J.; Bott, S. G.; Atwood, J. L.; Rausch, M. D., Formation and molecular structures of (η^5-pentabenzylcyclopentadienyl)- and (η^5-pentaphenylcyclopentadienyl)dicarbonyl derivatives of cobalt and rhodium. *Organometallics* **1986,** *5* (8), 1635-1641.

5. Harder, S.; Ruspic, C., Insight in cyclopentadienyl metal complexes with superbulky ligands: The crystal structure of $[Cp^{BIG}K]_\infty$. *J Organomet Chem* **2009,** *694* (7), 1180-1184.

6. Schumann, H.; Janiak, C.; Khani, H., Cyclopentadienylthallium(I) compounds with bulky cyclopentadienyl ligands. *J Organomet Chem* **1987,** *330* (3), 347-355.

7. Panda, T. K.; Gamer, M. T.; Roesky, P. W., An Improved Synthesis of Sodium and Potassium Cyclopentadienide. *Organometallics* **2003,** *22* (4), 877-878.

8. Tabner, B. J.; Walker, T., Radical-anion intermediates. Part VII. Reactions of the 1,2,3,4-tetraphenylcyclopenta-1,3-diene radical anion. *J Chem Soc, Perkin Trans 2* **1975,** (12), 1304-1306.

9. Holl, S.; Bock, H.; Gharagozloo-Hubmann, K., Tris(1,2-dimethoxyethane-O,O)sodium pentaphenylcyclopentadienide. *Acta Crystallogr E* **2001,** *57*, M31-M32.

10. Field, L. D.; Lindall, C. M.; Masters, A. F.; Clentsmith, G. K. B., Penta-arylcyclopentadienyl complexes. *Coord Chem Rev* **2011,** *255* (15), 1733-1790.

11. (a) Kuchenbecker, D.; Harder, S.; Jansen, G., Insight in Structures of Superbulky Metallocenes with the CpBIG Ligand: Theoretical Considerations of Decaphenyl Metallocenes. *Zeitschrift für anorganische und allgemeine Chemie* **2010,** *636* (12), 2257-2261; (b) Orzechowski, L.; Piesik, D. F. J.; Ruspic, C.; Harder, S., Superbulky metallocene complexes of the heavier alkaline-earth metals strontium and barium. *Dalton Trans* **2008,** (35), 4742-4746.

12. Ruspic, C.; Moss, J. R.; Schürmann, M.; Harder, S., Remarkable Stability of Metallocenes with Superbulky Ligands: Spontaneous Reduction of SmIII to SmII. *Angew Chem Int Ed* **2008,** *47* (11), 2121-2126.

13. Turner, Z. R.; Buffet, J.-C.; O'Hare, D., Chiral Group 4 Cyclopentadienyl Complexes and Their Use in Polymerization of Lactide Monomers. *Organometallics* **2014,** *33* (14), 3891-3903.

14. Jones, S. C.; Roussel, P.; Hascall, T.; O'Hare, D., Convenient Solution Route To Alkylated Pentalene Ligands: New Metal Monoalkylpentalenyl Complexes. *Organometallics* **2006,** *25* (1), 221-229.

15. Stezowski, J. J.; Hoier, H.; Wilhelm, D.; Clark, T.; Schleyer, P. v. R., The structure of an aromatic 10π electron 'dianion': dilithium pentalenide. *J Chem Soc, Cheml Commun* **1985,** (18), 1263-1264.

16. Barroso, J.; Mondal, S.; Cabellos, J. L.; Osorio, E.; Pan, S.; Merino, G., Structure and Bonding of Alkali-Metal Pentalenides. *Organometallics* **2017,** *36* (2), 310-317.

17. Dinnebier, R. E.; Behrens, U.; Olbrich, F., Solid State Structures of Cyclopentadienyllithium, -sodium, and -potassium. Determination by High-Resolution Powder Diffraction. *Organometallics* **1997,** *16* (17), 3855-3858.

18. Ashley, A. E.; Cowley, A. R.; O'Hare, D., The hexamethylpentalene dianion and other reagents for organometallic pentalene chemistry. *Chem Commun* **2007,** (15), 1512-1514.

19. Behrens, U.; Dinnebier, R. E.; Neander, S.; Olbrich, F., Solid-State Structures of Base-Free Rubidium and Cesium Pentamethylcyclopentadienides. Determination by High-Resolution Powder Diffraction. *Organometallics* **2008,** *27* (20), 5398-5400.

20. Cloke, F. G. N.; Kuchta, M. C.; Harker, R. M.; Hitchcock, P. B.; Parry, J. S., Trialkylsilyl-Substituted Pentalene Ligands. *Organometallics* **2000,** *19* (26), 5795-5798.

21. Cole, M. L.; Jones, C.; Junk, P. C., Ether and crown ether adduct complexes of sodium and potassium cyclopentadienide and methylcyclopentadienide—molecular structures of $[Na(dme)Cp]_{\infty}$, $[K(dme)_{0.5}Cp]_{\infty}$, [Na(15-crown-5)Cp], [Na(18-crown-6)CpMe] and the "naked Cp–" complex $[K(15\text{-crown-}5)_2][Cp]$. *J Chem Soc, Dalton Trans* **2002,** (6), 896-905.

22. Janiak, C., (Organo)thallium (I) and (II) chemistry: Syntheses, structures, properties and applications of subvalent thallium complexes with alkyl, cyclopentadienyl, arene or hydrotris(pyrazolyl)borate ligands. *Coord Chem Rev* **1997,** *163*, 107-216.

23. Katz, T. J.; Mrowca, J. J., The Pentalenylcycloocta-1,5-dienerhodium Anion and Hydropentalenyl Complexes of Thallium, Platinum, and Rhodium. *J Am Chem Soc* **1967,** *89* (5), 1105-1111.

24. Ustynyuk, Y. A.; Shestakova, A. K.; Chertkov, V. A.; Zemlyansky, N. N.; Borisova, I. V.; Gusev, A. I.; Tchuklanova, E. B.; Chernyshev, E. A., Synthesis, structure and fluxional behaviour of isomeric bis(trimethylstannyl)dihydropentalenes. *J Organomet Chem* **1987,** *335* (1), 43-57.

25. Le Goff, E., The Synthesis of Hexaphenylpentalene. *J Am Chem Soc* **1962,** *84* (20), 3975-3976.

26. Cooper, R. T.; Chadwick, F. M.; Ashley, A. E.; O'Hare, D., Synthesis and Characterization of Group 4 Permethylpentalene Dichloride Complexes. *Organometallics* **2013,** *32* (7), 2228-2233.

27. Chadwick, F. M.; Ashley, A. E.; Cooper, R. T.; Bennett, L. A.; Green, J. C.; O'Hare, D. M., Group 9 bimetallic carbonyl permethylpentalene complexes. *Dalton Trans* **2015,** *44* (46), 20147-20153.

28. Krieck, S.; Schüler, P.; Görls, H.; Westerhausen, M., Straightforward synthesis of rubidium bis(trimethylsilyl)amide and complexes of the alkali metal bis(trimethylsilyl)amides with weakly coordinating 2,2,5,5-tetramethyltetrahydrofuran. *Dalton Trans* **2018,** *47* (36), 12562-12569.

29. Ojeda-Amador, A. I.; Martínez-Martínez, A. J.; Kennedy, A. R.; O'Hara, C. T., Structural Studies of Cesium, Lithium/Cesium, and Sodium/Cesium Bis(trimethylsilyl)amide (HMDS) Complexes. *Inorg Chem* **2016,** *55* (11), 5719-5728.

30. Drake, N. L.; Adams, J. R., Some 1,4-Diaryl-1,3-cyclopentadienes. *J Am Chem Soc* **1939,** *61* (6), 1326-1329.

31. Greifenstein, L. G.; Lambert, J. B.; Nienhuis, R. J.; Drucker, G. E.; Pagani, G. A., Response of Acidity and Magnetic-Resonance Properties to Aryl Substitution in Carbon Acids and Derived Carbanions - 1-Aryl-4-Phenylcyclopenta-1,3-Dienes - Dependence of Ionic Structure on Aryl Substitution. *J Am Chem Soc* **1981,** *103* (26), 7753-7761.

32. Clennan, E. L.; Mehrsheikh-Mohammadi, M. E., Mechanism of endoperoxide formation. 3. Utilization of the Young and Carlsson kinetic techniques. *J Am Chem Soc* **1984,** *106* (23), 7112-7118.

Chapter 4: Synthesis and reactions of mixed alkyl-aryl dihydropentalenes

4.1 Introduction

4.1.1 Cyclopentadienes with alkyl and aryl substituents

As discussed in chapter 3, replacing phenyl groups in **CpH** derivatives with alkyl-substituted aryl-groups can overcome the solubility issues experienced by the phenyl substituted-species. An alternate approach is to replace the phenyl groups with alkyl-substituents bound directly to the **Cp** ring.

Tetraphenylcyclopentadienone, which functions as a precursor for **Ph_5CpH** (Section 2.1.2), can also be used to synthesise **(Alkyl)Ph_4CpH** derivatives (Figure 1). **MePh_4CpH** has been prepared by reacting tetraphenylcyclopentadienone with MeMgBr, followed by reduction of the alcohol product.[1] Alternatively, tetraphenylcyclopentadienone has first be converted into a tosylate, which then undergoes a S_N2 reaction with the Grignard reagent.[2] Other **(Alkyl)Ph_4CpH** species, such as **EtPh_4CpH** and **^{n}BuPh_4CpH,** have also be prepared by this route.

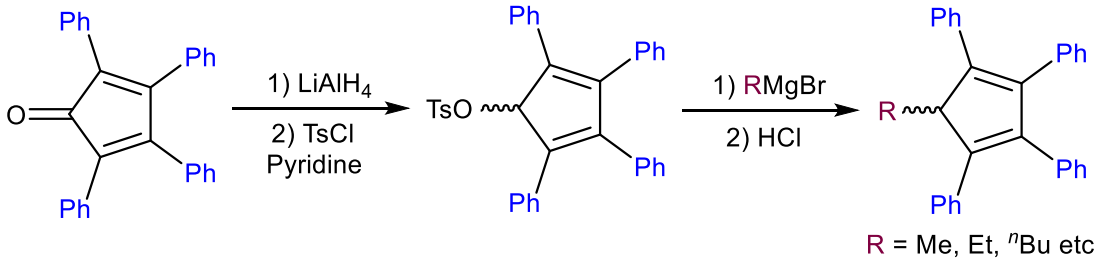

Figure 1: Synthesis of alkyltetraphenylcyclopentadienes from tetraphenylcyclopentadienone

MePh_4CpH has also been prepared by treating **2,3,4,5-Ph_4Fv**[3] with hydroiodic acid in refluxing acetic acid.[4] This fulvene has also been used as a precursor for other **(Alkyl)Ph_4CpH** species through reactions

with Grignard reagents (Figure 2). For example, reacting **2,3,4,5-Ph$_4$Fv** with MeMgBr leads to formation of **EtPh$_4$CpH**.[5]

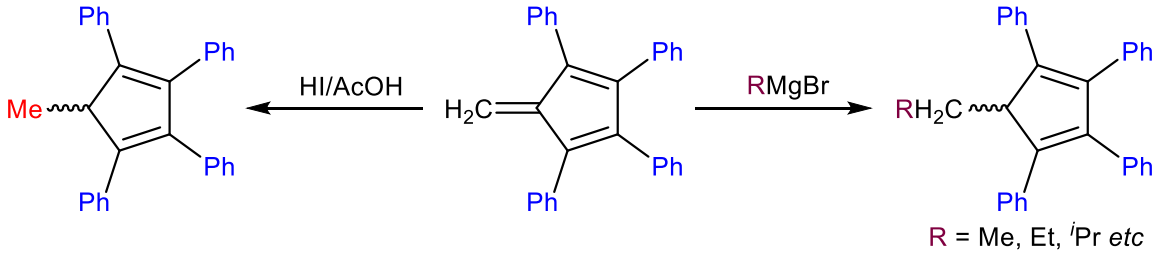

Figure 2: Synthesis of alkyltetraphenylcyclopentadienes from 2,3,4,5-tetraphenylfulvene

The melting point of **MePh$_4$CpH** is 98-99 °C,[5] considerably lower than for **Ph$_5$CpH** which melts at 260 °C. This suggests that the methyl group disrupts the packing of the molecule and therefore significantly decreases the lattice energy. It could also be that having less phenyl groups decreases the lattice energy through decreased π-π interactions between molecules. This decrease in melting point may be expected to translate into an increase in solubility compared to the entirely phenyl-substituted species.

Thewalt *et al.*[6] reported the preparation of the potassium salt of **MePh$_4$Cp**$^-$ by treating **MePh$_4$CpH** with KH suspended in THF (Figure 3), although characterisation of this species is limited. Few complexes of **MePh$_4$CpH** are reported in the literature. An example is provided by Martin-Matute *et al.*[1] who reacted **MePh$_4$PnH** with $Ru_3(CO)_{12}$ in boiling decane to obtain **(MePh$_4$Cp)Ru(CO)$_2$H**, which either dimerises to give **[(MePh$_4$Cp)Ru(CO)]$_2$** or is converted by treatment with chloroform into **(MePh$_4$Cp)Ru(CO)$_2$Cl**.

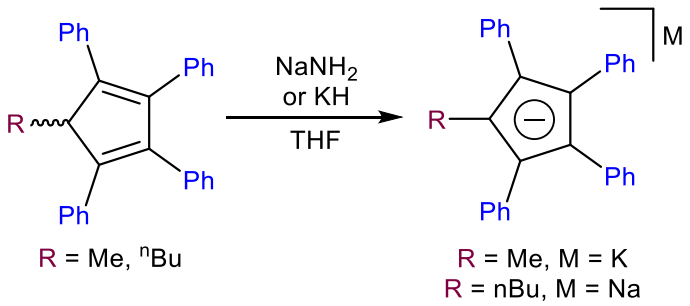

Figure 3: Synthesis of 1-alkyl-tetraphenylcyclopentadienes and conversion into their alkali-metal salts

Schumann and Lentz[7] reported that the sodium salt of **^{n}BuPh$_4$Cp$^-$** can prepared by reacting **^{n}BuPh$_4$CpH** $NaNH_2$ in THF (Figure 3), and that the reaction with TlOEt gives **Tl(^{n}BuPh$_4$Cp)**. They also report that the direct reaction of **^{n}BuPh$_4$CpH** with $FeCl_2$ gives **Fe(^{n}BuPh$_4$Cp)$_2$**, whereas the analogous reaction of **Ph$_5$CpH** fails to give the relevant ferrocene derivative.

More highly methylated phenyl-substituted **CpH**s have also been described. Various **Me$_2$Ph$_3$CpH** and **Me$_3$Ph$_2$CpH** species have been synthesised, typically from cyclopentenones synthesised through Nazarov cyclisations of divinylketones.[8] However, little exploration of their organometallic chemistry has been reported.

Cp*H can be synthesised by reacting 2-butenylliuthium with ethyl acetate, followed by acid-catalysed dehydration.[9] Threlkel and Bercaw[10] reported that replacing the ethyl acetate with ethyl benzoate allows the synthesis of **Me$_4$PhCpH** (Figure 4).

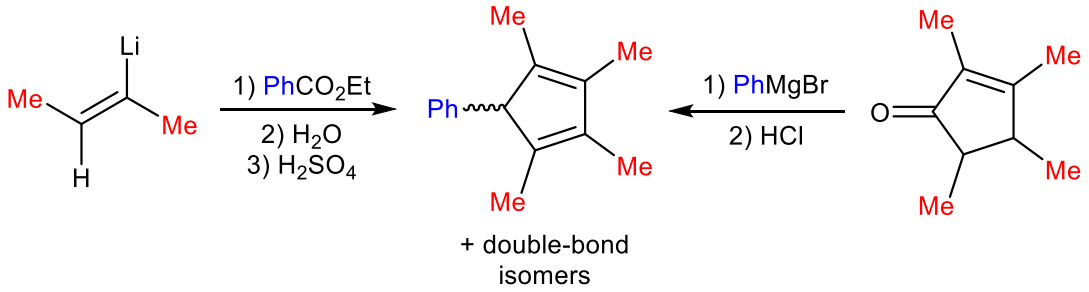

Figure 4: Synthesis of phenyltetramethylcylcopentadiene

Alternatively, **Me$_4$PhCpH** has been synthesised by reacting 2,3,4,5-tetramethylcyclopent-2-enone with PhMgBr, followed by acid-catalysed dehydration (Figure 4).[11] Morris *et al.*[12] reported that

reacting **Me_4PhCpH** with $IrCl_3$ gave an Ir dimer that can be used as precursor for amino acid-**Ir[Me_4PhCp]** complexes. These complexes were shown to be suitable catalysts for the asymmetric transfer hydrogenation with a variety of substrates that the analogous amino acid-**IrCp*** fail to react with.

4.1.2 Properties of methyl substituents

While methyl groups are smaller than phenyl groups, they are still able to exert a larger steric demand than a simple hydrogen atom. The 'A' value (Section 2.1.1) for a methyl group is 1.70 kcal mol^{-1}, compared to 3.00 kcal mol^{-1} for phenyl. This steric demand creates a destabilising effect in **Cp*$^-$** as compared to **Cp$^-$**, as solvation of the anion is inhibited by steric clashing with the methyl substituents.[13]

The electronic properties of methyl also affect the reactivity of **Cp** derivatives. The Hammett parameters (see section 2.1.1) for methyl groups are -0.07 for σ_m and -0.17 for σ_p. This suggests that methyl substituents are mildly electron-donating by inductive effects, and that resonance effects increase the donating-effect. This results in an increase in pK_a for methyl-substituted **Cp** derivatives due to destabilisation of the conjugate anion, with addition of each methyl group raising the pKa by approximately 2.0.[13]

The increased electron density in **Cp*$^-$** compared to **Cp$^-$** leads to this ligand bonding more strongly to metals, characterised by shorter metal-Cp bond distance.[14] This ligand is therefore harder displace than **Cp$^-$** and is better able to stabilise electron-deficient metals. This stronger M-ligand binding is also evident from the structure of Pn* species (Section 3.1.1).

4.1.3 Methyl-phenyl-substituted dihydropentalenes

There are limited examples of dihydropentalenes bearing both methyl and phenyl substituents, and these come from the same reports as the **Ph_2PnH_2** examples provided in section 2.1.3. As described by Kaiser and Hafner[15] **6-Me-6-(NMe_2-vinyl)Fv** cyclises at 106 °C to give **1-Me-3-(NMe_2)-PnH_2**, which

can be converted into **1-Me-3-PhPnH$_2$** by reacting it with PhLi, followed by amine elimination at ambient temperatures (Figure 5).

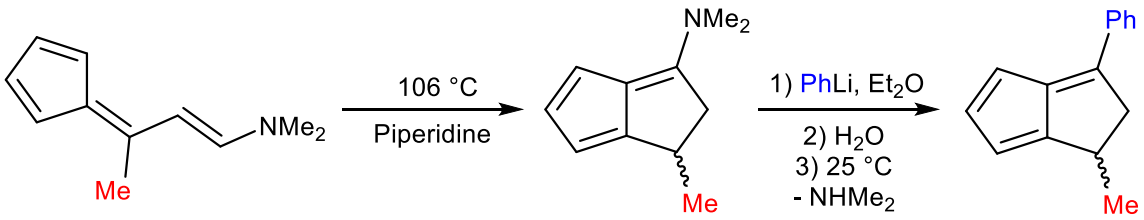

Figure 5: Synthesis of 1-methyl-3-phenyldihydropentalene

This species is not thermolabile like the parent **PnH$_2$** and exists as a stable solid at room temperature.[15] Its melting point is 36-37 °C, 25 °C lower than that of **3-PhPnH$_2$**.[15] This suggests that the single methyl group disrupts packing in the solid state, decreasing the lattice energy. This could in turn lead to this species being more soluble, although this would be dependent on the solvent being used.

Griesbeck[9] used the reaction of **CpH** and 4-phenyl-3-buten-2-one to synthesise **3-Me-1-PhPnH$_2$** (Figure 6). The yield of this species is higher than the analogous synthesis of **Ph$_2$PnH$_2$** (Section 2.1.3), and the reaction time is much shorter. The isomerisation of the 1,2-isomer to the 1,5-isomer can be induced either by flash vacuum thermolysis or chromatography on alumina. Coskum *et al.*[16] also report the synthesis of **3-Me-1-PhPnH$_2$** through the reaction of **6-PhFv** with acetone and pyrrolidine (Section 1.2.6)

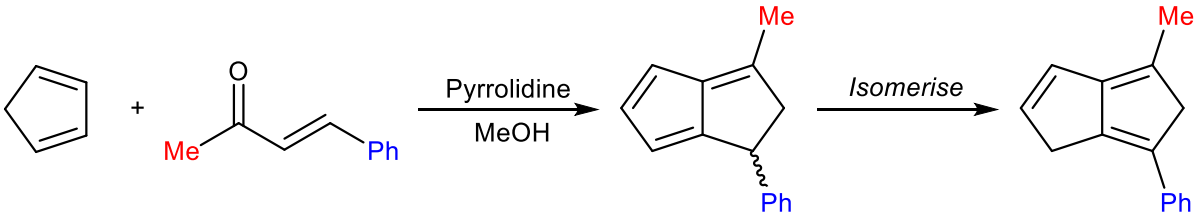

Figure 6: Synthesis of 3-methyl-1-phenyldihydropentalene

While this species has seemingly not been used as a **Pn^{2-}** species, it has been used to synthesise bridged **PnH$_3^-$** species for *ansa*-metallocenes through its reactions with anionic cyclopentadienyl derivatives (Figure 7).[17] A wider library of **PnH$_2$** derivatives would potentially allow further exploration of the

potential catalytic properties of these metallocenes. However, that is outside the scope of this investigation.

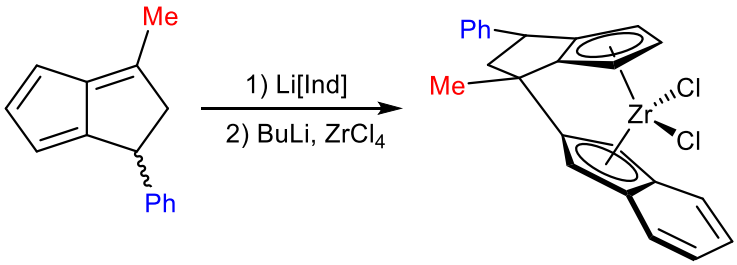

Figure 7: 3-methyl-1-phenyldihydropentalene as a precursor for a zirconocene derivative

4.1.4 Aims

In chapter 3 issues of solubility for phenyl-substituted $\mathbf{Pn^{2-}}$ derivatives were discussed. It was supposed that replacing some of the phenyl groups with methyl groups would create species that would be more soluble in the organic solvents typically used for transmetalation chemistry. Increased solubility would also allow full characterisation of the $\mathbf{Pn^{2-}}$ salts by NMR. An additional effect of this methyl substitution would $\mathbf{Pn^{2-}}$ with asymmetrical binding sites could further enhance solubility of these species due to disrupted packing effects. Having two electronically distinct rings could also create different binding environments in metal complexes, potentially leading to different reactivity at each metal centre in a bimetallic complex.

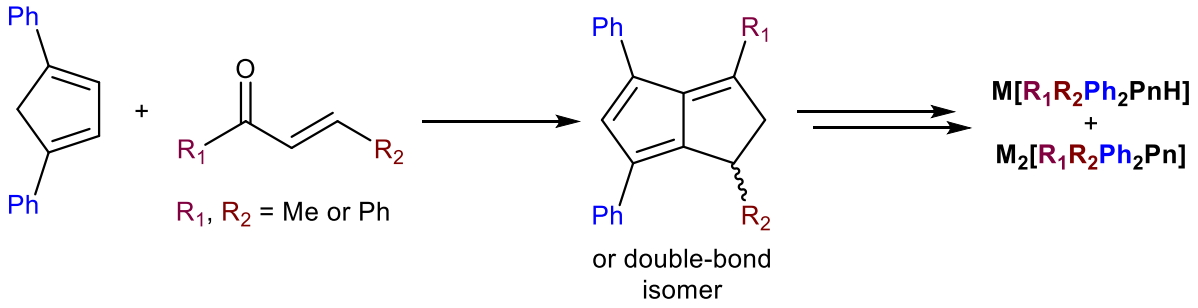

Figure 8: Synthesis of mixed methyl-phenyl tetrasubstituted-dihydropentalenes

In this chapter the synthesis of several methyl-phenyl substituted $\mathbf{PnH_2}$ (Figure 8) species is described using the methods described for the synthesis of $\mathbf{Ph_4PnH_2}$ (Section 2.4.2). It was supposed that these

could function as precursors for methyl-phenyl substituted **PnH**$^{-}$ and **Pn**$^{2-}$ species. It was shown that a range of bases might be suitable for this (Chapter 3), so these reagents were employed to attempt to access the desired anionic species.

4.2 Synthesis of dihydropentalenes with methyl and phenyl substituents

4.2 1 Synthesis of 3-methyl-1,4,6-triphenyldihydropentalene

4-phenyl-3-buten-2-one was identified as a suitable material for synthesising **PnH$_2$** derivatives, as this species is commercially available and was shown by Griesbeck[9] to react with **CpH** to give **1-Ph-3-MePnH$_2$** (see above). It was therefore supposed that the reaction of **Ph$_2$CpH** (see section 2.2.5) with 4-phenyl-3-buten-2-one would furnish **3-Me-1,4,6-Ph$_3$PnH$_2$.**

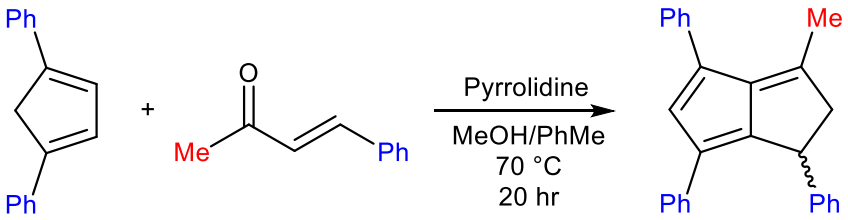

Figure 9: Synthesis of 3-methyl-1,4,6-triphenyldihydropentalene from 1,4-diphenylcyclopentadiene

Adding pyrrolidine to **Ph$_2$CpH** and 4-phenyl-3-buten-2-one in a 1:1 mixture of methanol and toluene led to the formation of **3-Me-1,4,6-Ph$_3$PnH$_2$** after heating at 70 °C overnight (Figure 9). The formation of this species required a shorter reaction time than the analogous formation of **Ph$_4$PnH$_2$**, presumably due to the increased reactivity of the enone and decreased steric hinderance for the ring closing step. The purification of **3-Me-1,4,6-Ph$_3$PnH$_2$** is straightforward, requiring only a biphasic workup, stripping through silica and recrystallisation from ethanol. By this route the dark red crystalline product can be obtained in high yields, up to 80%. While commercial 4-phenyl-3-buten-2-one can be purified by recrystallisation from petroleum ether, this was found to be unnecessary and did not improve the yield.

This melting point of this species is 151-152 °C, 29 °C lower than Ph_4PnH_2. This is likely due to the decreased phenyl substitution leading to less intermolecular π-π interactions, decreasing the lattice energy for **3-Me-1,4,6-Ph_3PnH_2**. While crystals of **3-Me-1,4,6-Ph_3PnH_2** suitable for XRD could not be obtained, the NMR spectrum of this species showed that it exists as exclusively the 1,2-H_2 isomer (Figure 10). It does not undergo rearrangement to the 1,5-H_2 isomer as reported for **3-Me-1-PhPnH_2**,[9] and the isomerisation could not be induced by prolonged heating or treating with silica or alumina.

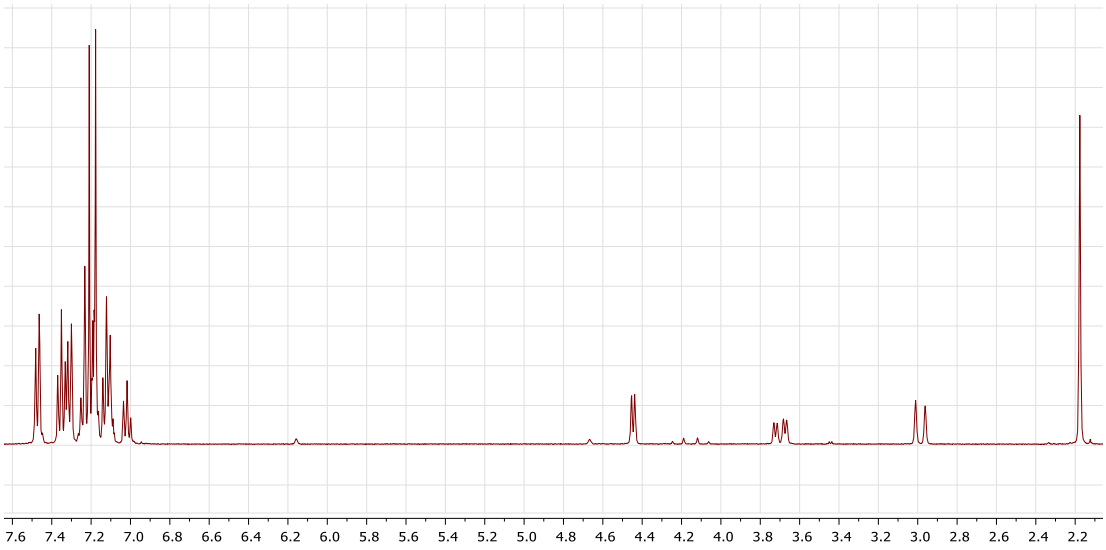

Figure 10: ^{1}H-NMR (500 MHz) spectrum of 3-methyl-1,4,6-triphenyldihydropentalene

The 1,2-H_2 nature of this species was shown by a NMR signal at 4.45 ppm, corresponding to the C1 hydrogen, and two signals at 3.70 and 2.99 ppm, corresponding to the C2-hydrogens (Figure 11). The two C2-hydrogens were differentiated by their Karplus relationship to the C1-hydrogen. The signal at 4.45 ppm couples to the signal at 3.70 ppm with a coupling constant of 6.99 Hz. This means these hydrogens were assigned as 'cis' to each other as a dihedral angle close to 0° gives a large coupling constant. The signals at 4.45 and 2.99 ppm couple to each other with a coupling constant of only 0.97 Hz, so these hydrogens were assigned as being 'trans' to each other.

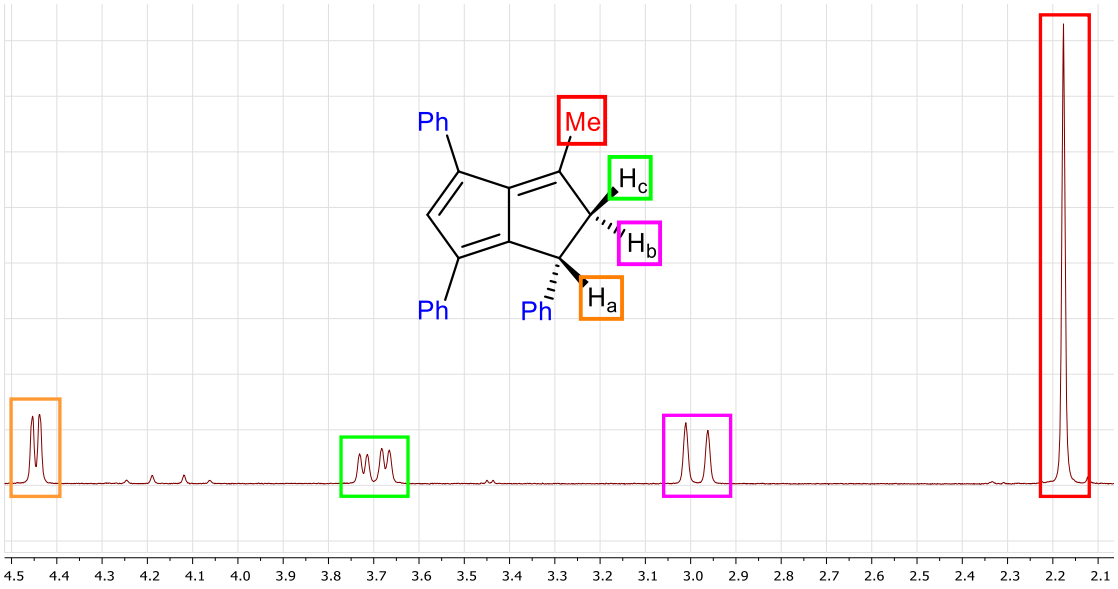

Figure 11: ^{1}H-NMR (500 MHz) spectrum showing 1,2-H_2 isomeric nature of 3-methyl-1,4,6-triphenyldihydropentalene

Then UV/vis spectrum of **3-Me-1,4,6-Ph_3PnH_2** was acquired using a 1.13x10^{-5} mol dm^{-3} THF solution of this species (Figure 12). The spectrum showed a strong absorbance in the UV region at λ_{max} of 296 nm, which had an ε of 42863 dm^3 mol^{-1} cm^{-1}. The magnitude of this ε suggests this absorbance is caused by a fully spin-, symmetry- and orbital-allowed transition. This is likely a π-π* transition in involving the diene ring of **3-Me-1,4,6-Ph_3PnH_2**, like what was supposed for **1,3,4,6-Ph_4PnH_2** (Section 2.4.2).

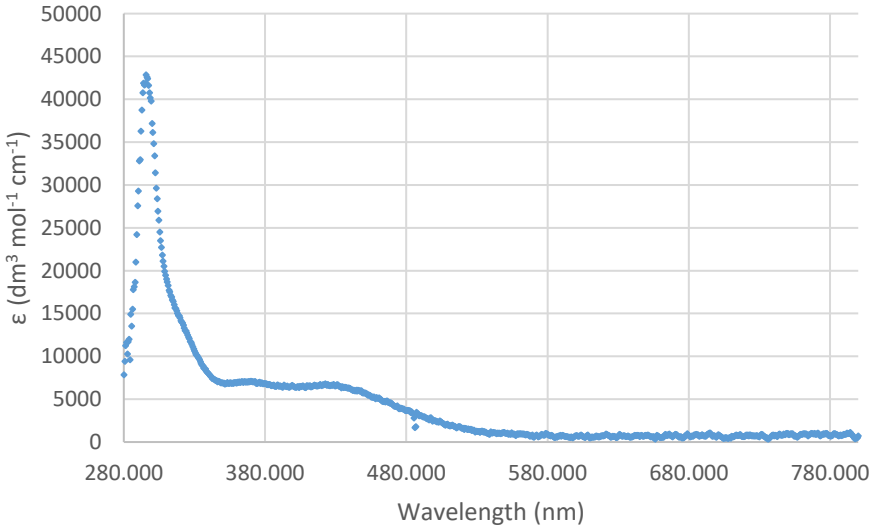

Figure 12: UV/vis spectrum of 3-methyl-1,4,6-triphenyldihydropentalene

The UV/vis spectrum also showed a broad absorbance between 350 and 480 nm, with small peaks at λ_{max} of 370 and 422 nm. These peaks have ε values of 7081 and 6795 $dm^3\ mol^{-1}\ cm^{-1}$ respectively. This suggests these are caused spin-allowed but symmetry- or orbital-forbidden π-π* transition, likely involving the fulvene-like π-system. As this absorbance crosses into the visible region is likely responsible for the intense red colour observed for **3-Me-1,4,6-Ph_3PnH_2**.

Fulvenes have been shown to be precursors for **PnH_2**s via their reaction with ketones (Section 2.4.2). Coskum *et al.*[16] showed that acetone and pyrrolidine is an effective system for transforming 6-substituted-**Fv**s into 3-methyl-substituted **PnH_2**s. Therefore, it was supposed **1,3,6-Ph_3Fv** and acetone could be used to synthesise **3-Me-1,4,6-Ph_3PnH_2** (Figure 13).

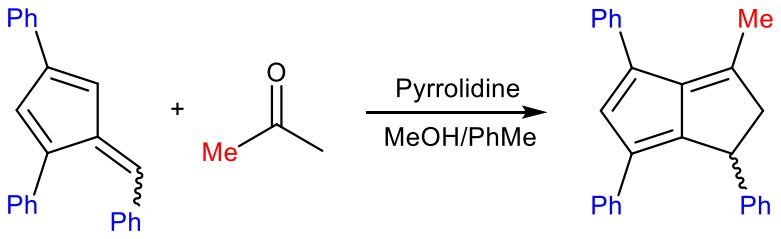

Figure 13: Synthesis of 3-methyl-1,4,6-triphenyldihydropentalene from 1,3,6-triphenylfulvene

Heating **1,3,6-Ph_3Fv** with pyrrolidine and a large excess of acetone gave **3-Me-1,4,6-Ph_3PnH_2** in 55% yield. As the synthesis of **1,3,6-Ph_3Fv** gives a yield of 95%, the overall conversion of **Ph_2CpH** into **3-Me-1,4,6-Ph_3PnH_2** across the two steps is 52%. This is lower than the reaction with 4-phenyl-3-buten-2-one, which is the method of choice for obtaining this **PnH_2** derivative.

4.2.2 Synthesis of 1,3-dimethyl-4,6-diphenyldihydropentalene

Replacing the 1- and 3-position phenyl groups in **Ph_4PnH_2** with methyl would give a **PnH_2** derivative with one phenyl-substituted ring and one methyl-substituted ring. It was supposed this would enable access to **1,3-Me_2-4,6-Ph_2Pn^{2-}**, a species that would contain a **Ph_2Cp^-** unit and a **Me_2Cp^-** unit (Figure 14). This would give an electron-poor binding site for metals and an electron-rich one, potentially altering the reactivity of the metal atoms within bimetallic complexes.

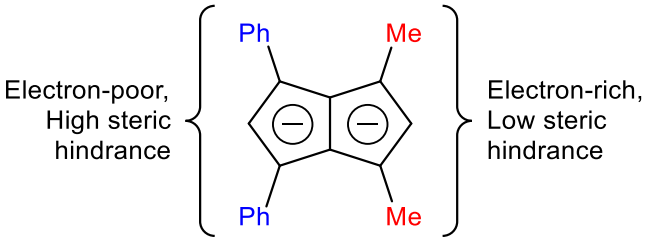

Figure 14: Two binding sites of 1,3-dimethyl-4,6-diphenylpentalenide

The pyrrolidine-facilitated reaction of **Ph_2CpH** with 3-penten-2-one gave **1,3-Me_2-4,6-Ph_2PnH_2** in high yields (Figure 15). Commercial 3-penten-2-one was acquired as 70% grade, containing 28% mesityl oxide and 2% ethanol. Surprisingly this could be used without any separation of the components or drying of the material.

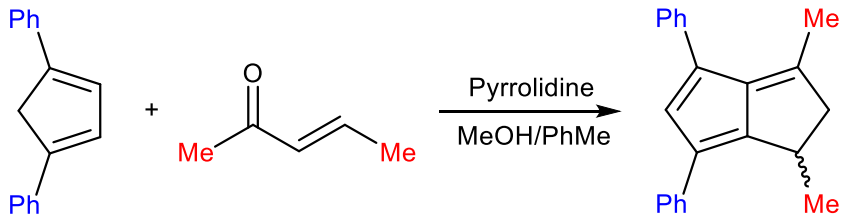

Figure 15: Synthesis of 1,3-dimethyl-4,6-diphenyldihydropentalene from 1,4-cyclopentadiene

A large excess of the enone is used, and presumably the 3-penten-2-one reacts more rapidly with **Ph_2CpH** than the mesityl oxide does as no unwanted **1,1,3-Me_3-4,6-Ph_2PnH** is observed in the worked-up product. Pure samples of **1,3-Me_2-4,6-Ph_2PnH_2** can be obtained by stripping through silica followed by recrystallisation from ethanol, giving a yield of 67 %. This species has a melting point of 122-123 °C, 29 °C lower than **3-Me-1,4,6-Ph_3PnH_2** likely due to the decreased phenyl-substitution leading to less intermolecular π-π interactions.

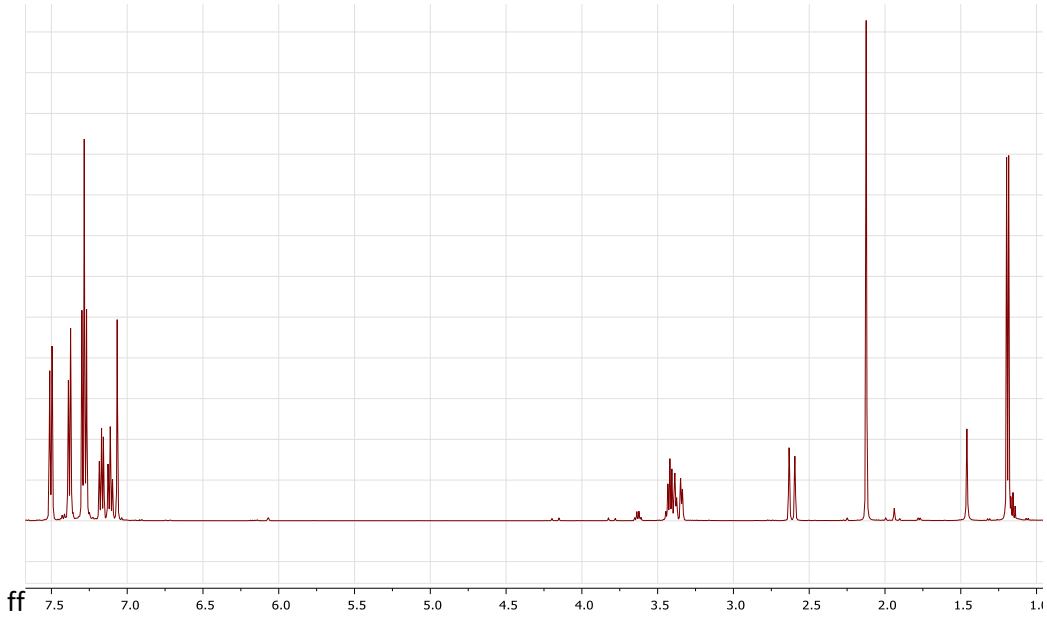

Figure 16: ^{1}H-NMR (500 MHz) spectrum of 1,3-dimethyl-4,6-diphenyldihydropentalene

The ^{1}H-NMR spectrum of **1,3-Me$_2$-4,6-Ph$_2$PnH$_2$** showed that this species was exclusively the 1,2-H$_2$ isomer (Figure 16). A pair of overlayed ^{1}H-NMR signals at 3.40 ppm corresponded to the C1-hydrogen and the C2-hydrogen *cis* to it (Figure 17). A signal at 2.16 ppm was assigned to the C2-hydrogen *trans* to the C1-hydrogen since any ^{3}J-coupling present was too small to be is observed. This is because the dihedral angel between these protons is shown by XRD (see below) to be 118 °, which according to the Karplus relationship will give a small ^{3}J-coupling constant.

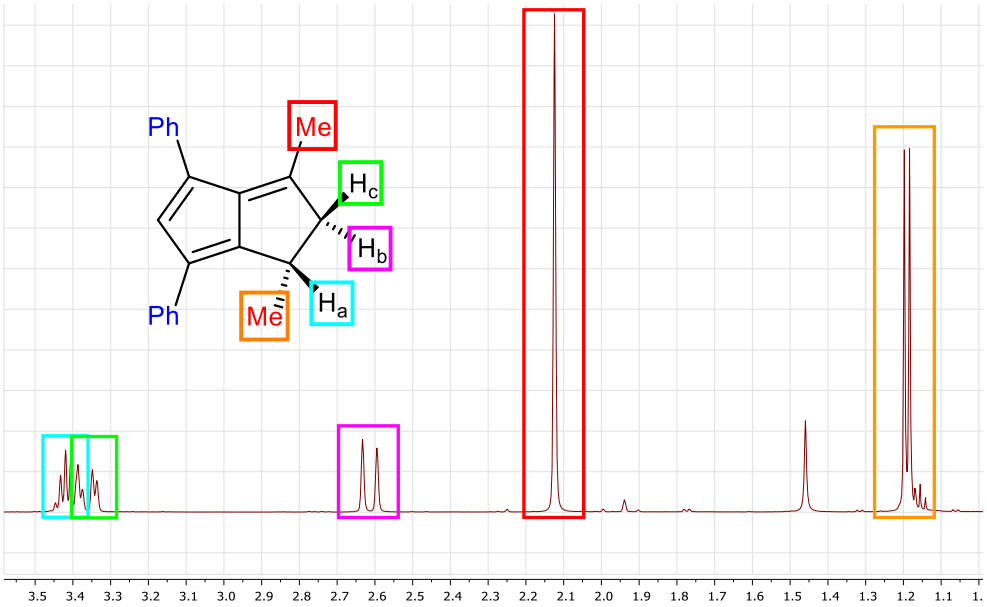

Figure 17: ^{1}H-NMR (500 MHz) spectrum showing 1,2-H_2 isomeric nature of 1,3-dimethyl-4,6-diphenyldihydropentalene

Crystals of **1,3-Me_2-4,6-Ph_2PnH$_2$** were grown from ethanol at -20 °C and were found to be suitable for XRD analysis (Figure 18). The crystal that was analysed was shown to contain the *S*-enantiomer, but as this species forms as a racemic mixture, other solids in the sample presumably contained the *R*-enantiomer or a mixture or the two. If this fractional crystallisation could be reproduced it could be useful for obtaining enantio-enriched samples of **1,3-Me_2-4,6-Ph_2PnH$_2$**, which could be useful for synthesis of single enantiomers of **1,3-Me_2-4,6-Ph_2PnH$^-$** (Section 3.1.2).

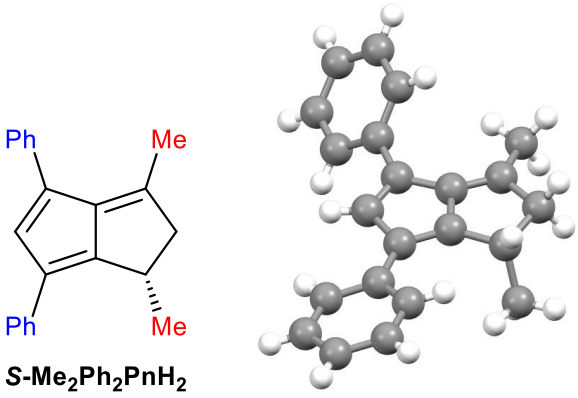

Figure 18: Crystal structure of (S)-1,3-dimethyl-4,6-diphenyldihydropentalene

The crystal structure of **1,3-Me$_2$-4,6-Ph$_2$PnH$_2$** showed the **PnH$_2$** core of this species to be almost identical to the core of **1,3,4,6-Ph$_4$PnH$_2$** (Section 2.4.2). The fulvene-like bond in **1,3-Me$_2$-4,6-Ph$_2$PnH$_2$** was 1.357(2) Å, identical to the analogous bond in **1,3,4,6-Ph$_4$PnH$_2$**, suggesting the substituent in the C3-position does not have a large effect of the length of this bond. The C-C bond lengths in the diene ring were 1.362(2)-1.368(2) Å and 1.452(2)-1.473(2) Å, close to the lengths observed in **1,3,4,6-Ph$_4$PnH$_2$**.

The UV/vis spectrum of **1,3-Me$_2$-4,6-Ph$_2$PnH$_2$** was acquired using a 2.07x10^{-5} mol dm^{-3} THF solution of this species (Figure 19). The spectrum showed two absorbances - one sharp absorbance in the UV range with λ_{max} at 300 nm, and a broad absorbance in the visible range with λ_{max} at 415 nm.

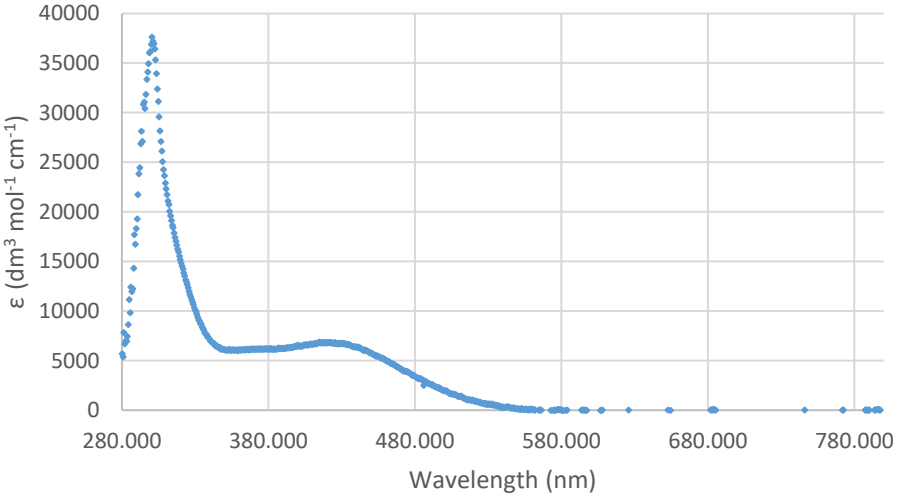

Figure 19: UV/vis spectrum of 1,3-dimethyl-4,6-diphenyldihydropentalene

The absorbance at 300 nm has an ε value of 37637 dm^3 mol^{-1} cm^{-1}. The magnitude of ε suggest this absorbance is arising from a fully spin-, symmetry- and orbital-allowed transition. As for **3-Me-1,4,6-Ph$_3$PnH$_2$** this transition is like a π-π* transition involving the diene ring. The absorbance at 415 nm has an ε value of 6859 dm^3 mol^{-1} cm^{-1}. This is likely arising from a spin-allowed but symmetry- or orbital-forbidden π-π* transition involving the fulvene-like bond. As with **3-Me-1,4,6-Ph$_3$PnH$_2$** this visible region absorbance is likely the cause of the bright red colour of **1,3-Me$_2$-4,6-Ph$_2$PnH$_2$**.

4.3. Reactions of methyl-phenyl dihydropentalenes

4.3.1 Deprotonation of 3-methyl-1,4,6-triphenyldihydropentalene

Lithium amides were shown to be useful bases for generating **Li[Ph$_4$PnH]** from **Ph$_4$PnH$_2$**, (section 3.2.1), so it was supposed they would be suitable for deprotonating **3-Me-1,4,6-Ph$_3$PnH$_2$**. However, unlike **Ph$_4$PnH$_2$** **3-Me-1,4,6-Ph$_3$PnH$_2$** has two sites that can be deprotonated in a manner that deposits the negative charge into the unsaturated C_5-ring (Figure 20).

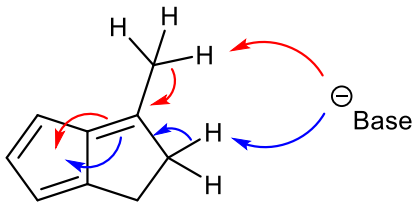

Figure 20: Two deprotonation sites of 3-methyl-substituted dihydropentalene

Deprotonation at the 2-position would lead to the 2,3-double bond structure observed for **Ph$_4$PnH** (Section 3.2) and other examples such as **Pn*H**$^-$.[18] However, the methyl group in the 3-position could also be deprotonated in manner analogous to the deprotonation of **6-MeFv**.[19] This would lead to an exocyclic alkene product forming rather than an endocyclic one.

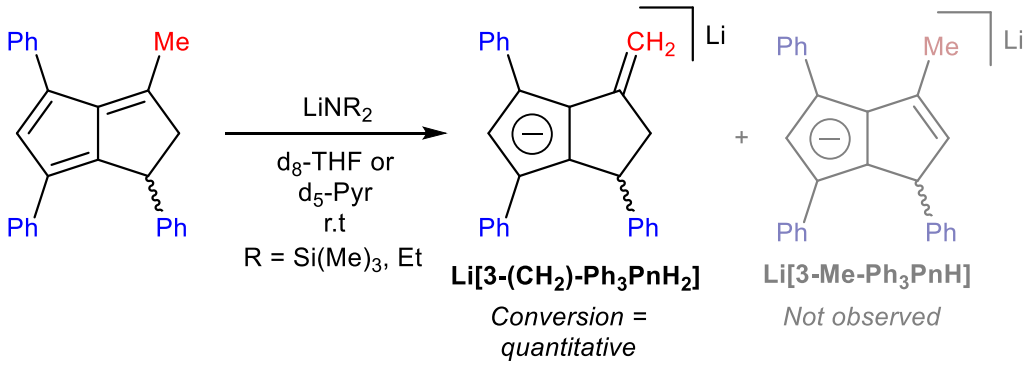

Figure 21: Deprotonation of 3-methyl-1,4,6-triphenyldihydropentalene with lithium amides

3-Me-1,4,6-Ph$_3$PnH$_2$ was treated with LiHMDS in d_8-THF, and NMR analysis of the reaction showed it to contain exclusively **Li[3-(CH$_2$)-Ph$_3$PnH$_2$]**, with no formation of **Li[3-Me-Ph$_3$PnH]** observed (Figure

21). Using the less hindered but more basic $LiNEt_2$ led to same species forming. Allowing solutions of **3-Me-1,4,6-Ph_3PnH_2** to stand for several weeks did not result in any conversion to the endocyclic alkene product, and prolonged heating at 70 °C also did not result in any interconversion.

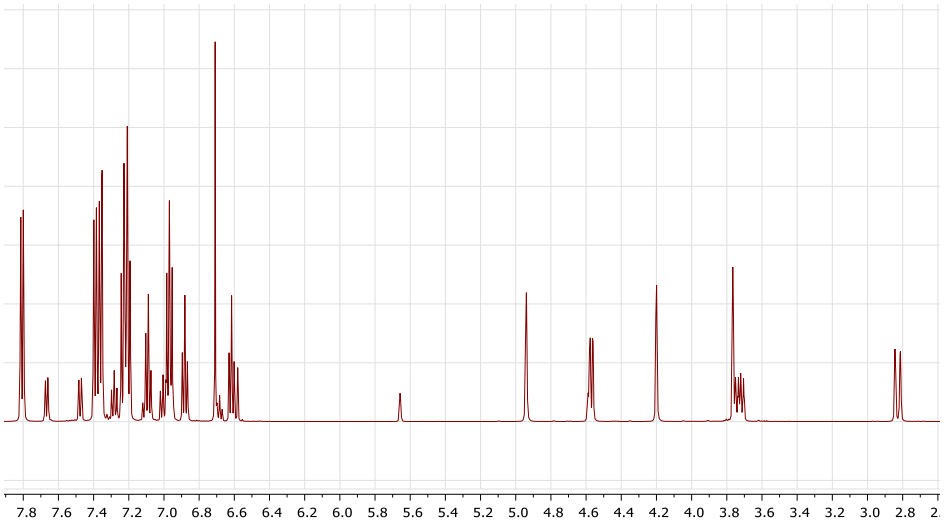

Figure 22: ^{1}H-NMR (500 MHz) spectrum of lithium 3-vinyl-1,4,6-triphenyl-1,2,2-trihydropentaleneide

The exocyclic structure of this reaction product was assigned by the disappearance of the ^{1}H-NMR signal at 2.18 ppm for the methyl group in **3-Me-1,4,6-Ph_3PnH_2**. This corresponded to the appearance of two signals at 4.20 and 4.94 ppm, one corresponding to the alkene proton oriented towards the neighbouring phenyl groups and one oriented away. The HSQC spectrum showed that these hydrogens are attached to a carbon that had a $^{13}C\{^1H\}$-NMR signal at 87.4 ppm, shifted downfield 70.3 ppm compared to the analogous carbon in **3-Me-1,4,6-Ph_3PnH_2** due to its conversion from a sp^3 centre to an sp^2 one.

In **Li[3-(CH_2)-Ph_3PnH_2]** the C2-ring bound hydrogens showed two ^{1}H signals at 2.58 and 3.71 ppm, similar to the two signals at 2.99 and 3.70 ppm observed in **3-Me-1,4,6-Ph_3PnH_2**. The $^{13}C\{^1H\}$ signal for the C2 carbon was 51.9 ppm, close to the chemical shift of 57.4 ppm for the analogous carbon in the precursor. This showed that deprotonation had not occurred at the C2 position. The deprotonation of the methyl group could be due to these protons being more kinetically accessible than the ring-bound protons. It is also possible that the exocyclic alkene product is more stable than the endocyclic product

due to decreased strain within the C_5-ring. This would result in the methyl-group protons being more acidic, even though deprotonation at this site results in a less-substituted alkene product.

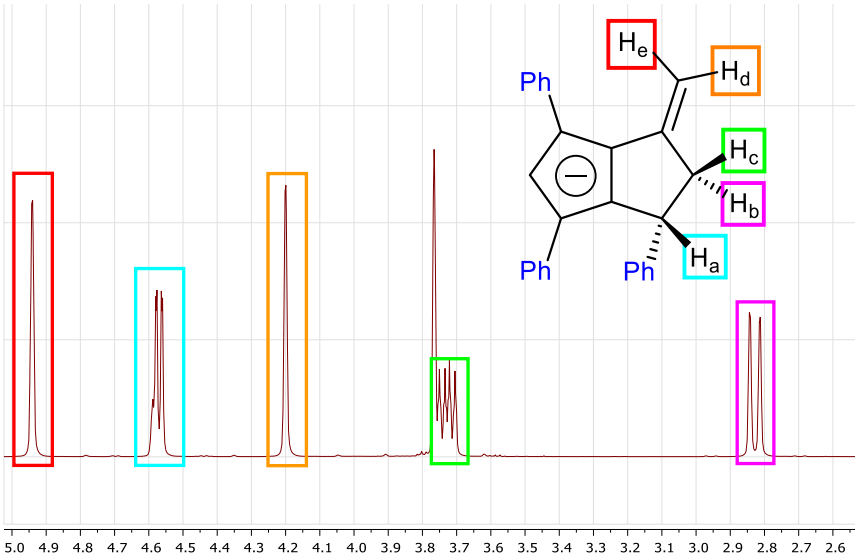

Figure 23: ^{1}H-NMR (500 MHz) spectrum of lithium 3-vinyl-1,4,6-triphenyl-1,2,2-trihydropentaleneide between 2.55-5.00 ppm

The ^{1}H-NMR showed that the C5-hydrogen signal was shifted upfield from 7.10 to 6.70 ppm upon deprotonation. The $^{13}C\{^1H\}$-NMR spectrum showed the C5-carbon signal is shifted upfield from 136.7 ppm in **3-Me-1,4,6-Ph$_3$PnH$_2$** to 111.7 ppm in **Li[3-(CH$_2$)-Ph$_3$PnH$_2$]**. The increased shielding of this carbon is caused by the 6π-anionic system in the C4/5/6/7/8 ring. The *para*-position carbons for the phenyls attached to the anionic ring showed $^{13}C\{^1H\}$-NMR signals of 118.5 and 119.9, shifted upfield by 6.2-7.0 ppm. This extra shielding could be arising from partial delocalisation of the negative charge into the π-system of the phenyl substituents. The phenyl-group attached to the neutral ring of **Li[3-(CH$_2$)-Ph$_3$PnH$_2$]**, which cannot participate in charge delocalisation, showed a $^{13}C\{^1H\}$-NMR signal of 127.2 ppm, shifted downfield by 1.1 ppm compared to the precursor.

This species potentially possesses both the stereocentre and the planar chirality of typical **PnH$^-$** structures (section 2.1.2) so could find utility as ligand in chiral complexes. However, the exocyclic double-bond, being less substituted than an endocyclic one would be in this case, could be less stable

towards unwanted side-reactions. As with **M[Ph$_4$PnH]** (section 3.2) crystals of this **PnH$^-$** salt could not be grown. This means that the structure of the **[3-(CH$_2$)-Ph$_3$PnH$_2$]** anion could not be analysed by XRD.

The further deprotonation of **Li[3-(CH$_2$)-Ph$_3$PnH$_2$]** was attempted using a variety of strong bases (Figure 23). The **Pn^{2-}** derivative was the desired target, but this would require a hydrogen-shift at some point in the reaction to give the correct configuration of the double bond. Another possible dianion would have the second charge in a partially exocyclic allyl-type arrangement and, while, this would not require hydrogen rearrangement, it would not form the 10π-aromatic system that stabilises **Pn^{2-}** species.

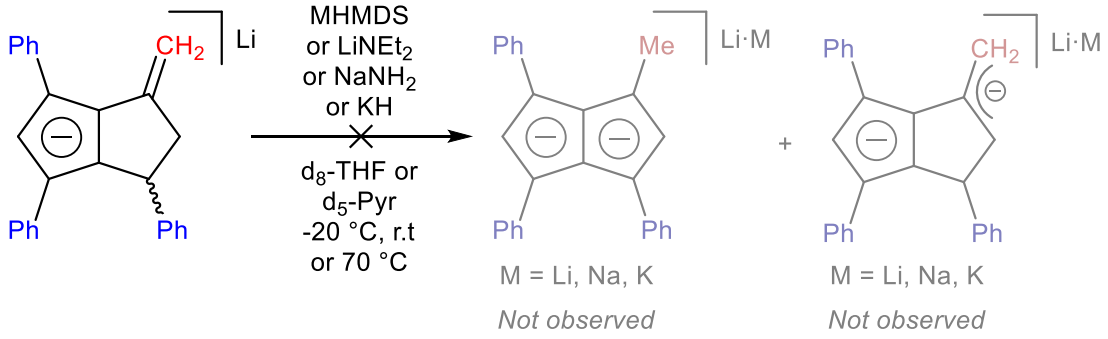

Figure 23: Attempted reaction of lithium 3-vinyl-1,4,6-triphenyl-1,2,2-trihydropentaleneide with amide and hydride bases

Treating **Li[3-(CH$_2$)-Ph$_3$PnH$_2$]** with either excess LiHMDS or LiNEt$_2$ in did not lead to any reaction occurring as observed by ^{1}H-NMR, and the samples remain visually unchanged. As **Pn^{2-}**s with different cations were found to be far more soluble (section 3.3.5), **Li[3-(CH$_2$)-Ph$_3$PnH$_2$]** was treated with NaNH$_2$ or KH to test if product solubility was preventing it being observed on the NMR spectra. Amide and hydride reagents can undergo addition reactions to double bonds, so it was also possible that these bases would undergo nucleophilic attack to the exocyclic double bond. However, no deprotonation or addition reaction was observed by ^{1}H-NMR with either NaNH$_2$ or KH.

4.3.2 Deprotonation of 1,3-dimethyl-4,6-diphenyldihydropentalene

The deprotonation of **$Me_2Ph_2PnH_2$** were investigated using the same conditions described for **$Me_2Ph_2PnH_2$** (Section 4.3.1). As with that species there is a methyl group in the 3-position, meaning that there are two possible deprotonation sites. The ring-bound protons might be more kinetically accessible in this derivative due to the neighbouring phenyl group being replaced with a smaller methyl group. This decreased steric bulk might also result in decreased ring strain in the endocyclic alkene product, which could make this product more thermodynamically favourable.

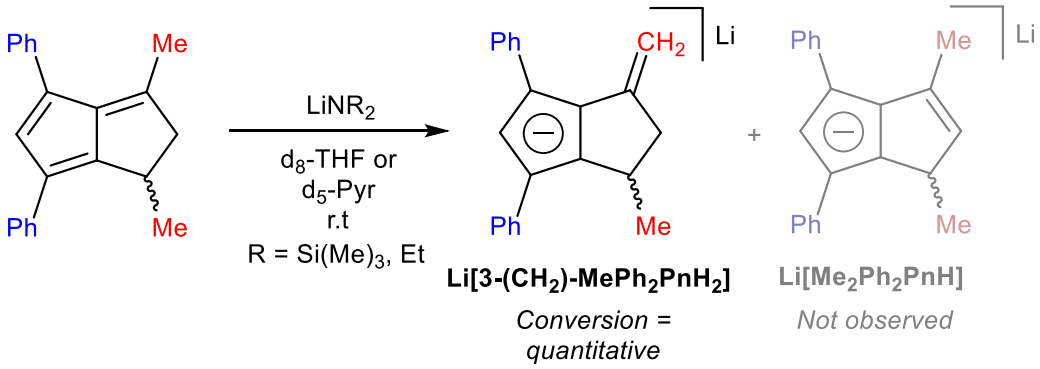

Figure 24: Reaction of 1,3-dimethyl-4,6-diphenyldihydropentalene with lithium amides

However, when **$Me_2Ph_2PnH_2$** was treated with either LiHMDS or $LiNEt_2$ in d_8-THF or d_5-pyridine no endocyclic alkene product was observed. Instead, the precursor was quantitively converted into **Li[3-(CH_2)-$MePh_2PnH_2$]** (Figure 24). Heating solutions of this species at 70 °C did not result in any interconversion into **Li[Me_2Ph_2PnH]**.

The formation of the exocyclic double-bond was shown by the disappearance of the ^{1}H-NMR signal at 2.12 ppm for the 3-position methyl group, which coincided with the appearance of two ^{1}H-NMR signals at 4.64 and 3.99 ppm (Figure 25). These signals corresponded to the two exocyclic alkene hydrogens, one oriented towards the neighbouring phenyl group and one oriented away. The HSQC spectrum showed that these two hydrogens are attached to a carbon that showed a $^{13}C\{^1H\}$-NMR signal at 87.0 ppm. This is shifted downfield by 69.4 ppm compared to the analogous carbon in **$Me_2Ph_2PnH_2$** due to its conversion from a sp^3 centre to a sp^2 one upon deprotonation.

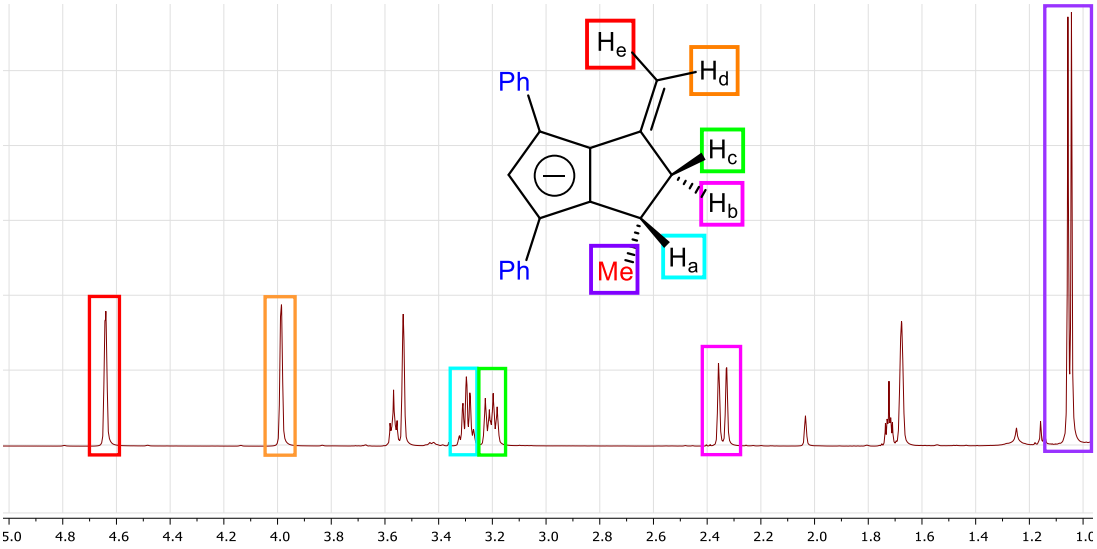

Figure 25: ^{1}H-NMR (500 MHz) spectrum of lithium 1-methyl-3-vinyl-4,6-diphenyl-1,2,2-trihydropentaleneide between 1.00-5.00 ppm

The C1/C2-hydrogens in **Li[3-(CH$_2$)-MePh$_2$PnH$_2$]** showed ^{1}H-NMR signals at 3.30, 3.20 and 3.24 (Figure 25). This is similar to the ^{1}H-NMR signals at 3.46, 3.32 and 2.61 ppm for the C1/C2-hydrogens in **Me$_2$Ph$_2$PnH$_2$**. The ^{13}C{^{1}H}-NMR spectrum of **Li[3-(CH$_2$)-MePh$_2$PnH$_2$]** showed signals at 49.2 and 55.4 ppm for the C1- and C2-carbons, close to the signals for analogous carbons in **Me$_2$Ph$_2$PnH$_2$** which had chemical shifts of 31.5 and 55.4 ppm. This showed that deprotonation had occurred at the C2-position.

As for **Li[3-(CH$_2$)-Ph$_3$PnH$_2$]** the ^{1}H-NMR signal for the C5-hydrogen of **Li[3-(CH$_2$)-MePh$_2$PnH$_2$]** was shifted upfield compared to neutral precursor, shifting from 7.07 to 6.31 ppm (Figure 26). The negative charge in **Li[3-(CH$_2$)-MePh$_2$PnH$_2$]** caused the ^{13}C{^{1}H}-NMR signal for the C5-carbon to be shifted to 111.9 ppm, 37.0 ppm upfield from the analogous carbon in **Me$_2$Ph$_2$PnH$_2$**.

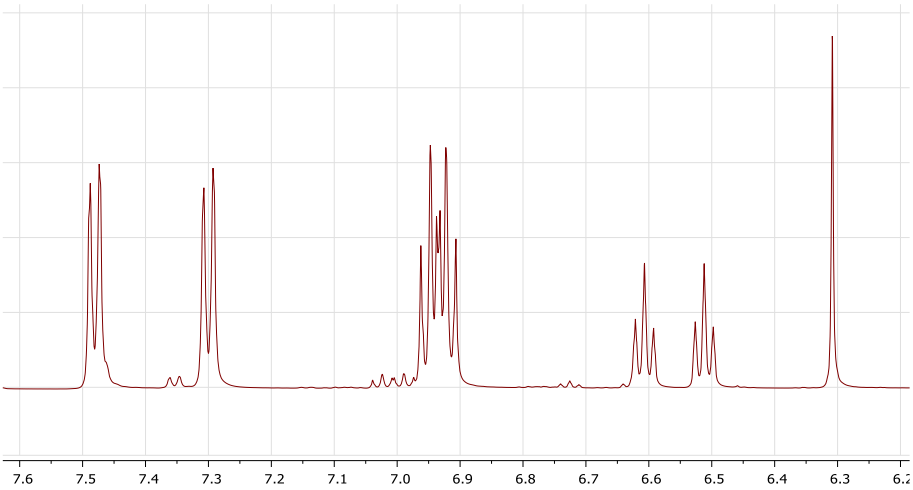

Figure 26: ^{1}H-NMR (500 MHz) spectrum of lithium 1-methyl-3-vinyl-4,6-diphenyl-1,2,2-trihydropentaleneide between 6.20-7.60 ppm

The *para*-position carbons in the phenyl-substituents of **Li[3-(CH$_2$)-MePh$_2$PnH$_2$]** showed ^{13}C{^{1}H}-NMR signals at 118.4 and 119.6 ppm. These signals were 6.5-7.4 ppm upfield of the *para*-carbon ^{13}C{^{1}H} signals in **Me$_2$Ph$_2$PnH$_2$**, perhaps due to π-delocalisation of the negative charge. However, to determine the degree of charge delocalisation in both **Li[3-(CH$_2$)-MePh$_2$PnH$_2$]** and **Li[3-(CH$_2$)-Ph$_3$PnH$_2$]** DFT calculations would be required, which is beyond the scope of this investigation.

The further deprotonation of **Li[3-(CH$_2$)-MePh$_2$PnH$_2$]** was attempted using a large excess of either LiHMDS or LiNEt$_2$ (Figure 27). However, no reaction was observed, and prolonged heating at 70 °C also did not lead to deprotonation occurring. Attempts to make a mixed alkali-metal product by deprotonating the lithium salt with either NaNH$_2$ or KH also failed. The starting material remained unreacted in both cases meaning that no nucleophilic addition reactions were occurring.

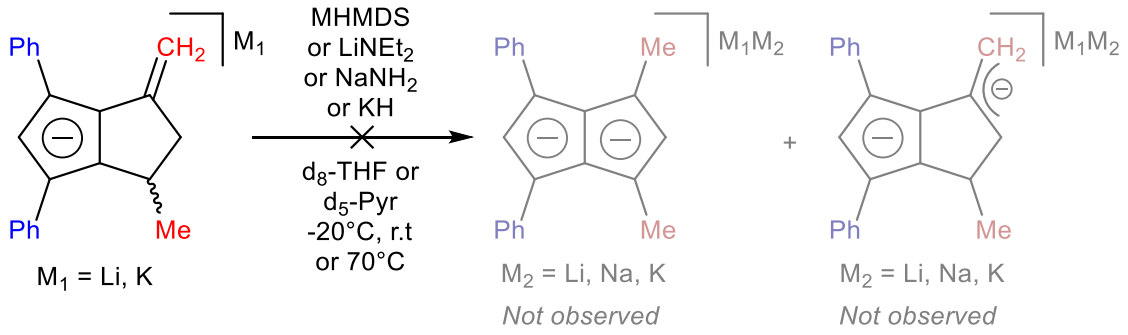

Figure 27: Attempted reaction of lithium 1-methyl-3-vinyl-4,6-diphenyl-1,2,2-trihydropentaleneide with amide and hydride bases

4.4 Conclusion and future work

In this chapter the synthesis of two novel **PnH_2** derivatives containing both methyl and phenyl substituents was described. As for phenyl substituted **PnH_2**s (Chapter 2) pyrrolidine is an effective reagent for facilitating **PnH_2** formation through annulation reactions of **CpH**s. These syntheses were high yielding and produced high purity material with straightforward workup procedures.

$MePh_3PnH_2$ and **$Me_2Ph_2PnH_2$** were both shown to produce, upon deprotonation, a monoanion with an exocyclic double bond rather than the typically endocyclic one. These structures are atypical of monoanionic **Pn** derivatives and could produce interesting compounds if complexed with d- or f-block metals. Due to these species being very soluble crystals suitable for XRD could not be obtained.

Both **$MePh_3PnH_2$** and **$Me_2Ph_2PnH_2$** proved unsuitable for synthesising **Pn^{2-}** derivatives because of the structures of the formed monoanions. Both these **PnH_2**s have methyl groups in the 3-position, and the hydrogens on this group are acidified by their positioning with respect to the fulvene-like double-bond.

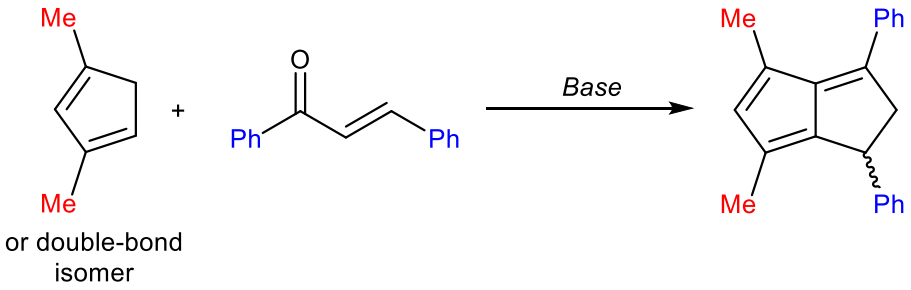

Figure 28: Synthesis of 4,6-dimethyl-1,3-diphenyldihydropentalene from 1,3-dimethylcyclopentadiene

A solution to this problem could be provided by synthesising isomers of these derivatives (Figure 28). For example, if **1,3-Me$_2$CpH**[20] was condensed with 1,3-diphenylprop-2-en-1one it could give **4,6-Me$_2$-1,3-Ph$_2$PnH$_2$**. If this **PnH$_2$** does not isomerise it would lack the acidic proton that enables the exocyclic double-bond to form upon deprotonation. It is therefore supposed that this species could be deprotonated to give **4,6-Me$_2$-1,3-Ph$_2$PnH$^-$**, which could then be further deprotonated to give **4,6-Me$_2$-1,3-Ph$_2$Pn^{2-}** (Figure 29).

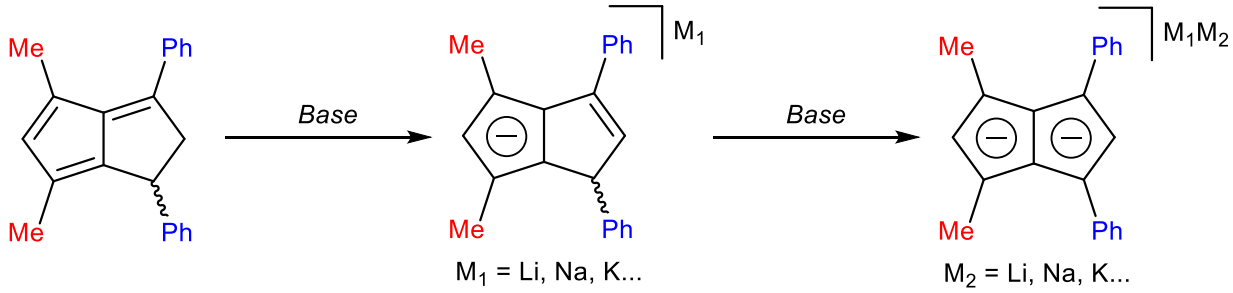

Figure 29: Synthesis of 4,6-dimethyl-1,3-diphenyldihydropentalenide and 4,6-dimethyl-1,3-diphenylpentalenide

One drawback to this approach is that **1,3-Me$_2$CpH** is reported to be thermolabile so could not be stored like **1,4-Ph$_2$CpH** and might degrade when exposed to the reaction conditions required to form the **PnH$_2$** derivative. The **1,3-Me$_2$CpH** could be 'trapped' by deprotonation, as **M[1,3-Me$_2$Cp]** would be resistant to the degradation **1,3-Me$_2$CpH** is susceptible to.[20b] It was shown that **MCp** derivatives can react with enones to give **PnH$_2$**s (Chapter 2) so **M[1,3-Me$_2$Cp]** could potentially be directly reacted with 1,3-diphenylprop-2-en-1one to give **4,6-Me$_2$-1,3-Ph$_2$PnH$_2$**.

Replacing the methyl groups with different alkyl substituents could prevent the unwanted reactivity of **MePh$_3$PnH$_2$** and **Me$_2$Ph$_2$PnH$_2$**. Isopropyl and cyclohexyl, for example, are likely to be inappropriate as they have acidic protons that could be removed if these substituents were placed in the 3-position of the **PnH$_2$** derivative. The additional substitution would likely further favour formation of the exocyclic double bond, unless steric clashing with the neighbouring phenyl-substituent prevent planarisation.

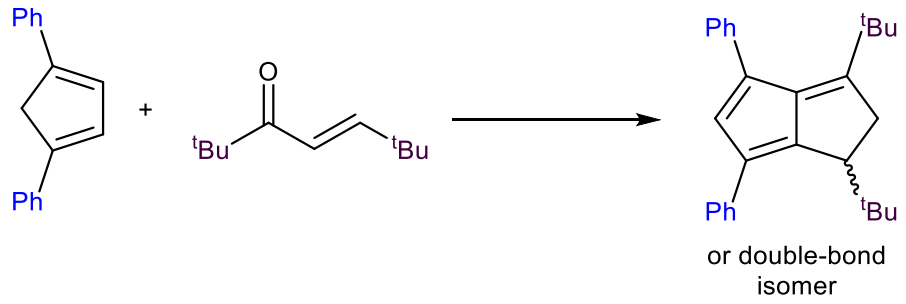

Figure 30: Synthesis of 1,3-di(tert-butyl)-4,6-diphenyldihydropentalene

However, tert-butyl groups would be resistant to deprotonation. If **1,4-Ph$_2$CpH** was condensed with 2,2,6,6-tetramethyl-4-hepten-3-one[21] if could furnish **1,3-^{t}Bu$_2$-4,6-Ph$_2$PnH$_2$** (Figure 30). It is supposed that this species would be a suitable precursor for **1,3-^{t}Bu$_2$-4,6-Ph$_2$PnH$^-$** and **1,3-^{t}Bu$_2$-4,6-Ph$_2$Pn^{2-}** species. This **Pn^{2-}** derivative would have a **^{t}Bu$_2$Cp$^-$** unit that would be very electron-rich but also more sterically hindered than the electron-poor **Ph$_2$Cp$^-$** unit. This ligand would potentially provide electronically asymmetric environments in bimetallic complexes (section 4.1.4). If a **Me$_2$Ph$_2$Pn^{2-}** species could be successfully obtained (see above) the organometallic chemistry of it, **^{t}Bu$_2$Ph$_2$Pn^{2-}** and **Ph$_4$Pn^{2-}** could be compared to probe the effects of electronics on the binding of these ligands.

In this chapter only tetrasubstituted **PnH$_2$** derivatives have been described. In order to synthesise more highly substituted **PnH$_2$**s with aryl and alkyl substituents trisubstituted **CpH**s are required. In chapter 2 it was shown that the pinacol coupling of 1,2,5-triphenyl-pentan-1,5-dione provided access to **1,2,3-Ph$_3$CpH**. It is supposed that pinacol coupling of other trisubstituted pentan-1,5-diones could yield trisubstituted **CpH**s (Figure 31).

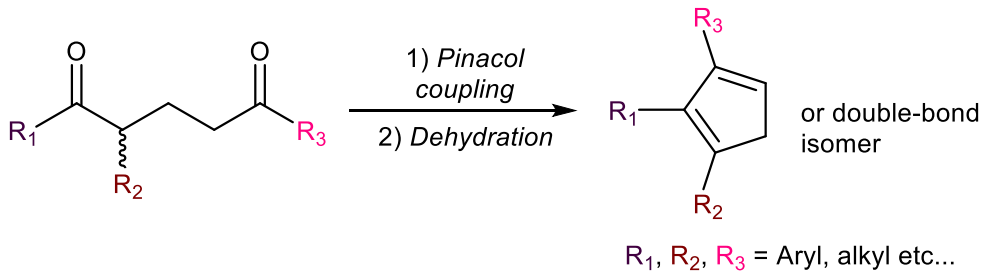

Figure 31: Synthesis of 1,2,3-trisubstituted cyclopentadienes from trisubstituted pentan-1,5-diones

An alternative route was described by Csáky *et al*.[22] who used furfural as starting material for a range **CpH** derivatives. Furfural is functionalised by stepwise addition of the appropriate organolithium or Grignard reagents, with intermediate isomerisation or dehydration steps (Figure 32). This allowed a modular approach to the functionalisation of the trisubstituted **CpH** derivative, with incorporated substituents including Me, Ph, *p*-OMePh, and *p*-CF_3Ph. It is supposed that this method could be extended to incorporate other substituents, such as longer-chain alkyl groups. These **CpHs** could then be used as precursors for **PnH_2** derivatives using the methods described in chapter 2.

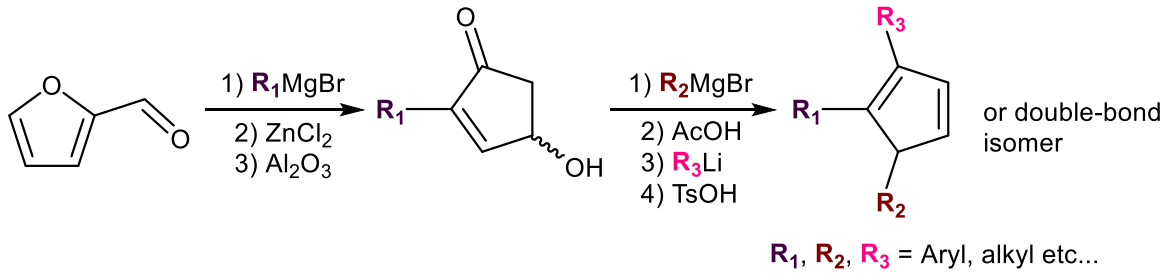

Figure 32: Synthesis of 1,2,3-trisubstituted cyclopentadienes from furfural

4.5 Experimental

General: All reactions and workups were carried out in air unless specified otherwise. Reactions under argon were performed using standard Schlenk techniques or an MBraun Unilab Plus glovebox. NMR spectroscopy was conducted using a 500 MHz Bruker Avance III. Chemical shifts (δ) are reported in ppm. Mass spectrometry was carried out at the EPSRC UK National Mass Spectrometry Facility in Swansea. Single crystal X-ray diffraction analysis was carried out by Dr Gabriele Kociok-Köhn at the University of Bath using a RIGAKU SuperNova Dual. UV/Vis spectroscopy was conducted using an Avantes AvaLight-DH-S-BAL light source and an Avantes AvaSpec-2048L spectrometer. Commercially available materials were obtained from Sigma Aldrich, Fisher or Acros. Methanol was dried by distillation from magnesium. Toluene was dried by distillation from sodium. THF, Et_2O and hexane were dried by distillation from potassium. d_8-THF and C_6D_6 were dried by distillation from potassium and stored over a sodium mirror. *Tert*-butanol and d_5-pyridine were dried by distillation from calcium hydride and stored over 4 Å molecular sieves. Pyrrolidine was purified by drying over sodium followed by distillation.

3-methyl-1,4,6-triphenyldihydropentalene:

Method A: 1,4-diphenyl-1,3-cyclopentadiene (0.50 g, 2.29 mmol) and 4-phenyl-3-buten-2-one (0.37 g, 2.52 mmol) were dissolved in 10 ml dry methanol and 10 ml dry toluene under argon. Pyrrolidine (0.25 ml, 2.29 mmol) was added and the resulting mixture was stirred at 70 °C for 42 hours. To the red solution was added 1 ml acetic acid in air, and the solvent was removed under reduced pressure. The crude material was dissolved in 150 ml diethyl ether and washed with 3x100 ml water then 100 ml aqueous Na_2CO_3, 100 ml water and 100 ml brine. The ether fraction was dried over $MgSO_4$ and the solvent removed reduced pressure. The fraction was then filtered through silica using 1:1 diethyl ether:hexane as the eluent, and the solvent removed under reduced pressure. The resulting red solid was recrystallized from ethanol to give a red crystalline solid. (0.63 g, 1.83 mmol, 80%)

Method B: 1,3,6-triphenylfulvene (0.50 g, 1.63 mmol) and acetone (0.15 ml, 1.96 mmol) were dissolved in 15 ml dry toluene and 15 ml dry methanol under argon, and to this was added pyrrolidine (0.14, 1.63 mmol). The resulting solution was stirred at 70 °C for 22 hours. 1 ml acetic acid was added in air, and the solvent was removed under reduced pressure. The crude material was dissolved in 100 ml diethyl ether and washed with 3x100 ml water then 100 ml aqueous Na_2CO_3, 100 ml water and 100 ml brine. The ether fraction was dried over $MgSO_4$ and the solvent removed reduced pressure. The fraction was then filtered through silica using 1:1 diethyl ether:hexane as the eluent, and the solvent removed under reduced pressure. The resulting red solid was recrystallized from ethanol to give a red crystalline solid (0.31 g, 0.90 mmol, 55%)

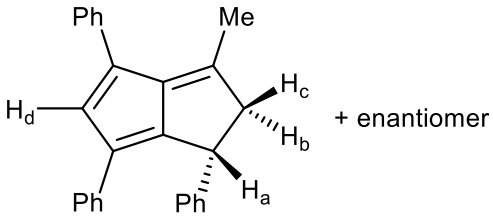

^{1}H NMR (500 MHz, $CDCl_3$): δ (ppm) = 7.47 (***o*-Ph**, d, 2H, $^3J_{HH}$ = 8.33 Hz), 7.29-7.38 (***o*-Ph**, ***m*-Ph**, m, 4H), 7.16-7.26 (***o*-Ph**, ***m*-Ph**, m, 6H), 7.08-7.15 (***p*-Ph**, **H_d**, m, 3H), 7.02 (***p*-Ph**, t, 1H, $^3J_{HH}$ = 7.23 Hz), 4.45 (**H_a**, d, 1H, $^3J_{HH}$ = 6.72 Hz), 3.70 (**H_c**, dd, 1H, $^2J_{HH}$ = 19.55 Hz ,$^3J_{HH}$ = 6.72 Hz), 2.99 (**H_b**, d, 1H, $^2J_{HH}$ = 19.55 Hz), 2.18 (**Me**, s, 3H);

$^{13}C\{^1H\}$ NMR (125 MHz, $CDCl_3$): δ = 156.4, 147.7, 144.3, 136.6, 135.3, 130.15, 128.5, 128.2, 128.1, 127.2, 126.3, 126.2, 125.8, 57.6, 42.9, 17.2;

HR ASAP-MS (+): m/z (expected) = 347.1800 [M+H]; (found) = 347.1799 [M+H]

UV/vis: $\lambda_{max}(\varepsilon)$ = 296 nm (42863 $dm^3\ mol^{-1}\ cm^{-1}$), 338 nm (7081 $dm^3\ mol^{-1}$), 338 nm (6795 $dm^3\ mol^{-1}$)

Melting point: 151-152 °C

1,3-dimethyl-4,6-diphenyldihydropentalene: 1,4-diphenyl-1,3-cyclopentadiene (0.35 g, 1.61 mmol) and 70 % 3-penten-2-one (0.25 ml, 1.77 mmol) were dissolved in 10ml dry methanol and 10ml dry toluene under argon. Pyrrolidine (0.17 ml, 1.61 mmol) was added and the resulting mixture was stirred at 70 °C for 20 hours. To the red solution was added 1 ml acetic acid in air, and the solvent was removed under reduced pressure. The crude material was dissolved in 100 ml diethyl ether and washed with 4x100 ml water, then 100 ml aqueous Na_2CO_3, 100 ml water and 100 ml brine. The ether fraction was dried over $MgSO_4$ and the solvent removed reduced pressure. The fraction was then filtered through silica using 1:1 diethyl ether:hexane as the eluent, and the solvent removed under reduced pressure. The resulting red solid was recrystallized from ethanol to give a red crystalline solid (0.31 g, 1.09 mmol, 67%).

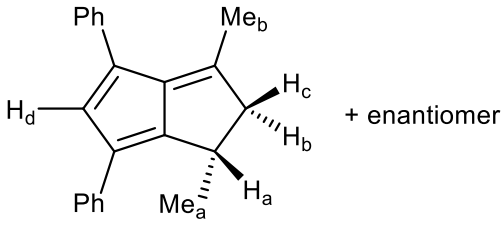

^{1}H NMR (500 MHz, $CDCl_3$): δ = 7.50 (***o*-Ph**, d, 2H, $^3J_{HH}$ = 7.51 Hz), 7.38, (***o*-Ph**, d, 2H, $^3J_{HH}$ = 7.39 Hz), 7.28 (***m*-Ph**, m, 4H), 7.17 (***p*-Ph**, t, 1H, $^3J_{HH}$ = 7.33 Hz), 7.17 (***p*-Ph**, t, 1H, $^3J_{HH}$ = 7.33 Hz), 7.11 (***p*-Ph**, t, 1H, $^3J_{HH}$ = 7.38 Hz), 7.07 (**H$_d$**, s, 1H), 3.32-3.46 (**H$_a$**, **H$_c$** , m, 2H), 2.61 (**H$_b$**, d, 1H, $^2J_{HH}$ = 19.17Hz), 2.12 (**Me$_b$**, s, 3H), 1.19 (**Me$_a$**, d, 3H, $^3J_{HH}$ = 6.95 Hz);

$^{13}C\{^1H\}$ NMR (125 MHz, $CDCl_3$): δ = 157.46, 151.50, 146.33, 137.10, 136.88, 128.51, 128.17, 127.68, 126.22, 126.15, 125.79, 55.42, 31.49, 19.35, 17.40;

HR ASAP-MS (+): m/z (expected) = 285.1643 [M+H]; (found) = 285.1640 [M+H]

UV/vis: $\lambda_{max}(\varepsilon)$ = 300 nm (37637 $dm^3\ mol^{-1}\ cm^{-1}$), 415 nm (6859 $dm^3\ mol^{-1}\ cm^{-1}$)

Melting point: 122-123 °C

Lithium 3-vinyl-1,4,6-triphenyl-1,2,2-trihydropentaleneide: Under argon **3-Me-1,4,6-Ph_3PnH_2** (10.0 mg, 0.029 mmol) in 0.2 ml d_8-THF was added dropwise to $LiNEt_2$ (2.5 mg, 0.032 mmol) in 0.2 ml d_8-THF under argon. The bright yellow solution was allowed to stand for 30 mins, and then was filtered into a J. Young NMR tube. The ^{1}H-NMR spectrum showed quantitative conversion of the starting material into **Li[3-(CH_2)-Ph_3PnH_2]**.

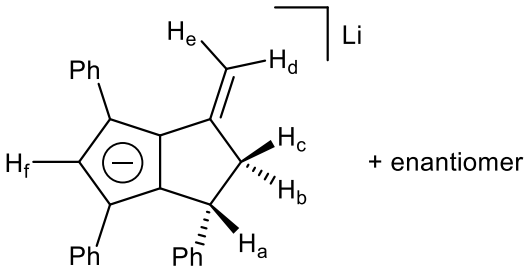

^{1}H NMR (500 MHz, d_8-THF): δ = 7.80 (***o*-Ph**, d, 2H, $^3J_{HH}$ = 8.14 Hz), 7.39 (***o*-Ph**, d, 2H, $^3J_{HH}$ = 8.46 Hz), 7.32 (***o*-Ph**, d, 2H, $^3J_{HH}$ = 8.10 Hz), 7.15-7.24 (***m*-Ph**, m, 4H), 7.24 (***p*-Ph**, t, 1H, $^3J_{HH}$ = 7.26 Hz), 6.95 (***m*-Ph**, t, 2H, $^3J_{HH}$ = 7.80 Hz), 6.87 (***p*-Ph**, t, 1H, $^3J_{HH}$ = 7.33 Hz), 6.71 (**H_f**, s, 1H), 6.61 (***p*-Ph**, t, 1H, $^3J_{HH}$ = 7.19 Hz), 4.94 (**H_e**, d, 1H, $^2J_{HH}$ = 1.32 Hz), 4.56 (**H_a**, dd, 1H, $^3J_{HH}$ = 8.28 Hz, $^3J_{HH}$ = 1.71 Hz), 4.20 (**H_d**, d, 1H, $^2J_{HH}$ = 1.27 Hz), 3.71 (**H_c**, m, 1H), 2.58 (**H_b**, dd, 1H, $^2J_{HH}$ = 14.50 Hz, $^3J_{HH}$ = 1.65 Hz);

^{13}C{^{1}H} NMR (125 MHz, d_8-THF): δ = 150.4, 148.6, 143.3, 141.8, 136.8, 127.4, 127.2, 127.0, 126.7, 126.1, 125.7, 124.3, 122.9, 119.9, 118.5, 116.1, 114.5, 111.6, 87.4, 51.6, 45.9;

Lithium 1-methyl-3-vinyl-4,6-diphenyl-1,2,2-trihydropentaleneide: Under argon **1,3-Me_2-4,6-Ph_2PnH_2** (10.0 mg, 0.035 mmol) in 0.2 ml d_8-THF was added dropwise to LiHMDS (6.5 mg, 0.039 mmol) in 0.2 ml d_8-THF. The bright yellow solution was allowed to stand for 30 mins, and then was filtered into a J. Young NMR tube. The ^{1}H-NMR spectrum showed quantitative conversion of the starting material into **Li[3-(CH_2)-$MePh_2PnH_2$]**.

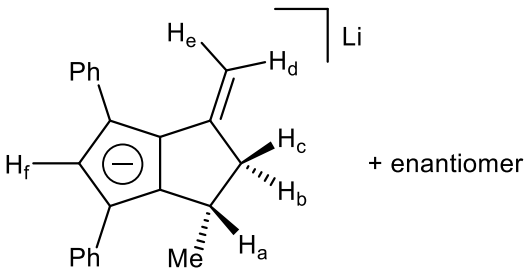

^{1}H NMR (500 MHz, d_8-THF): δ = 7.48 (***o*-Ph**, d, 2H, $^{3}J_{HH}$ = 8.05 Hz), 7.30 (***o*-Ph**, d, 2H, $^{3}J_{HH}$ = 8.37 Hz), 6.93 (***m*-Ph**, m, 4H), 6.61 (***p*-Ph**, t, 1H, $^{3}J_{HH}$ = 7.31 Hz), 6.51 (***p*-Ph**, t, 1H, $^{3}J_{HH}$ = 7.25 Hz), 6.31 (**H_f**, s, 1H), 4.64 (**H_e**, d, 1H, $^{2}J_{HH}$ = 1.57 Hz), 3.99 (**H_d**, d, 1H, $^{2}J_{HH}$ = 1.57 Hz), 3.30 (**H_a**, m, 1H), 3.20 (**H_c** , m, 1H), 2.34 (**H_b**, dd, 1H, $^{2}J_{HH}$ = 14.60 Hz, $^{3}J_{HH}$ = 0.98 Hz), 1.05 (**Me**, d, 1H, $^{3}J_{HH}$ = 6.63 Hz);

^{13}C{^{1}H} NMR (500 MHz, d_8-THF): δ = 147.4, 141.7, 140.9, 138.9, 125.5, 125.1, 123.7, 123.3, 121.6, 117.9, 116.7, 114.3, 112.2, 109.9, 85.0. 47.4, 31.9, 20.4;

4.6 Bibliography

1. Martín-Matute, B.; Edin, M.; Bogár, K.; Kaynak, F. B.; Bäckvall, J.-E., Combined Ruthenium(II) and Lipase Catalysis for Efficient Dynamic Kinetic Resolution of Secondary Alcohols. Insight into the Racemization Mechanism. *J Am Chem Soc* **2005,** *127* (24), 8817-8825.

2. Brand, R. A.; Mulvaney, J. E., Ring-opening reactions of anionic cyclopropyl compounds. 3. *J Org Chem* **1980,** *45* (4), 633-636.

3. Schreiber, E. C.; Becker, E. I., 1,2,3,4-Tetraphenylfulvalene. *J Am Chem Soc* **1954,** *76* (23), 6125-6127.

4. Fuson, R. C.; York, O., The Addition Of Grignard Reagents TO 1,2,3,4-Tetraphenylfulvene. *J Org Chem* **1953,** *18* (5), 570-574.

5. Bonagura, A. G.; Meyers, M. B.; Storfer, S. J.; Becker, E. I., The Reaction of 1,2,3,4-Tetraphenylfulvene with Grignard Reagents. *J Am Chem Soc* **1954,** *76* (23), 6122-6125.

6. Thewalt, U.; Schmid, G., Titan(IV)-Verbindungen mit hochphenylierten π-Cyclopentadienylliganden. Die Struktur von $(\pi\text{-}C_5H_5)(\pi\text{-}C_5Ph_5)TiCl_2$. *J Organomet Chem* **1991,** *412* (3), 343-353.

7. Schumann, H.; Lentz, A., 1,4-Bis(4-acylphen-1 -yl) 1,3-cy clopentadiene und 1,2,3,4-Tetra(4-alkylphen-1-yl)-1,3-cyclopentadiene und deren Natrium-, Thallium(I)- und Eisen(II)-Komplexe / 1,4-Bis(4-acylphen-1-yl)-1,3-cyclopentadienes and 1,2,3,4-Tetra(4-alkylphen-1-yl)- 1,3-cyclopentadienes and their Sodium, Thallium (I) and Iron(II) Complexes. In *Zeitschrift für Naturforschung B*, 1997; Vol. 52, p 45.

8. (a) Nishina, Y.; Tatsuzaki, T.; Tsubakihara, A.; Kuninobu, Y.; Takai, K., Synthesis of Multisubstituted Cyclopentadienes from Cyclopentenones Prepared via Catalytic Double Aldol Condensation and Nazarov Reaction Sequence. *Synlett* **2011,** *2011* (17), 2585-2589; (b) Wang, M.; Han, F.; Yuan, H.; Liu, Q., Tandem Nazarov cyclization–halovinylation of divinyl ketones under

Vilsmeier conditions: synthesis of highly substituted cyclopentadienes. *Chem Commun* **2010,** *46* (13), 2247-2249.

9. Griesbeck, A. G., Notizen/Notes Synthesis of 1-Phenyl-1,2- and 4-Phenyl-1,5-dihydropentalenes. *Chem Ber* **1991,** *124* (2), 403-405.

10. Threlkel, R. S.; Bercaw, J. E., A convenient synthesis of Alkyltetramethylcyclopentadienes and Phenyltetramethylcyclopentadiene. *JbOrganomet Chem* **1977,** *136* (1), 1-5.

11. Brown, L. C.; Ressegue, E.; Merola, J. S., Rapid Access to Derivatized, Dimeric, Ring-Substituted Dichloro(cyclopentadienyl)rhodium(III) and Iridium(III) Complexes. *Organometallics* **2016,** *35* (24), 4014-4022.

12. Morris, D. M.; McGeagh, M.; De Peña, D.; Merola, J. S., Extending the range of pentasubstituted cyclopentadienyl compounds: The synthesis of a series of tetramethyl(alkyl or aryl)cyclopentadienes (Cp∗R), their iridium complexes and their catalytic activity for asymmetric transfer hydrogenation. *Polyhedron* **2014,** *84*, 120-135.

13. Bordwell, F. G.; Bausch, M. J., Methyl effects on the basicities of cyclopentadienide and indenide ions and on the chemistry of their transition metal complexes. *J Am Chem Soc* **1983,** *105* (19), 6188-6189.

14. (a) Dinnebier, R. E.; Behrens, U.; Olbrich, F., Solid State Structures of Cyclopentadienyllithium, -sodium, and -potassium. Determination by High-Resolution Powder Diffraction. *Organometallics* **1997,** *16* (17), 3855-3858; (b) Behrens, U.; Dinnebier, R. E.; Neander, S.; Olbrich, F., Solid-State Structures of Base-Free Rubidium and Cesium Pentamethylcyclopentadienides. Determination by High-Resolution Powder Diffraction. *Organometallics* **2008,** *27* (20), 5398-5400.

15. Kaiser, R.; Hafner, K., A Simple Synthesis of 1,2-Dihydropentalene and its Substitution Products. *Angew Chem Int Ed Eng* **1970,** *9* (11), 892-893.

16. Coşkun, N.; Ma, J.; Azimi, S.; Gärtner, C.; Erden, I., 1,2-Dihydropentalenes from Fulvenes by [6 + 2] Cycloadditions with 1-Isopropenylpyrrolidine. *Org Lett* **2011,** *13* (22), 5952-5955.

17. Aulbach, M.; Kuber, F.; Riedel, M.; Helmer-Metzmann, F., Stereorigid metallocene compound. Google Patents: 2000.

18. Ashley, A. E.; Cowley, A. R.; O'Hare, D., The hexamethylpentalene dianion and other reagents for organometallic pentalene chemistry. *Chem Commum* **2007,** (15), 1512-1514.

19. Paradies, J.; Erker, G.; Fröhlich, R., Functional-Group Chemistry of Organolithium Compounds: Photochemical [2+2] Cycloaddition of Alkenyl-Substituted Lithium Cyclopentadienides. *Angew Chem In Ed* **2006,** *45* (19), 3079-3082.

20. (a) Deno, N. C.; Richey, H. G.; Liu, J. S.; Lincoln, D. N.; Turner, J. O., Carbonium Ions. XIX. The Intense Conjugation in Cyclopropyl Carbonium Ions1. *J Am Chem Soc* **1965,** *87* (20), 4533-4538; (b) McLean, S.; Haynes, P., Substitution in the cyclopentadienide anion series: Methylation of the cyclopentadienide and methylcyclopentadienide anions. *Tetrahedron* **1965,** *21* (9), 2313-2327.

21. Bowers, K. W.; Giese, R. W.; Grimshaw, J.; House, H. O.; Kolodny, N. H.; Kronberger, K.; Roe, D. K., Reactions involving electron transfer. I. Reduction of 2,2,6,6-tetramethyl-4-hepten-3-one. *J Am Chem Soc* **1970,** *92* (9), 2783-2799.

22. Csáky, A. G.; Contreras, C.; Mba, M.; Plumet, J., Regioselective Synthesis of Trisubstituted Cyclopentadienyl Ligands from Furans. *Synlett* **2002,** *2002* (09), 1451-1454.

Chapter 5: Conclusion and future work

5.1 Conclusion

In this investigation the synthesis and characterisation of three novel **PnH_2** derivatives has been described – **1,3,4,6-Ph_4PnH_2**, **3-Me-1,4,6-Ph_3PnH_2** and **1,3-Me_2-4,6-Ph_2PnH_2** (Figure 1). These species were all stable, high-melting point solids in contrast to the parent **PnH_2**, which is thermolabile. These **PnH_2**s were synthesised in high yields from inexpensive, commercially available enones and **1,4-Ph_2CpH**, which was synthesised from similarly inexpensive starting materials. These syntheses only require standard Schlenk techniques and laboratory equipment, making them more accessible than the **PnH_2**s that require specialised pyrolysis reactors (Section 1.2.2).

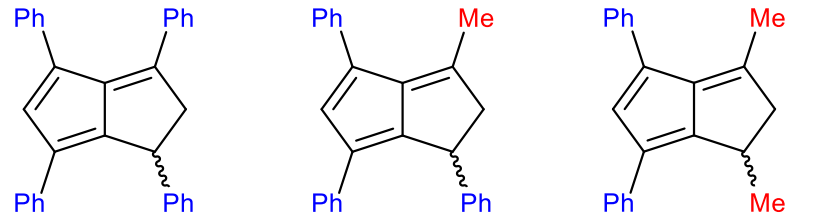

Figure 1: Three novel dihydropentalenes synthesised in this investigation

These **PnH_2** derivatives were used to synthesise several mono-anionic derivatives. **1,3,4,6-Ph_4PnH_2** was deprotonated with a range of bases to give alkali metal salts of the **1,3,4,6-Ph_4PnH^-** anion (Figure 2). This is the first **PnH^-** derivative to be synthesised with different alkali metal cations. The **M[1,3,4,6-Ph_4PnH]** species were shown to be highly soluble in co-ordinating solvents, which allowed characterisation by ^{1}H- and ^{13}C{^{1}H}-NMR but prevented the growth of crystals suitable for XRD analysis.

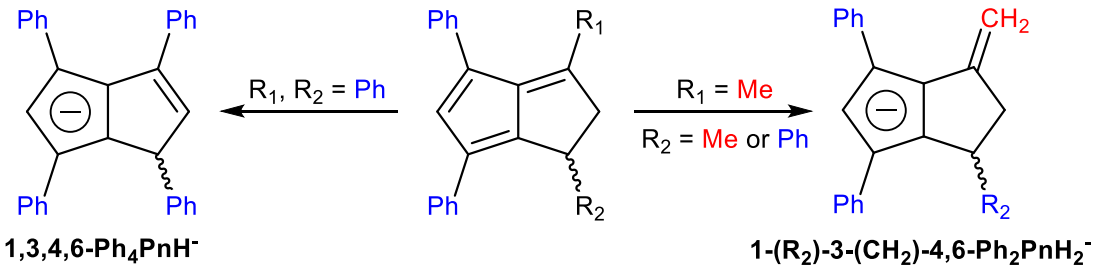

Figure 2: Mono-anionic derivatives of tetra-substituted dihydropentalenes

The **1,2-PnH$_2$** derivatives with a methyl substituent in the C3-position were shown to be inappropriate for the formation of **PnH$^-$** anions. Instead, it was found that the methyl group is deprotonated upon treatment with bases to give vinyl-substituted-**PnH$_2^-$** anions (Figure 2). The lithium salts of **3-(CH$_2$)-1,4,6-Ph$_3$PnH$_2^-$** and **1-Me-3-(CH$_2$)-Ph2PnH$_2^-$** were characterised by ^{1}H- and ^{13}C{^{1}H}-NMR, but crystals of these species could not be grown to analyse them by XRD. It was shown that these vinyl-substituted-**PnH$_2^-$**s do not undergo a second deprotonation when treated with strong bases, meaning **3-Me-1,4,6-Ph$_3$PnH$_2$** and **1,3-Me$_2$-4,6-Ph$_2$PnH$_2$** cannot function as precursors for **Pn^{2-}** species.

1,3,4,6-Ph$_4$PnH$_2$ was doubly deprotonated to give several **Ph$_4$Pn^{2-}** species. Dilithium, disodium and dipotassium salts of **Ph$_4$Pn^{2-}** (Figure 3) were characterised by XRD, the first **Pn^{2-}** derivative to be crystallographically characterised with different alkali metal cations. However, these homo-bimetallic salts were found to be insufficiently soluble in organic solvents to be analysed by NMR spectroscopy.

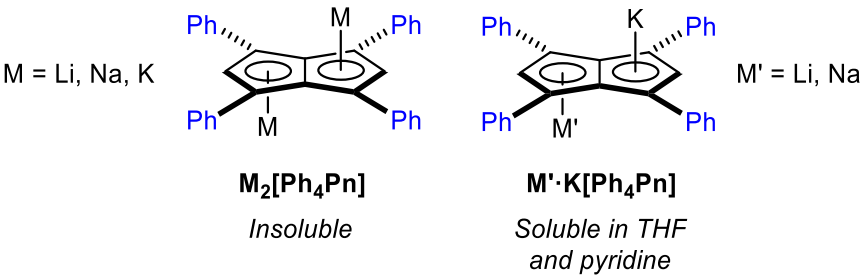

Figure 3: Homo- and hetero-bimetallic alkali metal salts of 1,3,4,6-tetraphenylpentalenide

In order to address this issue of solubility, heterobimetallic salts of **Ph$_4$Pn^{2-}** (Figure 3) were synthesised by stepwise deprotonation. **Li·K[Ph$_4$Pn]** and **Na·K[Ph$_4$Pn]** were sufficiently soluble in coordinating solvents to characterise by them ^{1}H- and ^{13}C{^{1}H}-NMR. Attempts to grow crystals of these

heterobimetallic species lead to formation of crystals of the homobimetallic derivatives, meaning that slow cation exchange must be occurring in solution. Therefore, these mixed-cation species would need to be synthesised immediately prior to any transmetalation reaction.

5.2 Future work

Future work would be split into two components – further synthesis of $\mathbf{Pn^{2-}}$s, and exploration of the organometallic chemistry of these $\mathbf{Pn^{2-}}$s. The ligand synthesis would focus on acquiring $\mathbf{Pn^{2-}}$ derivatives that address the problems encountered with the mixed phenyl- and methyl substituted species reported here. The alkali metal salts of $\mathbf{Ph_4Pn^{2-}}$ were shown to suffer issues of solubility. This insolubility could affect transmetalation reactions performed with this ligand and could lead to formation of insoluble metal complexes. To address this the phenyl substituents could be replaced with substituted-aryl groups (Figure 4). This could potentially enhance the solubility of this species, and also allow tuning of the steric and electronic properties of metal complexes derived from this ligand. It is supposed that $\mathbf{(\textit{p}\text{-Tol})_4Pn^{2-}}$ would be readily accessible using the methods described in Chapters 2 and 3, and therefore this would be a primary synthetic target.

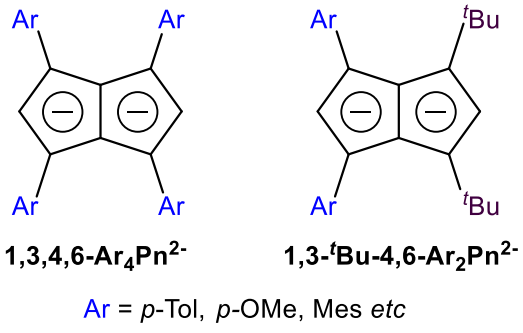

Figure 4: 1,3,4,6-tetraarylpentalenide (left) and 1,3-tert-butyl-4,6-diarylpentalenide (right)

Because the methyl substituted $\mathbf{PnH_2}$s in this investigation were found to undergo unwanted deprotonations they were unsuitable for us as $\mathbf{Pn^{2-}}$ precursors. Replacing the methyl substituents with *tert*-butyl groups would prevent this unwanted reactivity and potentially allow access to the desired

anionic derivatives. **1,3-^{t}Bu-4,6-Ar$_2$Pn^{2-}** (Figure 4) would be a ligand that provides a high degree of steric shielding and would provide two electronically different binding sites.

The investigation of the organometallic chemistry of these novel **Pn^{2-}**s would look at both early and late transition metals. **Pn^{2-}** complexes of early transition metals have found interest as polymerisation catalysts. **3-Me-1-PhPnH$_2$** has been used as a precursor for *ansa*-metallocene zirconium complexes (Section 4.1.3),[1] and these complexes have been used as catalysts for the polymerisation of propylene. Starting with **1,3,4,6-Ar$_4$PnH$_2$** could enable synthesis of tetraaryl-substituted *ansa*-metallocenes (Figure 5), with the high steric demand of the aryl substituents potentially the catalytic activity of these complexes.

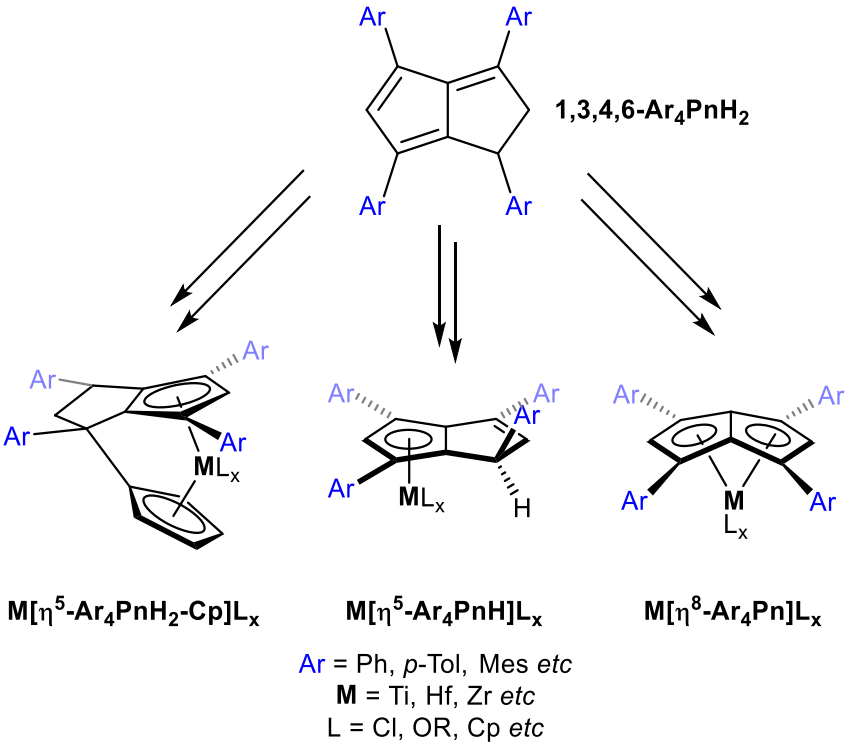

Figure 5: Potential structures of early-transition metal complexes derived from 1,3,4,6-tetraaryldihydropentalenes

Turner *et al.*[2] showed that **Pn*H$^-$** titanium, zirconium and hafnium complexes are initiators for lactide polymerisation, and Fraser *et al.*[3] showed that **Pn*$^{2-}$** titanium and zirconium complexed can be used as catalysts for the polymerisation of ethylene. Therefore, it is supposed that **Ar$_4$PnH$^-$**s and **Ar$_4$Pn^{2-}**

could be used as ligands in analogous complexes (Figure 5), and the catalytic activity of these complexes could be explored.

Bimetallic late transition metal $\mathbf{Pn^{2-}}$ complexes are of interest because of the high degree of electronic communication offered by the $\mathbf{Pn^{2-}}$ core. Jones *et al.*[4] showed that in *anti*-$\mathbf{[Mn(CO)_3]_2Pn}$ the two metal atoms are strongly electronically coupled, enabling full delocalization of the metal oxidation states. This property would potentially allow *anti*-bimetallic $\mathbf{Ar_4Pn^{2-}}$ complexes (Figure 6) to display reactivity that is not available to monometallic $\mathbf{Cp^-}$ complexes.

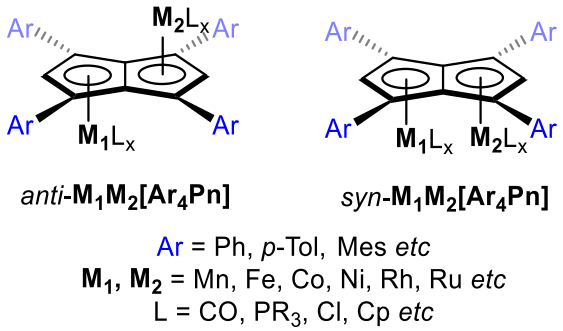

Figure 6: anti- and syn-bimetallic late transition-metal complexes of 1,3,4,6-tetraarylpentalenide

Syn-bimetallic $\mathbf{Ar_4Pn^{2-}}$ complexes (Figure 6) would have the additional property of the metal atoms being held in close proximity. This could potentially allow reversible formation of metal-metal bonds which, combined with the strong electronic communication through the ligand core, could give rise to interesting redox properties. The ultimate aim would be to synthesise bimetallic first row transition metals $\mathbf{Pn^{2-}}$ complexes. While these metals typically perform one electron processes, it is hoped that the electronic properties of $\mathbf{Pn^{2-}}$ would allow a pair of metal atoms to perform the two-electron bond-formation/bond-breaking reactions typical of second and third row transition metals.

5.3 Bibliography

1. Aulbach, M.; Kuber, F.; Riedel, M.; Helmer-Metzmann, F., Stereorigid metallocene compound. Google Patents: 2000.

2. Turner, Z. R.; Buffet, J.-C.; O'Hare, D., Chiral Group 4 Cyclopentadienyl Complexes and Their Use in Polymerization of Lactide Monomers. *Organometallics* **2014,** *33* (14), 3891-3903.

3. Fraser, D. A. X.; Turner, Z. R.; Buffet, J.-C.; O'Hare, D., Titanium and Zirconium Permethylpentalene Complexes, Pn*MCpRX, as Ethylene Polymerization Catalysts. *Organometallics* **2016,** *35* (16), 2664-2674.

4. Jones, S. C.; Hascall, T.; Barlow, S.; O'Hare, D., Pentalene Complexes of Group 7 Metal Carbonyls: An Organometallic Mixed-Valence System with Very Large Metal−Metal Electronic Coupling. *J Am Chem Soc* **2002,** *124* (39), 11610-11611.

Appendix

Crystal data and structure refinement for 1,3,4,6-tetraphenyldihydropentalene

Identification code	s17uh2	
Empirical formula	C32 H24	
Formula weight	408.51	
Temperature	150.00(10) K	
Wavelength	1.54184 Å	
Crystal system	Monoclinic	
Space group	I2/a	
Unit cell dimensions	a = 22.4778(7) Å	□= 90°.
	b = 5.7087(2) Å	□= 91.370(3)°.
	c = 17.2058(5) Å	□ = 90°.
Volume	2207.20(12) $Å^3$	
Z	4	
Density (calculated)	1.229 Mg/m^3	
Absorption coefficient	0.524 mm^{-1}	
F(000)	864	
Crystal size	0.200 x 0.150 x 0.040 mm^3	
Theta range for data collection	3.934 to 73.020°.	
Index ranges	-26<=h<=27, -5<=k<=7, -21<=l<=21	
Reflections collected	6989	
Independent reflections	2188 [R(int) = 0.0230]	
Completeness to theta = 67.684°	100.0 %	
Absorption correction	Semi-empirical from equivalents	
Max. and min. transmission	1.00000 and 0.80138	
Refinement method	Full-matrix least-squares on F^2	
Data / restraints / parameters	2188 / 0 / 235	
Goodness-of-fit on F^2	1.222	
Final R indices [I>2sigma(I)]	R1 = 0.0735, wR2 = 0.1552	
R indices (all data)	R1 = 0.0790, wR2 = 0.1574	
Extinction coefficient	n/a	
Largest diff. peak and hole	0.147 and -0.182 $e.Å^{-3}$	

Table 2. Atomic coordinates (x 10^4) and equivalent isotropic displacement parameters ($Å^2$x 10^3) for s17uh2. U(eq) is defined as one third of the trace of the orthogonalized U^{ij} tensor.

	x	y	z	U(eq)
C(1)	3685(1)	5249(6)	3096(1)	46(1)
C(2)	3726(1)	3091(7)	2736(2)	58(1)
C(3)	4246(2)	1788(6)	2782(2)	58(1)
C(4)	4731(1)	2625(5)	3198(2)	52(1)
C(5)	4695(1)	4754(6)	3574(2)	49(1)
C(6)	4173(1)	6059(5)	3528(1)	42(1)
C(7)	3162(4)	7126(12)	3007(5)	32(2)
C(8)	2953(5)	8637(15)	3669(6)	40(2)
C(9)	2413(2)	10102(10)	3340(3)	34(1)
C(10)	1963(12)	10160(50)	3861(14)	37(5)
C(11)	1780(3)	12350(11)	4256(4)	45(1)
C(12)	1305(8)	12660(40)	4758(12)	57(4)
C(13)	925(4)	10710(20)	4851(5)	56(2)
C(14)	1035(3)	8635(15)	4477(4)	52(2)
C(15)	1515(4)	8378(17)	3989(6)	45(2)
C(16)	2302(2)	8941(11)	2560(3)	33(1)
C(17)	1882(4)	8862(12)	1970(5)	34(2)
C(18)	2127(5)	7264(13)	1384(6)	33(2)
C(19)	2679(2)	6459(9)	1596(2)	31(1)
C(20)	3148(11)	5060(40)	1104(12)	25(3)
C(21)	2898(3)	3191(11)	693(4)	47(1)
C(22)	3288(4)	2089(13)	203(5)	65(2)
C(23)	3861(8)	2890(30)	156(10)	56(4)
C(24)	4052(3)	4792(18)	541(4)	52(2)
C(25)	3663(4)	5937(16)	1022(6)	39(2)
C(26)	2793(2)	7409(11)	2378(3)	32(1)

Table 3. Bond lengths [Å] for s17uh2.

C(1)-C(2)	1.384(4)
C(1)-C(6)	1.389(4)
C(1)-C(7)	1.594(8)
C(2)-C(3)	1.386(4)
C(2)-H(2)	0.9500
C(3)-C(4)	1.375(4)
C(3)-H(3)	0.9500
C(4)-C(5)	1.380(4)
C(4)-H(4)	0.9500
C(5)-C(6)	1.391(4)
C(5)-H(5)	0.9500
C(6)-H(6)	0.9500
C(7)-C(26)	1.358(10)
C(7)-C(8)	1.512(12)
C(8)-C(9)	1.569(12)
C(8)-H(8A)	0.9900
C(8)-H(8B)	0.9900
C(9)-C(10)	1.37(3)
C(9)-C(16)	1.511(7)
C(9)-H(9)	1.0000
C(10)-C(15)	1.45(3)
C(10)-C(11)	1.49(2)
C(11)-C(12)	1.401(18)
C(11)-H(11)	0.9500
C(12)-C(13)	1.413(17)
C(12)-H(12)	0.9500
C(13)-C(14)	1.374(13)
C(13)-H(13)	0.9500
C(14)-C(15)	1.390(12)
C(14)-H(14)	0.9500
C(15)-H(15)	0.9500
C(16)-C(17)	1.369(10)
C(16)-C(26)	1.449(6)
C(17)-C(18)	1.475(12)
C(18)-C(19)	1.365(11)
C(18)-H(18)	0.9500

C(19)-C(26)	1.467(6)
C(19)-C(20)	1.585(18)
C(20)-C(25)	1.27(3)
C(20)-C(21)	1.39(2)
C(21)-C(22)	1.383(9)
C(21)-H(21)	0.9500
C(22)-C(23)	1.371(17)
C(22)-H(22)	0.9500
C(23)-C(24)	1.337(19)
C(23)-H(23)	0.9500
C(24)-C(25)	1.382(11)
C(24)-H(24)	0.9500
C(25)-H(25)	0.9500

Table 4. Bond angles [°] for s17uh2.

C(2)-C(1)-C(6)	118.4(3)
C(2)-C(1)-C(7)	127.8(4)
C(6)-C(1)-C(7)	113.5(4)
C(1)-C(2)-C(3)	121.2(3)
C(1)-C(2)-H(2)	119.4
C(3)-C(2)-H(2)	119.4
C(4)-C(3)-C(2)	120.0(3)
C(4)-C(3)-H(3)	120.0
C(2)-C(3)-H(3)	120.0
C(3)-C(4)-C(5)	119.7(3)
C(3)-C(4)-H(4)	120.2
C(5)-C(4)-H(4)	120.2
C(4)-C(5)-C(6)	120.3(3)
C(4)-C(5)-H(5)	119.9
C(6)-C(5)-H(5)	119.9
C(1)-C(6)-C(5)	120.4(3)
C(1)-C(6)-H(6)	119.8
C(5)-C(6)-H(6)	119.8
C(26)-C(7)-C(8)	109.7(7)
C(26)-C(7)-C(1)	126.3(6)
C(8)-C(7)-C(1)	123.6(7)
C(7)-C(8)-C(9)	106.5(7)

C(7)-C(8)-H(8A)	110.4
C(9)-C(8)-H(8A)	110.4
C(7)-C(8)-H(8B)	110.4
C(9)-C(8)-H(8B)	110.4
H(8A)-C(8)-H(8B)	108.6
C(10)-C(9)-C(16)	118.9(12)
C(10)-C(9)-C(8)	110.7(12)
C(16)-C(9)-C(8)	101.4(5)
C(10)-C(9)-H(9)	108.5
C(16)-C(9)-H(9)	108.5
C(8)-C(9)-H(9)	108.5
C(9)-C(10)-C(15)	127.6(18)
C(9)-C(10)-C(11)	122(2)
C(15)-C(10)-C(11)	108.6(16)
C(12)-C(11)-C(10)	127.7(15)
C(12)-C(11)-H(11)	116.1
C(10)-C(11)-H(11)	116.1
C(11)-C(12)-C(13)	116.2(16)
C(11)-C(12)-H(12)	121.9
C(13)-C(12)-H(12)	121.9
C(14)-C(13)-C(12)	120.7(13)
C(14)-C(13)-H(13)	119.6
C(12)-C(13)-H(13)	119.6
C(13)-C(14)-C(15)	121.6(8)
C(13)-C(14)-H(14)	119.2
C(15)-C(14)-H(14)	119.2
C(14)-C(15)-C(10)	124.7(12)
C(14)-C(15)-H(15)	117.6
C(10)-C(15)-H(15)	117.6
C(17)-C(16)-C(26)	109.5(5)
C(17)-C(16)-C(9)	140.2(6)
C(26)-C(16)-C(9)	110.2(4)
C(16)-C(17)-C(18)	105.5(7)
C(19)-C(18)-C(17)	112.1(7)
C(19)-C(18)-H(18)	124.0
C(17)-C(18)-H(18)	124.0
C(18)-C(19)-C(26)	105.0(5)
C(18)-C(19)-C(20)	129.7(10)

C(26)-C(19)-C(20)	124.9(9)
C(25)-C(20)-C(21)	127.1(14)
C(25)-C(20)-C(19)	118.7(14)
C(21)-C(20)-C(19)	113.0(17)
C(22)-C(21)-C(20)	113.8(11)
C(22)-C(21)-H(21)	123.1
C(20)-C(21)-H(21)	123.1
C(23)-C(22)-C(21)	119.7(11)
C(23)-C(22)-H(22)	120.2
C(21)-C(22)-H(22)	120.2
C(24)-C(23)-C(22)	122.1(16)
C(24)-C(23)-H(23)	118.9
C(22)-C(23)-H(23)	118.9
C(23)-C(24)-C(25)	118.8(11)
C(23)-C(24)-H(24)	120.6
C(25)-C(24)-H(24)	120.6
C(20)-C(25)-C(24)	118.0(11)
C(20)-C(25)-H(25)	121.0
C(24)-C(25)-H(25)	121.0
C(7)-C(26)-C(16)	110.7(5)
C(7)-C(26)-C(19)	141.0(5)
C(16)-C(26)-C(19)	107.7(4)

Table 5. Anisotropic displacement parameters ($Å^2 x\ 10^3$) for s17uh2. The anisotropic displacement factor exponent takes the form: $-2\pi^2[h^2 a^{*2} U^{11} + ... + 2 h k a^* b^* U^{12}]$

	U^{11}	U^{22}	U^{33}	U^{23}	U^{13}	U^{12}
C(1)	35(1)	77(2)	26(1)	3(1)	4(1)	11(1)
C(2)	51(2)	86(2)	35(1)	-1(2)	1(1)	-4(2)
C(3)	75(2)	56(2)	43(2)	8(1)	6(1)	8(2)
C(4)	54(2)	54(2)	48(2)	17(1)	7(1)	20(1)
C(5)	36(1)	67(2)	43(1)	16(1)	1(1)	7(1)
C(6)	39(1)	57(2)	32(1)	11(1)	2(1)	9(1)
C(7)	32(3)	32(4)	31(3)	-5(4)	0(2)	14(4)
C(8)	38(4)	52(6)	32(3)	-13(4)	4(3)	10(4)
C(9)	35(2)	32(3)	36(3)	-7(2)	1(2)	6(2)

C(10)	24(9)	56(6)	30(5)	6(4)	-3(5)	-11(4)
C(11)	47(4)	37(3)	52(4)	-14(3)	11(3)	0(3)
C(12)	56(10)	55(7)	61(6)	-24(5)	13(6)	3(6)
C(13)	39(4)	94(7)	36(4)	7(5)	9(3)	9(4)
C(14)	39(3)	69(5)	48(4)	6(4)	-7(3)	-6(3)
C(15)	51(6)	40(5)	44(3)	-1(4)	-8(4)	2(4)
C(16)	33(3)	36(3)	30(2)	-1(2)	5(2)	10(2)
C(17)	43(3)	32(4)	26(3)	0(4)	4(2)	11(4)
C(18)	37(3)	36(5)	26(3)	-1(4)	-6(2)	6(4)
C(19)	37(2)	30(3)	25(2)	-2(2)	3(2)	8(2)
C(20)	17(8)	39(6)	21(3)	-11(4)	9(3)	5(6)
C(21)	54(4)	36(3)	52(3)	-12(3)	3(3)	1(3)
C(22)	77(5)	51(4)	66(5)	-32(3)	6(4)	6(4)
C(23)	48(11)	74(13)	46(6)	-17(7)	-2(7)	17(7)
C(24)	39(3)	81(6)	37(4)	-2(4)	9(3)	17(4)
C(25)	41(5)	40(5)	36(3)	-6(3)	-2(3)	10(3)
C(26)	35(3)	30(3)	29(2)	-3(2)	3(2)	8(2)

Table 6. Hydrogen coordinates (x 10^4) and isotropic displacement parameters (Å^{2}x 10^3) for s17uh2.

	x	y	z	U(eq)
H(2)	3392	2491	2451	69
H(3)	4267	316	2527	69
H(4)	5089	1742	3226	62
H(5)	5028	5331	3865	58
H(6)	4150	7514	3794	51
H(8A)	3277	9689	3854	48
H(8B)	2828	7648	4109	48
H(9)	2550	11743	3249	41
H(11)	2012	13701	4155	54
H(12)	1241	14098	5022	69
H(13)	591	10838	5176	68
H(14)	776	7344	4553	63
H(15)	1552	6933	3721	54
H(18)	1923	6846	914	40

H(21)	2496	2716	745	57
H(22)	3159	785	-100	78
H(23)	4132	2064	-159	68
H(24)	4447	5347	484	63
H(25)	3777	7338	1284	47

Table 7. Torsion angles [°] for s17uh2.

C(6)-C(1)-C(2)-C(3)	-1.8(4)
C(7)-C(1)-C(2)-C(3)	170.6(5)
C(1)-C(2)-C(3)-C(4)	0.5(4)
C(2)-C(3)-C(4)-C(5)	0.7(4)
C(3)-C(4)-C(5)-C(6)	-0.6(4)
C(2)-C(1)-C(6)-C(5)	2.0(4)
C(7)-C(1)-C(6)-C(5)	-171.6(4)
C(4)-C(5)-C(6)-C(1)	-0.8(4)
C(2)-C(1)-C(7)-C(26)	-27.1(10)
C(6)-C(1)-C(7)-C(26)	145.7(6)
C(2)-C(1)-C(7)-C(8)	144.0(6)
C(6)-C(1)-C(7)-C(8)	-43.3(8)
C(26)-C(7)-C(8)-C(9)	-4.3(9)
C(1)-C(7)-C(8)-C(9)	-176.7(6)
C(7)-C(8)-C(9)-C(10)	136.9(14)
C(7)-C(8)-C(9)-C(16)	9.8(7)
C(16)-C(9)-C(10)-C(15)	35(3)
C(8)-C(9)-C(10)-C(15)	-81(2)
C(16)-C(9)-C(10)-C(11)	-129.9(17)
C(8)-C(9)-C(10)-C(11)	113.5(19)
C(9)-C(10)-C(11)-C(12)	175.5(17)
C(15)-C(10)-C(11)-C(12)	8(3)
C(10)-C(11)-C(12)-C(13)	-6(3)
C(11)-C(12)-C(13)-C(14)	1(2)
C(12)-C(13)-C(14)-C(15)	-0.7(18)
C(13)-C(14)-C(15)-C(10)	3.9(18)
C(9)-C(10)-C(15)-C(14)	-173.5(16)
C(11)-C(10)-C(15)-C(14)	-7(2)
C(10)-C(9)-C(16)-C(17)	45.8(17)

C(8)-C(9)-C(16)-C(17)	167.3(9)
C(10)-C(9)-C(16)-C(26)	-133.8(13)
C(8)-C(9)-C(16)-C(26)	-12.3(7)
C(26)-C(16)-C(17)-C(18)	-1.5(9)
C(9)-C(16)-C(17)-C(18)	179.0(8)
C(16)-C(17)-C(18)-C(19)	-1.8(9)
C(17)-C(18)-C(19)-C(26)	4.1(8)
C(17)-C(18)-C(19)-C(20)	-169.3(13)
C(18)-C(19)-C(20)-C(25)	121.7(16)
C(26)-C(19)-C(20)-C(25)	-50(2)
C(18)-C(19)-C(20)-C(21)	-47(2)
C(26)-C(19)-C(20)-C(21)	140.9(12)
C(25)-C(20)-C(21)-C(22)	7(3)
C(19)-C(20)-C(21)-C(22)	174.1(11)
C(20)-C(21)-C(22)-C(23)	-0.5(17)
C(21)-C(22)-C(23)-C(24)	-4(2)
C(22)-C(23)-C(24)-C(25)	2(2)
C(21)-C(20)-C(25)-C(24)	-8(3)
C(19)-C(20)-C(25)-C(24)	-174.9(12)
C(23)-C(24)-C(25)-C(20)	3.2(19)
C(8)-C(7)-C(26)-C(16)	-3.6(9)
C(1)-C(7)-C(26)-C(16)	168.5(6)
C(8)-C(7)-C(26)-C(19)	-173.1(8)
C(1)-C(7)-C(26)-C(19)	-1.0(14)
C(17)-C(16)-C(26)-C(7)	-169.1(6)
C(9)-C(16)-C(26)-C(7)	10.6(9)
C(17)-C(16)-C(26)-C(19)	4.0(8)
C(9)-C(16)-C(26)-C(19)	-176.3(4)
C(18)-C(19)-C(26)-C(7)	164.8(9)
C(20)-C(19)-C(26)-C(7)	-21.4(17)
C(18)-C(19)-C(26)-C(16)	-4.9(8)
C(20)-C(19)-C(26)-C(16)	168.9(12)

Crystal data and structure refinement for dilithium 1,3,4,6-tetraphenylpentalenide

Identification code	s18uh6	
Empirical formula	C48 H54 Li2 O4	
Formula weight	708.79	
Temperature	150.00(10) K	
Wavelength	1.54184 Å	
Crystal system	Monoclinic	
Space group	$P2_1/n$	
Unit cell dimensions	a = 14.2476(2) Å	□= 90°.
	b = 8.82290(10) Å	□= 93.4200(10)°.
	c = 16.0040(3) Å	□ = 90°.
Volume	2008.20(5) $Å^3$	
Z	2	
Density (calculated)	1.172 Mg/m^3	
Absorption coefficient	0.556 mm^{-1}	
F(000)	760	
Crystal size	0.514 x 0.411 x 0.152 mm^3	
Theta range for data collection	4.284 to 73.162°.	
Index ranges	-17<=h<=17, -8<=k<=10, -19<=l<=19	
Reflections collected	22952	
Independent reflections	4008 [R(int) = 0.0396]	
Completeness to theta = 67.684°	100.0 %	
Absorption correction	Semi-empirical from equivalents	
Max. and min. transmission	1.00000 and 0.38597	
Refinement method	Full-matrix least-squares on F^2	
Data / restraints / parameters	4008 / 0 / 262	
Goodness-of-fit on F^2	1.039	
Final R indices [I>2sigma(I)]	R1 = 0.0506, wR2 = 0.1340	
R indices (all data)	R1 = 0.0544, wR2 = 0.1380	
Extinction coefficient	n/a	
Largest diff. peak and hole	0.388 and -0.360 $e.Å^{-3}$	

Table 2. Atomic coordinates (x 10^4) and equivalent isotropic displacement parameters ($Å^2$x 10^3) for s18uh6. U(eq) is defined as one third of the trace of the orthogonalized U^{ij} tensor.

	x	y	z	U(eq)
Li	4161(2)	2880(3)	4842(1)	29(1)
O(1)	3023(1)	1773(1)	4439(1)	35(1)
O(2)	4484(1)	1703(1)	5863(1)	33(1)
C(1)	3854(1)	5336(1)	4486(1)	23(1)
C(2)	2853(1)	5696(1)	4506(1)	24(1)
C(3)	2358(1)	5492(2)	5227(1)	29(1)
C(4)	1400(1)	5766(2)	5233(1)	39(1)
C(5)	901(1)	6248(2)	4511(1)	42(1)
C(6)	1369(1)	6454(2)	3788(1)	38(1)
C(7)	2331(1)	6194(2)	3781(1)	31(1)
C(8)	4256(1)	4657(1)	3794(1)	24(1)
C(9)	5191(1)	4174(1)	3990(1)	23(1)
C(10)	5758(1)	3343(2)	3410(1)	25(1)
C(11)	5609(1)	3550(2)	2540(1)	33(1)
C(12)	6128(1)	2748(2)	1980(1)	44(1)
C(13)	6818(1)	1744(2)	2266(1)	47(1)
C(14)	6986(1)	1534(2)	3118(1)	40(1)
C(15)	6455(1)	2308(2)	3682(1)	30(1)
C(16)	5414(1)	4643(1)	4846(1)	22(1)
C(17)	2512(1)	1941(2)	3644(1)	50(1)
C(18)	1784(2)	725(3)	3623(2)	67(1)
C(19)	1546(2)	633(4)	4524(2)	91(1)
C(20)	2428(1)	1055(3)	5002(1)	60(1)
C(21)	4144(1)	2173(2)	6655(1)	41(1)
C(22)	4910(6)	1979(7)	7285(5)	56(2)
C(23)	5435(3)	638(5)	6932(3)	50(1)
C(22A)	4840(5)	1395(7)	7341(4)	44(1)
C(23A)	5723(3)	1259(6)	6885(3)	48(1)
C(24)	5358(1)	911(2)	6013(1)	43(1)

Table 3. Bond lengths [Å] for s18uh6.

Li-O(2)	1.968(2)
Li-O(1)	1.968(3)
Li-C(1)	2.276(3)
Li-C(8)	2.306(3)
Li-C(16)#1	2.314(3)
Li-C(9)	2.357(3)
Li-C(16)	2.367(3)
O(1)-C(20)	1.422(2)
O(1)-C(17)	1.4359(18)
O(2)-C(24)	1.4353(18)
O(2)-C(21)	1.4437(19)
C(1)-C(8)	1.4109(18)
C(1)-C(16)#1	1.4483(17)
C(1)-C(2)	1.4639(16)
C(2)-C(3)	1.4001(19)
C(2)-C(7)	1.4098(18)
C(3)-C(4)	1.3876(19)
C(3)-H(3)	0.9500
C(4)-C(5)	1.387(2)
C(4)-H(4)	0.9500
C(5)-C(6)	1.380(2)
C(5)-H(5)	0.9500
C(6)-C(7)	1.3903(19)
C(6)-H(6)	0.9500
C(7)-H(7)	0.9500
C(8)-C(9)	1.4161(17)
C(8)-H(8)	1.0000
C(9)-C(16)	1.4475(17)
C(9)-C(10)	1.4638(17)
C(10)-C(15)	1.400(2)
C(10)-C(11)	1.4077(19)
C(11)-C(12)	1.388(2)
C(11)-H(11)	0.9500
C(12)-C(13)	1.381(3)
C(12)-H(12)	0.9500
C(13)-C(14)	1.384(3)

C(13)-H(13)	0.9500
C(14)-C(15)	1.391(2)
C(14)-H(14)	0.9500
C(15)-H(15)	0.9500
C(16)-C(16)#1	1.449(2)
C(17)-C(18)	1.491(3)
C(17)-H(17A)	0.9900
C(17)-H(17B)	0.9900
C(18)-C(19)	1.504(4)
C(18)-H(18A)	0.9900
C(18)-H(18B)	0.9900
C(19)-C(20)	1.480(3)
C(19)-H(19A)	0.9900
C(19)-H(19B)	0.9900
C(20)-H(20A)	0.9900
C(20)-H(20B)	0.9900
C(21)-C(22)	1.451(8)
C(21)-C(22A)	1.591(7)
C(21)-H(21A)	0.9900
C(21)-H(21B)	0.9900
C(21)-H(21C)	0.9900
C(21)-H(21D)	0.9900
C(22)-C(23)	1.526(10)
C(22)-H(22A)	0.9900
C(22)-H(22B)	0.9900
C(23)-C(24)	1.488(5)
C(23)-H(23A)	0.9900
C(23)-H(23B)	0.9900
C(22A)-C(23A)	1.496(9)
C(22A)-H(22C)	0.9900
C(22A)-H(22D)	0.9900
C(23A)-C(24)	1.492(5)
C(23A)-H(23C)	0.9900
C(23A)-H(23D)	0.9900
C(24)-H(24A)	0.9900
C(24)-H(24B)	0.9900
C(24)-H(24C)	0.9900
C(24)-H(24D)	0.9900

Table 4. Bond angles [°] for s18uh6.

O(2)-Li-O(1)	99.07(11)
O(2)-Li-C(1)	137.89(13)
O(1)-Li-C(1)	104.38(10)
O(2)-Li-C(8)	160.40(13)
O(1)-Li-C(8)	100.49(10)
C(1)-Li-C(8)	35.86(6)
O(2)-Li-C(16)#1	105.87(11)
O(1)-Li-C(16)#1	137.66(12)
C(1)-Li-C(16)#1	36.77(6)
C(8)-Li-C(16)#1	59.28(7)
O(2)-Li-C(9)	127.82(11)
O(1)-Li-C(9)	125.48(12)
C(1)-Li-C(9)	60.73(7)
C(8)-Li-C(9)	35.34(5)
C(16)#1-Li-C(9)	60.23(7)
O(2)-Li-C(16)	101.86(10)
O(1)-Li-C(16)	158.94(13)
C(1)-Li-C(16)	60.55(7)
C(8)-Li-C(16)	58.54(7)
C(16)#1-Li-C(16)	36.03(6)
C(9)-Li-C(16)	35.68(5)
C(20)-O(1)-C(17)	108.56(13)
C(20)-O(1)-Li	121.59(12)
C(17)-O(1)-Li	127.10(12)
C(24)-O(2)-C(21)	109.04(12)
C(24)-O(2)-Li	123.60(12)
C(21)-O(2)-Li	120.22(11)
C(8)-C(1)-C(16)#1	106.11(10)
C(8)-C(1)-C(2)	123.39(11)
C(16)#1-C(1)-C(2)	129.90(11)
C(8)-C(1)-Li	73.24(9)
C(16)#1-C(1)-Li	73.06(9)
C(2)-C(1)-Li	111.99(10)
C(3)-C(2)-C(7)	116.83(12)
C(3)-C(2)-C(1)	121.93(11)
C(7)-C(2)-C(1)	121.17(12)

C(4)-C(3)-C(2)	121.82(13)
C(4)-C(3)-H(3)	119.1
C(2)-C(3)-H(3)	119.1
C(5)-C(4)-C(3)	120.20(15)
C(5)-C(4)-H(4)	119.9
C(3)-C(4)-H(4)	119.9
C(6)-C(5)-C(4)	119.33(13)
C(6)-C(5)-H(5)	120.3
C(4)-C(5)-H(5)	120.3
C(5)-C(6)-C(7)	120.68(14)
C(5)-C(6)-H(6)	119.7
C(7)-C(6)-H(6)	119.7
C(6)-C(7)-C(2)	121.13(14)
C(6)-C(7)-H(7)	119.4
C(2)-C(7)-H(7)	119.4
C(1)-C(8)-C(9)	111.93(11)
C(1)-C(8)-Li	70.90(9)
C(9)-C(8)-Li	74.28(9)
C(1)-C(8)-H(8)	124.0
C(9)-C(8)-H(8)	124.0
Li-C(8)-H(8)	124.0
C(8)-C(9)-C(16)	105.91(11)
C(8)-C(9)-C(10)	123.84(11)
C(16)-C(9)-C(10)	130.23(11)
C(8)-C(9)-Li	70.38(9)
C(16)-C(9)-Li	72.56(9)
C(10)-C(9)-Li	120.68(10)
C(15)-C(10)-C(11)	117.07(12)
C(15)-C(10)-C(9)	122.47(12)
C(11)-C(10)-C(9)	120.45(12)
C(12)-C(11)-C(10)	121.15(15)
C(12)-C(11)-H(11)	119.4
C(10)-C(11)-H(11)	119.4
C(13)-C(12)-C(11)	120.65(15)
C(13)-C(12)-H(12)	119.7
C(11)-C(12)-H(12)	119.7
C(12)-C(13)-C(14)	119.31(14)
C(12)-C(13)-H(13)	120.3

C(14)-C(13)-H(13)	120.3
C(13)-C(14)-C(15)	120.37(16)
C(13)-C(14)-H(14)	119.8
C(15)-C(14)-H(14)	119.8
C(14)-C(15)-C(10)	121.42(14)
C(14)-C(15)-H(15)	119.3
C(10)-C(15)-H(15)	119.3
C(9)-C(16)-C(1)#1	144.03(11)
C(9)-C(16)-C(16)#1	108.05(13)
C(1)#1-C(16)-C(16)#1	107.91(13)
C(9)-C(16)-Li#1	120.95(10)
C(1)#1-C(16)-Li#1	70.17(9)
C(16)#1-C(16)-Li#1	73.99(11)
C(9)-C(16)-Li	71.75(9)
C(1)#1-C(16)-Li	121.32(10)
C(16)#1-C(16)-Li	69.99(11)
Li#1-C(16)-Li	143.98(6)
O(1)-C(17)-C(18)	105.10(15)
O(1)-C(17)-H(17A)	110.7
C(18)-C(17)-H(17A)	110.7
O(1)-C(17)-H(17B)	110.7
C(18)-C(17)-H(17B)	110.7
H(17A)-C(17)-H(17B)	108.8
C(17)-C(18)-C(19)	102.37(17)
C(17)-C(18)-H(18A)	111.3
C(19)-C(18)-H(18A)	111.3
C(17)-C(18)-H(18B)	111.3
C(19)-C(18)-H(18B)	111.3
H(18A)-C(18)-H(18B)	109.2
C(20)-C(19)-C(18)	104.39(18)
C(20)-C(19)-H(19A)	110.9
C(18)-C(19)-H(19A)	110.9
C(20)-C(19)-H(19B)	110.9
C(18)-C(19)-H(19B)	110.9
H(19A)-C(19)-H(19B)	108.9
O(1)-C(20)-C(19)	107.72(17)
O(1)-C(20)-H(20A)	110.2
C(19)-C(20)-H(20A)	110.2

O(1)-C(20)-H(20B)	110.2
C(19)-C(20)-H(20B)	110.2
H(20A)-C(20)-H(20B)	108.5
O(2)-C(21)-C(22)	107.4(4)
O(2)-C(21)-C(22A)	104.7(3)
O(2)-C(21)-H(21A)	110.2
C(22)-C(21)-H(21A)	110.2
O(2)-C(21)-H(21B)	110.2
C(22)-C(21)-H(21B)	110.2
H(21A)-C(21)-H(21B)	108.5
O(2)-C(21)-H(21C)	110.8
C(22A)-C(21)-H(21C)	110.8
O(2)-C(21)-H(21D)	110.8
C(22A)-C(21)-H(21D)	110.8
H(21C)-C(21)-H(21D)	108.9
C(21)-C(22)-C(23)	101.4(5)
C(21)-C(22)-H(22A)	111.5
C(23)-C(22)-H(22A)	111.5
C(21)-C(22)-H(22B)	111.5
C(23)-C(22)-H(22B)	111.5
H(22A)-C(22)-H(22B)	109.3
C(24)-C(23)-C(22)	103.4(4)
C(24)-C(23)-H(23A)	111.1
C(22)-C(23)-H(23A)	111.1
C(24)-C(23)-H(23B)	111.1
C(22)-C(23)-H(23B)	111.1
H(23A)-C(23)-H(23B)	109.0
C(23A)-C(22A)-C(21)	101.8(4)
C(23A)-C(22A)-H(22C)	111.4
C(21)-C(22A)-H(22C)	111.4
C(23A)-C(22A)-H(22D)	111.4
C(21)-C(22A)-H(22D)	111.4
H(22C)-C(22A)-H(22D)	109.3
C(24)-C(23A)-C(22A)	102.5(4)
C(24)-C(23A)-H(23C)	111.3
C(22A)-C(23A)-H(23C)	111.3
C(24)-C(23A)-H(23D)	111.3
C(22A)-C(23A)-H(23D)	111.3

H(23C)-C(23A)-H(23D)	109.2
O(2)-C(24)-C(23)	104.8(2)
O(2)-C(24)-C(23A)	107.8(2)
O(2)-C(24)-H(24A)	110.8
C(23)-C(24)-H(24A)	110.8
O(2)-C(24)-H(24B)	110.8
C(23)-C(24)-H(24B)	110.8
H(24A)-C(24)-H(24B)	108.9
O(2)-C(24)-H(24C)	110.1
C(23A)-C(24)-H(24C)	110.1
O(2)-C(24)-H(24D)	110.1
C(23A)-C(24)-H(24D)	110.1
H(24C)-C(24)-H(24D)	108.5

Symmetry transformations used to generate equivalent atoms:

#1 -x+1,-y+1,-z+1

Table 5. Anisotropic displacement parameters ($Å^2 x\ 10^3$) for s18uh6. The anisotropic displacement factor exponent takes the form: $-2\pi^2[h^2 a^{*2} U^{11} + ... + 2 h k a^* b^* U^{12}]$

	U^{11}	U^{22}	U^{33}	U^{23}	U^{13}	U^{12}
Li	24(1)	33(1)	29(1)	3(1)	-3(1)	1(1)
O(1)	28(1)	42(1)	34(1)	4(1)	-7(1)	-3(1)
O(2)	27(1)	40(1)	33(1)	4(1)	-4(1)	5(1)
C(1)	16(1)	28(1)	24(1)	2(1)	-3(1)	0(1)
C(2)	16(1)	24(1)	29(1)	0(1)	-4(1)	0(1)
C(3)	19(1)	34(1)	35(1)	3(1)	-1(1)	-1(1)
C(4)	21(1)	46(1)	50(1)	1(1)	7(1)	-2(1)
C(5)	16(1)	47(1)	64(1)	-2(1)	-4(1)	3(1)
C(6)	25(1)	39(1)	49(1)	-1(1)	-15(1)	8(1)
C(7)	23(1)	34(1)	32(1)	1(1)	-6(1)	5(1)
C(8)	19(1)	30(1)	22(1)	2(1)	-3(1)	-1(1)
C(9)	17(1)	29(1)	23(1)	1(1)	-1(1)	-1(1)
C(10)	17(1)	30(1)	27(1)	-4(1)	2(1)	-6(1)
C(11)	24(1)	48(1)	27(1)	-5(1)	2(1)	-9(1)
C(12)	34(1)	70(1)	29(1)	-15(1)	9(1)	-17(1)
C(13)	33(1)	58(1)	50(1)	-28(1)	20(1)	-14(1)
C(14)	26(1)	37(1)	56(1)	-14(1)	12(1)	-3(1)

C(15)	23(1)	32(1)	35(1)	-5(1)	5(1)	-2(1)
C(16)	15(1)	27(1)	23(1)	2(1)	0(1)	1(1)
C(17)	54(1)	46(1)	46(1)	4(1)	-25(1)	-9(1)
C(18)	63(1)	65(1)	69(1)	-2(1)	-23(1)	-23(1)
C(19)	62(2)	130(3)	81(2)	-27(2)	10(1)	-54(2)
C(20)	38(1)	89(2)	52(1)	12(1)	4(1)	-16(1)
C(21)	43(1)	39(1)	41(1)	1(1)	9(1)	-2(1)
C(22)	84(4)	53(4)	32(2)	6(3)	-5(2)	-11(3)
C(23)	43(2)	48(2)	55(2)	19(2)	-25(2)	-12(2)
C(22A)	45(2)	56(4)	32(2)	10(3)	-7(2)	-14(3)
C(23A)	29(2)	61(3)	52(2)	20(2)	-13(2)	-9(2)
C(24)	34(1)	47(1)	48(1)	5(1)	-5(1)	13(1)

Table 6. Hydrogen coordinates (x 10^4) and isotropic displacement parameters ($Å^2$x 10^3) for s18uh6.

	x	y	z	U(eq)
H(3)	2688	5156	5727	35
H(4)	1084	5624	5733	47
H(5)	245	6435	4513	51
H(6)	1030	6775	3291	46
H(7)	2642	6356	3280	37
H(8)	3928	4562	3226	29
H(11)	5146	4252	2332	40
H(12)	6006	2892	1395	53
H(13)	7174	1203	1880	56
H(14)	7467	858	3320	48
H(15)	6568	2130	4265	36
H(17A)	2935	1811	3180	60
H(17B)	2215	2953	3595	60
H(18A)	2040	-248	3428	80
H(18B)	1228	1008	3256	80
H(19A)	1033	1347	4640	109
H(19B)	1349	-406	4668	109
H(20A)	2292	1755	5463	72
H(20B)	2738	140	5247	72
H(21A)	3599	1546	6794	49

H(21B)	3945	3247	6627	49
H(21C)	3491	1823	6710	49
H(21D)	4164	3290	6710	49
H(22A)	4674	1739	7839	68
H(22B)	5313	2893	7333	68
H(23A)	6101	625	7148	60
H(23B)	5136	-334	7074	60
H(22C)	4936	2040	7845	53
H(22D)	4606	389	7506	53
H(23C)	6084	2218	6908	57
H(23D)	6127	429	7118	57
H(24A)	5891	1533	5839	52
H(24B)	5351	-59	5702	52
H(24C)	5815	1244	5608	52
H(24D)	5259	-194	5945	52

Table 7. Torsion angles [°] for s18uh6.

C(8)-C(1)-C(2)-C(3)	140.94(13)
C(16)#1-C(1)-C(2)-C(3)	-28.8(2)
Li-C(1)-C(2)-C(3)	57.04(16)
C(8)-C(1)-C(2)-C(7)	-35.76(19)
C(16)#1-C(1)-C(2)-C(7)	154.47(13)
Li-C(1)-C(2)-C(7)	-119.66(13)
C(7)-C(2)-C(3)-C(4)	-0.1(2)
C(1)-C(2)-C(3)-C(4)	-176.90(13)
C(2)-C(3)-C(4)-C(5)	0.4(2)
C(3)-C(4)-C(5)-C(6)	-0.1(3)
C(4)-C(5)-C(6)-C(7)	-0.5(2)
C(5)-C(6)-C(7)-C(2)	0.9(2)
C(3)-C(2)-C(7)-C(6)	-0.6(2)
C(1)-C(2)-C(7)-C(6)	176.29(13)
C(16)#1-C(1)-C(8)-C(9)	2.84(15)
C(2)-C(1)-C(8)-C(9)	-169.01(12)
Li-C(1)-C(8)-C(9)	-63.35(11)
C(16)#1-C(1)-C(8)-Li	66.19(10)
C(2)-C(1)-C(8)-Li	-105.66(13)
C(1)-C(8)-C(9)-C(16)	-3.05(15)

Li-C(8)-C(9)-C(16)	-64.38(10)
C(1)-C(8)-C(9)-C(10)	175.74(12)
Li-C(8)-C(9)-C(10)	114.41(14)
C(1)-C(8)-C(9)-Li	61.33(11)
C(8)-C(9)-C(10)-C(15)	-150.08(13)
C(16)-C(9)-C(10)-C(15)	28.4(2)
Li-C(9)-C(10)-C(15)	-64.23(16)
C(8)-C(9)-C(10)-C(11)	29.26(19)
C(16)-C(9)-C(10)-C(11)	-152.26(13)
Li-C(9)-C(10)-C(11)	115.12(13)
C(15)-C(10)-C(11)-C(12)	0.7(2)
C(9)-C(10)-C(11)-C(12)	-178.70(13)
C(10)-C(11)-C(12)-C(13)	-1.3(2)
C(11)-C(12)-C(13)-C(14)	0.5(2)
C(12)-C(13)-C(14)-C(15)	1.0(2)
C(13)-C(14)-C(15)-C(10)	-1.7(2)
C(11)-C(10)-C(15)-C(14)	0.81(19)
C(9)-C(10)-C(15)-C(14)	-179.83(12)
C(8)-C(9)-C(16)-C(1)#1	-178.56(17)
C(10)-C(9)-C(16)-C(1)#1	2.8(3)
Li-C(9)-C(16)-C(1)#1	118.5(2)
C(8)-C(9)-C(16)-C(16)#1	2.01(17)
C(10)-C(9)-C(16)-C(16)#1	-176.68(13)
Li-C(9)-C(16)-C(16)#1	-60.90(13)
C(8)-C(9)-C(16)-Li#1	-79.78(13)
C(10)-C(9)-C(16)-Li#1	101.54(15)
Li-C(9)-C(16)-Li#1	-142.68(8)
C(8)-C(9)-C(16)-Li	62.90(10)
C(10)-C(9)-C(16)-Li	-115.78(15)
C(20)-O(1)-C(17)-C(18)	-25.1(2)
Li-O(1)-C(17)-C(18)	173.71(16)
O(1)-C(17)-C(18)-C(19)	34.2(3)
C(17)-C(18)-C(19)-C(20)	-30.6(3)
C(17)-O(1)-C(20)-C(19)	5.2(3)
Li-O(1)-C(20)-C(19)	167.7(2)
C(18)-C(19)-C(20)-O(1)	16.4(3)
C(24)-O(2)-C(21)-C(22)	12.9(3)
Li-O(2)-C(21)-C(22)	-138.6(3)

C(24)-O(2)-C(21)-C(22A)	-7.2(2)
Li-O(2)-C(21)-C(22A)	-158.7(2)
O(2)-C(21)-C(22)-C(23)	-30.7(4)
C(21)-C(22)-C(23)-C(24)	37.1(5)
O(2)-C(21)-C(22A)-C(23A)	27.6(4)
C(21)-C(22A)-C(23A)-C(24)	-36.3(5)
C(21)-O(2)-C(24)-C(23)	11.5(2)
Li-O(2)-C(24)-C(23)	161.8(2)
C(21)-O(2)-C(24)-C(23A)	-16.3(3)
Li-O(2)-C(24)-C(23A)	133.9(2)
C(22)-C(23)-C(24)-O(2)	-30.0(4)
C(22A)-C(23A)-C(24)-O(2)	34.0(4)

Symmetry transformations used to generate equivalent atoms:

#1 -x+1,-y+1,-z+1

Crystal data and structure refinement for Disodium 1,3,4,6-tetraphenylpentalenide

Identification code	s19uh6	
Empirical formula	C56 H70 Na2 O6	
Formula weight	885.10	
Temperature	150.01(10) K	
Wavelength	1.54184 Å	
Crystal system	Monoclinic	
Space group	$P2_1/n$	
Unit cell dimensions	a = 10.75710(10) Å	□= 90°.
	b = 12.92160(10) Å	□= 97.8400(10)°.
	c = 17.4019(2) Å	□ = 90°.
Volume	2396.24(4) $Å^3$	
Z	2	
Density (calculated)	1.227 Mg/m^3	
Absorption coefficient	0.767 mm^{-1}	
F(000)	952	
Crystal size	0.290 x 0.202 x 0.141 mm^3	
Theta range for data collection	4.276 to 73.115°.	
Index ranges	-13<=h<=13, -16<=k<=16, -21<=l<=21	
Reflections collected	46889	
Independent reflections	4790 [R(int) = 0.0333]	
Completeness to theta = 67.684°	100.0 %	
Absorption correction	Semi-empirical from equivalents	
Max. and min. transmission	1.00000 and 0.82349	
Refinement method	Full-matrix least-squares on F^2	
Data / restraints / parameters	4790 / 0 / 298	
Goodness-of-fit on F^2	1.019	
Final R indices [I>2sigma(I)]	R1 = 0.0381, wR2 = 0.0964	
R indices (all data)	R1 = 0.0406, wR2 = 0.0983	
Extinction coefficient	n/a	
Largest diff. peak and hole	0.316 and -0.326 $e.Å^{-3}$	

Table 2. Atomic coordinates (x 10^4) and equivalent isotropic displacement parameters ($Å^2$x 10^3) for s19uh6. U(eq) is defined as one third of the trace of the orthogonalized U^{ij} tensor.

	x	y	z	U(eq)
Na	3788(1)	3582(1)	4234(1)	28(1)
C(1)	4715(1)	5372(1)	4719(1)	21(1)
C(2)	5333(1)	5288(1)	4033(1)	22(1)
C(3)	6275(1)	4529(1)	4202(1)	23(1)
C(4)	6254(1)	4084(1)	4944(1)	22(1)
C(5)	4982(1)	5695(1)	3251(1)	22(1)
C(6)	3735(1)	5935(1)	2951(1)	24(1)
C(7)	3407(1)	6236(1)	2184(1)	29(1)
C(8)	4309(1)	6323(1)	1688(1)	31(1)
C(9)	5549(1)	6103(1)	1970(1)	31(1)
C(10)	5880(1)	5798(1)	2736(1)	27(1)
C(11)	6948(1)	3149(1)	5193(1)	22(1)
C(12)	8062(1)	2884(1)	4894(1)	27(1)
C(13)	8683(1)	1961(1)	5080(1)	32(1)
C(14)	8233(1)	1258(1)	5578(1)	34(1)
C(15)	7144(1)	1500(1)	5883(1)	31(1)
C(16)	6515(1)	2426(1)	5701(1)	25(1)
O(1)	3173(1)	2233(1)	4978(1)	39(1)
C(17)	3620(2)	1194(1)	4922(1)	41(1)
C(18)	3552(2)	675(1)	5690(1)	56(1)
C(19)	3225(3)	1649(2)	6239(2)	37(1)
C(19A)	2510(3)	1137(3)	5941(2)	49(1)
C(20)	2623(2)	2344(1)	5675(1)	47(1)
O(2)	4408(1)	2576(1)	3278(1)	34(1)
C(21)	5466(2)	1907(1)	3317(1)	43(1)
C(22)	6250(1)	2296(1)	2717(1)	48(1)
C(23)	5387(2)	2996(1)	2194(1)	49(1)
C(24)	4147(1)	2924(1)	2489(1)	42(1)
O(3)	1750(1)	4020(1)	3683(1)	36(1)
C(25)	1027(1)	4055(1)	2927(1)	33(1)
C(26)	-293(1)	4348(1)	3054(1)	36(1)
C(27)	-57(1)	5000(1)	3785(1)	42(1)
C(28)	1012(1)	4420(1)	4246(1)	39(1)

Table 3. Bond lengths [Å] for s19uh6.

Na-O(2)	2.2812(10)
Na-O(1)	2.3203(10)
Na-O(3)	2.3385(10)
Na-C(1)	2.6128(12)
Na-C(1)#1	2.6351(12)
Na-C(2)	2.8113(12)
Na-C(4)	2.8450(12)
Na-C(3)	2.9498(12)
C(1)-C(1)#1	1.445(2)
C(1)-C(4)#1	1.4466(16)
C(1)-C(2)	1.4483(15)
C(2)-C(3)	1.4115(16)
C(2)-C(5)	1.4595(15)
C(3)-C(4)	1.4153(15)
C(3)-H(3)	0.9500
C(4)-C(11)	1.4553(16)
C(5)-C(6)	1.4059(16)
C(5)-C(10)	1.4106(16)
C(6)-C(7)	1.3896(16)
C(6)-H(6)	0.9500
C(7)-C(8)	1.3880(18)
C(7)-H(7)	0.9500
C(8)-C(9)	1.3870(19)
C(8)-H(8)	0.9500
C(9)-C(10)	1.3880(17)
C(9)-H(9)	0.9500
C(10)-H(10)	0.9500
C(11)-C(16)	1.4076(16)
C(11)-C(12)	1.4129(16)
C(12)-C(13)	1.3849(18)
C(12)-H(12)	0.9500
C(13)-C(14)	1.387(2)
C(13)-H(13)	0.9500
C(14)-C(15)	1.3859(19)
C(14)-H(14)	0.9500
C(15)-C(16)	1.3897(17)

C(15)-H(15)	0.9500
C(16)-H(16)	0.9500
O(1)-C(20)	1.4283(17)
O(1)-C(17)	1.4342(17)
C(17)-C(18)	1.506(2)
C(17)-H(17A)	0.9900
C(17)-H(17B)	0.9900
C(18)-C(19A)	1.392(4)
C(18)-C(19)	1.648(4)
C(18)-H(18A)	0.9900
C(18)-H(18B)	0.9900
C(18)-H(18C)	0.9900
C(18)-H(18D)	0.9900
C(19)-C(20)	1.419(3)
C(19)-H(19A)	0.9900
C(19)-H(19B)	0.9900
C(19A)-C(20)	1.635(4)
C(19A)-H(19C)	0.9900
C(19A)-H(19D)	0.9900
C(20)-H(20A)	0.9900
C(20)-H(20B)	0.9900
C(20)-H(20C)	0.9900
C(20)-H(20D)	0.9900
O(2)-C(21)	1.4237(17)
O(2)-C(24)	1.4350(16)
C(21)-C(22)	1.514(2)
C(21)-H(21A)	0.9900
C(21)-H(21B)	0.9900
C(22)-C(23)	1.509(2)
C(22)-H(22A)	0.9900
C(22)-H(22B)	0.9900
C(23)-C(24)	1.496(2)
C(23)-H(23A)	0.9900
C(23)-H(23B)	0.9900
C(24)-H(24A)	0.9900
C(24)-H(24B)	0.9900
O(3)-C(25)	1.4363(15)
O(3)-C(28)	1.4378(16)

C(25)-C(26)	1.5155(19)
C(25)-H(25A)	0.9900
C(25)-H(25B)	0.9900
C(26)-C(27)	1.517(2)
C(26)-H(26A)	0.9900
C(26)-H(26B)	0.9900
C(27)-C(28)	1.509(2)
C(27)-H(27A)	0.9900
C(27)-H(27B)	0.9900
C(28)-H(28A)	0.9900
C(28)-H(28B)	0.9900

Table 4. Bond angles [°] for s19uh6.

O(2)-Na-O(1)	96.48(4)
O(2)-Na-O(3)	101.00(4)
O(1)-Na-O(3)	95.05(4)
O(2)-Na-C(1)	127.09(4)
O(1)-Na-C(1)	127.57(4)
O(3)-Na-C(1)	102.31(4)
O(2)-Na-C(1)#1	125.77(4)
O(1)-Na-C(1)#1	101.15(4)
O(3)-Na-C(1)#1	127.52(4)
C(1)-Na-C(1)#1	31.97(4)
O(2)-Na-C(2)	96.83(4)
O(1)-Na-C(2)	151.24(4)
O(3)-Na-C(2)	107.24(4)
C(1)-Na-C(2)	30.69(3)
C(1)#1-Na-C(2)	50.77(3)
O(2)-Na-C(4)	95.64(4)
O(1)-Na-C(4)	104.41(4)
O(3)-Na-C(4)	152.74(4)
C(1)-Na-C(4)	50.60(3)
C(1)#1-Na-C(4)	30.30(3)
C(2)-Na-C(4)	48.91(3)
O(2)-Na-C(3)	82.33(4)
O(1)-Na-C(3)	130.55(4)
O(3)-Na-C(3)	133.93(4)

C(1)-Na-C(3)	48.03(3)
C(1)#1-Na-C(3)	47.88(3)
C(2)-Na-C(3)	28.23(3)
C(4)-Na-C(3)	28.20(3)
C(1)#1-C(1)-C(4)#1	108.13(12)
C(1)#1-C(1)-C(2)	107.94(12)
C(4)#1-C(1)-C(2)	143.93(10)
C(1)#1-C(1)-Na	74.86(8)
C(4)#1-C(1)-Na	107.26(7)
C(2)-C(1)-Na	82.25(6)
C(1)#1-C(1)-Na#1	73.17(8)
C(4)#1-C(1)-Na#1	82.90(6)
C(2)-C(1)-Na#1	107.62(7)
Na-C(1)-Na#1	148.03(4)
C(3)-C(2)-C(1)	106.05(9)
C(3)-C(2)-C(5)	122.18(10)
C(1)-C(2)-C(5)	130.70(10)
C(3)-C(2)-Na	81.35(7)
C(1)-C(2)-Na	67.06(6)
C(5)-C(2)-Na	108.43(7)
C(2)-C(3)-C(4)	111.87(10)
C(2)-C(3)-Na	70.42(6)
C(4)-C(3)-Na	71.78(6)
C(2)-C(3)-H(3)	124.1
C(4)-C(3)-H(3)	124.1
Na-C(3)-H(3)	125.3
C(3)-C(4)-C(1)#1	105.91(10)
C(3)-C(4)-C(11)	122.56(10)
C(1)#1-C(4)-C(11)	130.64(10)
C(3)-C(4)-Na	80.02(6)
C(1)#1-C(4)-Na	66.80(6)
C(11)-C(4)-Na	110.51(7)
C(6)-C(5)-C(10)	116.37(10)
C(6)-C(5)-C(2)	122.58(10)
C(10)-C(5)-C(2)	120.91(10)
C(7)-C(6)-C(5)	121.53(11)
C(7)-C(6)-H(6)	119.2
C(5)-C(6)-H(6)	119.2

C(8)-C(7)-C(6)	120.83(11)
C(8)-C(7)-H(7)	119.6
C(6)-C(7)-H(7)	119.6
C(9)-C(8)-C(7)	118.89(11)
C(9)-C(8)-H(8)	120.6
C(7)-C(8)-H(8)	120.6
C(8)-C(9)-C(10)	120.43(11)
C(8)-C(9)-H(9)	119.8
C(10)-C(9)-H(9)	119.8
C(9)-C(10)-C(5)	121.93(11)
C(9)-C(10)-H(10)	119.0
C(5)-C(10)-H(10)	119.0
C(16)-C(11)-C(12)	116.18(11)
C(16)-C(11)-C(4)	122.56(10)
C(12)-C(11)-C(4)	121.13(10)
C(13)-C(12)-C(11)	121.88(12)
C(13)-C(12)-H(12)	119.1
C(11)-C(12)-H(12)	119.1
C(12)-C(13)-C(14)	120.81(12)
C(12)-C(13)-H(13)	119.6
C(14)-C(13)-H(13)	119.6
C(15)-C(14)-C(13)	118.51(12)
C(15)-C(14)-H(14)	120.7
C(13)-C(14)-H(14)	120.7
C(14)-C(15)-C(16)	121.13(12)
C(14)-C(15)-H(15)	119.4
C(16)-C(15)-H(15)	119.4
C(15)-C(16)-C(11)	121.49(11)
C(15)-C(16)-H(16)	119.3
C(11)-C(16)-H(16)	119.3
C(20)-O(1)-C(17)	109.40(11)
C(20)-O(1)-Na	125.56(9)
C(17)-O(1)-Na	122.85(9)
O(1)-C(17)-C(18)	107.46(13)
O(1)-C(17)-H(17A)	110.2
C(18)-C(17)-H(17A)	110.2
O(1)-C(17)-H(17B)	110.2
C(18)-C(17)-H(17B)	110.2

H(17A)-C(17)-H(17B)	108.5
C(19A)-C(18)-C(17)	103.02(18)
C(17)-C(18)-C(19)	102.39(15)
C(17)-C(18)-H(18A)	111.3
C(19)-C(18)-H(18A)	111.3
C(17)-C(18)-H(18B)	111.3
C(19)-C(18)-H(18B)	111.3
H(18A)-C(18)-H(18B)	109.2
C(19A)-C(18)-H(18C)	111.2
C(17)-C(18)-H(18C)	111.2
C(19A)-C(18)-H(18D)	111.2
C(17)-C(18)-H(18D)	111.2
H(18C)-C(18)-H(18D)	109.1
C(20)-C(19)-C(18)	101.26(18)
C(20)-C(19)-H(19A)	111.5
C(18)-C(19)-H(19A)	111.5
C(20)-C(19)-H(19B)	111.5
C(18)-C(19)-H(19B)	111.5
H(19A)-C(19)-H(19B)	109.3
C(18)-C(19A)-C(20)	103.1(2)
C(18)-C(19A)-H(19C)	111.1
C(20)-C(19A)-H(19C)	111.1
C(18)-C(19A)-H(19D)	111.1
C(20)-C(19A)-H(19D)	111.1
H(19C)-C(19A)-H(19D)	109.1
C(19)-C(20)-O(1)	108.79(16)
O(1)-C(20)-C(19A)	101.56(16)
C(19)-C(20)-H(20A)	109.9
O(1)-C(20)-H(20A)	109.9
C(19)-C(20)-H(20B)	109.9
O(1)-C(20)-H(20B)	109.9
H(20A)-C(20)-H(20B)	108.3
O(1)-C(20)-H(20C)	111.5
C(19A)-C(20)-H(20C)	111.5
O(1)-C(20)-H(20D)	111.5
C(19A)-C(20)-H(20D)	111.5
H(20C)-C(20)-H(20D)	109.3
C(21)-O(2)-C(24)	106.65(11)

C(21)-O(2)-Na	128.53(8)
C(24)-O(2)-Na	118.72(9)
O(2)-C(21)-C(22)	106.41(12)
O(2)-C(21)-H(21A)	110.4
C(22)-C(21)-H(21A)	110.4
O(2)-C(21)-H(21B)	110.4
C(22)-C(21)-H(21B)	110.4
H(21A)-C(21)-H(21B)	108.6
C(23)-C(22)-C(21)	105.06(12)
C(23)-C(22)-H(22A)	110.7
C(21)-C(22)-H(22A)	110.7
C(23)-C(22)-H(22B)	110.7
C(21)-C(22)-H(22B)	110.7
H(22A)-C(22)-H(22B)	108.8
C(24)-C(23)-C(22)	105.07(13)
C(24)-C(23)-H(23A)	110.7
C(22)-C(23)-H(23A)	110.7
C(24)-C(23)-H(23B)	110.7
C(22)-C(23)-H(23B)	110.7
H(23A)-C(23)-H(23B)	108.8
O(2)-C(24)-C(23)	106.25(12)
O(2)-C(24)-H(24A)	110.5
C(23)-C(24)-H(24A)	110.5
O(2)-C(24)-H(24B)	110.5
C(23)-C(24)-H(24B)	110.5
H(24A)-C(24)-H(24B)	108.7
C(25)-O(3)-C(28)	109.45(10)
C(25)-O(3)-Na	137.99(8)
C(28)-O(3)-Na	112.47(8)
O(3)-C(25)-C(26)	105.91(10)
O(3)-C(25)-H(25A)	110.6
C(26)-C(25)-H(25A)	110.6
O(3)-C(25)-H(25B)	110.6
C(26)-C(25)-H(25B)	110.6
H(25A)-C(25)-H(25B)	108.7
C(25)-C(26)-C(27)	102.05(11)
C(25)-C(26)-H(26A)	111.4
C(27)-C(26)-H(26A)	111.4

C(25)-C(26)-H(26B)	111.4
C(27)-C(26)-H(26B)	111.4
H(26A)-C(26)-H(26B)	109.2
C(28)-C(27)-C(26)	101.46(11)
C(28)-C(27)-H(27A)	111.5
C(26)-C(27)-H(27A)	111.5
C(28)-C(27)-H(27B)	111.5
C(26)-C(27)-H(27B)	111.5
H(27A)-C(27)-H(27B)	109.3
O(3)-C(28)-C(27)	105.53(11)
O(3)-C(28)-H(28A)	110.6
C(27)-C(28)-H(28A)	110.6
O(3)-C(28)-H(28B)	110.6
C(27)-C(28)-H(28B)	110.6
H(28A)-C(28)-H(28B)	108.8

Symmetry transformations used to generate equivalent atoms:

#1 -x+1,-y+1,-z+1

Table 5. Anisotropic displacement parameters ($Å^2 x\ 10^3$) for s19uh6. The anisotropic displacement factor exponent takes the form: $-2\pi^2[h^2 a^{*2} U^{11} + ... + 2 h k a^* b^* U^{12}]$

	U^{11}	U^{22}	U^{33}	U^{23}	U^{13}	U^{12}
Na	27(1)	26(1)	30(1)	-1(1)	0(1)	-4(1)
C(1)	20(1)	21(1)	20(1)	0(1)	0(1)	-4(1)
C(2)	21(1)	23(1)	20(1)	1(1)	2(1)	-4(1)
C(3)	21(1)	26(1)	21(1)	0(1)	3(1)	-2(1)
C(4)	19(1)	24(1)	21(1)	0(1)	1(1)	-3(1)
C(5)	26(1)	19(1)	20(1)	-1(1)	2(1)	-4(1)
C(6)	26(1)	24(1)	22(1)	0(1)	3(1)	-1(1)
C(7)	30(1)	30(1)	25(1)	1(1)	-2(1)	2(1)
C(8)	41(1)	32(1)	19(1)	3(1)	1(1)	-1(1)
C(9)	35(1)	34(1)	24(1)	2(1)	9(1)	-5(1)
C(10)	25(1)	31(1)	25(1)	2(1)	3(1)	-3(1)
C(11)	21(1)	24(1)	20(1)	-3(1)	-1(1)	-2(1)
C(12)	24(1)	32(1)	26(1)	1(1)	2(1)	0(1)
C(13)	27(1)	36(1)	33(1)	-6(1)	2(1)	6(1)
C(14)	37(1)	26(1)	35(1)	-2(1)	-2(1)	7(1)

C(15)	39(1)	24(1)	29(1)	1(1)	2(1)	-3(1)
C(16)	26(1)	25(1)	23(1)	-2(1)	2(1)	-2(1)
O(1)	53(1)	32(1)	34(1)	2(1)	10(1)	-3(1)
C(17)	57(1)	31(1)	35(1)	-1(1)	0(1)	-3(1)
C(18)	74(1)	45(1)	48(1)	13(1)	0(1)	-4(1)
C(19)	33(1)	50(2)	28(1)	6(1)	5(1)	-1(1)
C(19A)	46(2)	53(2)	46(2)	18(2)	8(1)	-2(2)
C(20)	44(1)	58(1)	40(1)	-1(1)	13(1)	-1(1)
O(2)	30(1)	43(1)	31(1)	-2(1)	2(1)	1(1)
C(21)	47(1)	38(1)	41(1)	-4(1)	-4(1)	10(1)
C(22)	32(1)	57(1)	56(1)	-15(1)	6(1)	8(1)
C(23)	46(1)	51(1)	53(1)	6(1)	19(1)	4(1)
C(24)	31(1)	59(1)	34(1)	6(1)	3(1)	3(1)
O(3)	29(1)	48(1)	32(1)	-3(1)	1(1)	1(1)
C(25)	36(1)	34(1)	29(1)	-2(1)	3(1)	-1(1)
C(26)	34(1)	40(1)	34(1)	4(1)	0(1)	0(1)
C(27)	43(1)	39(1)	45(1)	-4(1)	14(1)	2(1)

Table 6. Hydrogen coordinates (x 10^4) and isotropic displacement parameters ($Å^2$x 10^3) for s19uh6.

	x	y	z	U(eq)
H(3)	6854	4340	3860	27
H(6)	3102	5891	3281	29
H(7)	2555	6385	1996	35
H(8)	4081	6529	1163	37
H(9)	6177	6162	1638	37
H(10)	6735	5655	2918	32
H(12)	8395	3354	4554	33
H(13)	9427	1806	4865	39
H(14)	8660	626	5707	40
H(15)	6822	1025	6223	37
H(16)	5777	2575	5924	30
H(17A)	4496	1198	4806	50
H(17B)	3092	818	4501	50
H(18A)	4363	349	5896	68
H(18B)	2883	144	5647	68

H(18C)	3432	-82	5626	68
H(18D)	4322	806	6059	68
H(19A)	2657	1435	6613	45
H(19B)	3996	1956	6526	45
H(19C)	2544	1080	6511	58
H(19D)	1721	820	5687	58
H(20A)	2726	3064	5867	56
H(20B)	1715	2187	5573	56
H(20C)	1789	2679	5576	56
H(20D)	3171	2747	6070	56
H(21A)	5194	1186	3200	51
H(21B)	5957	1928	3841	51
H(22A)	6990	2684	2968	58
H(22B)	6543	1713	2420	58
H(23A)	5701	3717	2225	59
H(23B)	5316	2759	1649	59
H(24A)	3729	3608	2464	50
H(24B)	3592	2426	2175	50
H(25A)	1031	3372	2670	40
H(25B)	1375	4576	2598	40
H(26A)	-801	3728	3134	44
H(26B)	-721	4754	2613	44
H(27A)	189	5715	3669	50
H(27B)	-804	5021	4060	50
H(28A)	1519	4890	4613	47
H(28B)	690	3849	4543	47

Table 7. Torsion angles [°] for s19uh6.

C(1)#1-C(1)-C(2)-C(3)	-1.76(14)
C(4)#1-C(1)-C(2)-C(3)	178.20(15)
Na-C(1)-C(2)-C(3)	-73.03(8)
Na#1-C(1)-C(2)-C(3)	75.73(9)
C(1)#1-C(1)-C(2)-C(5)	166.36(12)
C(4)#1-C(1)-C(2)-C(5)	-13.7(2)
Na-C(1)-C(2)-C(5)	95.09(12)
Na#1-C(1)-C(2)-C(5)	-116.15(11)
C(1)#1-C(1)-C(2)-Na	71.27(10)

C(4)#1-C(1)-C(2)-Na	-108.77(17)
Na#1-C(1)-C(2)-Na	148.76(6)
C(1)-C(2)-C(3)-C(4)	3.02(13)
C(5)-C(2)-C(3)-C(4)	-166.36(10)
Na-C(2)-C(3)-C(4)	-59.98(9)
C(1)-C(2)-C(3)-Na	63.00(7)
C(5)-C(2)-C(3)-Na	-106.38(10)
C(2)-C(3)-C(4)-C(1)#1	-3.03(13)
Na-C(3)-C(4)-C(1)#1	-62.21(7)
C(2)-C(3)-C(4)-C(11)	167.22(10)
Na-C(3)-C(4)-C(11)	108.04(10)
C(2)-C(3)-C(4)-Na	59.18(8)
C(3)-C(2)-C(5)-C(6)	142.46(12)
C(1)-C(2)-C(5)-C(6)	-24.03(18)
Na-C(2)-C(5)-C(6)	51.18(12)
C(3)-C(2)-C(5)-C(10)	-33.03(16)
C(1)-C(2)-C(5)-C(10)	160.49(12)
Na-C(2)-C(5)-C(10)	-124.30(10)
C(10)-C(5)-C(6)-C(7)	1.37(17)
C(2)-C(5)-C(6)-C(7)	-174.31(11)
C(5)-C(6)-C(7)-C(8)	-0.87(19)
C(6)-C(7)-C(8)-C(9)	0.01(19)
C(7)-C(8)-C(9)-C(10)	0.27(19)
C(8)-C(9)-C(10)-C(5)	0.3(2)
C(6)-C(5)-C(10)-C(9)	-1.10(17)
C(2)-C(5)-C(10)-C(9)	174.66(11)
C(3)-C(4)-C(11)-C(16)	-147.59(11)
C(1)#1-C(4)-C(11)-C(16)	20.02(18)
Na-C(4)-C(11)-C(16)	-56.48(12)
C(3)-C(4)-C(11)-C(12)	28.09(16)
C(1)#1-C(4)-C(11)-C(12)	-164.30(11)
Na-C(4)-C(11)-C(12)	119.19(10)
C(16)-C(11)-C(12)-C(13)	0.82(17)
C(4)-C(11)-C(12)-C(13)	-175.11(11)
C(11)-C(12)-C(13)-C(14)	-0.42(19)
C(12)-C(13)-C(14)-C(15)	0.15(19)
C(13)-C(14)-C(15)-C(16)	-0.32(19)
C(14)-C(15)-C(16)-C(11)	0.78(18)

C(12)-C(11)-C(16)-C(15)	-0.99(16)
C(4)-C(11)-C(16)-C(15)	174.88(11)
C(20)-O(1)-C(17)-C(18)	-10.28(17)
Na-O(1)-C(17)-C(18)	153.75(11)
O(1)-C(17)-C(18)-C(19A)	32.7(2)
O(1)-C(17)-C(18)-C(19)	-9.39(19)
C(17)-C(18)-C(19)-C(20)	25.5(2)
C(17)-C(18)-C(19A)-C(20)	-38.7(2)
C(18)-C(19)-C(20)-O(1)	-33.0(2)
C(17)-O(1)-C(20)-C(19)	29.4(2)
Na-O(1)-C(20)-C(19)	-134.07(16)
C(17)-O(1)-C(20)-C(19A)	-12.60(19)
Na-O(1)-C(20)-C(19A)	-176.09(14)
C(18)-C(19A)-C(20)-O(1)	33.1(2)
C(24)-O(2)-C(21)-C(22)	30.86(15)
Na-O(2)-C(21)-C(22)	-120.70(11)
O(2)-C(21)-C(22)-C(23)	-16.55(16)
C(21)-C(22)-C(23)-C(24)	-3.16(18)
C(21)-O(2)-C(24)-C(23)	-33.07(16)
Na-O(2)-C(24)-C(23)	121.79(11)
C(22)-C(23)-C(24)-O(2)	21.69(17)
C(28)-O(3)-C(25)-C(26)	-8.51(14)
Na-O(3)-C(25)-C(26)	175.43(9)
O(3)-C(25)-C(26)-C(27)	29.76(14)
C(25)-C(26)-C(27)-C(28)	-38.59(14)
C(25)-O(3)-C(28)-C(27)	-16.59(15)
Na-O(3)-C(28)-C(27)	160.56(9)
C(26)-C(27)-C(28)-O(3)	34.52(14)

Symmetry transformations used to generate equivalent atoms:

#1 -x+1,-y+1,-z+1

Crystal data and structure refinement for dipotassium 1,3,4,6-tetraphenylpentalenide

Identification code	s18uh2	
Empirical formula	C24 H27 K O2	
Formula weight	386.55	
Temperature	150.01(10) K	
Wavelength	1.54184 Å	
Crystal system	Triclinic	
Space group	P-1	
Unit cell dimensions	a = 9.3187(2) Å	= 91.443(2)°.
	b = 10.3999(3) Å	= 103.837(2)°.
	c = 12.2070(2) Å	= 114.291(2)°.
Volume	1036.74(4) $Å^3$	
Z	2	
Density (calculated)	1.238 Mg/m^3	
Absorption coefficient	2.350 mm^{-1}	
F(000)	412	
Crystal size	0.300 x 0.200 x 0.120 mm^3	
Theta range for data collection	3.766 to 73.134°.	
Index ranges	-11<=h<=11, -12<=k<=12, -15<=l<=15	
Reflections collected	19692	
Independent reflections	4136 [R(int) = 0.0270]	
Completeness to theta = 67.684°	100.0 %	
Absorption correction	Semi-empirical from equivalents	
Max. and min. transmission	1.00000 and 0.76236	
Refinement method	Full-matrix least-squares on F^2	
Data / restraints / parameters	4136 / 0 / 244	
Goodness-of-fit on F^2	1.043	
Final R indices [I>2sigma(I)]	R1 = 0.0340, wR2 = 0.0904	
R indices (all data)	R1 = 0.0346, wR2 = 0.0910	
Extinction coefficient	n/a	
Largest diff. peak and hole	0.487 and -0.300 $e.Å^{-3}$	

Table 2. Atomic coordinates (x 10^4) and equivalent isotropic displacement parameters (Å^{2}x 10^3) for s18uh2. U(eq) is defined as one third of the trace of the orthogonalized U^{ij} tensor.

	x	y	z	U(eq)
K	7725(1)	4737(1)	4649(1)	27(1)
O(1)	6970(1)	2843(1)	2839(1)	39(1)
C(1)	5391(2)	1661(2)	2633(2)	43(1)
C(2)	4653(2)	1432(2)	1374(2)	53(1)
C(3)	6144(2)	1818(2)	913(1)	43(1)
C(4)	7447(2)	3035(2)	1801(1)	41(1)
O(2)	9459(1)	3349(1)	5821(1)	30(1)
C(5)	8786(2)	1897(2)	5294(1)	34(1)
C(6)	7355(2)	1126(2)	5775(2)	44(1)
C(7)	7943(3)	1873(2)	6984(2)	55(1)
C(8)	9406(2)	3263(2)	6990(1)	39(1)
C(9)	4817(2)	5100(1)	4410(1)	19(1)
C(10)	3437(2)	3825(1)	3772(1)	20(1)
C(11)	2454(2)	3566(1)	2595(1)	20(1)
C(12)	1423(2)	2174(2)	2023(1)	26(1)
C(13)	458(2)	1931(2)	914(1)	31(1)
C(14)	485(2)	3062(2)	322(1)	34(1)
C(15)	1487(2)	4436(2)	861(1)	30(1)
C(16)	2451(2)	4689(2)	1977(1)	24(1)
C(17)	3019(2)	2867(1)	4574(1)	21(1)
C(18)	4027(2)	3498(1)	5692(1)	20(1)
C(19)	3591(2)	2917(1)	6704(1)	21(1)
C(20)	3856(2)	3795(1)	7697(1)	24(1)
C(21)	3331(2)	3222(2)	8623(1)	32(1)
C(22)	2518(2)	1761(2)	8589(1)	35(1)
C(23)	2246(2)	871(2)	7623(1)	34(1)
C(24)	2780(2)	1437(2)	6701(1)	28(1)

Table 3. Bond lengths [Å] for s18uh2.

K-O(1)	2.6742(11)
K-O(2)#1	2.7672(10)
K-O(2)	2.7677(10)
K-C(9)	2.8354(12)
K-C(18)#2	2.8954(12)
K-C(9)#2	2.9296(12)
K-C(17)#2	3.0341(12)
K-C(10)#2	3.0508(12)
K-C(19)#2	3.4468(12)
K-C(1)	3.5127(18)
K-C(5)	3.5313(15)
K-K#1	3.9168(5)
O(1)-C(4)	1.4335(19)
O(1)-C(1)	1.434(2)
C(1)-C(2)	1.494(2)
C(1)-H(1A)	0.9900
C(1)-H(1B)	0.9900
C(2)-C(3)	1.528(3)
C(2)-H(2A)	0.9900
C(2)-H(2B)	0.9900
C(3)-C(4)	1.513(2)
C(3)-H(3A)	0.9900
C(3)-H(3B)	0.9900
C(4)-H(4A)	0.9900
C(4)-H(4B)	0.9900
O(2)-C(5)	1.4377(17)
O(2)-C(8)	1.4426(18)
C(5)-C(6)	1.512(2)
C(5)-H(5A)	0.9900
C(5)-H(5B)	0.9900
C(6)-C(7)	1.512(2)
C(6)-H(6A)	0.9900
C(6)-H(6B)	0.9900
C(7)-C(8)	1.524(2)
C(7)-H(7A)	0.9900
C(7)-H(7B)	0.9900

C(8)-H(8A)	0.9900
C(8)-H(8B)	0.9900
C(9)-C(9)#2	1.440(2)
C(9)-C(18)#2	1.4429(17)
C(9)-C(10)	1.4436(18)
C(10)-C(17)	1.4198(17)
C(10)-C(11)	1.4580(17)
C(11)-C(16)	1.4070(18)
C(11)-C(12)	1.4100(18)
C(12)-C(13)	1.3854(19)
C(12)-H(12)	0.9500
C(13)-C(14)	1.391(2)
C(13)-H(13)	0.9500
C(14)-C(15)	1.381(2)
C(14)-H(14)	0.9500
C(15)-C(16)	1.3908(19)
C(15)-H(15)	0.9500
C(16)-H(16)	0.9500
C(17)-C(18)	1.4170(17)
C(17)-H(17)	1.0000
C(18)-C(19)	1.4612(17)
C(19)-C(20)	1.4068(18)
C(19)-C(24)	1.4076(19)
C(20)-C(21)	1.3897(19)
C(20)-H(20)	0.9500
C(21)-C(22)	1.385(2)
C(21)-H(21)	0.9500
C(22)-C(23)	1.386(2)
C(22)-H(22)	0.9500
C(23)-C(24)	1.386(2)
C(23)-H(23)	0.9500
C(24)-H(24)	0.9500

Table 4. Bond angles [°] for s18uh2.

O(1)-K-O(2)#1	93.30(3)
O(1)-K-O(2)	85.95(3)

O(2)#1-K-O(2)	89.91(3)
O(1)-K-C(9)	103.36(4)
O(2)#1-K-C(9)	125.45(3)
O(2)-K-C(9)	142.00(3)
O(1)-K-C(18)#2	114.34(4)
O(2)#1-K-C(18)#2	96.84(3)
O(2)-K-C(18)#2	158.05(3)
C(9)-K-C(18)#2	29.14(3)
O(1)-K-C(9)#2	121.26(4)
O(2)#1-K-C(9)#2	136.54(3)
O(2)-K-C(9)#2	115.91(3)
C(9)-K-C(9)#2	28.87(4)
C(18)#2-K-C(9)#2	47.20(3)
O(1)-K-C(17)#2	141.80(4)
O(2)#1-K-C(17)#2	91.57(3)
O(2)-K-C(17)#2	131.95(3)
C(9)-K-C(17)#2	45.74(4)
C(18)#2-K-C(17)#2	27.52(3)
C(9)#2-K-C(17)#2	45.03(3)
O(1)-K-C(10)#2	148.46(4)
O(2)#1-K-C(10)#2	111.79(3)
O(2)-K-C(10)#2	111.86(3)
C(9)-K-C(10)#2	46.66(3)
C(18)#2-K-C(10)#2	46.30(3)
C(9)#2-K-C(10)#2	27.84(3)
C(17)#2-K-C(10)#2	26.98(3)
O(1)-K-C(19)#2	99.07(3)
O(2)#1-K-C(19)#2	78.26(3)
O(2)-K-C(19)#2	167.34(3)
C(9)-K-C(19)#2	48.21(3)
C(18)#2-K-C(19)#2	24.73(3)
C(9)#2-K-C(19)#2	71.41(3)
C(17)#2-K-C(19)#2	45.23(3)
C(10)#2-K-C(19)#2	69.32(3)
O(1)-K-C(1)	21.89(4)
O(2)#1-K-C(1)	114.98(4)
O(2)-K-C(1)	89.17(4)
C(9)-K-C(1)	87.54(4)

C(18)#2-K-C(1)	106.58(4)
C(9)#2-K-C(1)	100.50(4)
C(17)#2-K-C(1)	132.24(4)
C(10)#2-K-C(1)	128.32(4)
C(19)#2-K-C(1)	99.84(4)
O(1)-K-C(5)	65.87(4)
O(2)#1-K-C(5)	100.60(3)
O(2)-K-C(5)	22.47(3)
C(9)-K-C(5)	133.71(4)
C(18)#2-K-C(5)	162.53(4)
C(9)#2-K-C(5)	116.57(4)
C(17)#2-K-C(5)	149.45(4)
C(10)#2-K-C(5)	124.04(4)
C(19)#2-K-C(5)	164.90(3)
C(1)-K-C(5)	66.76(4)
O(1)-K-K#1	89.47(3)
O(2)#1-K-K#1	44.96(2)
O(2)-K-K#1	44.95(2)
C(9)-K-K#1	165.16(3)
C(18)#2-K-K#1	137.69(3)
C(9)#2-K-K#1	145.25(3)
C(17)#2-K-K#1	119.45(3)
C(10)#2-K-K#1	121.69(3)
C(19)#2-K-K#1	123.07(2)
C(1)-K-K#1	106.75(3)
C(5)-K-K#1	58.46(3)
C(4)-O(1)-C(1)	109.65(12)
C(4)-O(1)-K	130.36(9)
C(1)-O(1)-K	114.08(9)
O(1)-C(1)-C(2)	105.37(14)
O(1)-C(1)-K	44.03(7)
C(2)-C(1)-K	132.96(13)
O(1)-C(1)-H(1A)	110.7
C(2)-C(1)-H(1A)	110.7
K-C(1)-H(1A)	68.5
O(1)-C(1)-H(1B)	110.7
C(2)-C(1)-H(1B)	110.7
K-C(1)-H(1B)	113.7

H(1A)-C(1)-H(1B)	108.8
C(1)-C(2)-C(3)	102.49(14)
C(1)-C(2)-H(2A)	111.3
C(3)-C(2)-H(2A)	111.3
C(1)-C(2)-H(2B)	111.3
C(3)-C(2)-H(2B)	111.3
H(2A)-C(2)-H(2B)	109.2
C(4)-C(3)-C(2)	101.74(13)
C(4)-C(3)-H(3A)	111.4
C(2)-C(3)-H(3A)	111.4
C(4)-C(3)-H(3B)	111.4
C(2)-C(3)-H(3B)	111.4
H(3A)-C(3)-H(3B)	109.3
O(1)-C(4)-C(3)	106.76(13)
O(1)-C(4)-H(4A)	110.4
C(3)-C(4)-H(4A)	110.4
O(1)-C(4)-H(4B)	110.4
C(3)-C(4)-H(4B)	110.4
H(4A)-C(4)-H(4B)	108.6
C(5)-O(2)-C(8)	105.28(11)
C(5)-O(2)-K#1	117.05(8)
C(8)-O(2)-K#1	119.47(8)
C(5)-O(2)-K	110.16(8)
C(8)-O(2)-K	114.29(9)
K#1-O(2)-K	90.09(3)
O(2)-C(5)-C(6)	104.00(12)
O(2)-C(5)-K	47.37(6)
C(6)-C(5)-K	94.20(10)
O(2)-C(5)-H(5A)	111.0
C(6)-C(5)-H(5A)	111.0
K-C(5)-H(5A)	151.5
O(2)-C(5)-H(5B)	111.0
C(6)-C(5)-H(5B)	111.0
K-C(5)-H(5B)	72.0
H(5A)-C(5)-H(5B)	109.0
C(5)-C(6)-C(7)	103.46(14)
C(5)-C(6)-H(6A)	111.1
C(7)-C(6)-H(6A)	111.1

C(5)-C(6)-H(6B)	111.1
C(7)-C(6)-H(6B)	111.1
H(6A)-C(6)-H(6B)	109.0
C(6)-C(7)-C(8)	104.64(14)
C(6)-C(7)-H(7A)	110.8
C(8)-C(7)-H(7A)	110.8
C(6)-C(7)-H(7B)	110.8
C(8)-C(7)-H(7B)	110.8
H(7A)-C(7)-H(7B)	108.9
O(2)-C(8)-C(7)	106.52(13)
O(2)-C(8)-H(8A)	110.4
C(7)-C(8)-H(8A)	110.4
O(2)-C(8)-H(8B)	110.4
C(7)-C(8)-H(8B)	110.4
H(8A)-C(8)-H(8B)	108.6
C(9)#2-C(9)-C(18)#2	107.99(13)
C(9)#2-C(9)-C(10)	108.43(13)
C(18)#2-C(9)-C(10)	143.58(11)
C(9)#2-C(9)-K	79.20(9)
C(18)#2-C(9)-K	77.73(7)
C(10)-C(9)-K	109.06(8)
C(9)#2-C(9)-K#2	71.93(9)
C(18)#2-C(9)-K#2	110.94(8)
C(10)-C(9)-K#2	80.75(7)
K-C(9)-K#2	151.13(4)
C(17)-C(10)-C(9)	105.92(11)
C(17)-C(10)-C(11)	123.72(11)
C(9)-C(10)-C(11)	129.78(11)
C(17)-C(10)-K#2	75.85(7)
C(9)-C(10)-K#2	71.41(6)
C(11)-C(10)-K#2	111.37(7)
C(16)-C(11)-C(12)	116.41(12)
C(16)-C(11)-C(10)	121.84(12)
C(12)-C(11)-C(10)	121.73(12)
C(13)-C(12)-C(11)	121.64(13)
C(13)-C(12)-H(12)	119.2
C(11)-C(12)-H(12)	119.2
C(12)-C(13)-C(14)	120.69(13)

C(12)-C(13)-H(13)	119.7
C(14)-C(13)-H(13)	119.7
C(15)-C(14)-C(13)	118.87(13)
C(15)-C(14)-H(14)	120.6
C(13)-C(14)-H(14)	120.6
C(14)-C(15)-C(16)	120.76(13)
C(14)-C(15)-H(15)	119.6
C(16)-C(15)-H(15)	119.6
C(15)-C(16)-C(11)	121.63(13)
C(15)-C(16)-H(16)	119.2
C(11)-C(16)-H(16)	119.2
C(18)-C(17)-C(10)	111.30(11)
C(18)-C(17)-K#2	70.78(7)
C(10)-C(17)-K#2	77.16(7)
C(18)-C(17)-H(17)	124.2
C(10)-C(17)-H(17)	124.2
K#2-C(17)-H(17)	124.2
C(17)-C(18)-C(9)#2	106.30(10)
C(17)-C(18)-C(19)	122.31(11)
C(9)#2-C(18)-C(19)	129.41(11)
C(17)-C(18)-K#2	81.70(7)
C(9)#2-C(18)-K#2	73.13(7)
C(19)-C(18)-K#2	99.26(7)
C(20)-C(19)-C(24)	116.76(12)
C(20)-C(19)-C(18)	122.15(12)
C(24)-C(19)-C(18)	120.95(12)
C(20)-C(19)-K#2	83.44(7)
C(24)-C(19)-K#2	131.31(9)
C(18)-C(19)-K#2	56.00(6)
C(21)-C(20)-C(19)	121.29(13)
C(21)-C(20)-H(20)	119.4
C(19)-C(20)-H(20)	119.4
C(22)-C(21)-C(20)	120.60(14)
C(22)-C(21)-H(21)	119.7
C(20)-C(21)-H(21)	119.7
C(21)-C(22)-C(23)	119.28(13)
C(21)-C(22)-H(22)	120.4
C(23)-C(22)-H(22)	120.4

C(22)-C(23)-C(24)	120.34(14)
C(22)-C(23)-H(23)	119.8
C(24)-C(23)-H(23)	119.8
C(23)-C(24)-C(19)	121.71(13)
C(23)-C(24)-H(24)	119.1
C(19)-C(24)-H(24)	119.1

Symmetry transformations used to generate equivalent atoms:

#1 -x+2,-y+1,-z+1 #2 -x+1,-y+1,-z+1

Table 5. Anisotropic displacement parameters ($Å^2 x\ 10^3$) for s18uh2. The anisotropic displacement factor exponent takes the form: $-2\pi^2[h^2 a^{*2} U^{11} + ... + 2 h k a^* b^* U^{12}]$

	U^{11}	U^{22}	U^{33}	U^{23}	U^{13}	U^{12}
K	25(1)	29(1)	32(1)	5(1)	10(1)	16(1)
O(1)	37(1)	42(1)	32(1)	-2(1)	10(1)	12(1)
C(1)	37(1)	49(1)	40(1)	4(1)	14(1)	15(1)
C(2)	38(1)	71(1)	39(1)	-1(1)	7(1)	16(1)
C(3)	43(1)	53(1)	31(1)	0(1)	10(1)	20(1)
C(4)	43(1)	40(1)	41(1)	0(1)	19(1)	15(1)
O(2)	29(1)	25(1)	33(1)	4(1)	7(1)	11(1)
C(5)	40(1)	28(1)	34(1)	3(1)	11(1)	15(1)
C(6)	43(1)	32(1)	49(1)	2(1)	15(1)	7(1)
C(7)	64(1)	41(1)	50(1)	-1(1)	31(1)	6(1)
C(8)	35(1)	40(1)	33(1)	-3(1)	9(1)	9(1)
C(9)	18(1)	23(1)	19(1)	6(1)	8(1)	12(1)
C(10)	20(1)	21(1)	21(1)	4(1)	8(1)	10(1)
C(11)	17(1)	25(1)	21(1)	3(1)	8(1)	10(1)
C(12)	25(1)	27(1)	26(1)	2(1)	10(1)	11(1)
C(13)	26(1)	36(1)	27(1)	-5(1)	7(1)	8(1)
C(14)	27(1)	51(1)	19(1)	2(1)	4(1)	15(1)
C(15)	26(1)	42(1)	26(1)	13(1)	9(1)	16(1)
C(16)	20(1)	28(1)	25(1)	6(1)	7(1)	11(1)
C(17)	23(1)	19(1)	23(1)	4(1)	9(1)	10(1)
C(18)	20(1)	20(1)	22(1)	6(1)	8(1)	11(1)
C(19)	18(1)	25(1)	23(1)	9(1)	7(1)	11(1)
C(20)	22(1)	27(1)	25(1)	7(1)	9(1)	11(1)
C(21)	30(1)	43(1)	24(1)	7(1)	11(1)	16(1)

C(22)	35(1)	47(1)	30(1)	21(1)	17(1)	18(1)
C(23)	34(1)	30(1)	39(1)	18(1)	14(1)	12(1)
C(24)	32(1)	25(1)	29(1)	9(1)	11(1)	13(1)

Table 6. Hydrogen coordinates (x 10^4) and isotropic displacement parameters ($Å^2$x 10^3) for s18uh2.

	x	y	z	U(eq)
H(1A)	4706	1883	3043	51
H(1B)	5501	801	2888	51
H(2A)	4108	2064	1153	64
H(2B)	3851	429	1100	64
H(3A)	6436	1008	867	51
H(3B)	5955	2126	151	51
H(4A)	8526	3020	1904	49
H(4B)	7523	3959	1563	49
H(5A)	9602	1502	5493	40
H(5B)	8416	1825	4454	40
H(6A)	7105	103	5763	53
H(6B)	6366	1217	5341	53
H(7A)	8273	1291	7529	66
H(7B)	7074	2061	7189	66
H(8A)	9274	4084	7300	47
H(8B)	10429	3264	7465	47
H(12)	1390	1384	2408	31
H(13)	-229	981	554	38
H(14)	-174	2893	-440	40
H(15)	1519	5218	464	36
H(16)	3123	5644	2331	29
H(17)	2201	1846	4366	25
H(20)	4404	4800	7735	28
H(21)	3532	3837	9286	38
H(22)	2152	1373	9221	42
H(23)	1691	-132	7592	40
H(24)	2594	810	6049	34

Table 7. Torsion angles [°] for s18uh2.

C(4)-O(1)-C(1)-C(2)	-18.79(19)
K-O(1)-C(1)-C(2)	137.10(12)
C(4)-O(1)-C(1)-K	-155.89(15)
O(1)-C(1)-C(2)-C(3)	34.3(2)
K-C(1)-C(2)-C(3)	74.6(2)
C(1)-C(2)-C(3)-C(4)	-36.2(2)
C(1)-O(1)-C(4)-C(3)	-4.94(19)
K-O(1)-C(4)-C(3)	-155.63(11)
C(2)-C(3)-C(4)-O(1)	25.76(19)
C(8)-O(2)-C(5)-C(6)	40.96(15)
K#1-O(2)-C(5)-C(6)	176.37(10)
K-O(2)-C(5)-C(6)	-82.71(12)
C(8)-O(2)-C(5)-K	123.67(11)
K#1-O(2)-C(5)-K	-100.92(7)
O(2)-C(5)-C(6)-C(7)	-35.30(18)
K-C(5)-C(6)-C(7)	-82.34(14)
C(5)-C(6)-C(7)-C(8)	16.6(2)
C(5)-O(2)-C(8)-C(7)	-30.18(17)
K#1-O(2)-C(8)-C(7)	-164.28(12)
K-O(2)-C(8)-C(7)	90.83(14)
C(6)-C(7)-C(8)-O(2)	7.5(2)
C(9)#2-C(9)-C(10)-C(17)	-1.32(16)
C(18)#2-C(9)-C(10)-C(17)	178.45(16)
K-C(9)-C(10)-C(17)	83.29(9)
K#2-C(9)-C(10)-C(17)	-68.65(8)
C(9)#2-C(9)-C(10)-C(11)	170.04(13)
C(18)#2-C(9)-C(10)-C(11)	-10.2(3)
K-C(9)-C(10)-C(11)	-105.34(12)
K#2-C(9)-C(10)-C(11)	102.72(12)
C(9)#2-C(9)-C(10)-K#2	67.33(11)
C(18)#2-C(9)-C(10)-K#2	-112.91(18)
K-C(9)-C(10)-K#2	151.94(5)
C(17)-C(10)-C(11)-C(16)	152.15(12)
C(9)-C(10)-C(11)-C(16)	-17.9(2)
K#2-C(10)-C(11)-C(16)	65.26(13)
C(17)-C(10)-C(11)-C(12)	-26.27(18)

C(9)-C(10)-C(11)-C(12)	163.73(12)
K#2-C(10)-C(11)-C(12)	-113.15(11)
C(16)-C(11)-C(12)-C(13)	-0.17(19)
C(10)-C(11)-C(12)-C(13)	178.33(12)
C(11)-C(12)-C(13)-C(14)	0.5(2)
C(12)-C(13)-C(14)-C(15)	-0.3(2)
C(13)-C(14)-C(15)-C(16)	-0.2(2)
C(14)-C(15)-C(16)-C(11)	0.5(2)
C(12)-C(11)-C(16)-C(15)	-0.30(19)
C(10)-C(11)-C(16)-C(15)	-178.79(12)
C(9)-C(10)-C(17)-C(18)	2.38(14)
C(11)-C(10)-C(17)-C(18)	-169.65(11)
K#2-C(10)-C(17)-C(18)	-63.18(9)
C(9)-C(10)-C(17)-K#2	65.55(8)
C(11)-C(10)-C(17)-K#2	-106.47(11)
C(10)-C(17)-C(18)-C(9)#2	-2.48(14)
K#2-C(17)-C(18)-C(9)#2	-69.62(8)
C(10)-C(17)-C(18)-C(19)	162.89(11)
K#2-C(17)-C(18)-C(19)	95.75(11)
C(10)-C(17)-C(18)-K#2	67.14(9)
C(17)-C(18)-C(19)-C(20)	-140.06(13)
C(9)#2-C(18)-C(19)-C(20)	21.7(2)
K#2-C(18)-C(19)-C(20)	-54.07(13)
C(17)-C(18)-C(19)-C(24)	35.61(18)
C(9)#2-C(18)-C(19)-C(24)	-162.68(13)
K#2-C(18)-C(19)-C(24)	121.60(11)
C(17)-C(18)-C(19)-K#2	-85.99(11)
C(9)#2-C(18)-C(19)-K#2	75.72(12)
C(24)-C(19)-C(20)-C(21)	-0.32(19)
C(18)-C(19)-C(20)-C(21)	175.52(12)
K#2-C(19)-C(20)-C(21)	133.01(12)
C(19)-C(20)-C(21)-C(22)	-0.4(2)
C(20)-C(21)-C(22)-C(23)	0.6(2)
C(21)-C(22)-C(23)-C(24)	-0.1(2)
C(22)-C(23)-C(24)-C(19)	-0.7(2)
C(20)-C(19)-C(24)-C(23)	0.9(2)
C(18)-C(19)-C(24)-C(23)	-174.98(13)
K#2-C(19)-C(24)-C(23)	-104.91(15)

Crystal data and structure refinement for 1,3-dimethyl-4,6-diphenyldihydropentalene

Identification code	e18uh4	
Empirical formula	C22 H20	
Formula weight	284.38	
Temperature	150.01(10) K	
Wavelength	0.71073 Å	
Crystal system	Monoclinic	
Space group	$P2_1/c$	
Unit cell dimensions	a = 8.8682(4) Å	□= 90°.
	b = 8.5119(4) Å	□= 97.373(5)°.
	c = 20.7900(12) Å	□ = 90°.
Volume	1556.36(14) $Å^3$	
Z	4	
Density (calculated)	1.214 Mg/m^3	
Absorption coefficient	0.068 mm^{-1}	
F(000)	608	
Crystal size	0.450 x 0.250 x 0.200 mm^3	
Theta range for data collection	3.331 to 29.572°.	
Index ranges	-12<=h<=12, -11<=k<=11, -27<=l<=28	
Reflections collected	38391	
Independent reflections	4057 [R(int) = 0.0604]	
Completeness to theta = 25.242°	99.8 %	
Absorption correction	Semi-empirical from equivalents	
Max. and min. transmission	1.00000 and 0.92425	
Refinement method	Full-matrix least-squares on F^2	
Data / restraints / parameters	4057 / 0 / 201	
Goodness-of-fit on F^2	1.048	
Final R indices [I>2sigma(I)]	R1 = 0.0621, wR2 = 0.1236	
R indices (all data)	R1 = 0.0919, wR2 = 0.1337	
Extinction coefficient	n/a	
Largest diff. peak and hole	0.287 and -0.283 $e.Å^{-3}$	

Table 2. Atomic coordinates (x 10^4) and equivalent isotropic displacement parameters (Å^{2}x 10^3) for e18uh4. U(eq) is defined as one third of the trace of the orthogonalized U^{ij} tensor.

	x	y	z	U(eq)
C(1)	2510(2)	7008(2)	4830(1)	26(1)
C(2)	3208(2)	5947(2)	4336(1)	23(1)
C(3)	2319(2)	6072(2)	3658(1)	29(1)
C(4)	3133(2)	4341(2)	4638(1)	20(1)
C(5)	3424(2)	2799(2)	4516(1)	20(1)
C(6)	4135(2)	2091(2)	3986(1)	21(1)
C(7)	4955(2)	2992(2)	3590(1)	25(1)
C(8)	5657(2)	2304(2)	3103(1)	29(1)
C(9)	5579(2)	701(2)	3004(1)	31(1)
C(10)	4779(2)	-212(2)	3392(1)	33(1)
C(11)	4065(2)	470(2)	3875(1)	27(1)
C(12)	2910(2)	1897(2)	5052(1)	22(1)
C(13)	2314(2)	2848(2)	5482(1)	21(1)
C(14)	1758(2)	2338(2)	6085(1)	22(1)
C(15)	865(2)	989(2)	6092(1)	27(1)
C(16)	347(2)	479(2)	6656(1)	35(1)
C(17)	713(2)	1301(2)	7226(1)	38(1)
C(18)	1623(2)	2625(2)	7234(1)	34(1)
C(19)	2142(2)	3137(2)	6670(1)	27(1)
C(20)	2418(2)	4441(2)	5228(1)	20(1)
C(21)	1977(2)	5937(2)	5332(1)	22(1)
C(22)	1067(2)	6577(2)	5824(1)	26(1)

Table 3. Bond lengths [Å] for e18uh4.

C(1)-C(21)	1.507(2)
C(1)-C(2)	1.555(2)
C(1)-H(1A)	0.9900
C(1)-H(1B)	0.9900
C(2)-C(4)	1.510(2)
C(2)-C(3)	1.527(2)
C(2)-H(2)	1.0000
C(3)-H(3A)	0.9800

C(3)-H(3B)	0.9800
C(3)-H(3C)	0.9800
C(4)-C(5)	1.368(2)
C(4)-C(20)	1.452(2)
C(5)-C(6)	1.467(2)
C(5)-C(12)	1.473(2)
C(6)-C(7)	1.396(2)
C(6)-C(11)	1.399(2)
C(7)-C(8)	1.385(2)
C(7)-H(7)	0.9500
C(8)-C(9)	1.380(2)
C(8)-H(8)	0.9500
C(9)-C(10)	1.380(2)
C(9)-H(9)	0.9500
C(10)-C(11)	1.383(2)
C(10)-H(10)	0.9500
C(11)-H(11)	0.9500
C(12)-C(13)	1.362(2)
C(12)-H(12)	0.9500
C(13)-C(20)	1.464(2)
C(13)-C(14)	1.470(2)
C(14)-C(19)	1.396(2)
C(14)-C(15)	1.396(2)
C(15)-C(16)	1.382(2)
C(15)-H(15)	0.9500
C(16)-C(17)	1.379(3)
C(16)-H(16)	0.9500
C(17)-C(18)	1.385(3)
C(17)-H(17)	0.9500
C(18)-C(19)	1.384(2)
C(18)-H(18)	0.9500
C(19)-H(19)	0.9500
C(20)-C(21)	1.357(2)
C(21)-C(22)	1.485(2)
C(22)-H(22A)	0.9800
C(22)-H(22B)	0.9800
C(22)-H(22C)	0.9800

Table 4. Bond angles [°] for e18uh4.

C(21)-C(1)-C(2)	107.06(12)
C(21)-C(1)-H(1A)	110.3
C(2)-C(1)-H(1A)	110.3
C(21)-C(1)-H(1B)	110.3
C(2)-C(1)-H(1B)	110.3
H(1A)-C(1)-H(1B)	108.6
C(4)-C(2)-C(3)	113.73(13)
C(4)-C(2)-C(1)	101.98(12)
C(3)-C(2)-C(1)	111.54(13)
C(4)-C(2)-H(2)	109.8
C(3)-C(2)-H(2)	109.8
C(1)-C(2)-H(2)	109.8
C(2)-C(3)-H(3A)	109.5
C(2)-C(3)-H(3B)	109.5
H(3A)-C(3)-H(3B)	109.5
C(2)-C(3)-H(3C)	109.5
H(3A)-C(3)-H(3C)	109.5
H(3B)-C(3)-H(3C)	109.5
C(5)-C(4)-C(20)	109.00(13)
C(5)-C(4)-C(2)	140.56(14)
C(20)-C(4)-C(2)	110.23(12)
C(4)-C(5)-C(6)	129.99(14)
C(4)-C(5)-C(12)	106.02(13)
C(6)-C(5)-C(12)	123.97(13)
C(7)-C(6)-C(11)	117.39(14)
C(7)-C(6)-C(5)	121.62(14)
C(11)-C(6)-C(5)	120.95(14)
C(8)-C(7)-C(6)	121.09(15)
C(8)-C(7)-H(7)	119.5
C(6)-C(7)-H(7)	119.5
C(9)-C(8)-C(7)	120.56(15)
C(9)-C(8)-H(8)	119.7
C(7)-C(8)-H(8)	119.7
C(10)-C(9)-C(8)	119.27(15)
C(10)-C(9)-H(9)	120.4
C(8)-C(9)-H(9)	120.4

C(9)-C(10)-C(11)	120.43(16)
C(9)-C(10)-H(10)	119.8
C(11)-C(10)-H(10)	119.8
C(10)-C(11)-C(6)	121.25(15)
C(10)-C(11)-H(11)	119.4
C(6)-C(11)-H(11)	119.4
C(13)-C(12)-C(5)	111.79(13)
C(13)-C(12)-H(12)	124.1
C(5)-C(12)-H(12)	124.1
C(12)-C(13)-C(20)	105.37(13)
C(12)-C(13)-C(14)	125.84(14)
C(20)-C(13)-C(14)	128.74(13)
C(19)-C(14)-C(15)	117.85(15)
C(19)-C(14)-C(13)	121.83(14)
C(15)-C(14)-C(13)	120.28(14)
C(16)-C(15)-C(14)	121.18(16)
C(16)-C(15)-H(15)	119.4
C(14)-C(15)-H(15)	119.4
C(17)-C(16)-C(15)	120.15(17)
C(17)-C(16)-H(16)	119.9
C(15)-C(16)-H(16)	119.9
C(16)-C(17)-C(18)	119.70(16)
C(16)-C(17)-H(17)	120.2
C(18)-C(17)-H(17)	120.2
C(19)-C(18)-C(17)	120.21(17)
C(19)-C(18)-H(18)	119.9
C(17)-C(18)-H(18)	119.9
C(18)-C(19)-C(14)	120.89(16)
C(18)-C(19)-H(19)	119.6
C(14)-C(19)-H(19)	119.6
C(21)-C(20)-C(4)	110.85(13)
C(21)-C(20)-C(13)	141.12(14)
C(4)-C(20)-C(13)	107.80(12)
C(20)-C(21)-C(22)	130.35(14)
C(20)-C(21)-C(1)	109.52(13)
C(22)-C(21)-C(1)	120.09(13)
C(21)-C(22)-H(22A)	109.5
C(21)-C(22)-H(22B)	109.5

H(22A)-C(22)-H(22B)	109.5
C(21)-C(22)-H(22C)	109.5
H(22A)-C(22)-H(22C)	109.5
H(22B)-C(22)-H(22C)	109.5

Table 5. Anisotropic displacement parameters ($Å^2 x\ 10^3$) for e18uh4. The anisotropic displacement factor exponent takes the form: $-2\pi^2[h^2 a^{*2} U^{11} + ... + 2 h k a^* b^* U^{12}]$

	U^{11}	U^{22}	U^{33}	U^{23}	U^{13}	U^{12}
C(1)	30(1)	21(1)	25(1)	2(1)	-2(1)	3(1)
C(2)	23(1)	20(1)	24(1)	4(1)	2(1)	0(1)
C(3)	31(1)	28(1)	27(1)	4(1)	2(1)	2(1)
C(4)	20(1)	21(1)	20(1)	2(1)	0(1)	-1(1)
C(5)	20(1)	22(1)	20(1)	2(1)	1(1)	0(1)
C(6)	19(1)	26(1)	17(1)	1(1)	0(1)	3(1)
C(7)	24(1)	26(1)	24(1)	1(1)	2(1)	0(1)
C(8)	23(1)	40(1)	24(1)	4(1)	6(1)	1(1)
C(9)	28(1)	42(1)	25(1)	-5(1)	6(1)	8(1)
C(10)	40(1)	27(1)	31(1)	-4(1)	8(1)	7(1)
C(11)	32(1)	26(1)	24(1)	2(1)	7(1)	2(1)
C(12)	24(1)	19(1)	22(1)	2(1)	2(1)	1(1)
C(13)	21(1)	19(1)	21(1)	0(1)	2(1)	0(1)
C(14)	21(1)	24(1)	22(1)	3(1)	5(1)	7(1)
C(15)	29(1)	24(1)	28(1)	4(1)	6(1)	5(1)
C(16)	32(1)	32(1)	42(1)	14(1)	14(1)	6(1)
C(17)	35(1)	52(1)	29(1)	17(1)	15(1)	16(1)
C(18)	34(1)	48(1)	22(1)	0(1)	5(1)	15(1)
C(19)	26(1)	30(1)	26(1)	0(1)	4(1)	6(1)
C(20)	19(1)	21(1)	20(1)	0(1)	0(1)	-1(1)
C(21)	20(1)	22(1)	22(1)	-1(1)	-2(1)	0(1)
C(22)	26(1)	24(1)	30(1)	-4(1)	2(1)	4(1)

Table 6. Hydrogen coordinates (x 10^4) and isotropic displacement parameters ($Å^2$x 10^3) for e18uh4.

	x	y	z	U(eq)
H(1A)	3283	7752	5037	31
H(1B)	1645	7619	4609	31
H(2)	4293	6248	4321	27
H(3A)	2418	7138	3490	43
H(3B)	1244	5844	3680	43
H(3C)	2724	5316	3369	43
H(7)	5034	4095	3656	30
H(8)	6197	2941	2835	35
H(9)	6071	231	2672	38
H(10)	4718	-1316	3326	39
H(11)	3516	-174	4137	32
H(12)	2985	788	5093	26
H(15)	608	412	5703	32
H(16)	-263	-440	6650	42
H(17)	343	961	7612	45
H(18)	1891	3183	7627	41
H(19)	2767	4046	6680	32
H(22A)	1619	7449	6055	40
H(22B)	895	5749	6134	40
H(22C)	87	6954	5608	40

Table 7. Torsion angles [°] for e18uh4.

C(21)-C(1)-C(2)-C(4)	-4.82(16)
C(21)-C(1)-C(2)-C(3)	116.91(14)
C(3)-C(2)-C(4)-C(5)	55.7(3)
C(1)-C(2)-C(4)-C(5)	175.92(19)
C(3)-C(2)-C(4)-C(20)	-118.12(14)
C(1)-C(2)-C(4)-C(20)	2.09(16)
C(20)-C(4)-C(5)-C(6)	-179.63(14)
C(2)-C(4)-C(5)-C(6)	6.5(3)
C(20)-C(4)-C(5)-C(12)	-1.33(16)
C(2)-C(4)-C(5)-C(12)	-175.21(18)

C(4)-C(5)-C(6)-C(7)	15.2(2)
C(12)-C(5)-C(6)-C(7)	-162.86(14)
C(4)-C(5)-C(6)-C(11)	-167.39(16)
C(12)-C(5)-C(6)-C(11)	14.6(2)
C(11)-C(6)-C(7)-C(8)	0.6(2)
C(5)-C(6)-C(7)-C(8)	178.18(14)
C(6)-C(7)-C(8)-C(9)	-1.0(2)
C(7)-C(8)-C(9)-C(10)	0.7(3)
C(8)-C(9)-C(10)-C(11)	-0.1(3)
C(9)-C(10)-C(11)-C(6)	-0.2(3)
C(7)-C(6)-C(11)-C(10)	-0.1(2)
C(5)-C(6)-C(11)-C(10)	-177.64(15)
C(4)-C(5)-C(12)-C(13)	0.60(17)
C(6)-C(5)-C(12)-C(13)	179.03(14)
C(5)-C(12)-C(13)-C(20)	0.38(17)
C(5)-C(12)-C(13)-C(14)	-177.18(14)
C(12)-C(13)-C(14)-C(19)	134.25(17)
C(20)-C(13)-C(14)-C(19)	-42.7(2)
C(12)-C(13)-C(14)-C(15)	-43.5(2)
C(20)-C(13)-C(14)-C(15)	139.55(16)
C(19)-C(14)-C(15)-C(16)	1.4(2)
C(13)-C(14)-C(15)-C(16)	179.20(14)
C(14)-C(15)-C(16)-C(17)	-0.2(2)
C(15)-C(16)-C(17)-C(18)	-1.1(3)
C(16)-C(17)-C(18)-C(19)	1.1(3)
C(17)-C(18)-C(19)-C(14)	0.1(2)
C(15)-C(14)-C(19)-C(18)	-1.4(2)
C(13)-C(14)-C(19)-C(18)	-179.13(14)
C(5)-C(4)-C(20)-C(21)	-174.10(13)
C(2)-C(4)-C(20)-C(21)	1.76(17)
C(5)-C(4)-C(20)-C(13)	1.60(17)
C(2)-C(4)-C(20)-C(13)	177.46(12)
C(12)-C(13)-C(20)-C(21)	172.4(2)
C(14)-C(13)-C(20)-C(21)	-10.1(3)
C(12)-C(13)-C(20)-C(4)	-1.17(16)
C(14)-C(13)-C(20)-C(4)	176.29(14)
C(4)-C(20)-C(21)-C(22)	172.73(15)
C(13)-C(20)-C(21)-C(22)	-0.7(3)

C(4)-C(20)-C(21)-C(1)	-5.02(18)
C(13)-C(20)-C(21)-C(1)	-178.49(19)
C(2)-C(1)-C(21)-C(20)	6.27(17)
C(2)-C(1)-C(21)-C(22)	-171.75(13)